Functional implications of tau-fyn interactions in Alzheimer's disease

Lau, Hay Wun Dawn

Awarding institution:
King's College London

Functional implications of tau-fyn interactions in Alzheimer's disease

Dawn Hay Wun Lau

Thesis submitted in fulfilment of the degree of Doctor of Philosophy

Department of Basic and Clinical Neuroscience

King's College London

Institute of Psychiatry, Psychology and Neuroscience

December 2014

Declaration

I hereby declare that, with the exception of the western blots of human brain shown in Chapter 5, all of the work presented in this thesis is my own. Emma Phillips and Ksenia Kurbatskaya (PhD students), prepared the human brain homogenates. Marte Hogseth (MSc student), ran the brain samples on western blots and performed the initial quantification, and I performed statistical analysis of the blots of human brain.

Dawn Lau

December 2014

Acknowledgments

I would like to thank my two supervisors, Diane Hanger and Wendy Noble, for their continuous support, encouragement, and for keeping their faith in me. I feel very fortunate to have had the opportunity to work with both of them, and they have both contributed to my growth as a scientist. I have always felt appreciated, and their help was always at hand. I also thank Alzheimer's Research UK and the Croucher Foundation for funding the work presented in this thesis.

A special thanks goes to Amy Pooler, who taught me all the research skills I would need with plenty of patience, was a constant source of advice and humour, and was a fantastic role model, mentor, and friend. I would also like to thank Teresa for always listening, being so full of positive energy, and for the best office chats. Many thanks go to the rest of Team Tau, Emma for providing many hours of off-topic discussion both in and outside the office and lab, cake, and Iceland. Cara, Ksenia, and Marie for never failing to make me laugh. Matthew and Tong for always coming up with brilliant gems of wisdom, whether funny or serious. I would also like to thank everyone from the Gallo, Hirth, and Miller groups for their friendship, help, and support, especially Charlotte, Lizzie, and Sarah. Lizzie for being a constant source of advice and sharing the same hang-ups as I have, and both Lizzie and Charlotte for all the fun times we had, especially outside the lab. Also, Iceland.

Thank you to Selina Wray, who has always been a fantastic role model and encouraged me to go for this PhD. Thank you to my chemistry and physics teachers, Ms Berry and Mr Bhathena, for making science inspirational.

Big thanks to my UK friends, especially Anita, Cat, Tharni, and Wei for always listening to my problems and lots of laughter outside the lab. Huge thank you to my friends in Hong Kong, Canada, USA, and Australia, especially Eugenia, Gabo, Mandy, Stephanie for always being there for me when needed. I would also like to thank Toby (Dr Chan now) who read this thesis, never lost his faith in me, and always brought me back from a bad day.

Last but not least, thank you to my family, both in the UK and Hong Kong. Rosa for understanding my PhD woes and being a great friend, and to my aunt and uncle for taking me under their wing. My dad for providing our home with an endless supply of Scientific American magazines, and introducing me early to the world of technology. I would like to dedicate this thesis in memory of my mum, whose unfaltering love gave me strength throughout this journey.

Abstract

Alzheimer's disease (AD) is characterised by neuropathological deposits of amyloid plaques and neurofibrillary tangles. In AD, tau is abnormally phosphorylated and forms aggregates which spread trans-synaptically throughout the brain. The non-receptor-associated tyrosine kinase fyn is up-regulated in a subset of tangle-bearing neurons in AD brain and fyn also phosphorylates tau. Most tau is axonally located, where it promotes microtubule stability. Both tau and fyn are found in dendrites, where they stabilise receptor complexes at the post-synaptic density. Tau is also trafficked to the plasma membrane in a phosphorylation-dependent process that requires fyn. Tau is also present in the extracellular space, which could play an important role in the spread of tau pathology in AD. The function of tau at the membrane, and the precise role of fyn in tau trafficking are unclear, but they suggest that fyn could contribute to tau propagation.

Here, the role of fyn in tau release was investigated in organotypic brain slices. The neurotoxicity of soluble β-amyloid oligomers was examined in organotypic brain slices to investigate their impact on tau release. Interactions between tau and SH2 and SH3 domains of fyn were confirmed. Furthermore, the precise binding site between the proline-rich region of tau and the fyn-SH3 domain was identified. Lentiviruses containing tau mutations that alter the tau-fyn interaction were used to determine the downstream effects in organotypic brain slices. Changes in tau and fyn were investigated in human post-mortem brain tissue from individuals with AD and from unaffected controls.

The results presented in this thesis characterise tau-fyn binding and provide insight into the functional implications of this interaction in relation to tau propagation. Understanding the basis of the molecular interactions between tau and fyn will improve our understanding of these important molecular entities and may lead to the discovery of new therapeutic targets for dementia.

Table of Contents

List of Tables

List of Figures

Publications arising from this thesis

Lau, D.H.W., Pooler, A.M., Noble, W., and Hanger, D.P. Identification of the binding site between tau and fyn-SH3. (In preparation)

Rodríguez-Martín, T., Pooler, A.M., **Lau, D.H.W.**, Morotz, G., De Vos, K., Gilley, J., Coleman, M.P., and Hanger, D.P. Axonal mitochondrial number is reduced in neurons of mice expressing the P301L tau mutation associated with frontotemporal dementia. (In preparation)

Hanger, D.P., **Lau, D.H.W.**, Phillips, E.C., Bondulich, M.K., Guo, T., Woodward, B.W., Pooler, A.M., and Noble, W. Intracellular and extracellular roles for tau in neurodegenerative disease. (2014) J. Alzheimers Dis. 40:S37-45. PMID: 24595196

Pooler, A.M., Phillips, E., **Lau, D.H.W.**, Noble, W., and Hanger, D.P. (2013) Physiological release of endogenous tau is stimulated by neuronal activity. EMBO Rep. 14, 389-94. PMID: 23412472

Abbreviations

aa	Amino acid
ABCA7	ATP binding cassette transporter 7 gene
AD	Alzheimer's disease
Aβ	β-Amyloid
AECM	Albert Einstein College of Medicine
AGD	Argyrophilic grain disease
AMPA	α-Amino-3-hydroxy-5-methyl-4-isoxazolepropionic acid
ANOVA	Analysis of variance
ApoE	Apolipoprotein E
APP	Amyloid precursor protein
APS	Ammonium persulphate
BACE	β-site APP cleaving enzyme
BCA	Bicinchoninic acid
BIN1	Bridging integrator 1 gene
BSA	Bovine serum albumin
bp	Base pairs
BME	Basal medium Eagle
BRET	Bioluminescence resonance energy transfer
CBD	Corticobasal degeneration
CD2AP	CD2-associated protein gene
CD33	Myeloid surface antigen CD33 gene
Cdk5	Cyclin dependent kinase-5
CHO	Chinese hamster ovary
CK1	Casein kinase 1
CLU	Clusterin gene
CNS	Central nervous system
COS	CV-1 in Origin with SV40 genes
CR1	Complement receptor 1 gene

Csk	C-src kinase
C-terminus	Carboxyl-terminus
DIV	Days *in vitro*
DTT	Dithiothreitol
DMSO	Dimethyl sulfoxide
dNTP	Deoxyribonucleotide triphosphate
DSP	Dithiobis[succinimidyl propionate]
EBSS	Earl's balanced salt solution
E.coli	*Escherichia coli*
EDTA	Ethylenediaminetetraacetic acid
EGFP	Enhanced green fluorescent protein
EGTA	Ethylene glycol-bis(2-aminoethylether)-*N*,*N*,*N*′,*N*′-tetraacetic acid
ELISA	Enzyme-linked immunosorbent assay
EPHA1	Ephrin receptor A1 gene
ESLB	Extra strong lysis buffer
FAK	Focal adhesion kinase
FBS	Foetal bovine serum
FTD	Frontotemporal dementia
FTDP-17	Frontotemporal dementia and parkinsonism linked to chromosome 17
$g_{(av)}$	Average gravitational force
GFAP	Glial fibrillary acidic protein
GFP	Green fluorescent protein
GSK-3	Glycogen synthase kinase-3
GST	Glutathione-S-transferase
GWAS	Genome-wide association study
HBSS	Hank's balanced salt solution
HEK	Human embryonic kidney cells
HRP	Horseradish peroxidase
IgG	Immunoglobulin

iPSC	Induced pluripotent stem cell
IPTG	Isopropyl-1-thio-β-D-galactopyranoside
IRES	Internal ribosome entry site
JIP1	c-Jun N-terminal kinase-interacting protein 1
kDa	Kilodaltons
kb	Kilobases
LB	Luria-Bertani
LDH	Lactate dehydrogenase
LTD	Long-term depression
LTP	Long-term potentiation
MAP	Microtubule-associated protein
MARK	Microtubule affinity-regulating kinase
MAPT	Microtubule-associated protein tau gene
MCI	Mild cognitive impairment
MS4A	Membrane-spanning 4-domains, subfamily A gene
NMDA	N-methyl-D-aspartic acid
NR2b	NMDA receptor subtype 2B
NSE	Neuron-specific enolase
N-terminus	Amino-terminus
PAGE	Polyacrylamide gel electrophoresis
PBS	Phosphate-buffered saline
PBS-T	PBS-Tween
PCR	Polymerase chain reaction
PDL	Poly-D-lysine
PFA	Paraformaldehyde
PHF	Paired helical filaments
PICALM	Phosphatidylinositol-binding clathrin assembly protein gene
PKA	Cyclic AMP-dependent protein kinase
PP	Protein phosphatase

PrP^C	Cellullar prion protein
PSD-95	Post-synaptic density protein 95
PS1	Presenilin-1 gene
PS2	Presenilin-2 gene
PSP	Progressive supranuclear palsy
OD	Optical density
RIPA	Radioimmunoprecipitation assay
rpm	Revolutions per minute
RPTPα	Receptor protein tyrosine phosphatase-α
rSAP	Shrimp alkaline phosphatase
sAPPα	Soluble amyloid precursor protein α
sAPPβ	Soluble amyloid precursor protein β
SDS	Sodium dodecyl sulphate
SDS-PAGE	Sodium dodecyl sulphate-polyacrylamide gel electrophoresis
S.E.M.	Standard error of the mean
SOC	Super Optimal Broth with Catabolite repression
SH	Src homology
STEP61	Striatal enriched phosphatase 61
STS	Staurosporine
TAE	Tris-acetate-EDTA
TBS	Tris-buffered saline
TBS-T	TBS-Tween
TEMED	N,N,N',N' tetramethylethylenediamine
TMB	3,3',5,5'-Tetramethylbenzidine
TNE	Tris-NaCl-EDTA
TREM2	Triggering receptor expressed on myeloid cells 2
TU	Transducing units
Tween-20	Polyethylene glycol sorbitan monolaurate
X-Gal	5-bromo-4-chloro-3-indolyl-β-D-galactopyranoside

Amino acid code

Alanine	Ala	A	Methionine	Met	M
Cysteine	Cys	C	Asparagine	Asn	N
Aspartic acid	Asp	D	Proline	Pro	P
Glutamic acid	Glu	E	Glutamine	Gln	Q
Phenylalanine	Phe	F	Arginine	Arg	R
Glycine	Gly	G	Serine	Ser	S
Histidine	His	H	Threonine	Thr	T
Isoleucine	Ile	I	Valine	Val	V
Lysine	Lys	K	Tryptophan	Trp	W
Leucine	Leu	L	Tyrosine	Tyr	Y

Chapter 1 Introduction

1.1 Clinical overview of AD

The first formal diagnosis of what is now known as Alzheimer's disease (AD) was presented in 1906 by Alois Alzheimer (Alzheimer, 1907), who had examined a woman suffering from cognitive impairment that he had never seen before. His patient, Auguste Deter, was fifty years old when she was diagnosed with "senile dementia", although in the present day she would most likely have received a diagnosis of early-onset AD. Her symptoms included aphasia, paranoia, rapid memory loss, auditory hallucinations, and disorientation. After she died, her brain tissue was obtained by Dr Alzheimer for histopathological analysis. In his findings, he noted the presence of significant cortical atrophy, leaving in its place characteristic fibrils that we now know as neurofibrillary tangles, composed of the tau protein. He also noted the deposition of "miliar foci" in the cerebral cortex, filled with a "peculiar matter" which is now known to be the β-amyloid (Aβ) protein of amyloid plaques (Strassnig and Ganguli, 2005).

AD is the most common cause of dementia in the elderly population. The greatest risk factor for AD is age; typically, late-onset AD affects individuals aged 65 or above, whereas early onset forms of AD, usually caused by genetic mutations, are less common (Thies and Bleiler, 2011). Currently, the diagnostic criteria for AD are those proposed by the International Working Group for New Research Criteria for the Diagnosis of Alzheimer's Disease (Dubois et al., 2014). The diagnosis of the early stages of AD has been refined due to improvements in technology and detection of early changes (Dubois et al., 2014). There are three stages of AD: preclinical AD, prodromal AD, and dementia due to AD, all of which display progressively worse symptoms. The first stage is asymptomatic in that there may be visible changes in biomarker profile, but the individual will not have developed any cognitive symptoms. Changes in biomarker profile include positive positron emission tomography scans using the Pittsburgh compound B (PiB-PET), which detects deposits of Aβ protein, or changes in levels of Aβ or tau in the cerebrospinal fluid (Dubois et al., 2010). Subsequently, individuals with prodromal AD display clinical symptoms, which include episodic memory loss characterised by low free recall, but these cognitive impairments do not affect the individual's daily activities (Dubois et al., 2010). Cognitive testing is carried out using clinical tools such as the Mini-Mental State Exam which is a widely used screening test that measures several factors including orientation, memory, concentration, and language (Folstein et al., 1975). Finally, progression to the last stage of AD is typified by increasingly impaired episodic memory and impairment of

other cognitive functions, such as aphasia, apraxia, and agnosia with worsening of executive function (van der Flier et al., 2011). The progressive decline in cognitive function results in the individual eventually being unable to carry out daily tasks due to impaired judgment, disorientation, confusion, and problems with language and movement, therefore requiring full-time assistance. Those in the final stages of AD become extremely vulnerable to infections or complications due to immobility, ultimately leading to death.

1.2 Neuropathology of AD

Morphologically, post-mortem brains from AD patients display severe brain atrophy compared to a cognitively normal individual (Holtzman et al., 2011). At the microscopic level, the hallmarks of AD pathology are characterised by neuronal loss and degeneration with intraneuronal neurofibrillary tangles, composed of the microtubule-associated protein tau, and depositions of Aβ peptide in extracellular plaques (Figure 1.1) (Holtzman et al., 2011).

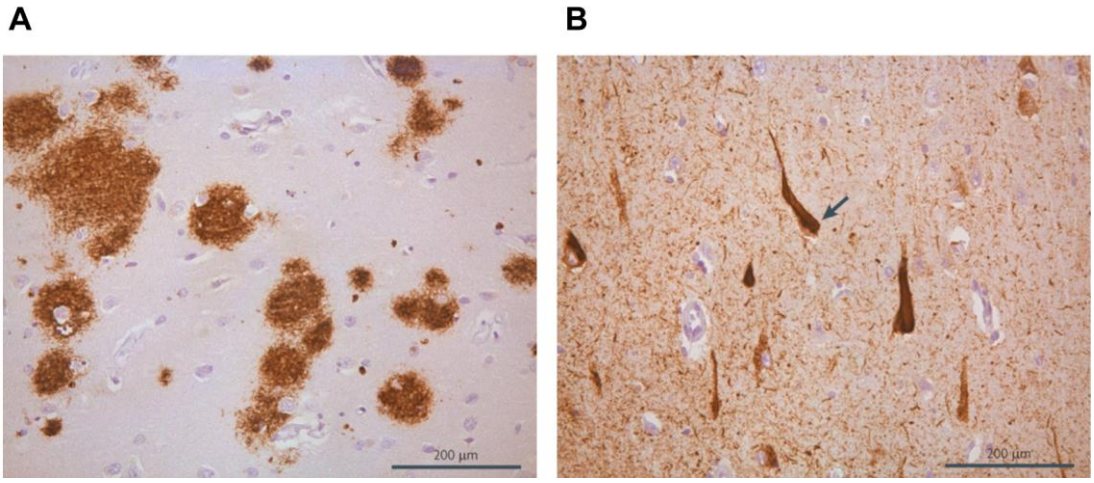

Figure 1.1 Neuropathology of Alzheimer's disease

Aggregates of (A) Aβ protein and (B) tau protein are observed in brains of late-stage AD individuals. Extracellular Aβ plaques stained with an Aβ-specific antibody (A) and intracellular neurofibrillary tangles containing tau stained with an antibody specific for phosphorylated tau (B). Image from (Aguzzi and O'Connor, 2010).

The inclusions of tau protein, in the form of pre-tangles, neurofibrillary tangles, and neuropil threads, occur long before the onset of clinical symptoms (Braak et al., 2013). Pre-tangles, which are composed of soluble but abnormally phosphorylated tau, start forming in the axon of diseased neurons, which then turn into neurofibrillary tangles positive for Gallyas silver iodide staining (Uchihara et al., 2001). Tangle-containing neurons can survive for several years, but following death of the neuron, extracellular "ghost tangles" can remain in the neuropil (Morsch et al., 1999). The formation of tau pathology follows a characteristic pattern of spreading throughout the brain during disease progression which is used to classify disease severity as Braak stages I-VI (Braak and Braak, 1991). At stages I and II, tau pathology is confined to the transentorhinal cortex. By stages III-IV, the pathology has progressed anatomically to involve the limbic region. In stages V-VI, severe tau pathology, including ghost tangles, is seen in the preceding regions and tau pathology finally consumes the isocortex (Braak and Braak, 1991; Braak et al., 2011).

Isolation and purification of the amyloid constituent from the plaques revealed a 4 kDa polypeptide termed Aβ (Glenner and Wong, 1984; Masters et al., 1985). Aβ is derived from cleavage of the amyloid precursor protein (APP), which was isolated and sequenced in 1986 (Kang et al., 1987). Extracellular depositions of aggregated Aβ peptide, including species ranging from 39 to 42 amino acids in length, but predominantly 40 or 42 ($A\beta_{40}$ or $A\beta_{42}$, respectively) give rise to the accumulation of amyloid plaques in AD brain. $A\beta_{42}$ is more abundant in AD brain due to its insolubility and propensity to fibrillise, compared to other species of Aβ (Serrano-Pozo et al., 2011). Amyloid plaques are classified into two categories. Dense-core plaques stain positive for β-sheet dyes such as Congo Red and Thioflavin S, and are associated with toxicity of the surrounding neuropil, characterised by dystrophic neurites, loss of synapses and neurons, and activation of glial cells (Serrano-Pozo et al., 2011). On the other hand, diffuse plaques can be found in cognitively "normal" individuals as well as in AD brain and the Aβ that makes up the majority of the protein content in these plaques is not in a fibrillar form (Selkoe, 2011). Aβ plaques occur much later after the presentation of abnormal tau inclusions, generally in the fourth decade when pre-tangle pathology can already be observed (Braak et al., 2011; Braak et al., 2013). In AD, amyloid plaques preferentially appear in the cerebral cortex, particularly the isocortex (Braak and Braak, 1991).

1.3 Genetics of AD

The relationship between plaques and tangles is not fully understood. However, it is generally accepted that Aβ accumulation in the brain initiates a pathological cascade triggering altered tau phosphorylation, resulting in the loss of neurons, eventually causing dementia. This is known as the amyloid cascade hypothesis (Hardy and Allsop, 1991; Hardy and Higgins, 1992). The strongest evidence for the amyloid cascade hypothesis came from the discovery of mutations in the *APP* gene on chromosome 21 in families with early-onset AD (Chartier-Harlin et al., 1991; Goate et al., 1991; Murrell et al., 1991; van Duijn et al., 1991). APP processing results in the production of both non-amyloidogenic products and several different Aβ species including those with 40 or 42 amino acids ($A\beta_{40}$ and $A\beta_{42}$) (O'Brien and Wong, 2011). The first mutations in *APP* were found in codon 717 which were point mutations that resulted in the substitution of valine with glycine, isoleucine, or phenylalanine (Chartier-Harlin et al., 1991; Goate et al., 1991; Murrell et al., 1991; Naruse et al., 1991). Although these mutations are rare, they are not found in healthy individuals or in individuals with late-onset AD, indicating that *APP* 717 mutations, located just beyond the C-terminus sequence encoding Aβ, are pathogenic for early-onset AD. Additionally, another *APP* mutation, resulting in substitution of alanine by glycine at residue 692, was found in a Dutch family with “presenile dementia” (Hendriks et al., 1992). In support of the pathogenicity of *APP* mutations, transgenic mice expressing V717F mutant APP exhibit extracellular Aβ deposits, dystrophic neurites, gliosis, and synaptic loss consistent with AD (Games et al., 1995).

Subsequently, a double mutation at residues 670/671 of *APP*, located in exon 16, was found in a large Swedish family with early-onset AD (Mullan et al., 1992). This mutation causes lysine-asparagine and methionine-leucine substitutions in the amino acid sequence of APP. In contrast to the *APP* 717 mutations, the 670/671 mutation resides at the N-terminus of the sequence encoding Aβ peptide. In cultured human embryonic kidney (HEK) 293 cells, overexpression of 670/671 mutant APP results in a six-to-eight-fold increase in Aβ production compared to wild-type (WT) APP-expressing cells (Citron et al., 1992). Furthermore, mutation of codon 693 of *APP* (E693G), termed the Arctic mutation, also contributes to familial AD, resulting in decreased plasma Aβ levels but without affecting the ratios of $A\beta_{40}/A\beta_{42}$ (Nilsberth et al., 2001). Overall, mutations in *APP* are rare, as they only account for a very small proportion of familial AD (Tanzi et al., 1992). Intriguingly, a recent mutation in *APP* (A673T) was discovered in an Icelandic cohort, with the finding that this mutated allele was actually protective for AD (Jonsson et al., 2012). This was suggested to be caused in part by altered processing

of APP by β-secretase enzyme, resulting in a decreased production of Aβ in transfected cells (Jonsson et al., 2012). However, a homozygous mutation at the same codon (A673V), is causative for AD and increases Aβ production and fibrillisation (Di Fede et al., 2009).

Mutations were later discovered in the presenilin-1 (*PS1*) and presenilin-2 (*PS2*) genes on chromosomes 14 and 1, respectively, in families with early-onset AD (Clark et al., 1995; Levy-Lahad et al., 1995; Rogaev et al., 1995; Sherrington et al., 1995; Wasco et al., 1995). In particular, mutations in *PS1* appear to be a frequent association in early-onset familial AD individuals, while mutations in *PS2* are rare in familial AD (Sherrington et al., 1996). In individuals with familial AD associated with mutations in *PS1* or *PS2*, elevated $A\beta_{42}$ was found in plasma compared to age-matched controls (Scheuner et al., 1996). Additionally, individuals bearing the E280A *PS1* mutation were found to have significantly increased $A\beta_{42}$ deposition when compared to sporadic AD individuals, indicating that these mutations enhance $A\beta_{42}$ production (Lemere et al., 1996). In further support of this suggestion, expression of *PS1* mutations both *in vitro* and *in vivo* upset the ratio of $A\beta_{40}/A\beta_{42}$ production, leading to an elevation of $A\beta_{42}$ which is more fibrillogenic than $A\beta_{40}$ (Borchelt et al., 1996; Duff et al., 1996; Citron et al., 1997).

There are also a number of genetic risk factors for AD. Most notably, the *APOE* gene has a significant effect on the risk of developing AD (Corder et al., 1993). There are three alleles in the *APOE* gene, *APOE*-ε2, *APOE*-ε3, and *APOE*-ε4. Individuals harbouring the ε4 allele have an increased risk of developing late-onset AD and this risk is further increased by homozygosity of the ε4 allele, whereas individuals with the ε2 allele have a reduced risk of AD or a later age of onset (Corder et al., 1993; Strittmatter et al., 1993; Chartier-Hariln et al., 1994; Blacker et al., 1997). Interestingly, the apolipoprotein E (ApoE) protein co-localises with neurofibrillary tangles as well as amyloid plaques, suggesting a pathogenic role of this protein in AD (William Rebeck et al., 1993; Benzing and Mufson, 1995), although its function in disease is not well understood. The presence of *APOE* alleles does not conclusively determine whether or not an individual will develop AD (Meyer et al., 1998).

More recently, genome-wide association studies (GWAS) have provided evidence of several other genetic risk factors for sporadic late-onset AD, including *CLU* (encodes clusterin protein), *CR1* (complement receptor 1), *PICALM* (phosphatidylinositol-binding clathrin assembly protein), *BIN1* (bridging integrator 1), *MS4A* (membrane-spanning 4-domains, subfamily A) gene cluster, *EPHA1* (ephrin receptor A1), *CD2AP* (CD2-associated protein), *CD33* (myeloid surface antigen CD33), *ABCA7* (ATP binding

cassette transporter 7), and *TREM2* (triggering receptor expressed on myeloid cells 2) (Harold et al., 2009; Lambert et al., 2009; Corneveaux et al., 2010; Seshadri et al., 2010; Hollingworth et al., 2012; Guerreiro et al., 2013; Jonsson et al., 2013). It is believed that these genes explain about 50% of late-onset AD, indicating there are remaining risk genes that have not yet been identified (Kamboh et al., 2012). Interestingly, the *FYN* gene, among others, has been flagged as a candidate gene in modulating *APOE*-ε4-dependent transcriptomic changes in AD (Rhinn et al., 2013).

Although tau pathology is evident in the brains of individuals with AD, to date, no mutations causative for AD have been found in the gene encoding the tau protein, *MAPT*. A seminal finding was reported in 1998 (Hutton et al., 1998) when mutations in the tau gene were found to be causative for frontotemporal dementia and parkinsonism linked to chromosome 17 (FTDP-17), demonstrating that tau dysfunction alone was sufficient to cause neurodegeneration (Dumanchin et al., 1998; Hutton et al., 1998; Spillantini et al., 1998b; Rizzu et al., 1999). While no evidence for mutations in the *MAPT* gene in AD individuals has been established, tau mutations in FTDP-17 support the hypothesis that tau is causative for neurodegenerative dementias.

1.3.1 Genetic alterations of tau in neurodegenerative disease

The genetic basis of tau-mediated neurodegeneration is supported by the existence of two haplotypes at the *MAPT* locus on chromosome 17q21. H1, the more common haplotype, has been associated with several tauopathies, including corticobasal degeneration and progressive supranuclear palsy (PSP) (Baker et al., 1999; Houlden et al., 2001). There have been several sub-haplotypes identified within the H1 haplotype, but it was later determined that only the sub-haplotype H1c is associated with PSP (Pittman et al., 2006). Conversely, the H2 haplotype is uncommon and involves a chromosomal inversion of ~900 kilobases, with a 238 base pair deletion in the intron upstream of exon 10 (Baker et al., 1999; Stefansson et al., 2005). It is negatively associated with PSP, suggesting that carriers of the H2 haplotype may be protected against disease (Baker et al., 1999). The H2 haplotype has been shown to be associated with increased expression of exon 3 of tau mRNA, especially in the frontal cortex (Caffrey et al., 2008; Trabzuni et al., 2012). The effect of *MAPT* haplotype on the risk of AD remains unclear. The H1c haplotype has been found to be associated with increased risk of AD (Myers et al., 2005; Myers et al., 2007), and a more recent study has provided more evidence for an association between the H1 haplotype and

AD (Gerrish et al., 2012). However, these studies need to be replicated with larger sample sizes.

To date, several pathogenic mutations in *MAPT* have been discovered, including missense, deletion, silent, and intronic mutations (Table 1.1) (Spillantini and Goedert, 2013). Although these mutations are pathogenic in tauopathies, none of them have been found to be causative for AD. Most of these mutations are coding mutations in exons 9-12 of *MAPT*. Mutations in tau are classified into two categories: mutations which act at the protein level and mainly affect microtubule binding or tau aggregation, and mutations which act at the mRNA level to influence the splicing of exon 10, therefore affecting the 3R to 4R tau ratio. For the most part, mutations which influence tau splicing tend to promote the inclusion of exon 10, resulting in over-production of 4R tau (Spillantini and Goedert, 2013). For example, evidence shows that tau containing frontotemporal dementia mutations such as P301L, R406W or ΔK280 tau accelerate aggregation of tau *in vitro* (Goedert et al., 1999; Nacharaju et al., 1999; Barghorn et al., 2000). These mutations suggest that tau-mediated neurodegeneration stems from a gain of function rather than loss of function, as none of the mutations in tau have been found to result in loss of protein (Wolfe, 2009).

Table 1.1 Tau mutations and their associated clinical phenotype

Mutation	Exon	Clinical phenotype	Reference
R5H	1	FTD	(Hayashi et al., 2002)
R5L	1	PSP	(Poorkaj et al., 2002)
K257T	9	FTD	(Pickering-Brown et al., 2000; Rizzini et al., 2000)
I260V	9	FTD	(Grover et al., 2003)
L266V	9	FTD	(Hogg et al., 2003; Kobayashi et al., 2003)
G272V	9	FTD	(Hutton et al., 1998)
G273R	9	FTD	(van der Zee et al., 2006)
-15, -10	Intron 9	FTD	(Malkani et al., 2006)
N279K	10	FTD	(Wszolek et al., 1992)
ΔK280	10	FTD	(Rizzu et al., 1999; Momeni et al., 2009)
L284L	10	FTD	(D'Souza et al., 1999)
L284R	10	PSP	(Rohrer et al., 2011)
ΔN296	10	PSP	(Pastor et al., 2001)
N296N	10	FTD	(Spillantini et al., 2000)
N296H	10	FTD	(Iseki et al., 2001)

P301L	10	FTD	(Dumanchin et al., 1998; Hutton et al., 1998; Spillantini et al., 1998a)
P301S	10	FTD	(Bugiani et al., 1999; Sperfeld et al., 1999; Lossos et al., 2003)
P301T	10	FTD	(Llado et al., 2007)
G303V	10	PSP	(Ros et al., 2005)
S305I	10	AGD	(Kovacs et al., 2008)
S305N	10	FTD	(Iijima et al., 1999; Kobayashi et al., 2002)
S305S	10	FTD, PSP	(Stanford et al., 2000; Skoglund et al., 2008)
+3, +11, +12, +13, +14, +16	Intron 10	FTD	(Hutton et al., 1998; Spillantini et al., 1998b; Yasuda et al., 2000; Miyamoto et al., 2001; Kowalska et al., 2002)
+19	Intron 10	FTD	(Stanford et al., 2003)
L315R	11	FTD	(van Herpen et al., 2003)
K317M	11	FTD	(Zarranz et al., 2005)
S320F	11	FTD	(Rosso et al., 2002)
P332S	11	FTD	(Deramecourt et al., 2012)
G335S	12	FTD	(Spina et al., 2007)
G335V	12	FTD	(Neumann et al., 2005)

Q336R	12	FTD	(Pickering-Brown et al., 2004)
V337M	12	FTD	(Sumi et al., 1992; Poorkaj et al., 1998)
E342V	12	FTD	(Lippa et al., 2000)
S352L	12	Other tauopathy	(Nicholl et al., 2003)
S356T	12	FTD	(Momeni et al.)
V363I	12	FTD	(Munoz et al., 2007; Anfossi et al., 2011)
P364S	12	FTD	(Rossi et al., 2012)
G366R	12	FTD	(Rossi et al., 2012)
K369I	12	FTD	(Neumann et al., 2001)
G389R	13	FTD	(Murrell et al., 1999; Pickering-Brown et al., 2000)
R406W	13	FTD	(Reed et al., 1997; Hutton et al., 1998)
N410H	13	CBD	(Kouri et al., 2014)
T427M	13	FTD	(Giaccone et al., 2005)

This table lists the known pathogenic mutations in *MAPT* and where they are located within the sequence (intron or exon). The clinical phenotype caused by each mutation is shown as well as the primary references. FTD, frontotemporal dementia. PSP, progressive supranuclear palsy. AGD, argyrophilic grain disease. CBD, corticobasal degeneration.

1.4 Amyloid beta

1.4.1 Amyloid precursor protein processing

APP is a transmembrane protein located in neurons that can be alternatively spliced into three major isoforms: APP695, APP751, and APP770, of which the shortest form APP695 is specifically expressed in the brain (Kang and Müller-Hill, 1990; O'Brien and Wong, 2011). Cleavage of APP can occur by two mutually exclusive pathways (Figure 1.2). In the non-amyloidogenic pathway, APP is first cleaved by α-secretase within the Aβ domain, releasing an extracellular soluble fragment, sAPPα. Subsequently, γ-secretase cleaves the remaining C-terminal fragment in the membrane (APP-CTFα) to produce the p3 fragment (Haass and Selkoe, 1993). In the amyloidogenic pathway, β-secretase, which was subsequently identified as β-site APP cleaving enzyme (BACE), cleaves APP and releases a soluble fragment called sAPPβ (Vassar et al., 1999). BACE cleavage releases a C99 membrane-bound fragment, which can be further cleaved by γ-secretase to generate Aβ (Vassar et al., 1999). γ-secretase is a complex composed of at least four proteins, including presenilin 1 (PS1) or its homologue presenilin 2 (PS2), nicastrin, anterior pharynx-defective-1 (APH-1), and presenilin enhancer-2 (PEN-2) (Kimberly et al., 2003). The Aβ peptide generated from γ-secretase cleavage of C99 at multiple sites ranges from 38-43 residues in length. Predominantly $A\beta_{40}$ (90%) is produced, followed by $A\beta_{42}$ (10%) which is believed to be the more toxic form of Aβ (Jarrett et al., 1993; LaFerla et al., 2007).

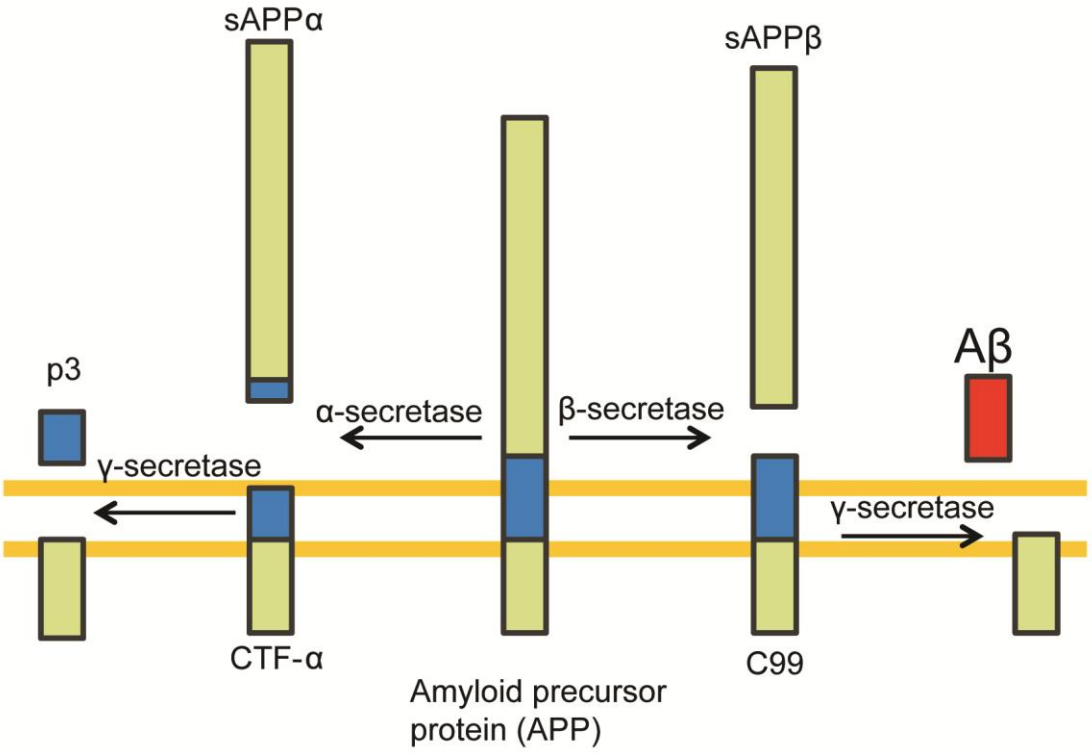

Figure 1.2 Non-amyloidogenic and amyloidogenic processing of APP

Cleavage of APP occurs on two mutually exclusive pathways: non-amyloidogenic and amyloidogenic. In the non-amyloidogenic pathway, APP is cleaved by α-secretase into sAPPα and CTF-α. CTF-α is then cleaved further by γ-secretase to release p3. In the amyloidogenic pathway, APP is first cleaved by β-secretase to produce sAPPβ and C99, which is retained in the membrane. C99 is subsequently cleaved by γ-secretase to release the Aβ fragment of mainly 40 or 42 amino acids.

1.4.2 Species, toxicity, and aggregation of Aβ

The amyloid cascade hypothesis postulates that Aβ plays a critical role in the pathogenesis of AD, driven by accumulation of toxic Aβ in neurons (Hardy and Selkoe, 2002). However, contrary to this hypothesis, the number of Aβ plaques in the brains of AD individuals does not correlate well with disease severity (Arriagada et al., 1992; Gómez-Isla et al., 1997; Giannakopoulos et al., 2003; Nelson et al., 2009), and transgenic mouse models of AD overexpressing mutant APP or presenilin do not exhibit a correlation between the amount of Aβ plaques and severity of neurodegeneration (Benilova et al., 2012). Therefore, attention has shifted to studying the intermediate forms of Aβ species that accumulate prior to the formation of Aβ plaques.

Soluble oligomeric Aβ extracted from brains of AD patients is a better correlate of disease progression than the presence of Aβ plaques (McLean et al., 1999; Mc Donald et al., 2010). Extracts of soluble Aβ oligomers, but not insoluble Aβ plaques, are able to induce synaptotoxicity in cultured rodent neurons, further supporting the idea that soluble species of Aβ are toxic while plaques are relatively inert (Shankar et al., 2008). Soluble Aβ resolves into several assemblies of various sizes on electrophoretic gels, but the smallest species that exert toxicity were proposed to be Aβ dimers (Shankar et al., 2008).

However, caution must be used in interpreting studies using Aβ oligomers, as it is difficult to determine whether the assemblies of Aβ studied in different laboratories are identical. Aβ oligomers can be generated synthetically (Lambert et al., 1998), extracted from AD brain tissue (Shankar et al., 2008), or purified from mammalian cells (Shankar et al., 2007), but depending on the origin, the toxicity of the Aβ species can be highly variable. Synthetic Aβ oligomers have been suggested to be less neurotoxic than Aβ oligomers derived from cells expressing mutant forms of APP (Townsend et al., 2006). Other studies have since confirmed the variability of Aβ toxicity and the relatively weaker potency of synthetic Aβ oligomers compared to human brain-derived Aβ (Jin et al., 2011). The exact nature of the toxic species of Aβ is still elusive and the reality may be that a mixture of oligomeric Aβ assemblies exert neurotoxicity at varying potencies *in vivo*, although reproducing this is difficult due to the heterogeneity of Aβ species reported in the literature (Benilova et al., 2012).

1.5 Tau

1.5.1 Tau structure

Tau is a microtubule-associated protein ubiquitously expressed in the brain (Binder et al., 1985) which binds to microtubules to promote their assembly and stabilisation. Tau protein is encoded by the *MAPT* gene on chromosome 17q21 and contains 16 exons (Neve et al., 1986; Andreadis et al., 1992). Alternative mRNA splicing gives rise to six possible isoforms of tau in the central nervous system (CNS), resulting from the inclusion or exclusion of exons 2, 3, and 10 (Cleveland et al., 1977; Couchie and Nunez, 1985; Goedert et al., 1989b). Alternative splicing of exon 10 gives rise to tau protein containing either three or four tandem repeat domains at its C-terminus (3R or 4R tau, respectively) (Goedert et al., 1989a). At the N-terminus, exons 2 and 3 each encode inserts of 29 amino acids, resulting in three possible combinations of tau: 0N, 1N, or 2N, in which exon 3 only appears if exon 2 is translated (Goedert et al., 1989b). Correspondingly, the combination of exons 2, 3, and 10 generate six isoforms of tau in the adult human brain, ranging from smallest to largest: 0N3R, 0N4R, 1N3R, 2N3R, 1N3R, 2N4R with molecular weights of 48 to 67kDa (Figure 1.3) (Goedert et al., 1989b; Goedert and Jakes, 1990). In addition to these isoforms, a 110 kDa isoform of tau (also known as big tau) is found specifically in the peripheral nervous system. The sequence of big tau is identical to that of CNS tau, but big tau has an additional insert of 254 amino acids at the N-terminus (Goedert et al., 1992).

All six isoforms of tau are present in adult human brain, but the pattern of isoform expression is developmentally regulated. Foetal tau is mostly comprised of 3R tau, but the ratio of 3R to 4R tau gradually reaches a 1:1 ratio in adults (Goedert et al., 1989a). Additionally, the inclusion of exons 2 and 3 is observed only in adult human brain; during foetal development, only the shortest isoform, 0N3R tau, is expressed (Goedert et al., 1989b).

The protein sequence of tau can be divided into distinct regions with differing functions. The N-terminus of tau, known as the projection domain, is overall negatively charged due to the high concentration of acidic residues (Himmler et al., 1989; Goedert et al., 1991). The negatively charged residues suggest that the N-terminus of tau can protrude from the microtubule surface, which act as cross-bridges between microtubules and may determine the amount of spacing between microtubules (Hirokawa et al., 1988; Chen et al., 1992). In transfected PC12 cells, expression of an N-terminal fragment of tau (aa 1-202, excluding the microtubule binding domain) did not result in microtubule binding; instead, this region of tau localised to the plasma

membrane (Brandt et al., 1995). Moreover, the N-terminus of tau plays an important role in mediating interactions between tau and plasma membrane-associated proteins such as src family kinases (Lee et al., 1998; Reynolds et al., 2008; Pooler et al., 2012).

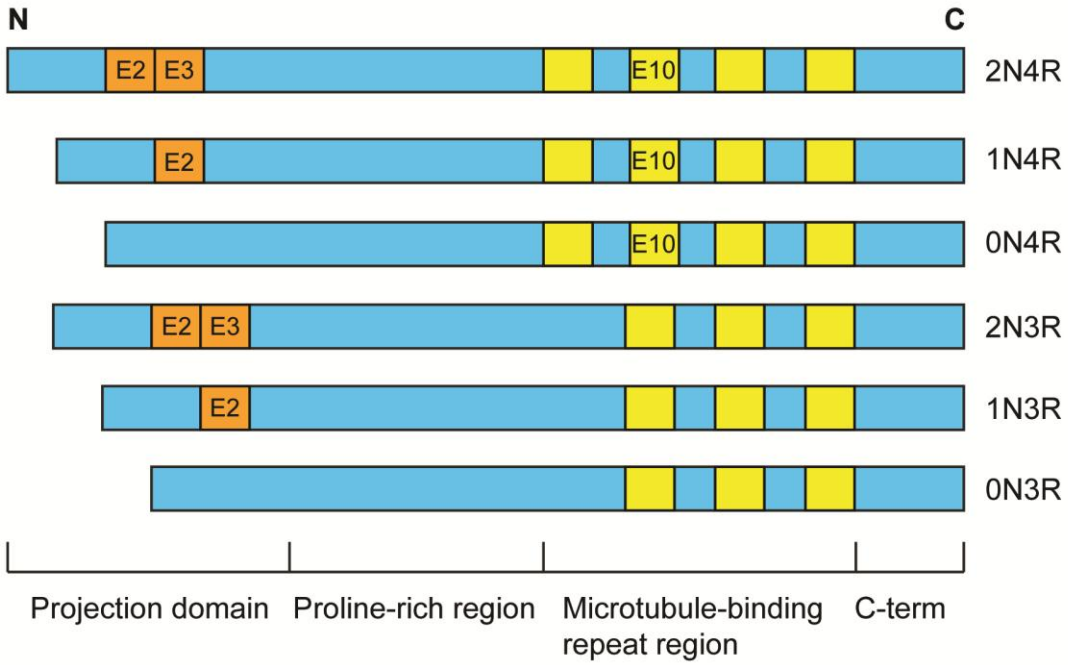

Figure 1.3 Isoforms of tau protein and their domains

There are six main isoforms of tau that arise from alternative splicing of exons 2, 3, and 10 (denoted E2, E3, and E10, respectively). Tau is comprised of distinct regions: the N-terminal projection domain, the proline-rich region, the microtubule-binding repeat region, and the C-terminus (C-term). The different isoforms (2N4R-0N3R) denote the presence or absence of the alternatively spliced exons in the N-terminal (N) or microtubule-binding repeat (R) domains.

Tau also contains a proline-rich region at residues 151-243 (Figure 1.4) (Kolarova et al., 2012), which is required for both microtubule bundling and the association between tau and microtubules (Kanai et al., 1992). Within the proline-rich domain, there are seven overlapping sequences of PXXP motifs, where P is proline and X is any other amino acid (Figure 1.4). These PXXP motifs, located between residues 176-236 of tau, are highly conserved candidate SH3 binding domains, indicating that tau can associate with proteins containing SH3 domains, such as fyn, phosphatidylinositol 3-kinase, and phospholipase Cγ1 (Cheadle et al., 1994; Sparks et al., 1994; Lee et al., 1998; Reynolds et al., 2008; Usardi et al., 2011).

```
MAEPRQEFEV MEDHAGTYGL GDRKDQGGYT MHQDQEGDTD AGLKESPLQT     50
PTEDGSEEPG SETSDAKSTP TAEDVTAPLV DEGAPGKQAA AQPHTEIPEG    100
TTAEEAGIGD TPSLEDEAAG HVTQARMVSK SKDGTGSDDK KAKGADGKTK    150
IATPRGAAPP GQKGQANATR IPAKTPPAPK TPPSSGEPPK SGDRSGYSSP    200
GSPGTPGSRS RTPSLPTPPT REPKKVAVVR TPPKSPSSAK SRLQTAPVPM    250
PDLKNVKSKI GSTENLKHQP GGGKVQIINK KLDLSNVQSK CGSKDNIKHV    300
PGGGSVQIVY KPVDLSKVTS KCGSLGNIHH KPGGGQVEVK SEKLDFKDRV    350
QSKIGSLDNI THVPGGGNKK IETHKLTFRE NAKAKTDHGA EIVYKSPVVS    400
GDTSPRHLSN VSSTGSIDMV DSPQLATLAD EVSASLAKQG L             441
```

Figure 1.4 Amino acid sequence of 2N4R tau

The amino acid sequence of the longest isoform of tau, 2N4R, is shown. Amino acid numbering is in the right hand column. The proline rich region (residues 151-243) in the N-terminal part of tau is underlined. The seven PXXP motifs are highlighted in yellow.

The C-terminal half of tau contains the microtubule binding domain, which comprises three or four imperfect repeats, dependent on the presence or absence of the alternatively spliced exon 10. In contrast to the acidic nature of the N-terminus, the C-terminus of tau is basic and therefore the terminal ends of tau have opposing net charges (Mandelkow and Mandelkow, 2012). A paperclip model for the structure of tau has been proposed, whereby the N- and C-terminal ends are brought together near the microtubule repeat region (Figure 1.5) (Jeganathan et al., 2006). Interestingly, the repeat domain alone has more propensity to aggregate than full-length tau (Wille et al., 1992). Additionally, two hexapeptide motifs (VQIVYK and VQIINK) in the repeat region of tau from 275-280 and 306-310 residues of tau, respectively, are essential for aggregation of tau, which is observed in AD and other tauopathies (von Bergen et al., 2000; von Bergen et al., 2001).

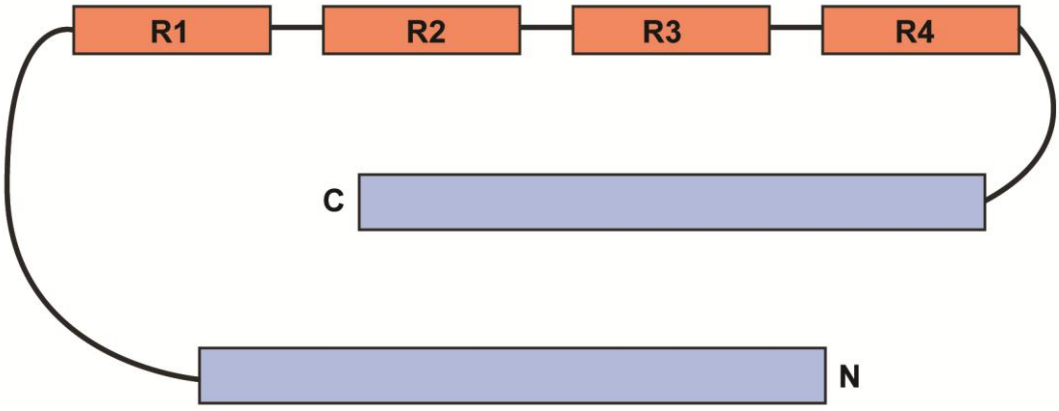

Figure 1.5 The paperclip model of tau

The paperclip model of tau folding has been proposed, whereby the N- and C-terminal ends of tau are brought towards the centre of the repeat domain (R1-4). This folding back of N- and C-terminals is thought to be transient but becomes more stable in pathologically folded tau.

1.5.2 Tau function

The main function of tau protein is to promote the assembly and stabilisation of microtubules (Weingarten et al., 1975; Cleveland et al., 1977; Mitchison and Kirschner, 1984; Drubin and Kirschner, 1986). In cultured neurons, tau binds to the most dynamic microtubules at the distal axon, towards the growth cone (Kempf et al., 1996). Tau knockout mice survive, but they display decreased microtubule number and density in axons as well as decreased microtubule stability in small-calibre axons (Harada et al., 1994). Tau-deficient mice also exhibit some muscle weakness and impaired motor coordination (Ikegami et al., 2000). The lack of a more severe phenotype due to loss of tau-dependent microtubule function appears to be indicative of a compensatory mechanism from other microtubule-associated proteins, particularly microtubule-associated protein 1A (MAP1A) (Harada et al., 1994), raising the possibility that tau may have functions other than microtubule stabilisation. To investigate whether tau was important in neuronal maturation, tau knockout mice were created by replacement of exon 1 with a neomycin expression cassette to disrupt translation of tau protein (Dawson et al., 2001). Neurons from these $tau^{-/-}$ mice exhibited delayed axonal elongation during development, but otherwise the mice were viable and displayed no overt phenotype. There was also increased MAP1A expression in knockout mice at birth but this decreased to comparable levels with WT mice after 12 months, suggesting that although MAPs other than tau may be upregulated to compensate for loss of tau, it is not sufficient to restore the role of tau in axonal extension. The upregulation of MAP1A has also been described in an additional tau knockout mouse line (Fujio et al., 2007).

Tau is also thought to play a role in regulating axonal transport by interfering with dynein and kinesin motility on microtubules, thereby affecting their ability to transport cellular cargoes (Dixit et al., 2008). However, examination of a third tau knockout mouse which produces a fusion protein of the first 31 amino acids of tau fused to enhanced green fluorescent protein (EGFP) and which does not display any overt phenotype when compared to WT mice (Tucker et al., 2001), showed that in this line, the loss of tau did not significantly affect axonal transport rates (Yuan et al., 2008). This is contrast to the findings of Dixit et al. (2008) and suggests that tau does not play a major role in axonal transport *in vivo.* To determine whether these findings are due to developmental defects caused by absence of tau, a conditional knockout mouse where tau expression is suppressed in adulthood could resolve the question of whether tau is required for neuronal function.

In addition to microtubule binding and stabilization, tau can also interact with actin filaments and this was shown *in vitro* and *in vivo* in *Drosophila* brain tissue (Fulga et al., 2007). Purified tau incubated with polymerised actin filaments was shown to increase bundled F-actin in a sedimentation assay, which was abolished by immunodepletion of tau. Upon treatment with an actin-depolymerising drug, actin filaments pre-incubated with tau were more resistant to depolymerisation than in the absence of tau (Fulga et al., 2007). Using electron microscopy, pre-incubation of actin filaments with tau induced actin bundling as observed by closely packed parallel fibres (Fulga et al., 2007). The interaction of tau with actin is thought to be mediated by the microtubule-binding domain and the proline-rich domain (Yu and Rasenick, 2006; He et al., 2009). Although the proline-rich domain binds to actin with a lower affinity than the microtubule binding alone, this study demonstrates that multiple domains can promote actin bundling (He et al., 2009).

Tau has also been detected in the nucleus in both neuronal cells and human brain tissue (Loomis et al., 1990; Wang et al., 1993; Brady et al., 1995; Liu and Götz, 2013), thereby suggesting a role for tau involving DNA interactions. Moreover, tau protein can form complexes with DNA *in vitro*, and heat stress was able to induce DNA damage in tau knockout neurons but not in WT neurons, indicating that tau has a neuroprotective role in maintaining DNA integrity (Sjöberg et al., 2006; Wei et al., 2008; Sultan et al., 2011). Indeed, overexpression of tau in tau knockout neurons rescued heat-induced DNA damage (Sultan et al., 2011). Studies focusing on the functions of nuclear tau are sparse, but evidence appears to suggest that the proline-rich domain of tau has more propensity to interact with DNA (Wei et al., 2008). Interestingly, rod-like tau deposits in the nucleus were recently reported in the brains of individuals with Huntington's disease and AD but rarely in control brain (Fernandez-Nogales et al., 2014). Moreover, neuroblastoma cells expressing truncated 4R tau (151-391) displayed nuclear localisation of transfected tau, in contrast to endogenous and full-length 2N4R tau which were predominantly localised to the cytoplasm (Paholikova et al.). As the tau protein encoded by this exogenously expressed tau included the proline-rich domain and the microtubule-binding domain, but excluded the N-terminus, this study suggests that the N-terminus of tau is not required for nuclear localisation.

In recent years, there has been a concentration of studies investigating the function of dendritic tau. Tau localisation at the dendritic spine and at synapses has been demonstrated in WT mice, and dendritic tau can co-immunoprecipitate with PSD-95 (postsynaptic density 95), a postsynaptic scaffolding protein (Ittner et al., 2010; Mondragon-Rodriguez et al., 2012; Frandemiche et al., 2014; Kimura et al., 2014). Thus the presence of tau at the synapse under normal, non-pathogenic conditions

indicates that there may be a physiological role of tau in synaptic function. Tau knockout mice show mislocalisation of the dendritic protein fyn to the neuronal cell body, and reduction of N-methyl-D-aspartate (NMDA) receptor stabilization (Ittner et al., 2010). NMDA receptor-induced long-term depression (LTD) results in a transient increase of tau phosphorylation at several epitopes (S199, S202, T205, T231, S235, S396, S404) without increasing total levels of tau (Mondragon-Rodriguez et al., 2012). Induction of long-term potentiation (LTP) and NMDA receptor activation also induced translocation of tau, PSD-95, fyn, and actin into the postsynaptic density fraction of cultured neurons, suggesting that tau is important in synaptic remodelling following synaptic plasticity (Frandemiche et al., 2014). Stabilisation of actin with an actin-polymerising compound also resulted in tau translocation to dendritic spines, indicating that tau can respond to actin-dependent spine remodelling (Frandemiche et al., 2014). In another study, tau was demonstrated to be required for LTD induction in the hippocampus, and LTD also caused phosphorylation at S396/S404 of tau (Kimura et al., 2014). Taken together, these data provide evidence for the hypothesis that tau plays an important role at the synapse.

Increasing evidence supports the idea that tau may also act as a signalling molecule. Several signalling molecules have been reported to interact with tau, including src family tyrosine kinases, phospholipase C γ, phosphatidylinositol 3-kinase, Grb2, histone deacetylase 6, and 14-3-3 (Jenkins and Johnson, 1998; Agarwal-Mawal et al., 2003; Reynolds et al., 2008; Perez et al., 2009; Usardi et al., 2011). More specifically, tau has been found to bind to and target the non-receptor-associated tyrosine kinase fyn to the postsynaptic site to act as a protein scaffold in dendrites (Ittner et al., 2010). In oligodendrocytes, tau binds to fyn and promotes outgrowth of oligodendrocytes by tethering tau to microtubules (Klein et al., 2002). In cultured cells, tau facilitates src-mediated actin remodelling induced by growth factor stimulation (Sharma et al., 2007). Whilst the function of membrane-associated tau remains to be fully elucidated, the presence of tau at the neuronal membrane supports the growing evidence for the involvement of tau as a signalling molecule at this site (Brandt et al., 1995; Maas et al., 2000; Reynolds et al., 2008; Pooler et al., 2012).

1.5.3 Tau phosphorylation and function in health and in neurodegenerative disease

Phosphorylation is the most common post-translational modification of tau, and abnormal phosphorylation of tau is observed in many tauopathies, including AD. There

are 85 serine, threonine, and tyrosine residues along the tau protein sequence, and approximately 19% of these sites are phosphorylated in normal brain, increasing to more than 50% in AD brain (Figure 1.6)(Hanger and Noble, 2011; Noble et al., 2013). Many of these phosphorylatable residues are clustered in the proline-rich domain of tau and phosphorylation at these sites is likely to play a role in modulating structure and/or tau function.

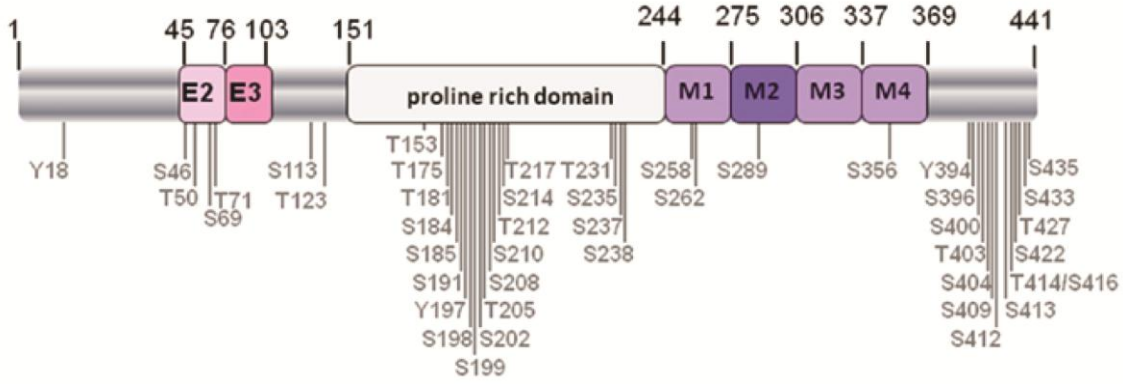

Figure 1.6 Phosphorylation sites on tau

Schematic of the longest isoform of tau and the relative positions of the phosphorylation sites on tau in Alzheimer brain. There are 85 serine, threonine, and tyrosine residues of tau which can be phosphorylated by kinases and are clustered around the proline-rich domain and the regions surrounding the microtubule binding domain. Image from Noble et al. (2013).

There is substantial evidence that phosphorylation of tau in and around the C-terminal repeat region can influence its ability to bind to microtubules. Overexpression of microtubule affinity-regulating kinase (MARK), a kinase which phosphorylates tau at KXGS motifs including S262, S324 and S356 in microtubule-binding repeats 1, 3 and 4 in tau, results in its detachment from microtubules and decreased microtubule stability (Drewes et al., 1997). Additionally, phosphorylation at these sites is protective against tau aggregation into paired helical filaments (Schneider et al., 1999). Phosphorylation at S214 also leads to the dissolution of tau binding to microtubules *in vitro* (Illenberger et al., 1998). Furthermore, phosphorylation of tau at T231 by glycogen synthase kinase-3β (GSK-3β) also decreases the association between tau and microtubules (Cho and Johnson, 2003). In contrast, tau phosphorylated at T231 can bind to prolyl isomerase Pin1, which restores its ability to bind to microtubules, illustrating the complex nature of the coupling of tau phosphorylation and function (Lu et al., 1999).

As tau phosphorylation is a key regulator of its interaction with microtubules, tau phosphorylation can also affect axonal transport of cellular cargoes. In transgenic mice

expressing the tau mutation K369I, which is causative for frontotemporal dementia, hyperphosphorylated tau has impaired interaction with c-Jun N-terminal kinase-interacting protein 1 (JIP1) (Ittner et al., 2009). This leads to the translocation of JIP1 from the axon to the cell body, which impedes the ability of JIP1 to mediate binding of cargoes to kinesin, thereby altering axonal transport (Ittner et al., 2009). Mitochondrial transport also appears to be regulated by tau phosphorylation. Phosphorylation of tau at S199, S202, and S205 by mutating each serine to aspartic acid in order to mimic phosphorylation, reduced the movement of mitochondria in neurite processes in PC12 cells as well as in axons of primary cortical neurons (Shahpasand et al., 2012). The phosphorylation of tau can also modulate tau transport along microtubules. Inhibition of GSK-3, a tau kinase, reduces tau phosphorylation. GSK-3 inhibition in primary rat cortical neurons expressing tau fused to EGFP reduced the rate of axonal tau transport (Cuchillo-Ibanez et al., 2008). Expression of pseudophosphorylated tau at 18 or 27 sites by substituting serine/threonine residues with glutamic acid significantly increased the rate of axonal tau transport, which was not due to differences in tau concentration (Cuchillo-Ibanez et al., 2008). In contrast, expression of a non-phosphorylatable tau mutant where 18 serine/threonine residues were mutated to alanine decreased the rate of tau transport (Cuchillo-Ibanez et al., 2008). This is thought to be mediated by the interaction between tau and kinesin-1, which is facilitated by GSK-3-induced phosphorylation of tau (Cuchillo-Ibanez et al., 2008).

The structure of tau is also tightly linked to its phosphorylation state, as evidenced by studies showing that tau phosphorylation precedes its aggregation. *In vitro* experiments with pseudophosphorylated tau at S396/S404 by mutation of serine to glutamic acid show that phosphorylation at these sites significantly potentiates rates of tau assembly into filaments (Abraha et al., 2000). Pseudophosphorylation at other residues in the C-terminal region of tau also resulted in enhanced propensity to aggregate into fibrils, whereas phosphorylation of N-terminal residues did not alter the self-aggregation of tau (Haase et al., 2004). These studies show that phosphorylation of tau differentially regulates its structure, dependent on the phosphorylated residue(s).

In pathological conditions, evidence suggests that aggregation of tau is preceded by its phosphorylation. Phosphorylated tau isolated from AD brain self-assembles into paired helical filaments (PHFs), and *in vitro* phosphorylation of recombinant tau was sufficient to induce self-assembly into PHFs (Alonso et al., 2001). Moreover, it has been shown in transgenic mouse models of tauopathy that increased tau phosphorylation occurs prior to the onset of tau PHFs (Sahara et al., 2002; Andorfer et al., 2003; Oddo et al., 2007; Delobel et al., 2008; Mastrangelo and Bowers, 2008). Likewise, lithium-mediated inhibition of GSK-3, a tau kinase, was able to decrease tau phosphorylation at specific

epitopes and reduce tau aggregation in a mouse model of tauopathy (Noble et al., 2005). These data imply that tau phosphorylation may play a role in the formation of tau aggregates under pathological conditions.

The subcellular localisation of tau may also be regulated by phosphorylation. For instance, membrane-associated tau is dephosphorylated at epitopes that are typically abnormally phosphorylated in AD (Arrasate et al., 2000; Maas et al., 2000; Pooler et al., 2012), whereas cytosolic tau contains a mixture of both dephosphorylated and phosphorylated tau. Furthermore, phosphomimetics of tau where residues at the N-terminal half of tau were mutated to mimic phosphorylation, were shown to result in a reduction in the amount of tau associated with the plasma membrane. However, mimicking phosphorylation of residues in the C-terminal half of tau by amino acid substitutions did not affect the proportion of membrane-associated tau (Pooler et al., 2012). The data agree with a previous report showing that pseudophosphorylation of tau at sites affected by AD, which are primarily in the C-terminal half of tau, reduces the binding of tau with the membrane in PC12 cells (Maas et al., 2000). Furthermore, phosphorylation of tau at tyrosine residues by pervanadate, which inhibits the activity of protein tyrosine phosphatases, also increases the association of tau with neuronal detergent-resistant membranes, or lipid rafts (Usardi et al., 2011). The interaction of tau with plasma membranes and lipid rafts is regulated by the presence of fyn, and the phosphorylation status of tau has also been shown to alter its binding with fyn (Usardi et al., 2011; Pooler et al., 2012). This suggests that tau phosphorylation at serine, threonine and tyrosine residues can regulate the association of tau with the plasma membrane, and its interactions with membrane-associated proteins, which could have further downstream effects on tau function.

Recent findings suggest that extracellular tau may also play a role in both health and disease, but it remains to be seen whether phosphorylation may alter the function of extracellular tau. Similar to intracellular membrane-associated tau, extracellular tau secreted from primary neurons and non-neuronal cells is dephosphorylated at epitopes typically associated with AD (Plouffe et al., 2012; Pooler et al., 2013a). It is unclear whether the phosphorylation status of intracellular tau is directly related to that of extracellular tau. However, there is some evidence that phosphorylation of intracellular tau can affect the process of tau release. In HeLa cells overexpressing a construct of human tau mutated to mimic phosphorylation at 12 sites, tau release was significantly increased compared to cells expressing WT tau (Plouffe et al., 2012). In contrast, neuroblastoma cells overexpressing tau containing mutations associated with frontotemporal dementia secrete significantly less tau when compared to cells expressing WT tau (Karch et al., 2012). Additionally, these authors also reported that

extracellular tau from neuroblastoma cells expressing human tau is phosphorylated at T181 (Karch et al., 2012). These studies indicate that phosphorylation of tau may modulate neuronal tau release, which could have an effect on the spread of tau pathology or other undiscovered roles of extracellular tau in cell-cell signalling.

1.5.4 Tau toxicity and propagation

Spreading of protein aggregates found in neurodegenerative disorders is a common mechanism, as evidenced by studies of α-synuclein in Parkinson's disease, and superoxide dismutase-1 in motor neuron disease (Spillantini et al., 1998a; Desplats et al., 2009; Münch et al., 2011). However, the mechanisms underlying the spread and uptake of tau from one brain region to another remains to be fully elucidated. This spread of pathological tau is termed "prion-like" propagation, since the propagation of pathology could involve the transfer of toxic proteins between cells that induce self-assembly when taken up by neighbouring cells, despite not being infectious.

In AD, the spread of tau pathology follows a specific, pre-defined characteristic pattern (as described above) that is defined by Braak staging from stage I to VI, which indicates the progression of disease. To provide an explanation for this spread of pathology, several studies support the hypothesis that tau pathology spreads via a trans-synaptic mechanism, whereby neuronal connectivity, not proximity, is the key determinant of the spatial localisation of pathology.

In vitro studies have shown that extracellular, exogenous tau aggregates can be taken up by neurons to induce oligomerisation of intracellular tau, which can then be released and transferred to adjacent or synaptically connected neurons (Frost et al., 2009; Guo and Lee, 2011; Kfoury et al., 2012; Wu et al., 2013). These studies indicate that tau pathology may be seeded by an initial event that causes the oligomerisation of tau, following which tau seeds may be released and this extracellular tau taken up by connected neurons. Such a mechanism provides a template through which further tau oligomerisation is induced in the recipient neurons, enabling the spread of tau pathology.

Recently, a series of studies carried out by independent groups has provided substantial evidence that tau pathology spreads throughout the brain *in vivo*. In one study, the authors took brain extract from transgenic mice which express mutant P301S tau, an FTD-causing mutation, and injected these extracts into mice overexpressing WT human tau (Clavaguera et al., 2009). The recipient mice would not normally

develop tau aggregates, but injection of the P301S brain extract induced the formation of tau filaments, and these were confirmed to be of both human and murine origin (Clavaguera et al., 2009). Several months after injection, tau pathology was not confined to the injection site, but had spread to neighbouring brain regions that were anatomically connected. The spread of tau pathology could not be explained by diffusion of the brain extract alone as a result of the extensive distance from the injection site.

In other studies, a model of tau transmission was created by generating a transgenic mouse where expression of mutant P301L tau was limited to layer II neurons of the medial entorhinal cortex, where tau pathology is first observed. As these mice aged, tau pathology was first observed only in the entorhinal cortex, and over time, the pathology spread to interconnected hippocampal regions, indicative of a trans-synaptic spread of tau (de Calignon et al., 2012; Harris et al., 2012; Liu et al., 2012). The lack of significant amounts of human tau mRNA in neurons that had taken up mutant tau showed that the source of the spreading tau pathology was the mutant tau originally expressed in the entorhinal cortex. Interestingly, the recipient transgenic mice did not display cognitive defects or neurodegeneration (Clavaguera et al., 2009; Harris et al., 2012), suggesting that the supposedly pathological tau species that propagates throughout the brain may not be toxic. Instead, there may be another, possibly soluble and/or oligomeric, tau species that could be responsible for neurotoxicity following the transmission of aggregated tau species.

Until recently, the toxic species of tau was thought to be the mature neurofibrillary tangles, but recent studies have shown that it is likely that soluble phosphorylated forms of tau are toxic to neurons. For instance, synapse loss and impaired synaptic function occurs in transgenic mice expressing mutant P301S tau, and this occurs several months before neurofibrillary tangles are detectable (Yoshiyama et al., 2007). Interestingly, in the rTg4510 inducible mouse model of tauopathy expressing mutant P301L tau, turning off the tau transgene resulted in recovery of memory impairment and prevented further loss of neurons, despite continued accumulation of neurofibrillary tangles (SantaCruz et al., 2005). Synapse loss in rTg4510 mice also precedes significant neurofibrillary tangle accumulation in regions of synaptic loss (Kopeikina et al., 2013). Moreover, injection of synthetic tau oligomers into WT mice, but not monomers or fibrils, results in impaired memory, loss of synapses, and mitochondrial dysfunction at the area of injection (Lasagna-Reeves et al., 2011). Furthermore, the visual response function of tangle-bearing neurons from rTg4510 mice is not impaired when compared to neighbouring neurons that do not contain tangles (Kuchibhotla et

al., 2014). These studies strongly suggest that soluble, oligomeric species of tau are responsible for neurotoxicity.

1.5.5 Kinases and phosphatases of tau

Several candidate kinases that phosphorylate tau have been identified, including GSK-3, cyclin-dependent kinase-5 (cdk5), cyclic AMP-dependent protein kinase (PKA), casein kinase 1 (CK1), prostate-derived sterile 20-like kinases, as well as several members of the mitogen-activated protein kinase family (Noble et al., 2013; Tavares et al., 2013). In addition, the five tyrosine residues on tau can be phosphorylated by tyrosine kinases including Lck, c-src, Syk, c-Abl, and fyn (Lee et al., 1998; Derkinderen et al., 2005; Reynolds et al., 2008). These kinases can be split into three classifications: proline-directed kinases, non-proline-directed kinases, and tyrosine kinases. There are also several phosphatases that dephosphorylate tau, including protein phosphatase (PP) 1, PP2A, and PP5 (Liu et al., 2005). These kinases and phosphatases work in concert to regulate tau phosphorylation, and it is believed that abnormal phosphorylation of tau in pathological conditions stems from an imbalance of kinase and phosphatase activity.

Phosphorylation of tau is negatively regulated by phosphatase activity. PP1, PP2A, PP2B, and PP5 dephosphorylate tau at overlapping sites (S202, T205, T212, S214, S235, S262, S396, S404, S409) *in vitro*, but have some specificity for other serine/threonine residues (Liu et al., 2005).Total PP activity in AD brain is reduced by approximately 50% compared to control brain tissue, with PP2A accounting for the majority of the phosphatase activity (Liu et al., 2005). PP2A has also been shown to dephosphorylate tau through regulation of other tau kinases, such as GSK-3 (Qian et al., 2010).

GSK-3 has two isoforms, GSK-3α and GSK-3β. GSK-3β (also known as TPK1, tau protein kinase I (Ishiguro et al., 1993)) is thought to be a key kinase of tau, and has been shown to phosphorylate tau at multiple sites *in vitro* and *in vivo* that are abnormally phosphorylated in AD (Hanger et al., 1992; Ishiguro et al., 1992; Lovestone et al., 1994; Zheng-Fischhöfer et al., 1998). GSK-3β-mediated phosphorylation of tau results in altered tau-microtubule binding and microtubule rearrangement (Wagner et al., 1996), and overexpression of GSK-3β in mouse models causes abnormal phosphorylation of tau and mislocalisation of tau from the axon to the somatodendritic area (Lucas et al., 2001). Lithium chloride, a non-specific inhibitor of GSK-3, has been shown to decrease tau phosphorylation at GSK-3β sites in mice expressing P301L

mutant tau as well as reducing insoluble tau aggregates and ameliorate axonal degeneration (Noble et al., 2005), supporting the role of GSK-3β in mediating tau-dependent neurodegeneration. A specific inhibitor of GSK-3, AR-A014418, also reduced the amount of insoluble tau in P301L mice, further supporting this conclusion (Noble et al., 2005).

Cdk5 is another major kinase of tau (Baumann et al., 1993). Cdk5 activity is regulated by interaction with its activator proteins p25, p35, and p39 (Noble et al., 2003) and multiple studies have shown the relevance of cdk5 phosphorylation of tau at disease-related epitopes (Michel et al., 1998; Patrick et al., 1999; Liu et al., 2002). Similar to GSK-3β, overexpression of cdk5 in mice results in abnormally phosphorylated tau and accumulation of tau pathology (Bian et al., 2002). When mice with elevated cdk5 activity were crossed with mice expressing mutant tau, the double transgenic mice displayed increased tau hyperphosphorylation and exacerbated the progression of pathology (Noble et al., 2003). Additionally, the activity of GSK-3 was elevated in double transgenic mice, suggesting that GSK-3 and cdk5 may act in concert to promote abnormally phosphorylated aggregates of tau (Noble et al., 2003). A subsequent study further examined the relationship between GSK-3 and cdk5 on tau phosphorylation. Aged transgenic mice overexpressing p25 led to an over-activation of cdk5, resulting in elevated tau phosphorylation at several epitopes normally found in AD brain, whereas young mice did not exhibit the increased phosphorylation (Plattner et al., 2006). This discrepancy may be explained by differential regulation of GSK-3β by cdk5. Activity of GSK-3β was decreased in young transgenic mice with elevated cdk5 activity, but this was reversed and activity was increased in aged mice. This difference in activity was proposed to be a result of inhibitory cross-talk between GSK-3β and cdk5, whereby cdk5 acts on protein phosphatase 1 and protein phosphatase 2A to regulate GSK-3β, thereby affecting tau phosphorylation (Plattner et al., 2006).

Of the tyrosine kinases that phosphorylate tau, fyn increases tyrosine phosphorylation of tau *in vitro*, and subsequent experiments revealed that fyn phosphorylates residue Y18 of tau (Lee et al., 1998; Lee et al., 2004). Phosphorylation of tau at Y18 by fyn did not have a significant effect on microtubule binding, but tau phosphorylated at Y18 has been found in AD brain tissue, and insoluble tau fibrils from AD brain contain tau phosphorylated at Y18, suggesting the relevance of this site in pathogenic conditions (Lee et al., 2004). The interaction of the SH2, but not SH3 domain of fyn with tau is increased following phosphorylation of tau at Y18 (Usardi et al., 2011), and this was shown to be important for the localisation of tau to membrane microdomains. There is also evidence suggesting that fyn-mediated phosphorylation of tau may be protective against filament-induced inhibition of fast axonal transport (Kanaan et al., 2013).

1.6 Fyn

1.6.1 Fyn structure and regulation of kinase activity

Fyn kinase is a member of the src family of non-receptor-associated tyrosine kinases. Since the discovery of the initial src kinase, nine src family kinases have been identified, which are src, lck, hck, blk, lyn, fgf, yes, yrk, and fyn. All src family kinases share similar sequence homology and contain four distinct Src homology (SH) domains (SH1-SH4; Figure 1.7) (Boggon and Eck, 2004). The SH1 (kinase) domain is located in the C-terminus of src. This region is responsible for catalytic activity, which is regulated by tyrosine autophosphorylation at tyrosine residue Y420 which will be discussed further in this section. The SH2 domain contains a phosphotyrosyl recognition pocket alongside another pocket that binds hydrophobic residues adjacent to the phosphotyrosine, and hence recognises phosphotyrosine residues on interacting proteins with a preference for the motif pY-E-E-I (Boggon and Eck, 2004). The SH3 domain recognises PXXP motifs in interacting proteins, such as those found in the proline-rich region of tau, which form a polyproline type II helix when bound to the SH3 domain. The SH4 domain is located at the N-terminus and this region targets the protein to the membrane via lipid modification. This region is always myristoylated and sometimes palmitoylated at the consensus sequence M-G-C at the N-terminus which promotes anchoring of the kinase to the plasma membrane (Hof and Resh, 1997; Liang et al., 2004). Each src family kinase has a unique domain located between the SH4 and SH3 domains at the N-terminus of the protein which distinguishes them from other src family kinases.

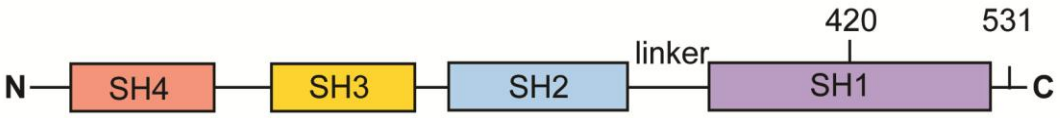

Figure 1.7 Structure of fyn kinase.

Schematic diagram of full-length fyn kinase. Fyn shares sequence and structural homology with other src family kinases, which all contain four SH domains. At the N-terminus is the SH4 domain (orange), which is also called the unique domain as its protein sequence distinguishes it from other kinases in the family. This is followed by the SH3 domain (yellow), which is important for interactions with PXXP motifs on binding partners. The SH2 domain (blue) recognises phosphotyrosine residues, and the SH1 domain at the C-terminus (purple) plays a role in catalytic activation of the kinase.

Alternative splicing of fyn results in three isoforms. Inclusion of exon 7B results in the generation of the isoform Fyn-B (referred to here as fyn), which is expressed ubiquitously but expression of which is highest in the brain (Cooke and Perlmutter, 1989; Resh, 1998). Isoform 2 (fyn-T) is expressed in hematopoietic cells, particularly T-cells (Resh, 1998). Fyn-T has a role in cell growth and proliferation, platelet activation, T- & B-cell receptor signalling, and axon guidance (Saito et al., 2010). Isoform 3 (FynΔ7) is less well characterised. It lacks exon 7 of full-length fyn and is expressed in hematopoietic cells, although other cell types have not been fully characterised (Goldsmith et al., 2002). In the brain, fyn expression has been demonstrated in the olfactory bulb, cortex, hippocampus, thalamus, and cerebellum, and it has been shown that fyn is expressed from embryonic day 8.5 to adulthood in mice (Yagi, 1999).

The kinase activity of fyn is regulated by tyrosine phosphorylation. Phosphorylation of tyrosine residue Y420 up-regulates, and Y531 down-regulates, the kinase activity of fyn, such that these two phosphorylation sites work in concert to regulate fyn activity. Upstream targets of fyn include C-terminal src kinase (Csk), which phosphorylates Y531 of src family kinases, resulting in kinase inactivation (Nada et al., 1991; Nada et al., 1993). This leads to a conformational change in fyn so that the SH2 domain binds to the C-terminal tail, and the SH3 domain binds to the linker located between the SH2 and the SH1 domain (Figure 1.8) (Superti-Furga et al., 1993; Sun et al., 1998). Knockouts of Csk result in embryonic lethality, in conjunction with increased src family kinase activity, demonstrating the importance of Csk as a regulator of members of src family kinases (Engen et al., 2008).

Activation of fyn is also regulated by receptor protein tyrosine phosphatase-α (RPTPα), which dephosphorylates Y531 (Bhandari et al., 1998; Sala and Sheng, 1999). This leads to a conformational change to the active conformation, resulting in autophosphorylation of fyn at Y420 and uncoupling of the SH2 domain to the C-terminal tail. Signalling transduction of the prion protein (PrP) has also been shown to act upstream of fyn. In 2000, it was first demonstrated that PrP can activate fyn by signalling via calveolin-1 (Mouillet-Richard et al., 2000), and subsequently this was also shown to be mediated by neural cell adhesion molecule (Santuccione et al., 2005). PrP knockout mice do not display an age-dependent increase in fyn expression when compared to WT mice (Schmitz et al., 2014), and the amount of active fyn was reduced in PrP knockout mice compared to WT (Santuccione et al., 2005). In contrast, Y420 of fyn is dephosphorylated by striatal enriched phosphatase 61 (STEP61), which results in kinase inactivation (Nguyen et al., 2002).

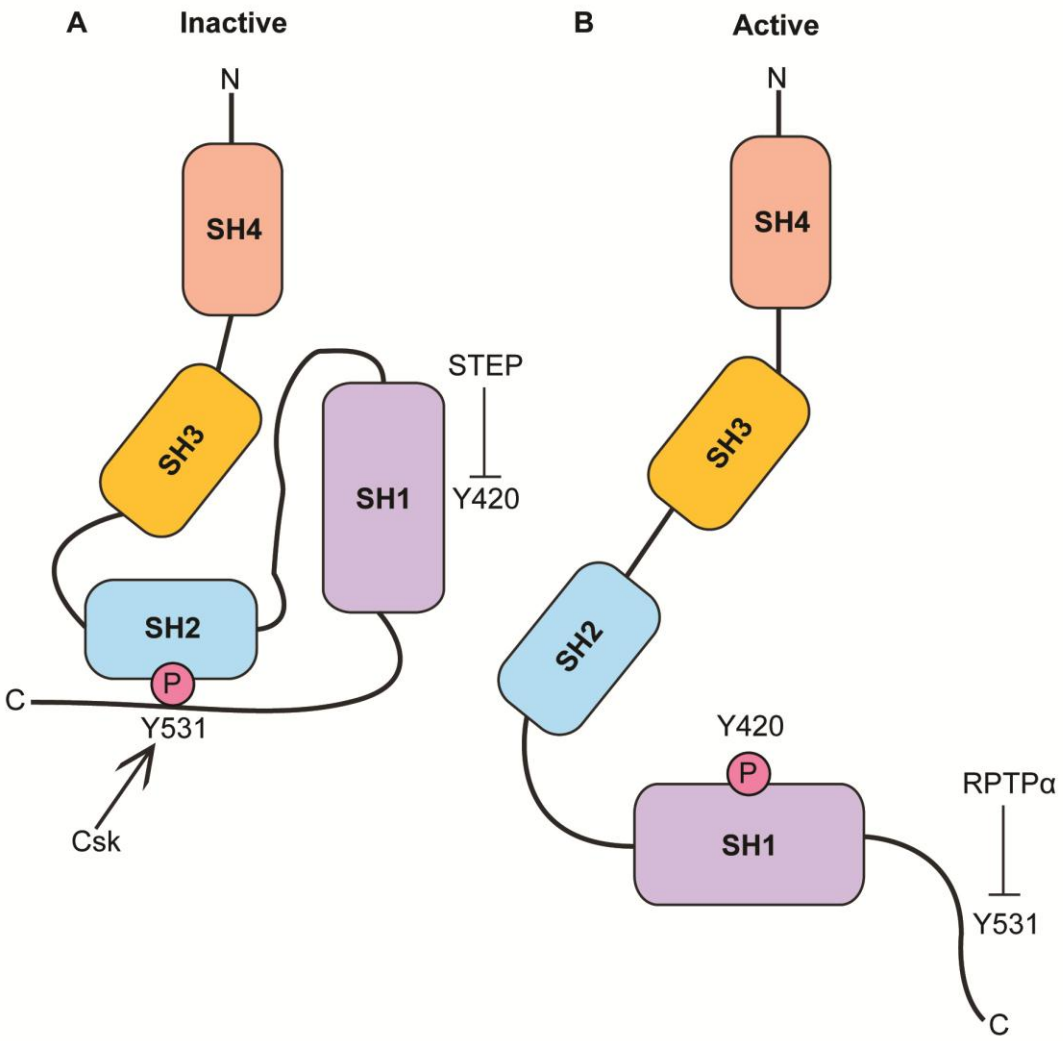

Figure 1.8 Active and inactive conformations of fyn

(A) In the inactive conformation of fyn, Y531 is phosphorylated allowing for binding of the SH2 domain to the C-terminal tail, while the SH3 domain binds the linker segment between the SH1 and SH2 domains. Inactivity of fyn is regulated by Csk-mediated phosphorylation of fyn at Y531, and STEP dephosphorylation of fyn at Y420. (B) When fyn is in the active conformation, Y531 is dephosphorylated by protein tyrosine phosphatases such as RPTPα, leading to autophosphorylation of Y420. This results in a conformational change so that SH2 is unbound from the C-terminal tail.

1.6.2 Function of fyn

Several substrates of fyn have been identified, including focal adhesion kinase (FAK) and the γ-aminobutyric $(GABA)_A$ receptor γ2 subunit. Reduction of fyn expression in transgenic mice led to reduced phosphorylation and decreased kinase activity of FAK (Grant et al., 1995). Moreover, fyn phosphorylation of the $GABA_A$ receptor γ2 subunit in the hippocampus supports a role for fyn in synaptic function (Jurd et al., 2010).

Fyn has also been shown to phosphorylate some important tau kinases. For example, fyn phosphorylates cdk5 at the Y15 residue, thus regulating cdk5 kinase activity in semaphorin-mediated neuronal guidance (Sasaki et al., 2002). In another study, fyn was also shown to phosphorylate GSK3-β. Neuroblastoma cells treated with insulin displayed a transient activation of GSK-3β and concomitant tau phosphorylation. Fyn was shown to phosphorylate GSK-3β *in vitro*, which was further increased by insulin stimulation (Lesort et al., 1999). Tau itself is a known fyn substrate. Fyn phosphorylates tau at Y18 (Lee et al., 2004) and it was recently shown that fyn is necessary for phosphorylation-dependent trafficking of tau to the membrane (Pooler et al., 2012). It is clear that a multitude of signalling pathways converge on fyn which can then act on several targets, which involve either targeting to the membrane or activation of signalling pathways.

In the brain, fyn is involved in neuronal growth and oligodendrocyte maturation (Sperber et al., 2001; Krämer-Albers and White, 2011). Mice lacking fyn protein are hypomyelinated, and mice expressing a kinase-dead mutant of fyn also show defects in myelination (Umemori et al., 1994; Sperber et al., 2001). In oligodendrocytes, fyn has been shown to interact with tau to promote process outgrowth (Klein et al., 2002), suggesting that this interaction is important for myelination. In addition, fyn and APP co-localise and interact in the somatodendritic area of neurons. Targeting of APP and the adaptor protein Disabled1 (Dab1) to lipid rafts is dependent on fyn in mice (Hoe et al., 2008; Minami et al., 2011). Cell surface expression of ephrin-A receptors is also dependent on fyn kinase activity which, in contrast to APP, negatively modulates expression (Baba et al., 2009).

The NMDA receptor is also a substrate of fyn, whereby the Y1472 of the NR2b subunit is the major phosphorylation site for fyn, and phosphorylation of this site facilitates synaptic plasticity (Suzuki and Okamuranoji, 1995; Nakazawa et al., 2001). Indeed, transgenic mice expressing constitutively active fyn exhibit significantly increased phosphorylation of NR2b at Y1472 (Kojima et al., 1998; Xia and Gotz, 2014). Several studies have demonstrated that fyn plays an important role in synaptic function by

associating with NMDA receptors to increase receptor stabilisation and activity. NMDA receptors are important for long-term potentiation and synaptic plasticity, and are involved in learning and memory. Co-expression of an active mutant form of fyn (Y531F) with NR2a subunit of the NMDA receptor in 293T cells resulted in increased tyrosine-phosphorylated NR2a (Tezuka et al., 1999). This was further compounded in the presence of PSD-95 (postsynaptic density 95), which was necessary for the formation of a complex involving PSD-95, NR2a, and fyn (Tezuka et al., 1999). The association of PSD-95 with fyn is mediated through its SH2 domain (Tezuka et al., 1999). Fyn is required for the dopamine D1 receptor-stimulated cell surface expression of NR2b-containing receptors (Dunah et al., 2004). Additionally, fyn can also bind to PSD-93, which is also a binding partner of NMDA receptors (Sato et al., 2008). In a more recent study, Ittner and colleagues (2010) showed that the phosphorylation of NR2b at Y1472 was significantly decreased when fyn is unable to be targeted to the postsynaptic density by tau. Mislocalised fyn was unable to bind to PSD-95, consequently de-stabilising the association between PSD-95 and NR2b. The sequestration of fyn in the cell body also conferred protection from pentylenetetrazole-induced seizures, suggesting that the presence of fyn at the PSD contributes to excitotoxic signalling through NMDA receptors (Ittner et al., 2010). Taken together, these data show that fyn stabilises the interaction between NR2b and PSD95, which in turn strengthens synaptic signalling.

Depletion of fyn in mice results in impaired spatial learning and long-term potentiation (LTP), and introduction of a fyn transgene rescued the impairment of LTP (Grant et al., 1992; Kojima et al., 1997). Interestingly, levels of src were increased in fyn knockout mice, suggesting that there may be compensatory mechanisms by other src family kinases which is not sufficient to rescue synaptic impairment (Kojima et al., 1997). In the cortex and hippocampus, there is an age-dependent decrease in dendritic spine density in fyn knockout mice (Babus et al., 2011). On the other hand, mice expressing a constitutively active form of fyn exhibit persistent tremor and increased hyperactivity when pups are separated from the rest of the litter (Xia and Gotz, 2014). Overexpression of active fyn in transgenic mice are also more susceptible to penthylenetetrazole-induced seizures (Kojima et al., 1998), suggesting that increases in fyn kinase activity can induce anxiety and hyperactivity.

Fyn can be both myristoylated and palmitoylated, and these modifications target fyn to the plasma membrane (Hof and Resh, 1997). In primary neurons, fyn was found to localise to lipid rafts, specialised membrane microdomains thought to play an important role in cell signalling (Pereira and Chao, 2007; Usardi et al., 2011). Subcellular fractionation of brain tissue also revealed the presence of fyn in synaptosomes,

predominantly the PSD fraction, although a smaller fraction was localised to the non-PSD fraction (Um et al., 2012). In hippocampal neurons, a small proportion of fyn can be seen in the cell body but it is predominantly localised to the dendrite (Ittner et al., 2010), and fyn was also observed at dendritic spines from human AD brain (Larson et al., 2012). Fyn is also required for the dynamic trafficking of tau between the membrane and cytoplasm (Pooler et al., 2012). In addition, the phosphorylation state of neuronal tau regulates its localisation suggesting that roles of tau, distinct from its microtubule-binding functions, are influenced by its phosphorylation and the presence of fyn (Pooler et al., 2012). Taken together, there is substantial evidence supporting the localisation of fyn to lipid rafts at dendrites, consistent with its role in synaptic function and membrane trafficking.

1.6.3 Potential involvement of fyn in Alzheimer's disease pathogenesis

The first evidence suggesting a role for fyn in the pathogenesis of AD came from studies of human post-mortem brain tissue. Fyn expression is increased in a subset of neurons from human AD brain; these neurons are also immunoreactive for abnormally phosphorylated tau, suggesting a possible association between tyrosine kinases and serine/threonine phosphorylation of tau in AD (Shirazi and Wood, 1993). In AD brain tissue, fyn was increased in the insoluble fraction but reduced in the soluble fraction, indicating that fyn may be sequestered into insoluble aggregates with progression of disease (Ho et al., 2005). Immunocytochemistry also revealed that fyn was decreased at synapses and mislocalised to the neuronal cell body in AD, where it co-localised with tau-containing tangles (Ho et al., 2005). Additionally, the decrease of soluble fyn displayed a significant correlation with the cognitive decline seen in AD patients (Ho et al., 2005). More recently, fyn activity was found to be increased in AD brains (Larson et al., 2012).

Transgenic mice overexpressing mutant APP exhibit reduced synaptophysin-positive presynaptic terminals compared to WT mice, but this is exacerbated when crossed with mice overexpressing fyn (Chin et al., 2004), implying that fyn can increase Aβ-induced synaptotoxicity. The double APP/fyn transgenic mice are able to learn the location of the platform in the Morris water maze test, but 24 hours after training they perform poorly in the maze and spend significantly less time in the target quadrant when compared to single APP or fyn transgenic mice (Chin et al., 2005). Thus the addition of fyn results in worsened memory deficits in an APP mouse model. Interestingly, the authors found that while total fyn expression was increased in the double transgenic

mice, fyn kinase activity was reduced compared to single transgenic fyn mice (Chin et al., 2005). In accordance with reduced fyn activity, STEP, which dephosphorylates fyn at Y420 and therefore inactivates fyn, was increased in double transgenic mice (Chin et al., 2005). Thus the exacerbation of Aβ-induced synaptic impairments may be due to a temporal difference in the elevation of fyn and STEP activity.

Behavioural studies also demonstrate that the synergistic effects of Aβ and fyn on exacerbating cognitive impairment in mouse models of AD that over-produce Aβ are dependent on the presence of tau (Roberson et al., 2011). It has been shown in multiple studies that fyn can mediate Aβ toxicity. In cell culture, fyn deficiency confers neuroprotection from Aβ toxicity and synaptotoxicity (Lambert et al., 1998; Williamson et al., 2008). In addition, elevation of Aβ results in activation of fyn, an increase in tyrosine phosphorylated tau, and re-distribution of fyn and tau in neurons (Williamson et al., 2002; Williamson et al., 2008; Um et al., 2012).

The interaction of tau and fyn has been under considerable scrutiny due to their synergistic roles in mediating Aβ neurotoxicity. Fyn phosphorylates tau at Y18, which is an epitope that is hyperphosphorylated in AD and is present in neurofibrillary tangles (Lee et al., 2004). In 2005, Bhaskar et al. (2005) showed that disease-related modifications in tau could affect tau-fyn binding *in vitro*. Phosphomimetics of tau at residues known to be phosphorylated in AD (T231, S235) reduced the binding between tau and fyn (Bhaskar et al., 2005). Interestingly, the authors found that the binding affinity of 3R tau to fyn was different to that of 4R tau. Mutation of S199/S202 and S396/S404 to aspartic acid, both of which are AD-related phosphoepitopes, resulted in pseudophosphorylation at these epitopes and an increase of the binding affinity of 4R, but not 3R, tau to fyn (Bhaskar et al., 2005). This suggests that the interaction of tau with fyn could be dependent on the association of tau with microtubules, which could be modified by phosphorylation of tau.

Since ablation of either tau or fyn can confer neuroprotection from Aβ toxicity, Ittner and colleagues (2010) initiated a series of experiments to investigate how these proteins can mediate Aβ toxicity. Transgenic mice expressing a tau deletion construct that lacked the microtubule binding domain resulted in sequestration of tau and fyn to the neuronal cell body (Ittner et al., 2010). In turn, the interaction of NMDA receptors and PSD-95 in dendrites was destabilised. Tau mutant mice crossed with mutant APP mice rescued premature mortality and memory deficits observed in single APP transgenic mice (Ittner et al., 2010). Reduction of total tau alone also ameliorated these impairments, suggesting that the targeting of fyn to the postsynaptic density by tau can specifically promote Aβ-induced toxicity (Ittner et al., 2010). In support of this

hypothesis, reduction of tau in a double transgenic mouse overexpressing mutant APP and fyn prevented cognitive deficits and premature mortality (Roberson et al., 2011). Thus there is considerable evidence that tau-fyn interactions could play a role in AD.

1.7 Synergistic toxicity between tau and Aβ in Alzheimer's disease

Synaptic loss is the best correlate of progressive cognitive decline in AD (DeKosky and Scheff, 1990; Terry et al., 1991), indicating that synaptotoxicity has a key role in the pathogenesis of disease. Both tau and Aβ have been shown to exert neurotoxic effects on synapses, raising the possibility that they might act in concert to synergistically promote synaptic loss in AD.

Using array tomography, soluble Aβ oligomers have been observed at individual synapses in post-mortem human brain tissue, and the presence of oligomers correlates with shrunken and degenerated spines (Koffie et al., 2012). Application of soluble Aβ to neurons causes impaired long-term potentiation and facilitates long-term depression (Lambert et al., 1998; Li et al., 2009). Extracts of Aβ oligomers from AD human post-mortem brain tissue also impairs synaptic plasticity and reduces dendritic spine density in neurons (Shankar et al., 2008). It has been suggested that Aβ exerts its synaptotoxic effects by acting on glutamatergic neurotransmitters receptors. The effect of Aβ on reducing levels of PSD-95 requires NMDA receptor activity (Shankar et al., 2007). Aβ oligomers also induce internalisation of α-amino-3-hydroxy-5-methyl-4-isoxazolepropionic acid (AMPA) and NMDA receptors, triggering the loss of dendritic spines (Snyder et al., 2005; Hsieh et al., 2006). Importantly, the effects of Aβ are mediated by the presence of tau, as reduction of tau reduced the susceptibility to excitotoxic seizures caused by Aβ (Roberson et al., 2007; Ittner et al., 2010; Roberson et al., 2011).

There is increasing evidence that tau can also exert toxicity on synapses. Synapse loss is evident in mouse models of tauopathy and precedes accumulation of tangles, indicating that soluble pre-tangle forms of tau can promote synaptotoxicity (Yoshiyama et al., 2007). Loss of spines is correlated with the missorting of tau in dendrites, suggesting that the mislocalisation of tau is linked to synaptic dysfunction (Zempel et al., 2010; Zempel and Mandelkow, 2014). Recent evidence suggests that accumulation of abnormally phosphorylated tau in dendritic spines mediates synaptic impairment in rTg4510 mice expressing mutant P301L tau (Hoover et al., 2010). Expression of

mutant tau is sufficient to cause impaired synaptic function and reduce the surface expression of AMPA and NMDA receptors (Hoover et al., 2010). Tau has also been observed at synapses and dendritic spines in both mouse models of tauopathy and in AD brain tissue (Tai et al., 2012; Kopeikina et al., 2013; Tai et al., 2014).

The link between tau and Aβ toxicity at synapses may be mediated by fyn. Ittner and colleagues (2010) demonstrated that tau plays an important role in trafficking of fyn to dendrites. Dendritic localisation of tau was shown to be important for positioning fyn in dendrites, where it phosphorylates the NMDA receptor subunit NR2b, thereby regulating the interaction between the NMDA receptor and PSD-95 (Ittner et al., 2010). The interaction of tau with fyn can influence Aβ-mediated neurotoxicity and excitotoxic seizures in mouse models of AD (Ittner et al., 2010). Therefore, the dendritic localisation of tau supports the hypothesis that AD pathology can be mediated by the interaction between fyn and tau. Another protein which has been recently found as a possible link between tau and Aβ is PrP^C, the cellular form of the prion protein. It was previously shown that PrP^C could bind to Aβ oligomers and that abolishing PrP expression blocked Aβ-induced synaptic impairment (Lauren et al., 2009). Subsequently, PrP^C was shown to form a complex with Aβ and fyn, resulting in abnormal phosphorylation of tau (Larson et al., 2012). This complex also appears to be mediated by mGluR5, a metabotropic glutamate receptor, which could mediate downstream effects of Aβ and tau on synapses (Um et al., 2013). Thus, it appears that Fyn may play a major role in mediating the development and progression of AD through interactions with Aβ and tau at synapses.

In 2012, it was reported that PrP^C acted as the receptor for Aβ, which then triggered activation of fyn kinase and subsequent downstream effects on tau (Larson et al., 2012). Fyn was found to be activated by Aβ oligomers when these were applied to cultured neurons, but activation of fyn was abolished in PrP^C knockout neurons or when PrP^C was immunodepleted (Um et al., 2012). Aβ treatment also increased the association between fyn and PrP. As early as fifteen minutes following Aβ application, NR2b phosphorylated at Y1472 by fyn was transiently increased accompanied by activation of fyn, but without any changes in STEP. Three hours post-Aβ, levels of STEP were increased while NR2b phosphorylation and levels of active fyn decreased (Um et al., 2012). This could point to compensatory up-regulation of STEP to counteract the Aβ-induced activation of fyn. Cell surface expression of NMDA receptors was also transiently increased in response to Aβ treatment in this study, and this was also followed by reduction of expression to levels below baseline, changes which were not seen in the absence of PrP^C or fyn (Um et al., 2012). The transient increase of cell surface NMDA receptor expression correlated with release of lactate dehydrogenase

(LDH), a measure of cell toxicity. Immunodepletion of PrP^C prevented the Aβ-induced LDH release (Um et al., 2012). This interaction was further confirmed when Larson and colleagues (2012) co-immunoprecipitated fyn, PrP^C, and soluble Aβ dimers from AD brain tissue, and these were found to co-localise at dendritic spines. Primary neurons treated with PrP^C antibody showed reduced phosphorylation of tau at the fyn-specific Y18 site, suggesting that PrP^C-dependent fyn activation can lead to downstream phosphorylation of tau (Larson et al., 2012). Furthermore, deletion of PrP^C in APP mutant transgenic mice reduced fyn activity, and lowered tau accumulation in the membrane fraction (Larson et al., 2012). On the other hand, overexpression of PrP^C in APP mutant mice resulted in an increased active fyn/total fyn ratio and potentiated the effects of APP on tau missorting and phosphorylation. Together, these studies provide evidence that links Aβ toxicity with PrP^C, fyn, and tau as a mechanistic pathway important for the pathogenesis of AD.

However, the role of fyn in AD is confounded by a study that showed reduction of fyn did not rescue AD-related impairments *in vivo*. 3xTg mice, which harbour mutations in APP, presenilin-1, and tau, are commonly used as models of AD. When crossed with fyn knockout mice, knockdown of fyn resulted in worsened spatial learning compared to controls (Minami et al., 2012). Similarly, genetic ablation of STEP, which leads to increased levels of active fyn, improved spatial learning and memory in the Morris water maze test, and enhanced LTP in the CA1 region of hippocampal slices from 3xTg mice (Zhang et al., 2010). These discrepancies clearly indicate that the role of fyn in AD is complex and requires further investigation. While the lack of fyn itself is sufficient to cause defects in synaptic plasticity and spatial learning (Grant et al., 1992), it remains possible that Aβ toxicity is mediated through specific functions of fyn, such as its association with tau or the PSD-95/NMDA receptor complex at the dendrite. These studies suggest that reduction of fyn alone may not be an appropriate therapeutic strategy for AD, but that it may be more beneficial to investigate downstream targets such as the association between tau and fyn.

Currently, it is known that the SH3 domain of fyn can bind to specific proline-rich sequences within PXXP motifs in tau (Lee et al., 1998; Usardi et al., 2011; Cochran et al., 2014). However, it is not known which of the seven PXXP sequences in tau has most importance for this interaction. Serine/threonine phosphorylation sites within and around the PXXP motifs have been identified in AD brain, suggesting that phosphorylation at these sites may regulate binding of tau to fyn (Reynolds et al., 2008). Given that tau-fyn binding can mediate phosphorylation-dependent trafficking of tau, and aberrant activation of fyn by Aβ leads to downstream pathological changes in tau, it is important to characterise the molecular mechanisms of tau-fyn interactions

with respect to normal and pathogenic conditions in order to find novel avenues for AD therapy.

1.8 Aims and objectives of the thesis

It is clear that tau and fyn are downstream of Aβ and that they are both able to modulate Aβ-induced neurotoxicity, but the mechanisms by which this occurs are unclear. Although studies have investigated tau-fyn interactions, the binding site for fyn on tau has yet to be fully defined. Moreover, the downstream consequences of such an interaction remain unclear. In addition, the role of fyn has not yet been investigated in the context of spreading of tau, either physiologically or pathologically. Therefore, the aims of this thesis are to:

1) Investigate the release of tau in organotypic brain slices, in comparison to tau release from primary neurons, and to determine whether fyn is involved in modulating tau release in this model;
2) Determine the effects of soluble Aβ oligomers on tau release;
3) Identify the critical binding site on tau that enables its interaction with fyn, and to determine the effects of inhibiting tau-fyn binding on tau release;
4) Determine whether there is any correlation between the presence of fyn and AD-related changes in tau in human post-mortem brain tissue.

Chapter 2 Materials & Methods

2.1 Materials

2.1.1 General molecular biology reagents

All reagents used were from Sigma-Aldrich (UK) and ultrapure water (Elga Maxima system) was used in the preparation of all solutions, unless otherwise stated.

Plasmids

All of the plasmids used in this thesis are listed in Table 2.1. Plasmids encoding glutathione-S-transferase (GST), or GST fused to the N-terminus of the src homology (SH) 2 or 3 domains of fyn were a gift from by Dr S. Anderson (University of Colorado Anschutz Medical Campus, Aurora, CO, USA) (Burton et al., 1997). Human full-length (2N4R) tau was previously cloned into pcDNA3.1-V5-His-TOPO vector by Dr Pascal Derkinderen in this laboratory (Derkinderen et al., 2005). Plasmids encoding 2N4R tau containing proline to alanine substitutions at residues 216 (P216A) or 233 (P233A) of tau was previously generated by Dr Alessia Usardi in this laboratory (Usardi et al., 2011). Plasmids pIRES2-EGFP and Lenti-GFP were provided by Dr Nina Balthasar (University of Bristol, UK).

Table 2.1. Plasmids used in this thesis

Plasmid	Vector	Source/Reference	Protein encoded
GST	pGEX	Dr S. Anderson (Burton et al., 1997)	GST
GST-fyn-SH2	pGEX	Dr S. Anderson (Burton et al., 1997)	SH2 domain of fyn fused to GST at the N-terminus
GST-fyn-SH3	pGEX	Dr S. Anderson (Burton et al., 1997)	SH3 domain of fyn fused to GST at the N-terminus
V5-tau	pcDNA3.1-V5-His-TOPO	Dr P. Derkinderen (Derkinderen et al.,	Wild-type (WT) human 2N4R tau tagged with V5 and

		2005)	His tags at the C-terminus
pIRES2-EGFP	pIRES2-EGFP	Clontech Laboratories (Palo Alto, CA, USA)	Internal ribosome entry site (IRES)-containing bicistronic vector expressing enhanced green fluorescent protein (EGFP)
Lenti-GFP	pTYF-SW-linker	Dr N. Balthasar (Liu et al., 2006)	EGFP under the control of human synapsin I promoter
P176A, P182A, P200A, P206A, P213A, P219A	pcDNA3.1-V5-His-TOPO	D. Lau	Tau containing individual proline to alanine substitutions at residues 176, 182, 200, 206, 213, or 219 of tau
P216A, P233A	pcDNA3.1-V5-His-TOPO	Dr A. Usardi (Usardi et al., 2011)	Tau containing individual proline to alanine substitutions at residues 216 or 233 of tau

Agarose gel electrophoresis of nucleic acids

Tris-acetate-EDTA (TAE) buffer	40 mM Tris, pH 8.0 20 mM acetic acid 1 mM ethylenediaminetetraacetic acid (EDTA)
DNA loading buffer	5X Green GoTaq® Reaction Buffer (Promega, Southampton, UK)
Nucleic acid molecular weight marker	Quick-Load® 1kb DNA Ladder (New England BioLabs, Hertfordshire, UK) Size (kb): 10, 8, 6, 5, 4, 3, 2, 1.5, 1, 0.5 TriDye™ 100 bp DNA Ladder (New England BioLabs, Hertfordshire, UK) Size (bp): 1517, 1200, 1000, 900, 800, 700, 600, 500/517, 400, 300, 200, 100

Plasmid DNA preparation

Plasmid DNA was prepared using the QIAprep Spin Miniprep Kit (Qiagen, Manchester, UK) and HiSpeed Plasmid Maxi Kit (Qiagen, Manchester, UK).

2.1.2 Site-directed mutagenesis

The QuikChange II XL Site-Directed Mutagenesis kit was purchased from Agilent Technologies, Cheshire, UK.

Primers

All primers were custom synthesised by Eurofins MWG Operon, Wolverhampton, UK. Primers used for site-directed mutagenesis are listed in Table 2.2. Full-length 2N4R human tau in pcDNA3.1-V5-His-TOPO was used as a template. The codons mutated to replace proline (P) with alanine (A) in the encoded protein are underlined.

Table 2.2. Forward and reverse primers used for site-directed mutagenesis of tau

Primer name	Primer sequence 5’ to 3’
Forward P176A	GATTCCAGCAAAAACCGCGCCCGCTCCAA
Reverse P176A	TTGGAGCGGGCGCGGTTTTTGCTGGAATC
Forward P176A-2	AGCAAAAACCGCGCCCGCTCCAAAG
Reverse P176A-2	CTTTGGAGCGGGCGCGGTTTTTGCT
Forward P176A-3	AGCAAAAACCGCTCCCGCTCCAAAG
Reverse P176A-3	CTTTGGAGCGGGAGCGGTTTTTGCT
Forward P182A	CGCTCCAAAGACAGCACCCAGCTCTGG
Reverse P182A	CCAGAGCTGGGTGCTGTCTTTGGAGCG
Forward P200A	GCTACAGCAGCGCCGGCTCCCCA
Reverse P200A	TGGGGAGCCGGCGCTGCTGTAGC
Forward P200A-2	TACAGCAGCGCAGGCTCCCCAG
Reverse P200A-2	TGGGGAGCCTGCGCTGCTGTA
Forward P200A-3	TACAGCAGCGCAGGCTCTCCAGGCACTC
Reverse P200A-3	GAGTGCCTGGAGAGCCTGCGCTGCTGTA
Forward P206A	GGCTCCCCAGGCACTGCCGGCAGC
Reverse P206A	GCTGCCGGCAGTGCCTGGGGAGCC
Forward P213A	GCTCCCGCACCGCGTCCCTTCCA

Reverse P213A	TGGAAGGGACGCGGTGCGGGAGC
Forward P219A	CCCTTCCAACCCCAGCCACCCGGG
Reverse P219A	CCCGGGTGGCTGGGGTTGGAAGGG

E.coli culture

IPTG	10 mM isopropyl-1-thio-β-D-galactopyranoside (IPTG) in H_2O, sterile filtered
X-Gal	20 mg/ml 5-bromo-4-chloro-3-indolyl-β-D-galactopyranoside (Thermo Scientific, Waltham, MA, USA)
Luria Bertani (LB) broth	20 g/l LB, sterilised by autoclaving For LB-ampicillin broth, 100 µg/ml ampicillin is added to sterile LB on day of use For LB-kanamycin broth, 50 µg/ml kanamycin is added to sterile LB on day of use
LB agar	32 g/L LB agar, sterilised by autoclaving For LB-ampicillin agar, 100 µg/ml ampicillin is added when agar is less than 55°C For LB-kanamycin broth, 50 µg/ml kanamycin is added when agar is less than 55°C
Super Optimal Broth with Catabolite repression (SOC) medium	1X SOC Outgrowth Medium (New England BioLabs, Hertfordshire, UK)

Plasmid sub-cloning

Primers to introduce stop codon in 2N4R tau in pcDNA3.1-V5-His-TOPO vector

All primers were custom synthesised by Eurofins MWG Operon, Wolverhampton, UK. PCR primers containing a single base mutation (underlined) were designed to amplify a fragment of tau to introduce a stop codon at the 3' end of the sequence encoding 2N4R human tau in pcDNA3.1-V5-His-TOPO (Table 2.3).

Table 2.3. Primers to introduce stop codon in 2N4R tau in pcDNA3.1-V5-His-TOPO

Primer name	Primer sequence 5' to 3'
Tau BsrGI forward	TGACCTTCCGCGAGAACGCCAAAGCCAAG
Tau EcoRV reverse	GTGCTGGATATCTGCAGAATTGCCCTTTGATCACAAACC

Restriction enzymes

All restriction enzymes and buffers were purchased from New England BioLabs, Hertfordshire, UK, unless otherwise stated.

DNA purification

Plasmid DNA was isolated for subcloning using the QIAquick Gel Extraction Kit (Qiagen, Manchester, UK).

Blunting, ligation and dephosphorylation

Quick Blunting Kit (New England BioLabs, Hertfordshire, UK)

T4 DNA ligase (New England BioLabs, Hertfordshire, UK)

Shrimp alkaline phosphatase (New England BioLabs, Hertfordshire, UK)

2.1.3 Transgenic mice

Wild-type, $fyn^{-/-}$, and $tau^{-/-}$ mice were obtained from The Jackson Laboratory, Maine, USA. $Fyn^{-/-}$ mice were maintained on a B6129SF2/J background, so this strain was used to provide wild-type controls for experiments involving $fyn^{-/-}$ mice.

B6;129S7-Fyn^{tm1Sor}/J ($fyn^{-/-}$) mice are viable and fertile without any overt phenotype. However, homozygous mutant mice have impaired T-cell receptor signalling and display a reduction in tyrosine-phosphorylated proteins. Neurological defects are also observed, including blunted long-term potentiation, impaired spatial learning, and altered hippocampal development.

$Mapt^{tm1(EGFP)Kit}$/J ($tau^{-/-}$) mice are viable and fertile without any overt phenotype. $Tau^{-/-}$ mice are maintained on a C57BL/6 background. The coding sequence of enhanced fluorescent green protein (EGFP) is knocked into the first exon, disrupting expression of the *Mapt* gene to produce the first 31 amino acids of tau fused to EGFP.

Mouse genotyping

Primers for genotyping fyn knockout ($^{-/-}$) and $tau^{-/-}$ mice are listed in Table 2.4 and Table 2.5, respectively.

Table 2.4. Primers for genotyping $fyn^{-/-}$ mice

Primer name (code)	Primer sequence 5' to 3'
Wild-type forward (10207)	AGGCCCAAGTTGACTATCCA
Common reverse (10208)	GGCAGCCTGTCTCAAAAGTC
Mutant fyn forward (oIMR9535)	GGGAGGATTGGGAAGACAAT

Table 2.5. Primers for genotyping $tau^{-/-}$ mice

Primer name (code)	Primer sequence 5' to 3'
Human tau forward (oIMR3115)	ACTTTGAACCAGGATGGCTGAGCCC
Human tau reverse (oIMR3116)	CTGTGCATGGCTGTCCACTAACCTT

Mouse tau forward (oIMR3092)	CTCAGCATCCCACCTGTCAC
Mouse tau reverse (oIMR3093)	CCAGTTGTGTATGTCCACCC
EGFP forward (oIMR0872)	AAGTTCATCTGCACCACCG
EGFP reverse (oIMR1416)	TCCTTGAAGAAGATGGTGCG

TEN9 buffer

15 mM Tris-HCl, pH 8.0
35 mM Tris
20 mM EDTA
40 mM NaCl

Proteinase K

50 mg/ml proteinase K in storage buffer:
50 mM Tris-HCl, pH 8.0
5 mM $CaCl_2$
50% (v/v) glycerol

Digestion mix

1% (w/v) SDS
1 mg/ml proteinase K
TEN9 buffer

2.1.4 General cell biology reagents

Protein buffering and lysis

Phosphate-buffered saline (PBS)	1 PBS tablet dissolved in 200 ml water
Tris-buffered saline (TBS)	50 mM Tris-HCl, pH 7.4 150 mM NaCl
PBS-T	PBS 0.1% (v/v) Tween-20
TBS-T	TBS 0.1% (v/v) Tween-20
Hypotonic buffer	10 mM $NaHCO_3$ 25 µg/ml DNAse Complete protease inhibitor cocktail without EDTA (Roche, West Sussex, UK) 1% (v/v) Phosphatase inhibitor cocktail 2
Bovine serum albumin (BSA) protein standards	Serial dilutions of 2 mg/ml BSA in H_2O were prepared in the appropriate lysis buffer to obtain concentrations of 125, 250, 500, 750, 1000, and 1500 µg/ml.
Extra strong lysis buffer (ESLB)	10 mM Tris-HCl, pH 7.5 0.5% (w/v) SDS 20 mM sodium deoxycholate 1% (v/v) Triton X-100 1 mM sodium orthovanadate 1.25 mM sodium fluoride 10 mM EDTA Complete protease inhibitor cocktail without EDTA (Roche, West Sussex, UK) 1% (v/v) Phosphatase inhibitor cocktail 2

Radioimmunoprecipitation assay (RIPA) buffer	50 mM Tris-HCl, pH 7.4 1% (v/v) Triton X-100 0.5% (w/v) sodium deoxycholate 0.1% (w/v) sodium dodecyl sulphate (SDS) 100 mM NaCl 1 mM ethylenediaminetetraacetic acid (EDTA) 10 mM iodoacetamide Complete protease inhibitor cocktail without EDTA (Roche) 1% (v/v) Phosphatase inhibitor cocktail 2
Hypotonic buffer for fractionation	10 mM $NaHCO_3$, pH 7.4 25 µg/ml DNAse Complete protease inhibitor cocktail without EDTA 1% (v/v) Phosphatase inhibitor cocktail 2
NETF buffer	100 mM NaCl 2 mM ethylene glycol tetraaectic acid (EGTA) 50 mM Tris-HCl, pH 7.4 1% (v/v) Nonidet P-40 (BDH Laboratories) Complete protease inhibitor cocktail without EDTA 1% (v/v) Phosphatase inhibitor cocktail 2
HEPES buffer	50 mM 4-(2-hydroxyethyl)-1-piperazineethanesulfonic acid (HEPES) 140 mM NaCl 0.5% (v/v) Triton X-100 Complete protease inhibitor cocktail without EDTA 1% (v/v) Phosphatase inhibitor cocktail 2

TBS-EGTA buffer	50 mM Tris, pH 7.4 150 mM NaCl 2 mM EGTA Complete protease inhibitor cocktail without EDTA 1% (v/v) Phosphatase inhibitor cocktail 2

Glutathione S-transferase (GST) pull-downs

Tris-NaCl-EDTA (TNE) buffer	25 mM Tris-HCl, pH 7.5 100 mM NaCl 1 mM EDTA Complete protease inhibitor cocktail (Roche, West Sussex, UK)
GST pull-down lysis buffer	25 mM Tris-HCl, pH 7.5 10% (v/v) glycerol 0.5% (v/v) Triton X-100 1 mM EDTA 1 mM ethylene glycol-bis(2-aminoethylether)-*N*,*N*,*N′*,*N′*-tetraacetic acid (EGTA) 150 mM NaCl Complete protease inhibitor cocktail (Roche, West Sussex, UK) 1% (v/v) Phosphatase inhibitor cocktail 2
GST pull-down wash buffer	50 mM Tris-HCl, pH 7.5 2 mM EDTA 0.5% (v/v) Triton X-100 150 mM NaCl Complete protease inhibitor cocktail (Roche, West Sussex, UK) 1% (v/v) Phosphatase inhibitor cocktail 2

Co-immunoprecipitation

Immunoprecipitation beads	Protein A agarose beads
IC261	3-[(2,4,6-Trimethoxyphenyl)methylidenyl]-indolin-2-one, SU5607 (IC261; Calbiochem)
Crosslinker	Dithiobis[succinimidyl propionate] (DSP, Thermo Scientific)

Bicinchoninic acid (BCA) protein assay

BCA Protein Assay Kit (Thermo Scientific, Waltham, MA, USA)	BCA Reagent A (containing sodium carbonate, sodium bicarbonate, bicinchoninic acid, sodium tartrate in 0.1M sodium hydroxide) BCA Reagent B (containing 4% cupric sulphate)

Cell toxicity assays

Lactate dehydrogenase (LDH) assay	CytoTox 96® Non-Radioactive Cytotoxicity Assay (Promega, Southampton, UK)
LIVE/DEAD assay	LIVE/DEAD® Fixable Far-Red Dead Cell Stain Kit (Life Technologies, Paisley, UK)

Immunocytochemistry

Fixing solution	4% (v/v) paraformaldehyde (PFA) in PBS
Hoescht	1 µg/ml Hoescht 33342 diluted in PBS

Mounting medium	Fluorescence mounting medium (DAKO, Cambridgeshire, UK)

2.1.5 Sodium dodecyl sulphate-polyacrylamide gel electrophoresis (SDS-PAGE)

Laemmli sample buffer (2x)	25 mM Tris-HCl, pH 6.8 4% (w/v) SDS 20% (v/v) glycerol 0.01% (w/v) Bromophenol blue 100 mM dithiothreitol (DTT)
Stock acrylamide (National Diagnostics, Hessle, UK)	30% (w/v) acrylamide 0.5% (w/v) bis-acrylamide (37.5:1)
Resolving gel	10% (w/v) acrylamide (National Diagnostics, Hessle, UK) 25% (v/v) resolving buffer, pH 8.8 (National Diagnostics, Hessle, UK) 0.01% (w/v) ammonium persulphate (APS, National Diagnostics, Hessle, UK) 0.1% (v/v) N,N,N',N' tetramethylethylenediamine (TEMED, National Diagnostics, Hessle, UK)
Stacking gel	4% (w/v) acrylamide 25% (v/v) stacking buffer, pH 6.8 (National Diagnostics, Hessle, UK) 0.075% (w/v) APS 0.15% (v/v) TEMED
Running buffer	25 mM Tris, pH 8.3 192 mM glycine 0.1% (w/v) SDS

Protein molecular weight markers	Precision Plus Protein™ All Blue Standards (Bio-Rad, Hertfordshire, UK) Molecular weight (kDa): 250, 150, 100, 75, 50, 37, 25, 20, 15, 10

Colloidal Coomassie blue staining

ProtoBlue Safe Working Solution	10% (v/v) ethanol 90% (v/v) ProtoBlue Safe (National Diagnostics, Hessle, UK)

Western blot (WB)

Transfer buffer	25 mM Tris, pH 8.3 192 mM glycine 20% (v/v) methanol
Blocking solution (WB)	5% (w/v) dried skimmed milk in TBS
Antibody diluent (WB)	3% (w/v) dried skimmed milk in TBS

2.1.6 General cell culture reagents

Poly-D-lysine	10 µg/ml poly-D-lysine (PDL)
Culture medium for primary neurons	Neurobasal® medium (Life Technologies, Paisley, UK) without Phenol red, supplemented with: 0.02% (v/v) B-27® (Life Technologies, Paisley, UK) 2 mM L-Glutamine (GE Healthcare, Buckinghamshire, UK) 100 U/ml penicillin (GE Healthcare, Buckinghamshire, UK)

	100 µg/ml streptomycin (GE Healthcare, Buckinghamshire, UK)
Papain solution (Worthington Biochemical Corporation, Lakewood, New Jersey, USA)	20 U/ml papain 1 mM L-cysteine 0.5 mM EDTA in Earle's Balanced Salt Solution with bicarbonate and phenol red (EBSS)
DNase I (Worthington Biochemical Corporation, Lakewood, New Jersey, USA)	2000 U/ml deoxyribonuclease in EBSS
Albumin-ovomucoid protease inhibitor (Worthington Biochemical Corporation, Lakewood, New Jersey, USA)	10 mg/ml ovomucoid inhibitor 10 mg/ml albumin in EBSS
Chinese Hamster Ovary (CHO) cells	HyClone™ Ham's Nutrient Mixture F-12 (GE Healthcare, Buckinghamshire, UK) supplemented with: 10% (v/v) foetal bovine serum (FBS, Biosera, Boussens, France) 2 mM L-glutamine 100 U/ml penicillin 100 µg/ml streptomycin
Trypsin	Trypsin-EDTA (GE Healthcare, Buckinghamshire, UK)

Organotypic mouse cortical brain slice culture

All medium was sterile filtered (0.2 µm) and stored at 4°C prior to use.

Dissection solution	1.25 mM KH_2PO_4, pH 7.4 124 mM NaCl 3 mM KCl 8.19 mM $MgSO_4$

	2.65 mM $CaCl_2$ 3.5 mM $NaHCO_3$ 10 mM glucose 2 mM ascorbic acid 39.4 µM ATP
Slicing medium	Basal medium Eagle (BME) 26.6 mM HEPES, pH 7.1 19.3 mM NaCl 5 mM $NaHCO_3$ 511 µM ascorbic acid 40 mM glucose 2.7 mM $CaCl_2$ 2.5 mM $MgSO_4$ 1% (v/v) GlutaMAX (Life Technologies, Paisley, UK) 0.033% (v/v) insulin 50 U/ml penicillin 50 µg/ml streptomycin 25% (v/v) horse serum
Serum-free medium	Minimum essential medium Eagle (MEM), phenol red-free 26.6 mM HEPES, pH 7.1 19.3 mM NaCl 5 mM $NaHCO_3$ 511 µM ascorbic acid 40 mM glucose 2.7 mM $CaCl_2$ 2.5 mM $MgSO_4$ 1% (v/v) GlutaMAX (Life Technologies, Paisley, UK) 0.033% (v/v) insulin 50 U/ml penicillin 50 µg/ml streptomycin

2.1.7 Antibodies

Table 2.6. Primary antibodies used for western blots and enzyme-linked immunosorbent assay (ELISA)

Antibody	Epitope/ specificity	Species/ Type	Dilution for western blots	Dilution for ELISA	Source/ Reference
DAKO	Tau (C-terminal half)	Rabbit polyclonal	1/10,000	1/1,000	DAKO, Cambridgeshire, UK
DA31	Tau (residues 150-190)	Mouse monoclonal		1/500	Peter Davies (Albert Einstein College of Medicine (AECM), NY, USA)
Tau-13	Human tau (residues 20-35)	Mouse monoclonal	1/5,000		Abcam, Cambridge, UK
Tau-5	Tau (residues 215-225)	Mouse monoclonal	1/1,000		Millipore, Darmstadt, Germany
Tau-1	Dephosphorylated tau (residues 199-205)	Mouse monoclonal	1/5,000		Millipore, Darmstadt, Germany
PHF-1	Tau phosphorylated at S396/404	Mouse monoclonal	1/5,000		Peter Davies (AECM, NY, USA)
CP13	Tau phosphorylated at S202	Mouse monoclonal	1/400		Peter Davies (AECM, NY, USA)
CP27	Human tau 130-150	Mouse monoclonal	1/1,000		Peter Davies (AECM, NY, USA)

Tau pS214	Tau phosphorylated at S214	Rabbit polyclonal	1/500		Abcam, Cambridge, UK
Tau pS262	Tau phosphorylated at S262	Rabbit polyclonal	1/500		Abcam, Cambridge, UK
Tau pY18	Tau phosphorylated at Y18	Rabbit polyclonal	1/500		Diane Hanger
Fyn	Fyn	Rabbit polyclonal	1/1,000		Sigma-Aldrich
Fyn (sc-16)	Peptide mapping at the N-terminus of human fyn	Rabbit polyclonal	1/500		Santa Cruz Laboratories, Santa Cruz, CA, USA
Fyn (sc-434)	Human fyn (residues 85-206)	Mouse monoclonal	1/250		Santa Cruz Laboratories, Santa Cruz, CA, USA
Fyn	Human fyn (residues 1-132)	Mouse monoclonal	1/500		BD Transduction Laboratories, San Jose, CA, USA
Fyn (CST)	Fyn	Rabbit polyclonal	1/250		Cell Signalling Technology, Beverly, MA, USA
Src pY416	Src and Fyn phosphorylated at Y416	Rabbit polyclonal	1/500		Cell Signalling Technology, Beverly, MA, USA
NSE	γ-enolase subunit of neuron specific enolase	Mouse monoclonal	1/10,000		DAKO, Cambridgeshire, UK

β-actin (AC-15)	N-terminal of the β isoform of actin	Mouse monoclonal	1/10,000		Abcam, Cambridge, UK
β-actin	β isoform of actin	Rabbit polyclonal	1/5,000		Abcam, Cambridge, UK
PSD-95	Post-synaptic density protein 95 (PSD-95)	Rabbit monoclonal	1/1,000		Cell Signalling Technology, Beverly, MA, USA
Synaptophysin (SP15)	Synaptophysin	Mouse monoclonal	1/1,000		Enzo Life Sciences, Exeter, UK
Drebrin (MX823)	Drebrin residues 632-649	Mouse monoclonal	1/5,000		My Bio Source, San Diego, CA, USA
V5	14 amino acid V5 epitope sequence: GKPIPNPLLGL NST	Mouse monoclonal	1/5,000		Life Technologies, Paisley, UK
GFP	GFP	Rabbit polyclonal	1/5,000		Abcam
GST	GST	Goat polyclonal	1/2,000		GE Healthcare, Buckinghamshire , UK
4G8	Amino acids 17-24 of amyloid beta	Mouse monoclonal	1/5,000		Covance, Princeton, NJ, USA
Cleaved caspase-3	Caspase-3 cleaved at D175	Rabbit polyclonal	1/1,000		Cell Signalling Technology, Beverly, MA, USA
GFAP	Glial fibrillary acidic protein (GFAP)	Mouse monoclonal	1/2,000		Vector Labs, Peterborough, UK

Table 2.7. Secondary antibodies used for western blots and ELISA

Antibody	Dilution for western blots	Source
Alexa Fluor® 680 goat anti-mouse	1/10,000	Life Technologies, Paisley, UK
IRDye ™ 800 conjugated goat anti-rabbit	1/10,000	Rockland Immunochemicals Inc., Pottstown, PA, USA
Horseradish peroxidase (HRP)-linked donkey anti-rabbit	1/500	GE Healthcare, Buckinghamshire, UK

2.1.8 Sandwich ELISA

Blocking solution (ELISA)

StartingBlock (TBS) Blocking Buffer (Thermo Scientific, Waltham, MA, USA)

Antibody diluent (ELISA)

20% (v/v) SuperBlock (PBS) Blocking Buffer (Thermo Scientific, Waltham, MA, USA) in TBS

3,3',5,5'-Tetramethylbenzidine (TMB)

1-Step Ultra TMB-ELISA Substrate Solution (Thermo Scientific, Waltham, MA, USA)

Coating buffer

15.6 mM K_2HPO_4, pH 7.2
25.6 mM KH_2PO_4
136.9 mM NaCl
1.27 mM EDTA
0.05% (w/v) sodium azide

Wash buffer

10 mM Tris-HCl, pH 7.4

100 mM NaCl
0.05% (v/v) Tween-20

2.1.9 Post-mortem human brain

Post-mortem human brain temporal or frontal (marked with an asterisk) cortex was obtained from the Medical Research Council London Neurodegenerative Diseases Brain Bank at the Institute of Psychiatry, Psychology and Neuroscience, King's College London. Case details are summarised in Table 2.8 and Table 2.9.

Table 2.8. Case details for control and late-stage Alzheimer's disease post-mortem human temporal cortex

Autopsy code	Sex	Age	Post-Mortem Delay (h)	Braak Stage	Pathology/Diagnosis
A011/06	F	82	43	Control	Normal brain
A140/07	F	81	17	I	Mild ageing changes Braak I
A153/06	F	92	17	Control	Control brain with some tau deposition
A134/00	M	86	6	Control	Normal adult brain
A358/08	F	55	12	Control	Minimal tau pathology consistent with HP-tau stage I
A192/09	M	80	21	Control	Widespread acute infarcts and acute ischaemic changes; old infarcts
A063/10	F	90	50	Control	Control brain - mild Alzheimer-type changes (modified Braak II) and mild amyloid angiopathy
A047/02	F	87	22	Control	Normal adult brain
A048/09	M	81	18	I	Control - old cerebral infarct (Braak I)
A239/03	M	78	10	Control	Ageing changes (mild)
A265/08	M	79	47	II	Early tau pathology Braak II, no neuritic plaques
A040/07	F	82	13	Control	Argyrophilic grains low to moderate density
A124/04	M	59	50	Control	Normal adult brain
A150/01	M	40	40	Control	Normal adult brain

A141/07	M	80	41	VI	Alzheimer's disease: Braak VI with severe amyloid angiopathy
A065/04	F	91	29	VI	Alzheimer's disease: Definite Braak VI
A094/04	M	88	46	VI	Alzheimer's disease: Definite Braak VI
A059/07	F	92	42	VI	Alzheimer's disease: Braak VI
A331/07	F	80	13	V	Alzheimer's disease: Braak V with mild amyloid angiopathy
A191/07	F	69	16	VI	Alzheimer's disease: Braak VI
A210/07	F	84	<24	V	Alzheimer's disease: Braak V
A167/05	F	81	<72	VI	Alzheimer's disease: Braak VI
A058/07	M	81	74	VI	Alzheimer's disease: Braak VI
A187/07	F	82	69	V	Alzheimer's disease: Braak V with mild amyloid angiopathy
A168/05	F	84	36	V/VI	Alzheimer's disease: Braak V/VI
A247/05	F	90	23	V/VI	Alzheimer's disease Braak V/VI
A350/09	F	98	3.5	IV	Alzheimer's disease BNE IV, CERAD probable
A065/02	M	82	80	V/VI	Alzheimer's disease definite Braak V/Vi
A318/09	M	72	5	VI	Alzheimer's disease: Braak VI with marked amyloid angiopathy
A181/09	F	89	15	IV	Alzheimer's disease (BNE stage IV) with amyloid angiopathy
A240/06	F	97	12	V	Alzheimer's disease: Braak V

A013/03	M	89	19	V/VI	Alzheimer's disease: definite Braak V/VI
A122/04	M	86	26	V	Alzheimer's disease: Braak V with moderate amyloid angiopathy
A332/07	F	87	48	VI	Alzheimer's disease: Braak VI with moderate amyloid angiopathy

Table 2.9. Case details for control and Braak I-VI Alzheimer's disease post-mortem human temporal cortex

Autopsy	Sex	Age	Post-Mortem Delay	Braak Stage	Pathology/Diagnosis
A047/02	F	87	22	Control	Normal adult brain
A134/00	M	86	6	Control	Normal adult brain
A124/04	M	59	50	Control	Normal adult brain
A150/01	M	40	40	Control	Normal adult brain
A239/03	M	78	10	Control	Ageing changes (mild)
A040/07	F	82	13	Control	Argyrophilic grains low to moderate density
A153/06	F	92	17	Control	Control brain with some tau deposition
A358/08	F	55	12	I	Minimal tau pathology consistent with HP-tau stage I
A140/07	F	81	17	I	Mild ageing changes Braak I
***A265/08**	M	79	47	II	Early tau pathology Braak II, no neuritic plaques

***A063/10**	F	90	50	II	Control brain- mild Alzheimer-type changes (modified Braak stage II) and mild amyloid angiopathy
***A073/05**	M	93	~33	II	Mild Alzheimer's type changes Braak II
***A310/09**	F	84	35	II	Alzheimer changes Braak II consistent with normal aging
***A276/05**	M	92	11	III	Mild Alzheimer's type changes due to ageing Braak III
***A209/08**	F	70	38	III	Possible Alzheimer's disease (CERAD) Braak III (limbic) BNE stage III
***A045/12**	M	86	52	III	Ageing changes (AD modified Braak stage 3) - suitable as control
***A097/13**	M	82	28	IV	Alzheimer's disease (modified Braak stage 4) with limbic TDP-43 pathology
***A078/13**	M	86	53	IV	Alzheimer's disease (modified Braak stage 4) with extensive severe amyloid angiopathy
***A223/12**	F	83	22	IV	Alzheimer's disease (limbic stage) (modified Braak stage 4) and moderate to severe amyloid angiopathy
***A175/12**	F	89	56	IV	Alzheimer's disease HP tau stage 4 severely affecting limbic system and moderately extending to neocortex.
A331/07	F	80	13	V	Alzheimer's disease Braak V with mild amyloid angiopathy
A187/07	F	82	69	V	Alzheimer's disease Braak V mild amyloid angiopathy
A122/04	M	86	26	V	Alzheimer's Braak V with moderate amyloid angiopathy
A168/05	F	84	36	VI	Alzheimer's disease Braak V/VI

A094/04	M	88	46	VI	Alzheimer's disease: Definite Braak VI
A059/07	F	92	42	VI	Alzheimer's disease Braak VI
A191/07	F	69	16	VI	Alzheimer's disease Braak VI

2.2 Methods

2.2.1 Breeding and maintenance of transgenic mice

Breeding of animals was performed with males at least 8 weeks of age, and females at least 6 weeks of age. All animal housekeeping and procedures were carried out in accordance with the UK Scientific Procedures (Animals) Act (1986) under the authority of Project Licence 70/7204 and appropriate personal licence.

2.2.2 Cell culture methods

Primary neuronal cell culture

100 ng/ml PDL in sterile H_2O was used to coat cell culture dishes. Dishes were incubated at 37°C for 1-24 h**.** Excess poly-D-lysine was removed immediately prior to plating of neurons and cell culture dishes were washed with sterile H_2O.

Isolation and papain dissociation of cortical neurons from embryonic rat brain

Embryonic day 18 (E18) Sprague-Dawley rat embryos (Charles River Laboratories, UK) were used to prepare primary cortical neurons following removal of the midbrain, cerebellum, and meninges. Dissected cortices were placed in Hank's balanced salt solution (HBSS) without calcium and magnesium. Papain dissociation was carried out according to the manufacturer's instructions (Section 2.1.6). Briefly, cortices were incubated in 5 ml papain solution containing 0.005% (v/v) DNAse I for 20 min at 37°C. Following vigorous trituration and straining (70 µm cell strainer, BD Falcon), a single cell suspension was produced. The cells were pelleted by centrifugation at 300 $g_{(av)}$ for 5 min at ambient temperature. The pelleted cells were resuspended in a solution of 2.7 ml EBSS mixed with 300 µl albumin-ovomucoid inhibitor solution and 150 µl DNase I. The cell suspension was layered onto 5 ml albumin-ovomucoid inhibitor solution and centrifuged at 70 $g_{(av)}$ for 5 min at ambient temperature to remove membrane fragments. The supernatant was removed, and pelleted cells were resuspended in 1 ml supplemented Neurobasal® medium per embryonic brain and counted using a

haemocytometer. Typically, 10 x 10^6 neurons were obtained from each embryonic brain.

Plating of primary rat cortical neurons

Cells were plated at the following densities:
200,000 cells/well in a 12-well plate
1 x 10^6 cells/well in a 6-well plate
4 x 10^6 cells/10 cm diameter dish

Culture of Chinese hamster ovary (CHO) cells

CHO cells were maintained in Ham's F-12 (Section 2.1.6) at 37°C, 5% CO_2. Cells were passaged when they reached 80-90% confluency. Cells were passaged by washing with HBSS without Ca^{2+}/Mg^{2+} followed by adding sufficient volume of trypsin-EDTA solution to cover the cells and incubating at 37°C for 5 min until cells detached. Cells were resuspended in culture medium to inactivate the trypsin.

Transient transfection of CHO cells

CHO cells were transfected at 70-80% confluency using jetPEI® (Polyplus Transfection) according to the manufacturer's instructions. Briefly, for each well of a 6-well plate, 3 µg of DNA was diluted in 150 mM NaCl to a final volume of 100 µl. Separately, 6 µl of jetPEI® reagent was added to 150 mM NaCl to a final volume of 100 µl. The jetPEI® solution was added to the DNA solution, vortexed, and incubated at ambient temperature for 15 min. Culture medium was removed from the CHO cells and replaced with 1 ml of fresh medium. 200 µl of the transfection mix was added dropwise to each well and cells were incubated for 24 h at 37°C. Cells were harvested 24 h post-transfection.

Long-term culture of mouse cortical organotypic brain slices

Postnatal day (P) 9-10 pups were used to prepare mouse cortical organotypic brain slice cultures. Pups were sacrificed by decapitation and the bisected heads were transferred immediately into oxygenated ice-cold dissection solution (Section 2.1.6). Following removal of the hippocampus and striatum, each half brain was placed into ice-cold oxygenated dissection solution. The corresponding half brain was cut into 350 µm coronal slices using a McIlwain tissue chopper. Three slices were plated into each well of a 6-well plate containing tissue culture inserts (0.4 µm, Millipore) and 1 ml slicing medium (Section 2.1.6) and incubated at 37°C in 5% CO_2. Three h after plating,

the medium was replaced with 1 ml fresh slicing medium, and slices were incubated at 37°C in 5% CO_2. The medium was changed every two days thereafter.

Lentiviral transduction of organotypic brain slices

Two different methods were used to assess the efficiency of lentivirus transduction into organotypic brain slices:

(1) Lentivirus was diluted to $1x10^9$ transducing units (TU)/ml in slicing medium. On the day of plating the slices, 10^7 TU lentivirus was pipetted per slice at the time of the first medium change.

(2) 1 µl lentivirus (approximately 10^7 TU) was injected into each slice using a Hamilton 2.5µl syringe at 3 equidistant locations.

(3) 20 multiplicities of infection (MOI) (approximately 10^7 TU) lentivirus was diluted directly into the culture medium.

Lentiviruses were allowed to transduce the cultures for at least 2 weeks before harvesting the slices.

2.2.3 Protein extraction and fractionation

Preparation of mouse brain homogenate

Mouse brain tissue was homogenised in 1 ml ice-cold lysis buffer (Section 2.1.4) per half brain using a Dounce homogeniser. The homogenate was rotated for 30 min at 4°C before being centrifuged at 16,000 $g_{(av)}$ for 45 min at 4°C. The supernatant was collected and diluted into 2x Laemmli sample buffer prior to western blotting.

Preparation of primary cortical neuronal cell lysate

Tissue culture medium was removed from rat cortical neuronal cultures. Cells were washed in ice-cold PBS and scraped into 2x Laemmli buffer (100 µl for each well of a 6-well plate or 400 µl per 10 cm diameter dish).

Preparation of organotypic brain slice lysate

Organotypic brain slices were washed with ice-cold PBS and scraped into PBS. Brain slices were centrifuged for 30 s at 16,100 $g_{(av)}$ at 4°C to pellet the slices, and supernatant was discarded. Extra strong lysis buffer (Section 2.1.4) was added prior to sonication with a Vibra-Cell™ (Sonics & Materials, Inc., Newtown, CT, USA) with 5 pulses at 40% output. Sonicated brain slices were then centrifuged at 16,100 $g_{(av)}$ for

20 min at 4°C. The resulting supernatant (brain slice lysate) was stored at -20°C until required.

Subcellular fractionation

PBS-washed rat cortical neurons or mouse brain tissue, on ice, were lysed in 1 ml ice-cold hypotonic buffer (Section 2.1.4) per 12 x 10^6 cells. Lysed cells were sonicated using a Vibra-Cell™ (Sonics & Materials, Inc., Newtown, CT, USA) with 5 pulses at 40% output, then centrifuged at 720 $g_{(av)}$ for 5 min at 4°C to remove unbroken cells. The supernatant was centrifuged at 100,000 $g_{(av)}$ for 1 h at 4°C. The resulting supernatant (cytosol) and pellet (membrane) fractions were resuspended in RIPA buffer or 2x Laemmli buffer.

Preparation of homogenates from human post-mortem brain tissue

Frozen human post-mortem brain tissue was thawed on ice and homogenised at 100 mg tissue/ml using a mechanical homogeniser (Ultra Turrax® T8, Werke GmbH & Co., Germany). To obtain total brain homogenates, tissue was homogenised in 2x Laemmli buffer. For isolation of soluble cytoplasmic proteins, brain tissue was homogenised in TBS-EGTA buffer (Section 2.1.4), and for immunoprecipitation, brain tissue was homogenised in extra strong lysis buffer (Section 2.1.4). All homogenates were sonicated briefly using a Vibra-Cell™ for 3 pulses of 3 seconds each at 40% output. All samples were centrifuged at 16,000 $g_{(av)}$ at 4°C for 20 min. The supernatants were collected and stored at -80°C until required.

Bicinchoninic acid (BCA) protein assay

Protein concentrations of cell lysates and tissue homogenates were determined using the BCA Protein Assay Kit (Thermo Scientific, Waltham, MA, USA) (Section 2.1.4) according to the manufacturer's instructions. Briefly, 25 µl of BSA protein standard or sample diluted in lysis buffer were pipetted in duplicate into a 96-well plate. Reagent A was mixed with Reagent B at a ratio of 1:50, and 100 µl of this solution was added to each well. After incubating the plate at 37°C for 30 min, the absorbance was read at 595 nm.

2.2.4 SDS-PAGE

Samples were mixed with 2x Laemmli sample buffer, heated at 100°C for 5 min, and centrifuged for 5 min at 16,000 $g_{(av)}$. Samples and molecular weight standards were loaded onto 10% (w/v) acrylamide gels. Gels were electrophoresed at 150V until the

dye front reached the end of the gel. In some experiments, the dye front was allowed to run off the gel for a period of 20 min.

2.2.5 Colloidal Coomassie blue staining

Gels were washed three times in H_2O for 5 min each wash. ProtoBlue Safe Working Solution (Section 2.1.5) was added to cover the gels, which were then heated to 100°C for 30 s in 10 second bursts. The gels were incubated on an orbital shaker for 5 min, rinsed several times with H_2O and incubated in H_2O with agitation until protein bands were visible.

2.2.6 Western blotting

All steps were performed at ambient temperature unless otherwise stated. SDS-PAGE gels were transferred onto nitrocellulose membranes (0.45 µm, Whatman, GE Healthcare, Buckinghamshire, UK) using a Bio-Rad (Hertfordshire, UK) wet transfer system. Nitrocellulose membranes, sponges, and filter papers (11 µm, Whatman) were soaked in transfer buffer prior to assembly in the blotting cassette as follows:

Anode
Sponge
10 filter papers
Nitrocellulose membrane
Gel
10 filter papers
Sponge
Cathode

Blotting cassettes were placed in transfer buffer (Section 2.1.5) with an ice pack, and electroblotted at 100V for 60 min.

Membranes were incubated in blocking solution (Section 2.1.5) for 1 h to minimise non-specific binding of primary antibody. Membranes were then incubated overnight in primary antibody (Section 2.1.5) at 4°C. Membranes were washed three times in PBS prior to incubation in secondary antibody (Section 2.1.5) for 1 h. Finally, membranes were washed three times in PBS and antigens were visualised using the Odyssey Infrared Imaging System (LI-COR Biosciences).

2.2.7 GST fusion protein pull-down

All steps were performed at 4°C unless otherwise stated. Cells in 6-well plates were washed with 100 µl per well of ice-cold PBS prior to lysis in GST pull-down lysis buffer (Section 2.1.4) and incubated on ice for 15 min with occasional vortexing. Lysates were centrifuged at 6,000 $g_{(av)}$ for 5 min to pellet cell debris. A 50% slurry of GST-beads was washed twice in GST pull-down wash buffer prior to use. To wash the beads, triple the bead volume of wash buffer was added to the beads, which were vortexed and centrifuged briefly. The supernatant was removed and washing step was repeated once. Each lysate was pre-cleared with 20 µl bead slurry by mixing for 1 h. The beads were pelleted by brief centrifugation. 20 µl of pre-cleared supernatant was collected, mixed with 20 µl 2x Laemmli sample buffer and stored at -20°C (total lysate).

The remaining supernatant was divided in two equal fractions and each was incubated with 20 µl 50% GST-only, GST-fyn-SH2, or GST-fyn-SH3 beads (Section 2.1.3). Samples were rotated overnight and the following day, the beads were pelleted at 6,000 $g_{(av)}$ for 5 min. The supernatant was discarded, beads were washed twice with wash buffer and resuspended in 30 µl 2x Laemmli sample buffer. Samples were heated at 100°C for 10 min and centrifuged at 16,000 $g_{(av)}$ for 1 min before analysing on western blots.

2.2.8 Co-immunoprecipitation

Pharmacological treatment and lysis of primary rat cortical neurons for co-immunoprecipitation

Primary rat cortical neurons were either untreated, or treated with vehicle (DMSO) or 4 µM IC261 for 2 h at 37°C, or crosslinked using DSP for 30 min at ambient temperature. Cells were washed in ice-cold PBS prior to lysis in the appropriate buffer (Section 2.1.4). Cells were incubated on ice for 15 min with regular vortexing, before being centrifuged at 16,000 $g_{(av)}$ for 30 min at 4°C. The supernatant was collected and stored on ice for subsequent co-immunoprecipitation studies.

Preparation of mouse brain homogenate for co-immunoprecipitation

Fresh mouse brain tissue was homogenised in ice-cold lysis buffer (Section 2.1.4) using a Dounce homogeniser. The homogenate was rotated for 30 min at 4°C before being centrifuged at 16,000 $g_{(av)}$ for 45 min at 4°C. The supernatant was collected and stored on ice for subsequent co-immunoprecipitation studies.

Subcellular fractionation of mouse brain homogenate for co-immunoprecipitation

Fresh mouse brain tissue was homogenised in ice-cold hypotonic buffer (Section 2.1.4) using a Dounce homogeniser. Homogenised tissue was sonicated using a Vibra-Cell™ (Sonics & Materials, Inc., Newtown, CT, USA) with 5 pulses at 40% output, then centrifuged at 720 $g_{(av)}$ for 5 min at 4°C to remove unbroken cells. The supernatant was centrifuged at 100,000 $g_{(av)}$ for 1 h at 4°C. The resulting supernatant (cytosol) and pellet (membrane) fractions were resuspended in RIPA buffer prior to subsequent co-immunoprecipitation studies.

Pervanadate treatment

50 µl of 200 mM sodium orthovanadate was mixed with 1.6 µl of 30% (v/v) hydrogen peroxide in a final volume of 1 ml H_2O, and incubated for 5 min at ambient temperature. Excess H_2O_2 was removed by adding 2 µl of 20 µg/ml catalase, and incubated for an additional 5 min at ambient temperature. CHO cells were treated with vehicle (0.04 µg/ml catalase) or 100 µM sodium pervanadate for 20 min at 37°C. Cells were washed in ice-cold PBS prior to lysis in the appropriate buffer (Section 2.1.4). Cells were incubated on ice for 15 min with regular vortexing, before being centrifuged at 16,000 $g_{(av)}$ for 30 min at 4°C. The supernatant was collected and stored on ice for subsequent co-immunoprecipitation studies.

Co-immunoprecipitation

A 50% (v/v) slurry of Protein A agarose beads was washed twice with lysis buffer (Section 2.1.4) prior to use. To wash the beads, a volume of buffer equivalent to three times the settled bead volume was added to the beads, which were then then vortexed and centrifuged at 8,000 $g_{(av)}$ for 1 min at 4°C. The supernatant was removed and washing steps were repeated. Homogenised brain tissue, or cell lysate was pre-cleared with 50% (v/v) washed bead slurry by mixing for 30 min at 4°C. The beads were pelleted by centrifugation at 8,000 $g_{(av)}$ for 1 min at 4°C. An aliquot of the pre-cleared supernatant from the homogenised brain tissue, or cell lysate (input) was mixed with 2x Laemmli sample buffer (Section 2.1), heated at 100°C for 5 min and stored at -20°C until required.

The remaining pre-cleared supernatant was incubated with 3 µg primary antibody for 16 h at 4°C. As negative controls, lysates were also incubated with an irrelevant antibody raised in the same species, or incubated without primary antibody. Lysate/antibody mixtures were incubated with 50% (v/v) washed bead slurry for 2 h at

4°C prior to centrifugation at 6,000 $g_{(av)}$ for 1 min at 4°C. The supernatant was discarded and the pellet (immunoprecipitate) was washed twice with the appropriate lysis buffer. 2x Laemmli sample buffer was added to each immunoprecipitate prior to analysis on western blots as detailed in Section 2.2.

2.2.9 Sandwich ELISA

A 96-well plate was coated with DA31 antibody, diluted 1/500 in coating buffer (Section 0), overnight at 4°C with shaking. The plate was washed three times with washing solution (Section 0) and incubated in 200 µl blocking solution (Section 0) for 1 h with shaking at ambient temperature. After washing five times with washing solution, 50 µl cell culture medium supernatant (culture medium which had been centrifuged at 16,100 $g_{(av)}$ at 4°C to remove cell debris) was added to triplicate wells. 50 µl of anti-tau detection antibody (manufactured by DAKO), diluted 1/1,000 in antibody diluent (Section 0), was mixed with the medium and the plate was sealed and incubated overnight at 4°C with constant agitation.

The plate was washed five times with PBS before and incubated in 100 µl 1/500 HRP-conjugated anti-rabbit secondary antibody (GE Healthcare, Buckinghamshire, UK) for 1 h with shaking. After washing five times in PBS, 100 µl TMB reagent was added and the plate was incubated for 5-10 min, before stopping the reaction with 100 µl 1N hydrochloric acid. Absorbance at 450 nm was read using a Victor3™ Multilabel Plate Reader (PerkinElmer Life Sciences, Waltham, USA).

2.2.10 Cell toxicity assays

Lactate dehydrogenase (LDH) assay

Cell culture medium was centrifuged for 5 min at 16,100 $g_{(av)}$ at 4°C to remove cell debris (pellet). 50 µl cell culture medium or cell lysate, diluted in medium, was pipetted in a 96-well plate in triplicate, with cell-free medium as a blank. 50 µl LDH substrate (Section 2.1.4) was added to each well and the plate was incubated at ambient temperature, protected from light, for 30 min, after which the plate was read at 490 nm to estimate the degree of LDH release.

LIVE/DEAD assay

Cells in a 12-well plate were washed with PBS and incubated in 300 µl per well of LIVE/DEAD solution (Section 2.1.4), diluted in 1/1,000 in PBS. After incubation at 37°C in a humidified chamber with 5% CO_2 for 30 min, cells were rinsed with PBS and fixed in 4% (w/v) PFA in PBS.

2.2.11 Immunocytochemistry

All steps were performed at ambient temperature unless otherwise stated. Culture medium was removed from organotypic brain slices and washed once with PBS. Slices were fixed in 4% (w/v) PFA in PBS (Section 2.1.4) for 15 min followed by three washes in PBS. To permeabilise, slices were incubated in 0.5% (v/v) Triton X-100 in PBS overnight at 4°C. The following day, slices were blocked in 20% (w/v) BSA in PBS for 4 h, after which they were washed 3x in PBS. Primary antibodies diluted in 5% (w/v) BSA in PBS (Section 2.1.4) were incubated with slices overnight at 4°C. Following three washes in PBS, secondary antibodies diluted in 5% (w/v) BSA in PBS were applied for 4 h, removed from light. Slices were washed three times in PBS and incubated in 1µg/ml Hoescht 3342 in PBS for 3 min in the dark. Finally, slices were washed twice with PBS and mounted onto glass slides using mounting medium (DAKO, Cambridgeshire, UK). Mounted slices were stored at 4°C, protected from light, until required. Images were captured using Nikon Imaging Software Elements-Advanced Research (NIS-Elements AR) on a Nikon Eclipse Ni-E Upright microscope equipped with a CSU-X1 Spinning Disk Confocal scanning unit and Andor Ixon3 EM-CCD camera.

2.2.12 Molecular biology methods

Site-directed mutagenesis

Polymerase chain reaction (PCR)-based mutant strand synthesis

Site-directed mutagenesis was carried out using the QuikChange II XL Site-Directed Mutagenesis Kit (Agilent Technologies, Cheshire, UK) according to the manufacturer's instructions. In brief, control and experimental reactions were prepared as shown below. PCR was used with cycling parameters listed in Table 2.10 in order to amplify the mutagenesis and control reaction.

All reactions were comprised of the following reagents:
5 µl 10x reaction buffer
1 µl dNTP mix
3 µl QuikSolution reagent
1 µl *PfuUltra* HF DNA polymerase (2.5 U/µl)

Control reactions contained:
2 µl (10 ng) pWhitescript 4.5-kb control plasmid (5 ng/µl)

1.25 µl (125 ng) oligonucleotide control primer #1 (34-mer, 100 ng/µl)
1.25 µl (125 ng) olignoucleotide control primer #2 (34-mer, 100 ng/µl)

Experimental reactions contained:
5 µl (10 ng) template DNA
125 ng each (forward and reverse) mutagenesis primer

H_2O was added to a final volume of 50 µl.

Table 2.10. PCR cycling parameters for site-directed mutagenesis

Step	Cycles	Temperature (°C)	Time
1. Initial denaturation	1	95	1 min
2. Denaturation, annealing, and elongation	18	95	50 s
		60 or 68	50 s
		68	7 min
3. Extension	1	68	7 min

Dpn I digestion of the PCR product

Following PCR cycling (Table 2.10), samples were placed on ice and 1 µl *Dpn* I (10 U/µl) was added. Samples were mixed and incubated at 37°C for 1 h to digest parental DNA, leaving mutant DNA intact.

Transformation of XL10-Gold ultracompetent cells

45 µl XL10-Gold ultracompetent cells was mixed with 2 µl of β-mercaptoethanol and incubated for 10 min on ice. 2 µl *Dpn* I-treated DNA, or 0.01 ng pUC18 control plasmid, was added to the ultracompetent cells, which were incubated on ice for 30 min. The cells were heated at 42°C for 30 s and placed on ice for 2 min. 0.5 ml of preheated (42°C) LB broth was added to each tube, incubated at 37°C for 1 h with shaking at 225-250 rpm. Transformed cells were plated onto LB-ampicillin agar plates, pre-spread with 10 mM IPTG and 20 mg/ml X-gal (Section 2.1.1), and incubated overnight at 37°C.

Preparation of plasmid DNA

Individual bacterial colonies were used to inoculate 5 ml LB-ampicillin broth and incubated at 37°C for 16 h with shaking at 225-250 rpm. Plasmid DNA was isolated using the QIAprep Spin Miniprep kit (Qiagen, Manchester, UK) according to the manufacturer's instructions.

Restriction enzyme digestion

5 µl plasmid cDNA was digested with 1 U *Bam*HI and *Pme*I restriction enzymes in their corresponding buffers, according to the manufacturer's instructions (Promega, Southampton, UK). After incubation at 37°C for 1-2 h, samples were mixed with DNA loading buffer and separated on a 1% (w/v) agarose gel containing 5% ethidium bromide at 120 V for 1 h. DNA was visualised in a GelDoc-It® (UVP, Upland, CA, USA) transilluminator at a wavelength of 302 nm.

DNA sequencing

Plasmid DNA was sequenced by Eurofins MWG Operon, Wolverhampton, UK using the T7 primer.

Lentiviral tau plasmids

Wild-type (WT) human tau (2N4R), along with mutant tau P213A, tau P216A, and P219A in pcDNA3.1-V5-His-TOPO were subcloned into Lenti-GFP (Table 2.1) in a multi-step process. It was necessary to first introduce a stop codon into the WT and mutant tau constructs, before subcloning into pIRES2-EGFP vector to allow for screening of viral transduction efficacy. Finally, Tau-IRES plasmids were subcloned into the lentiviral backbone. Refer to Chapter 4 for a diagram of cloning scheme.

Introduction of stop codon in WT and mutant tau in pcDNA3.1-V5-His-TOPO

Primers were designed (Table 2.3) to introduce a stop codon at nucleotide 2297, replacing A with T to produce the stop codon TGA. Primers were designed to amplify a 230 bp fragment of tau flanking the stop codon, to include restriction sites for *BsrGI* and *EcoRV*. PCR was used with the cycling parameters listed in Table 2.11 using WT tau as template.

The reaction comprised the following reagents:
10 µl 5x GoTaq Reaction buffer (Promega, Southampton, UK)
2.5 mM dNTP mix (GE Healthcare, Buckinghamshire, UK)
1 µl (100 ng) forward primer

1 µl (100 ng) reverse primer

1 ng template DNA

0.25 µl Taq polymerase (Promega, Southampton, UK)

H_2O was added to a final volume of 50 µl.

Table 2.11. PCR cycling parameters for introduction of stop codon

Step	Cycles	Temperature (°C)	Time
1. Initial denaturation	1	95	2 min
2. Denaturation, annealing, and elongation	20	95	50 s
		65	50 s
		72	7 min
3. Extension	1	72	7 min

The PCR reaction was resolved on a 1.5% (w/v) agarose gel and the 230 bp fragment (insert) was extracted using the QIAquick Gel Extraction Kit (Qiagen, Manchester, UK) according to the manufacturer's instructions. Extracted insert DNA containing stop codon, and 1 µg of vector DNA (WT, P213A, P216A, P219A tau) was digested with *BsrGI* and *EcoRV* overnight at 37°C. Double-digested vector DNA was resolved on a 0.7% (w/v) agarose gel and double-digested insert DNA was resolved on a 1.5% (w/v) agarose gel. Insert DNA fragment (169 bp) and vector DNA fragment (6718 bp) were extracted from the agarose gel and the following reaction was set up for ligation with T4 DNA ligase using a 1:6 vector to insert molar ratio with a total of 100 ng DNA per ligation. Ligation reaction was incubated overnight at ambient temperature.

100 µl of thawed DH5α *E.coli* competent cells were incubated with 1.2 ng ligated DNA on ice for 30 min and heat-shocked for 45 s at 42°C, then placed on ice for 2 min. 900 µl of SOC medium was added to each reaction and incubated at 37°C for 1 h with shaking at 225-250 rpm. Finally, transformed cells were plated onto LB-ampicillin agar plates and incubated overnight at 37°C. Individual bacterial colonies were used to inoculate 5 ml LB-ampicillin broth and incubated at 37°C for 16 h with shaking at 225-250 rpm. Plasmid DNA was isolated using the QIAprep Spin Miniprep kit according to

the manufacturer's instructions to produce tau constructs containing a stop codon (pcDNA3.1-tau-stop).

Generation of Tau-IRES

pcDNA3.1-tau-stop was placed into a pIRES2-EGFP vector to enable GFP screening of lentiviral transduction. pcDNA3.1-tau-stop (insert) was cut out using *EcoRI* and *EcoRV*, while pIRES2-EGFP (vector) was cut with *EcoRI* and *SmaI*. Digested insert (1370 bp) and vector (5278 bp) DNA was resolved on a 0.7% (w/v) agarose gel and extracted. Vector and insert DNA were ligated overnight and used to transform DH5α cells as above. Plasmid DNA was isolated using the QIAprep Spin Miniprep kit according to the manufacturer's instructions to produce Tau-IRES.

Generation of LV-tau

Tau-IRES was then transferred to a lentiviral backbone containing the human synapsin promoter. Lenti-GFP DNA was first digested with *SpeI* and *NotI* to remove the GFP transgene, which would then be replaced with tau-IRES. Following overnight digestion of Lenti-GFP with *SpeI* at 37°C, *SpeI*-cut Lenti-GFP was heat inactivated at 80°C for 20 min and blunted with Quick Blunting Kit (New England BioLabs, Hertfordshire, UK) according to the manufacturer's instructions.

The blunting reaction contained:
4 µg *SpeI*-digested DNA
2.5 µg 10x Blunting Buffer
100 µM dNTP mix
1 µl Blunt Enzyme mix
H_2O to 25 µl

The blunting reaction was incubated at ambient temperature for 15 min then heat inactivated at 70°C for 10 min. Blunt-*SpeI*-cut Lenti-GFP was resolved and extracted from a 0.8% agarose gel, then subsequently dephosphorylated using shrimp alkaline phosphatase (rSAP).

The dephosphorylation reaction contained:
1 pmol blunted DNA
2 µl 10x rSAP Reaction Buffer
1 µl rSAP (1 unit/µl)
H_2O to 20 µl

The dephosphorylation reaction was incubated at 37°C for 20 min and heat inactivated at 65°C for 5 min. Finally, blunt-*SpeI*-cut Lenti-GFP was digested with *NotI* and extracted from a 0.8% (w/v) agarose gel to produce the cut Lenti-GFP vector (8.1 kb).

Tau-IRES was digested with *AfeI* and *NotI* to produce insert DNA size of 2.7 kb. Vector and insert DNA were ligated as above and transformed into SURE2 competent cells. 100 µl of thawed SURE2 competent cells were incubated with 2 µl β-mercaptoethanol and incubated on ice for 10 min with mixing at 2 min intervals. 2 µl ligated DNA was added and cells were incubated on ice for 30 min. Cells were then heat-shocked for 30 s at 42°C, then placed on ice for 2 min. 900 µl of LB broth was added and incubated at 37°C for 1 h with shaking at 225-250 rpm. Finally, transformed cells were plated and bacterial colonies were used to inoculate 5 ml LB-ampicillin broth as above. Plasmid DNA was isolated as above to produce lentiviral constructs expressing tau-IRES-EGFP (LV-tau).

Preparation of endotoxin-free lentiviral plasmid DNA

Plasmid DNA used to produce lentivirus stocks must be endotoxin-free. LV-tau DNA was prepared using EndoFree Plasmid Maxi Kit (Qiagen, Manchester, UK) according to the manufacturer's instructions. Briefly, a single colony was picked from plates and used to inoculate 5 ml LB broth containing the appropriate antibiotic. Bacteria were grown for 8 h at 37°C in a shaking incubator, after which 2.5 ml culture was diluted into 250 ml LB broth containing the appropriate antibiotic. Bacteria were grown overnight at 37°C in a shaking incubator before being pelleted by centrifugation at 6,000 $g_{(av)}$ for 15 min at 4°C. Pellets were resuspended in 10 ml buffer P1, lysed with the addition of 10 ml buffer P2 and incubated for 10 min at ambient temperature. The lysis reaction was stopped by addition of 10 ml buffer P3. The resulting lysates were passed through a QIAfilter® cartridge and incubated for 10 min at ambient temperature to allow the precipitate to separate. Using the plunger, lysates were filtered through the cartridges into 50 ml Falcon tubes, and 2.5 ml of endotoxin removal (ER) buffer was added to each tube in order to remove endotoxins. Lysates containing ER buffer were incubated for 30 min on ice, after which they were applied to equilibrated QIAGEN-tip 500® columns. Lysates were allowed to enter the resin by gravity flow. The columns were washed twice with 30 ml QC buffer. To elute the DNA, 15 ml of QN buffer was added to the columns and allowed to enter the resin by gravity flow. The eluted DNA was collected in 30 ml endotoxin-free tubes. 10.5 ml of isopropanol was added to the eluted DNA to precipitate the DNA, and immediately centrifuged at 15,000 $g_{(av)}$ for 30 min at 4°C. The supernatant was removed, and the pellet was washed with 5 ml of endotoxin-free 70% ethanol, before centrifuging at 15,000 $g_{(av)}$ for 10 min at 4°C. The supernatant

was carefully decanted, and the pellets were air-dried at ambient temperature for 5-10 min. The DNA pellets were resuspended in 300-500 µl of endotoxin-free Tris-EDTA (TE) buffer and stored at -20°C until required.

Preparation of lentiviruses

Lentiviruses were prepared by Penn Vector Core, University of Pennsylvania, PA, USA.

DNA extraction

Ear punches from individual $fyn^{-/-}$ and $tau^{-/-}$ mice were incubated with 20 µl digestion mix containing proteinase K (Section 2.1.3) and incubated at 55°C for 20 min. Tubes were vortexed and incubated for an additional 20 min at 55°C. 80 µl of PCR-grade H_2O was added to each sample and vortexed before heating at 100°C for 10 min to inactivate proteinase K and melt DNA strands. Finally, 20 µl of sample was diluted with 60 µl of PCR-grade H_2O and the DNA was then used for PCR genotyping. PCR cycling parameters are listed in Table 2.11.

Genotyping

PCR reaction contained:

1 µl each primer (1.25 µM) (Section 2.1.3)
1 µl DNA
10 µl REDExtract-N-Amp PCR ReadyMix (Sigma)

H_2O was added to a final volume of 20 µl.

Table 2.12. PCR cycling parameters for genotyping of $fyn^{-/-}$ and $tau^{-/-}$ mice

Genotype	Cycle
$Fyn^{-/-}$ mice	94°C for 3 min (1 cycle) 94°C for 30 s, 60°C for 45 s, 72°C for 45 s (35 cycles) 72°C for 2 min (1 cycle), 4°C hold

Tau$^{-/-}$ mice	94°C for 3 min (1 cycle) 94°C for 30 s, 60°C for 1 min, 72°C for 1 min (35 cycles) 72°C for 2 min (1 cycle), 4°C hold

Preparation of recombinant GST fusion proteins

Frozen glycerol preparations of *E.coli* containing GST- and GST-fyn-SH3-encoding plasmids were streaked across LB-ampicillin agar plates and incubated overnight at 37°C. A single bacterial colony was used to inoculate 5 ml LB-amp broth and incubated overnight at 37°C with shaking. 2.5 ml overnight culture was then added to 250 ml LB-amp broth and incubated for 2 h at 37°C with shaking until an optical density (OD) of 0.6-1.0 nm was reached. IPTG was added to the cultures to a final concentration of 1 mM and cultures were incubated for a further 2 h with shaking. The culture was then centrifuged at 20,000 $g_{(av)}$ for 15 min at 4°C to pellet the bacteria. The pellet was resuspended in 12 ml TNE buffer (Section 2.1.4) and homogenised by sonication for six 15 s bursts on ice. Triton X-100 was added to a final concentration of 1% (v/v), mixed, and the samples were centrifuged at 30,000 $g_{(av)}$ for 10 min at 4°C. The supernatant, containing GST-fusion proteins, was collected and stored on ice.

Coupling of GST-fusion proteins to glutathione beads

A 50% (v/v) slurry of glutathione-4B beads (GE Healthcare, Buckinghamshire, UK) was washed three times in TNE buffer (Section 2.1.4) to remove ethanol. 750 µl glutathione-4B beads was added per 10 ml supernatant and rotated for 90 min at 4°C, then centrifuged at 3,300 $g_{(av)}$ for 1 min at 4°C to pellet the beads. Beads coupled to GST-fusion proteins were washed three times with TNE buffer and resuspended to a 50% slurry with TNE buffer.

2.2.13 Data analysis

Statistical analyses were performed using Microsoft Excel and GraphPad Prism 5. Data were tested for normal distribution using D'Agostino-Pearson normality test. When comparing two groups, Student's unpaired t-test was used to determine statistical significance. When comparing more than two groups, one-way analysis of variance (ANOVA) with Tukey's post-hoc test was used to determine differences between groups. For non-normally distributed data, Mann-Whitney test or Kruskal-Wallis test

was used to analyse comparisons between two or more than two groups, respectively. Spearman's rank correlations were used to determine correlations between proteins. Differences were considered statistically significant if $p < 0.05$.

Chapter 3 Tau release from organotypic brain slices

Tau has a well-established role as a microtubule-binding protein, but more recently, evidence has shown that tau may have novel functions related to its positioning in additional subcellular compartments. Notably, although considered to be a predominantly axonal protein, tau is known to mislocalise to the somatodendritic compartment of neurons in AD (Hoover et al., 2010; Zempel et al., 2010; Zempel and Mandelkow, 2014).

The appearance of tau pathology in Alzheimer's disease is initially observed in the entorhinal cortex, from where it spreads to anatomically connected regions (Braak and Del Tredici, 2011; Braak et al., 2011). It was previously suggested that the spread of tau pathology could be a passive process due to the death of neurons and subsequent release of toxic pathology-causing tau species (Gómez-Ramos et al., 2006; Simón et al., 2012b). However, several groups have now shown that tau pathology spreads through anatomically-connected regions of the brain, but the underlying mechanisms of this propagation has thus far been unclear (de Calignon et al., 2012; Liu et al., 2012; Clavaguera et al., 2013; Ahmed et al., 2014; Peeraer et al., 2014). Restricting expression of FTDP-17T-associated P301L tau to the entorhinal cortex in a transgenic mouse model showed trans-synaptic propagation of tau pathology (de Calignon et al., 2012; Liu et al., 2012). As the P301L tau mice aged, mutant tau pathology developed in an anterograde fashion through synaptically connected regions from the entorhinal cortex to the dentate gyrus. Initially it was proposed that tau pathology spread via tau release upon cell death and uptake by neighbouring cells (Gómez-Ramos et al., 2006; Frost et al., 2009; Simón et al., 2012b). However, evidence from cell studies now shows that tau can be found extracellularly, even in the absence of disease or cell death (Chai et al., 2012; Simón et al., 2012a; Pooler et al., 2013a). Taken together, these studies suggest that synaptic activity, rather than diffusion, may be involved in the transmission of tau pathology. Furthermore, *in vivo* microdialysis detected tau in the interstitial fluid of mice expressing either WT or P301L tau, further suggesting that tau may be released from neurons under both physiological and pathological conditions (Yamada et al., 2014). Taken together, these studies suggest that synaptic activity may be involved in the transmission of tau pathology, rather than tau spread occurring passively by the diffusion of mutant tau.

Several groups have shown that tau can be released from non-neuronal cells overexpressing tau, induced pluripotent stem cell-derived neurons, lamprey neurons, and mouse primary cortical neurons (Karch et al., 2012; Lee et al., 2012; Plouffe et al., 2012; Saman et al., 2012; Simón et al., 2012a; Pooler et al., 2013a; Mohamed et al.,

2014). These reports include studies from this laboratory showing that tau can be released from cultured primary cortical neurons following stimulation of neuronal activity by KCl or AMPA receptor agonists. Importantly, this secretion of tau is not accompanied by cell death, suggesting that tau release is a physiological process in healthy neurons that can be regulated by neuronal activity (Pooler et al., 2013a). Since tau spreads trans-synaptically in mouse brain (de Calignon et al., 2012; Liu et al., 2012), and tau release from neurons is activity-dependent and stopped upon blockade of pre-synaptic vesicle release (Pooler et al., 2013a), this suggests that synaptic activity may modulate release of physiological and pathogenic tau.

The mechanisms controlling the secretion of tau from neuronal cells remain to be elucidated. The phosphorylation state of tau can modify several tau functions, such as microtubule binding and association with membranes (Lindwall and Cole, 1984; Pooler et al., 2012). However, it is unclear whether tau phosphorylation and the activity of protein kinases affect tau release. This laboratory reported previously that fyn, a non-receptor-associated tyrosine kinase, was necessary for the phosphorylation-dependent movement of tau from the cytosol to the membrane (Pooler et al., 2012). Since fyn is required for trafficking of intracellular tau to the membrane, it is possible that fyn may also play a role in regulating the secretion of tau from healthy neurons.

Furthermore, the role of Aβ in tau propagation is unknown. The spread of tau pathology does not require the presence of toxic Aβ oligomers, as seen from several transgenic mouse models that harbour tau mutations (de Calignon et al., 2012; Liu et al., 2012; Michel et al., 2014). However, since Aβ exerts toxic effects on synapses, both indirectly and directly, and tau release is regulated by synaptic activity, it is important to determine whether Aβ can also alter tau release, as this could have implications for disease (Shankar et al., 2008; Ittner et al., 2010; Ripoli et al., 2014). Although soluble Aβ oligomers applied to primary cortical neurons did not appear to affect activity-dependent tau release (Pooler et al., 2013a), it is important to test the effects of Aβ in a more physiologically relevant system to better inform studies of potential synergistic effects between tau and Aβ.

In vivo studies using animal models are invariably the most physiologically relevant system available, but this requires extensive use of animals and high cost. Therefore culture of non-neuronal cells and primary neurons is frequently used to mitigate some of the disadvantages of using animal models. Despite their widespread use, primary neurons remain an imperfect *in vitro* model of a living animal. However, the use of non-neuronal cells to investigate mechanisms of disease is questionable, as this usually involves overexpression of exogenous target protein which could generate artifactual

data. Primary neurons are typically maintained as a monolayer and other components of the neuronal system are missing, such as glial cells and the complex connectivity that exists between neural cell types *in vivo* (Duff et al., 2002).

Long-term organotypic brain slice cultures are an attractive alternative to primary neurons and mouse models, as they retain synaptic plasticity and the cytoarchitecture of the brain *in vivo*, including a good representation of physiological neural cell composition (Gähwiler et al., 1997). Large numbers of brain slices can be prepared from a single animal, lessening the impact of animal use in research (Figure 3.1) (Duff et al., 2002).

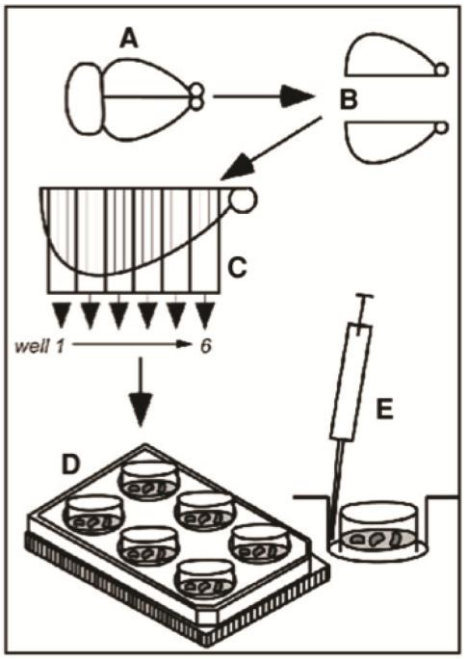

Figure 3.1 Schematic of organotypic brain slice preparation.

Organotypic brain slices are prepared from postnatal mouse pups. (A) The cortex is first bisected (B) and sliced into 350 µm sections (C) before plating on a cell culture plate lined with membrane inserts (D). Medium exchange of brain slices is carried out every two to three days (E). Image from (Duff et al., 2002).

It has been shown that organotypic hippocampal slices prepared from rat brain are developmentally comparable with acute hippocampal slices, when analysing synaptic transmission and morphology of spines (De Simoni et al., 2003). In contrast to acute slices, organotypic brain slices are also able to survive in long-term culture, which is advantageous for studies of neurodegeneration as this is usually a long-term process that cannot be replicated in acute slice cultures (Cho et al., 2007). Organotypic brain slices also offer an advantage over acute slices in that organotypic cultures recover from the slicing procedure and cells that have been damaged during dissection are removed after adaptation to the culture environment within 2-3 weeks (Gähwiler, 1981). Indeed, cultures of organotypic brain slices have previously been generated from P301S transgenic mice as a model of tauopathy (Mewes et al., 2012). Organotypic brain slices have also been used to evaluate drugs targeting tau aggregation (Congdon et al., 2012; Messing et al., 2013). Moreover, organotypic brain slices have been used to study a variety of other processes such as white matter injury, axonal regeneration, and epilepsy (Stoppini et al., 1997; Dean et al., 2011; Morin-Brureau et al., 2013). Once optimized, this technique provides a more physiological system than cell lines and primary neurons in which to model interactions between tau and fyn in normal and pathogenic conditions.

In the work described herein, we sought to further investigate neuronal tau release from organotypic brain slices prepared from WT and $fyn^{-/-}$ mice. The aims of this chapter were to establish whether (1) tau is secreted by organotypic brain slices under basal conditions and following stimulation of neuronal activity, (2) fyn is involved in this process, and (3) soluble Aβ oligomers affect tau release in a physiologically relevant model.

3.1 Results

3.1.1 Characterisation of wild-type and $fyn^{-/-}$ organotypic brain slices

The mechanisms underlying the release of tau are not clear, although they have been studied in various model systems. Mounting evidence supports the hypothesis that tau release from neurons is regulated by synaptic activity. Therefore, in order to ensure that tau release could be investigated in organotypic brain slices, these were initially characterised to investigate the expression of tau protein and synaptic proteins. Organotypic brain slices were also examined by immunocytochemistry to analyse the cytoarchitecture and arrangement of neurons and glia.

WT organotypic brain slices prepared from P9-10 mouse pups were prepared and cultured for 28 DIV before being harvested and fixed with PFA. Several studies report the presence of a ‘glial scar’ either on top or beneath brain slices maintained in long-term culture (del Rio and Soriano, 2010). In order to verify this, slices were stained with MAP2, a neuron-specific dendritic marker, GFAP, an astrocytic marker, and Hoescht 33342 to indicate nuclei. Double immunostaining with GFAP and MAP2 for astrocytic and neuronal cells shows the retained cytoarchitecture of the cortex by epifluorescence microscopy (Figure 3.2A). Slices were also labelled with tau and GFAP antibodies. Using confocal microscopy, representative images taken from the top, middle, and bottom of the slice show a higher density of GFAP-positive cells clustered on the top and bottom layers of the slice (Figure 3.2B). In contrast, tau-positive cells appear primarily between these layers of astrocytes, suggesting the presence of a ‘glial scar’ in long-term organotypic brain slices.

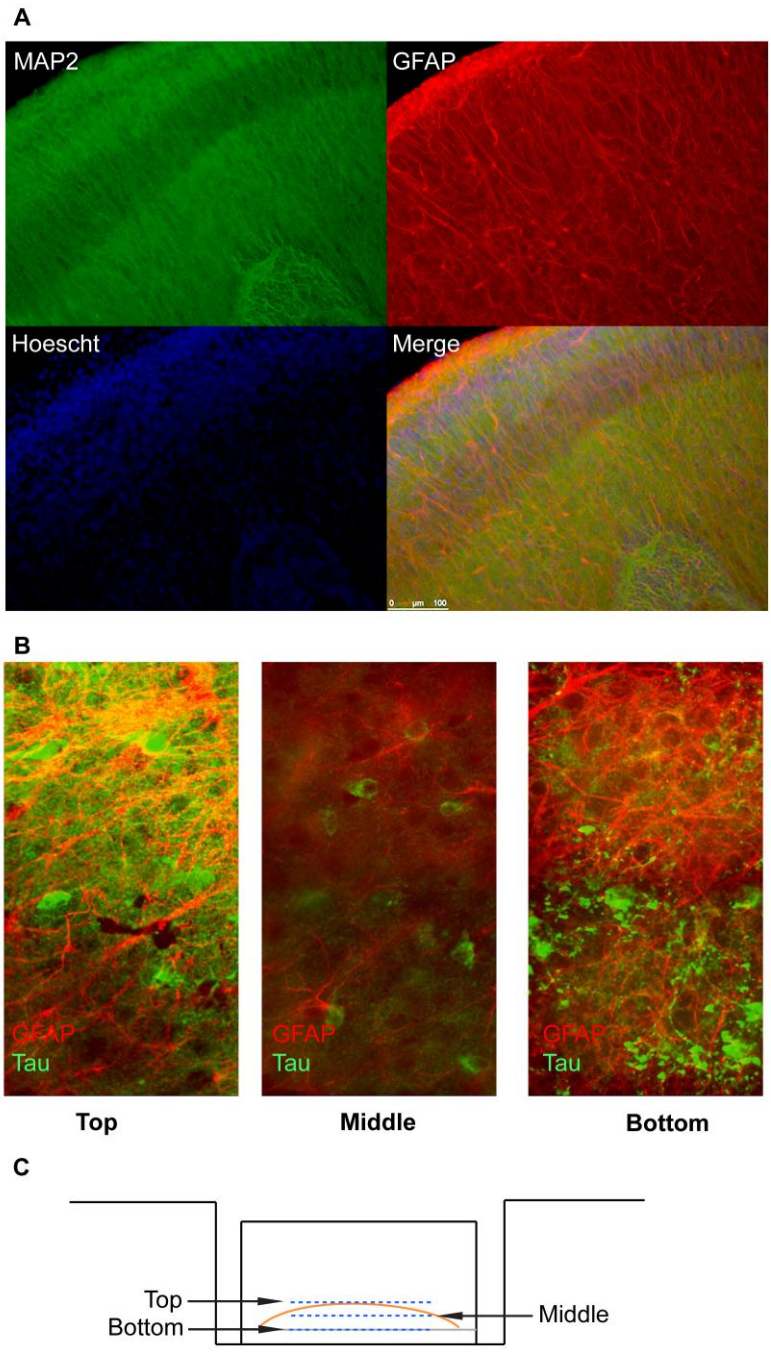

Figure 3.2 Immunocytochemistry of organotypic brain slices

Characterisation of 28 DIV wild-type organotypic brain slices by immunocytochemistry. (A) Slice stained with MAP2 (green), GFAP (red), and Hoescht 33342 nuclear marker (blue) shows that brain slices retain much cytoarchitecture of the intact brain. (B) Z-stack images from a confocal microscope showing image of a slice stained for tau (green) and GFAP (red). Top (left panel) and bottom (right panel) images show intense staining of GFAP-positive astrocytes. (C) Diagram of transverse view of brain slice (orange) in culture. Dashed lines (blue) indicate approximate planes of confocal images taken in (B).

It was next important to examine any differences between WT and fyn$^{-/-}$ organotypic brain slices. These were cultured for 14, 28, and 42 DIV before being harvested. Some brain slices did not remain viable for 42 DIV and, in these cases, only the earlier time points were investigated. Slices from each time point were lysed and processed together in order to reduce variability between experimental conditions. Slice lysates were analysed on western blots and quantified data were normalised to values for WT 14 DIV samples within each experimental repeat. The results show that there was no difference in the amount of tau present between WT and fyn$^{-/-}$ brain slices. Furthermore, increasing the time in culture from 14 to 42 DIV did not result in any change in the amount of tau present in either WT or fyn$^{-/-}$ brain slices (Figure 3.3A). Immunoblots probed with an antibody against dephosphorylated tau at S199/S202 (Tau-1) showed similar results to those obtained for total tau and there were no apparent changes in phosphorylation at this epitope over time in either WT or fyn$^{-/-}$ brain slices (Figure 3.3B). In contrast, an antibody against tau phosphorylated at S396/S404 (PHF-1) revealed significantly less PHF-1 tau, relative to total tau, present in fyn$^{-/-}$ brain slices at both 14 and 28 DIV compared to WT brain slices (Figure 3.3C). However, by 42 DIV, the amount of PHF-1 was similar in both WT and fyn$^{-/-}$ brain slices. These results show that whilst the amount of total tau and tau dephosphorylated at S199/S202 in WT and fyn$^{-/-}$ brain slices is similar for culture periods up to 42 DIV, tau phosphorylated at S396/S404 is decreased in fyn$^{-/-}$ brain slices, at least up to 28 DIV.

In order to investigate expression of synaptic proteins, western blots were probed with antibodies against pre-synaptic (synaptophysin) and post-synaptic (drebrin and PSD-95) proteins. Drebrin was present in WT brain slices at each of the three ages examined, but the amount of drebrin present was diminished at 42 DIV, although this did not reach significance when compared to 14 DIV (Figure 3.3D). This is consistent with previous reports of changes in developmental drebrin expression in rat brain tissue (Shirao et al., 1989). There are two isoforms in the rat, drebrin-E (embryonic) and drebrin-A (adult) which run at 130 and 140 kDa, respectively (Shirao et al., 1989). As the two bands may not be distinguishable on western blots, reduced density of drebrin bands in older slices may reflect loss of the embryonic drebrin band. The amount of drebrin in fyn$^{-/-}$ brain slices was significantly reduced at 28 DIV in fyn$^{-/-}$ compared to WT brain slices, indicating a possible difference in the development of dendritic spines between WT and fyn$^{-/-}$ brain slices maintained in long-term culture (Figure 3.3D). At 42 DIV, fyn$^{-/-}$ brain slices did not express any drebrin, indicating potential loss of viability in fyn$^{-/-}$ brain slices at this age.

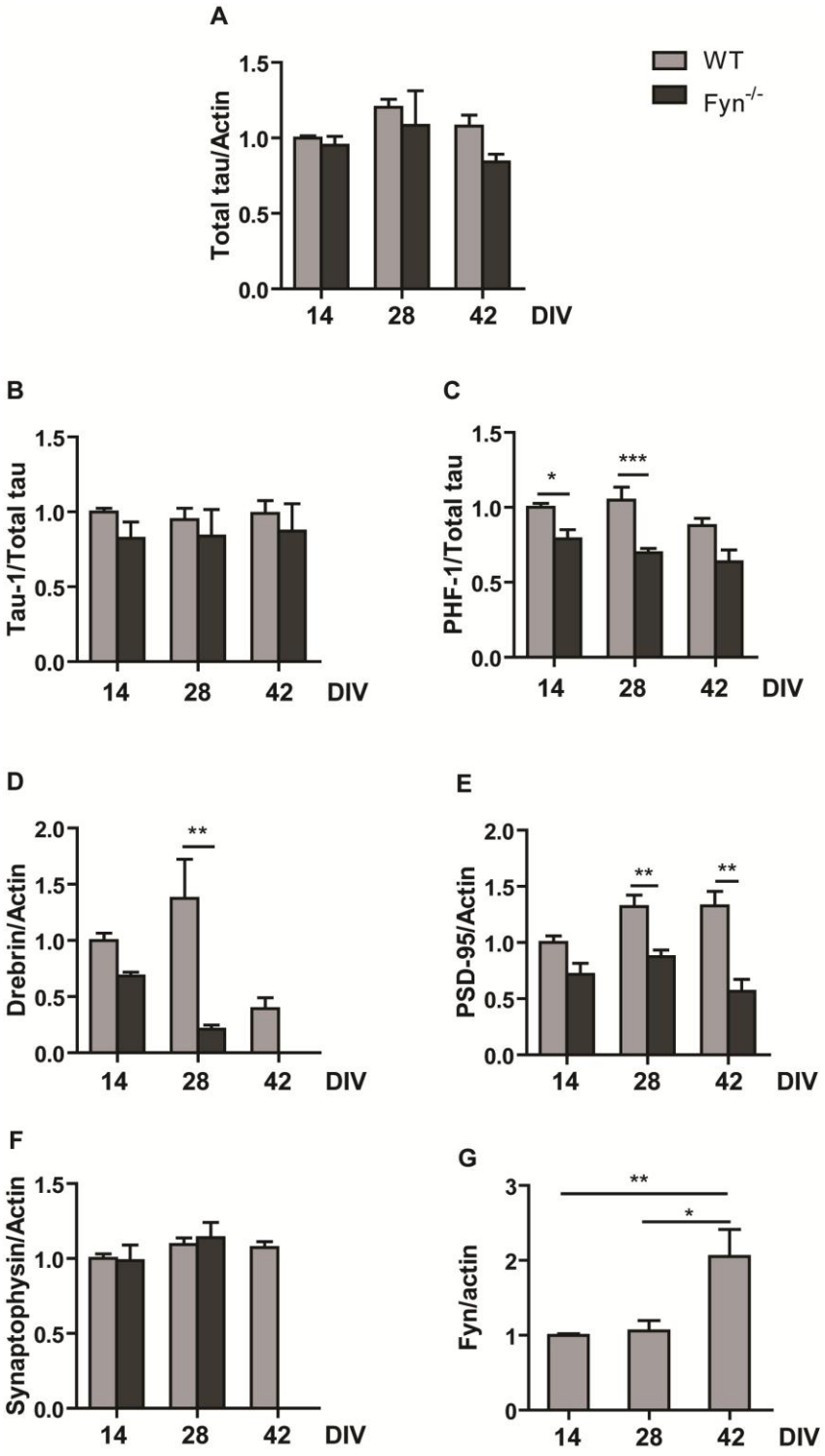

Figure 3.3 Characterisation of organotypic brain slice cultures

Quantification of (A) total tau, (B) tau-1 (tau dephosphorylated at S199/S202), (C) PHF-1 (tau pS396/S404), (D) drebrin, (E) PSD-95, (F) synaptophysin, and (G) fyn in WT (light grey bars) and fyn$^{-/-}$ (dark grey bars) cultured brain slices at 14, 28, and 42 days *in vitro* (DIV). Values represent mean ± SEM, n = 3-12. Two-way ANOVA with post-hoc Bonferroni's test, *$p < 0.05$, **$p < 0.01$, ***$p < 0.001$.

The amount of PSD-95, a post-synaptic scaffolding protein, was approximately equivalent in 14 DIV WT and fyn$^{-/-}$ slices, but it was significantly reduced in fyn$^{-/-}$ brain slices at 28 and 42 DIV compared to WT brain slices cultured for the same amount of time (Figure 3.3E). In contrast, synaptophysin was detected in similar amounts at all ages in WT brain slices and synaptophysin expression was not significantly different between WT and fyn$^{-/-}$ brain slices at 14 and 28 DIV (Figure 3.3F). However, synaptophysin was not detectable in fyn$^{-/-}$ slices at 42 DIV, which could indicate loss of cell viability at this age.

WT slices were also probed with an antibody against fyn, which showed that the amount of fyn remained stable at 14 and 28 DIV, but this increased approximately two-fold at 42 DIV (Figure 3.3G). The relative stability of synaptophysin and PSD-95 expression over time from 14 to 42 DIV suggests that the synaptic machinery such as synaptic vesicle scaffolding has been developed by 14 DIV and that slices are mature, at least for WT slices. Relative to WT brain slices, these results indicate that fyn$^{-/-}$ brain slices may have less developed dendritic spines as reflected by the decreased expression of drebrin and PSD-95 compared to WT. However, synaptophysin was not significantly different from WT brain slices. As the following experiments required use of reagents that would affect synaptic activity, such as KCl and Aβ, it was important to examine the expression of synaptic markers over time to select an appropriate age of slices for subsequent experiments. Based on these findings, slices cultured for periods between 28-42 DIV were used to strike a balance between slice viability and slice maturity.

3.1.2 Tau is secreted upon stimulation of neuronal activity in organotypic brain slices

Stimulation of neuronal activity by treatment with KCl and AMPA receptor agonists has been shown to induce the release of tau in primary neurons without affecting cell viability (Pooler et al., 2013a). As organotypic brain slices are a more physiologically relevant model than primary neurons in culture, basal and stimulated tau release was investigated in organotypic brain slices.

Organotypic brain slices exhibit relatively stable expression of synaptophysin and PSD-95 between 14 to 42 DIV, hence organotypic brain slices between 28-42 DIV were used to investigate tau release in this model system. Slices were washed with Hank's buffered saline solution (HBSS) to remove all traces of protein in the media before being treated with vehicle or 50 mM KCl for 30 minutes in HBSS containing calcium and magnesium. This concentration of KCl was selected because it has been shown to induce neuronal activity in primary neurons without affecting cell viability (Toescu, 1999; Zhou et al., 2009). In addition, concentrations up to 100 mM KCl have been used to stimulate neuronal activity for *in vivo* microdialysis studies for periods up to one hour without loss of neuronal viability (Yamada et al., 2014).

After exposure of slices to 50 mM KCl for 30 minutes, the conditioned medium was collected and analysed using a sandwich ELISA. This ELISA is optimised for detection of tau, using DA31 as the coating antibody, and tau (DAKO, Cambridgeshire, UK) as the capture antibody. Medium that did not come into contact with cells (unconditioned medium), but which was incubated for the same length of time in a humidified incubator with 5% CO_2, was used as a negative control and as a blank for the ELISA. Slices were harvested, lysed in hypotonic buffer, and the protein concentration of the slice lysates were determined by BCA assay (Section 2.2.3).

The intracellular compartment from which extracellular tau is derived is currently unknown. Studies have shown that in addition to cytosolic tau, a small proportion of tau localises to the plasma membrane. We found previously that the presence of fyn is required for trafficking of tau from the cytosol to the plasma membrane (Pooler et al., 2012). Thus, one possibility is that part of the pool of membrane-associated tau may be released into culture medium. Since fyn is necessary for the movement of tau from the cytosol to the membrane, it is reasonable to propose that fyn may also be involved in the release of membrane-associated tau. Therefore, organotypic brain slices from WT and $fyn^{-/-}$ mice were treated with vehicle or KCl for 30 minutes and the amount of tau released into the medium was measured using the sandwich ELISA.

In order to measure cell death, a lactate dehydrogenase (LDH) assay was used. LDH is a stable enzyme that is released from cells following damage to the plasma membrane, allowing for a quantitative assay in which LDH release is coupled to an enzymatic, colorimetric reaction. The amount of LDH released into the medium is compared to the total (intracellular and extracellular) amount of LDH present, to provide an indicator of the degree of cell death.

The amount of tau released from slices in the presence or absence of KCl was standardised to the protein concentration of the corresponding slice lysate. The amount of tau released into the medium from unstimulated WT brain slices was used to normalise the amount of tau release under different experimental conditions. Following KCl treatment, there was a statistically significant increase in tau release of approximately ten-fold in WT slices compared to unstimulated WT brain slices (Figure 3.4A). The proportion of LDH released increased from 2% to 4% of total LDH in KCl-treated slices, indicating that the release of tau was not due to the disintegration of the plasma membrane, but instead represents a physiological process in healthy brain slices (Figure 3.4B). There was no statistically significant difference between the amount of tau released from WT and $fyn^{-/-}$ slices not exposed to KCl (Figure 3.4A, $p > 0.05$). When $fyn^{-/-}$ slices were exposed to KCl, there was an approximate eight-fold increase in tau release compared to unstimulated $fyn^{-/-}$ slices (Figure 3.4A), which was similar to that observed in WT slices exposed to KCl. Similarly, the amount of LDH released was not significantly altered by the lack of fyn in the presence or absence of KCl (Figure 3.4B). These results show that KCl stimulates tau release in organotypic brain slices as well as in primary neurons and that the presence of fyn does not appear to affect this process. This suggests that, while fyn is necessary for phosphorylation-dependent translocation of tau to the membrane, it is not required for tau release, indicating that tau secretion may be regulated by non-fyn-dependent mechanisms.

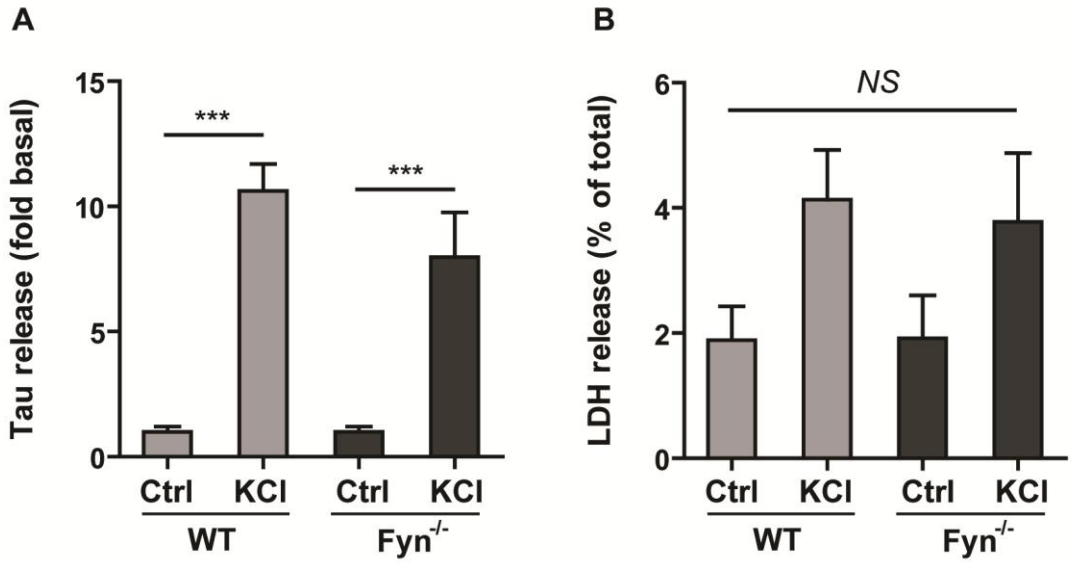

Figure 3.4 Tau release from organotypic brain slices from WT and fyn$^{-/-}$ mice

Tau release into culture medium from WT (light grey bars) or fyn$^{-/-}$ (dark grey bars) organotypic brain slices, with or without exposure to 50 mM KCl for 30 min, was quantified by sandwich ELISA, *n* = 16-27 (A). (B) The amount of LDH released was not significantly increased in KCl-treated slices compared to control, *n* = 10-13. Values represent mean ± SEM. One-way ANOVA with post-hoc Tukey's test, ***$p < 0.001$, *NS* = not significant.

Whole cell lysates of control and KCl-treated WT and fyn$^{-/-}$ organotypic brain slices were analysed on western blots to determine if KCl might affect the amount of intracellular tau. These results show that there was no difference in the amount of intracellular tau present in KCl-treated slices compared to untreated controls in either WT or fyn$^{-/-}$ slices (Figure 3.5). This suggests that the amount of tau released extracellularly is a small proportion of the total amount of intracellular tau.

Taken together, these results show that tau can be released into the extracellular space and that this is dependent on neuronal activity. The absence of fyn does not appear to regulate the release of tau under these experimental conditions.

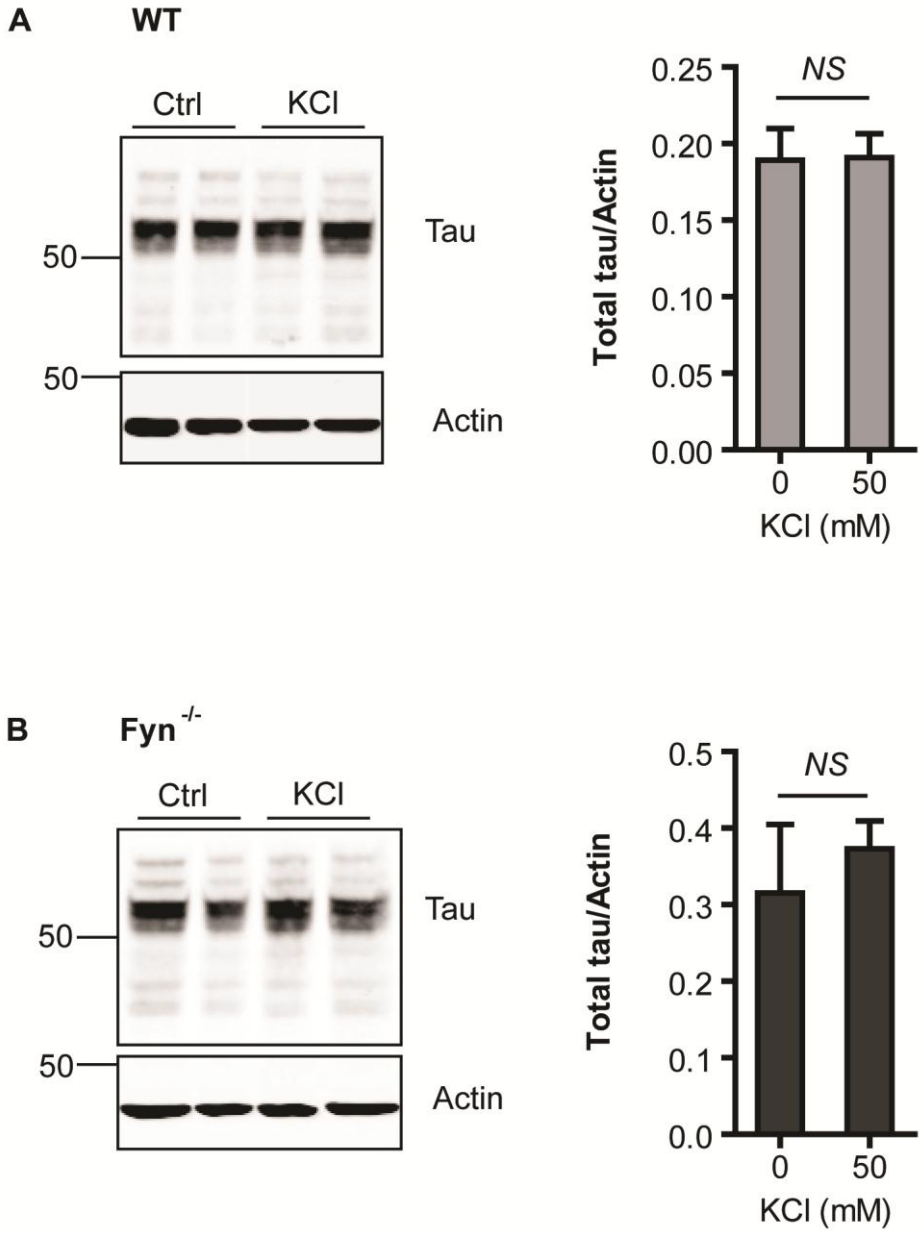

Figure 3.5 No detectable change in intracellular tau following exposure to KCl

Representative western blots of whole cell lysates of (A) WT or (B) fyn$^{-/-}$ organotypic brain slices treated with 50 mM KCl or vehicle. Molecular weight markers are shown on the left (kDa). Values represent mean ± SEM, *n* = 4-6. Student's t-test, *NS* = not significant.

3.1.3 Investigating the uptake of extracellular tau

The spreading of tau pathology is of great interest for the tauopathies, but the mechanisms of transmission are currently unclear. It has been shown that pathological tau may propagate between neurons in a manner dependent on synaptic connectivity.

Therefore, it is important to determine whether tau secreted in response to neuronal stimulation can be taken up by connected neurons, as a possible pathogenic mechanism. To do this, brain slices were prepared from tau$^{-/-}$ mice to see whether tau could be detected in these slices following exposure to extracellular tau derived from KCl-stimulated WT brain slices.

WT brain slices were treated with vehicle or 50 mM KCl for 30 min in HBSS containing calcium and magnesium to stimulate tau release. In parallel, a negative control comprising cell-free HBSS containing calcium and magnesium was incubated for 30 min at 37°C in a humidified incubator. After 30 min, conditioned (vehicle-treated and KCl-treated) medium and cell-free (unconditioned) medium was collected and centrifuged to remove debris. Separately maintained tau$^{-/-}$ slices were washed and exposed to vehicle-treated, KCl-treated, or unconditioned medium collected from the stimulated WT slices. The tau$^{-/-}$ slices were then incubated for 4 hours at 37°C in a humidified incubator before being harvested in hypotonic buffer. Tau$^{-/-}$ slices were then fractionated into membrane and cytosolic fractions to determine whether exogenous tau was membrane-associated or internalised into the cytosol. All fractions were run on western blots and probed with antibodies against tau to detect any uptake of tau. Lysates of WT brain slices were included as a positive control.

Probing the tau$^{-/-}$ slices exposed to tau-containing medium with an antibody against tau showed that no tau was detectable in any of the three conditions used (KCl, control, and unconditioned) in either total slice lysates or in membrane or cytosolic fractions, even at higher exposures (Figure 3.6). It had been determined previously that full-length, intact tau was amongst the tau species released upon stimulation of neuronal activity in primary neurons (Pooler et al., 2013a). However, in this experiment, there was no evidence of full-length, intact tau of the expected, molecular weight (~50 kDa), nor were any smaller cleaved fragments of tau detectable on western blots following exposure of tau$^{-/-}$ slices to tau-containing medium (Figure 3.6). The positive control of WT brain slice lysate shows that the tau antibody is able to detect tau, and sufficient protein loading was determined by probing with an antibody against β-actin. Membrane fractions were loaded in equivalent protein proportions to cytosolic fractions, so the decreased amount of β-actin in the membrane fraction reflects the greater abundance of β-actin in the cytosol relative to the membrane. Therefore, these results suggest that the absence of detectable tau in these preparations is not due to a lack of binding with tau antibody but rather that there is an insufficient amount of tau protein present in the tau$^{-/-}$ slices when incubated with conditioned medium containing secreted tau.

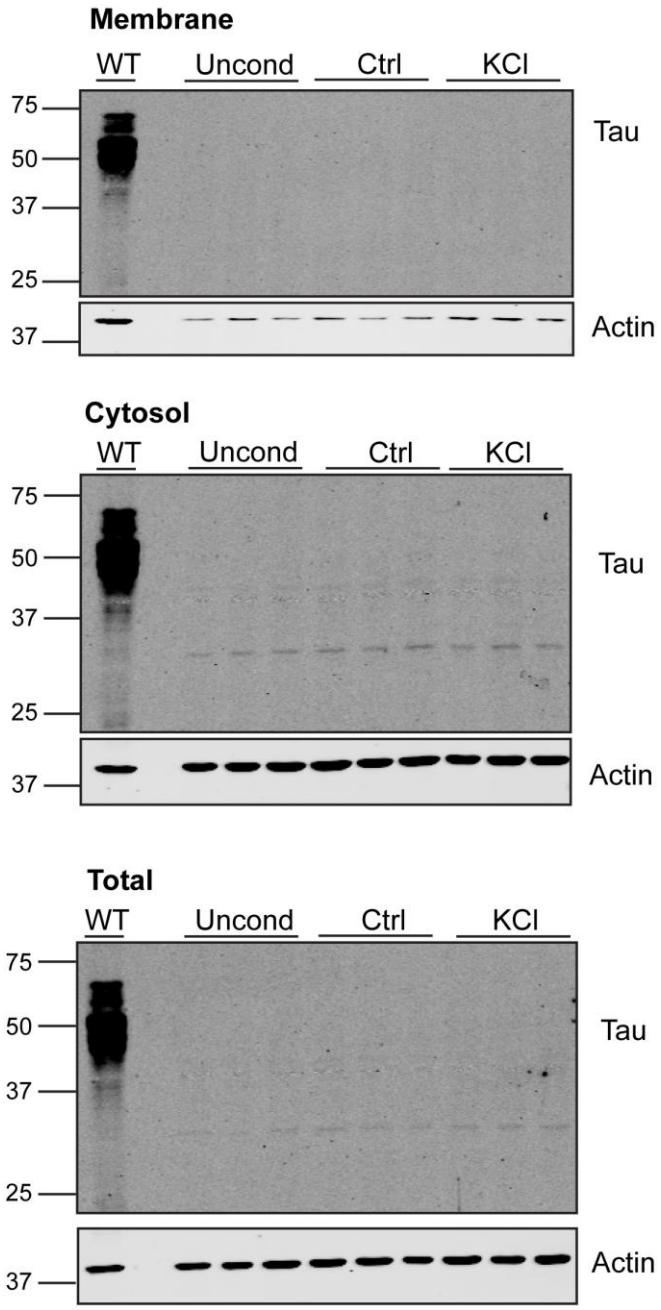

Figure 3.6 Tau uptake by tau$^{-/-}$ organotypic brain slices

Western blots of tau$^{-/-}$ organotypic brain slices treated with conditioned culture medium from WT slices exposed to 50 mM KCl or vehicle (Ctrl). Cell-free unconditioned medium (Uncond) was used as a negative control. Tau at the expected size (50 kDa) was not observed in membrane, cytosol, or total fractions. Whole cell lysate from WT slices was used as a positive control for tau. Molecular weight markers are shown on the left (kDa).

3.1.4 Characterisation of soluble Aβ oligomers

The aim of the following experiments was to determine whether soluble Aβ oligomers would have any effect on the release of tau from organotypic brain slices. First it was necessary to characterise the species of Aβ present in the preparation of soluble Aβ oligomers.

Human $Aβ_{1-42}$ peptide was used to prepare soluble Aβ by dissolving $Aβ_{1-42}$ peptide in autoclaved DI water, as this has been shown to reliably produce predominantly soluble Aβ species of oligomers and monomers (Town et al., 2002; Garwood et al., 2011; Atherton et al., 2014). In order to determine the species of soluble Aβ present in this preparation, 5 µg of freshly prepared 250 µM soluble Aβ was mixed with 2x Novex® Tricine SDS sample buffer (Life Technologies, Paisley, UK), heated for 5 min at 100°C before resolving on a 16% Tricine gel (Life Technologies, Paisley, UK). Western blots were incubated with the 4G8 antibody, which recognises amino acids 17-24 of Aβ and labels low molecular weight Aβ oligomers. Figure 3.7A shows that 4G8 recognises a predominant Aβ species of ~4-5 kDa, equivalent to monomeric Aβ, with a smaller proportion of the sample being composed of low molecular weight oligomers of 13 and 16 kDa, indicating the presence of Aβ trimers and tetramers. A minor proportion of this soluble Aβ preparation is comprised of 8 kDa dimers of Aβ (Figure 3.7A). It is possible that Aβ oligomers of higher molecular weight than the tetrameric forms are present in small amounts that are undetectable by 4G8, but the ratio of monomeric and oligomeric species of Aβ is similar to that reported previously by others (Town et al., 2002). Therefore, as this preparation is largely monomeric, concentrations of 10 µM Aβ or below should not contain significant amounts of toxic oligomeric species of Aβ.

Prior to treating organotypic brain slices with Aβ, each individual batch of Aβ was tested on cultures of primary rat cortical neurons to ensure the effectiveness of each Aβ preparation at inducing neuronal death and the expected changes in intracellular proteins, such as increased tau phosphorylation. 12 DIV primary rat cortical neurons were treated with 10 µM Aβ in Neurobasal® medium containing B27 and L-glutamine. Phenol red has previously been shown to interfere with the effects of Aβ and thus phenol red-free medium was used for these experiments (Ono et al., 2003; Porat et al., 2004; Necula et al., 2007). Neurons were treated with 0.5 µM staurosporine, which activates caspase-dependent apoptotic pathways (Yue et al., 1998; Zhang et al., 2004), as a positive control for cell death. Neurons were exposed to Aβ, vehicle (H_2O), or staurosporine for 48 hours before being harvested for cell toxicity assays, as described below.

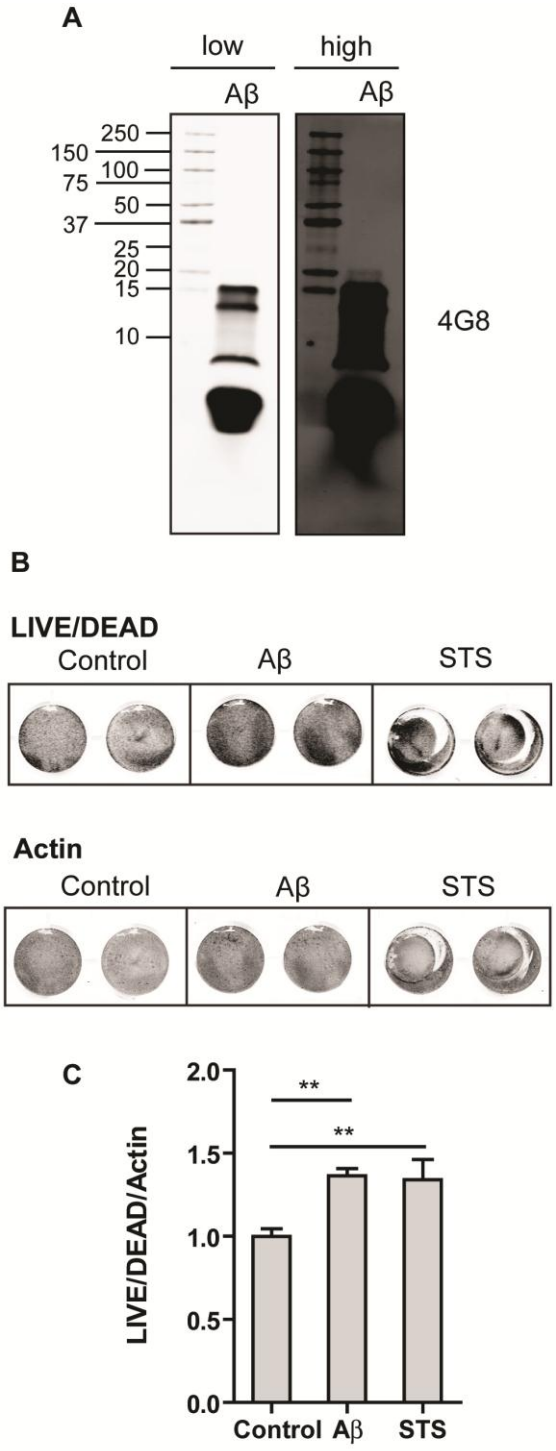

Figure 3.7 Characterisation of the soluble Aβ oligomeric preparation

(A) Western blot of 5 µg soluble Aβ oligomers at low and high exposures with an antibody against Aβ (4G8). Molecular weight markers are shown on the left (kDa). (B) Primary rat cortical neurons were treated with vehicle, 0.5 µM staurosporine (STS), or 10 µM soluble Aβ for 48 hours to assess neurotoxicity. Quantification of LIVE/DEAD, normalised to β-actin, shows significantly increased labelling of LIVE/DEAD in Aβ- and STS-treated neurons compared to control (C). Values represent mean ± SEM, n = 4-6. One-way ANOVA with post-hoc Dunnett's test, $^{**}p < 0.01$.

Cell toxicity was measured using a LIVE/DEAD assay, which enables quantitation of fluorescent ethidium homodimer-1 in cells with compromised membrane integrity. After incubating neurons with LIVE/DEAD according to the manufacturer's instructions, neurons were fixed and stained with β-actin as an internal control, before quantifying the ratio of LIVE/DEAD to β-actin staining using the Odyssey scanner. Under these conditions, Aβ induced cell death to a degree that was 1.3-fold higher than that of vehicle-treated control neurons which was statistically significant ($p < 0.01$) (Figure 3.7C).

3.1.5 Effects of soluble Aβ treatment on organotypic brain slices

As discussed above, the effects of Aβ, and potential interactions between Aβ, tau and fyn on tau release and propagation are not well understood. To determine if the effects of Aβ on tau release could be investigated in organotypic brain slice cultures, it was first necessary to determine the activity of Aβ in this model. The aim of this study was therefore to determine the effects of Aβ on tau phosphorylation and trafficking, and whether fyn could mediate the toxic effects of Aβ in organotypic brain slices.

The cytoskeletal protein α-spectrin undergoes calpain- and caspase-3-mediated cleavage in human post-mortem AD brain tissue (Atherton et al., 2014). α-Spectrin is a protein of 240 kDa, which is cleaved by calpain-1 and caspase-3, to generate 145-150 kDa fragments, or a 120 kDa fragment, respectively (Bahr et al., 1995; Martin et al., 1995). Exposure to Aβ has been shown to induce cleavage of α-spectrin in cultured primary neurons (Lee et al., 2000; Nicholson and Ferreira, 2009). Therefore, α-spectrin cleavage was examined following Aβ treatment in 21 DIV organotypic brain slices treated with 10 μM soluble Aβ for 24 or 48 hours. Slices were harvested and soluble proteins were extracted for protein analysis on western blots.

In contrast to previously reported findings in human AD brain, there were no significant changes in α-spectrin in Aβ-treated slices compared to vehicle-treated control slices. The amount of 140-150 kDa cleaved α-spectrin fragments as a proportion of total α-spectrin was equivalent in Aβ-treated and control slices, indicating that calpain cleavage was minimal under these conditions (Figure 3.8A,C). Similarly, there was no significant change in the amount of the 120 kDa caspase-cleaved product induced by Aβ as a proportion of total α-spectrin (Figure 3.8B,C). To further investigate changes in caspase-3 activity, blots of Aβ-treated slices were probed with an antibody that specifically recognises the active form (cleaved) of caspase-3. In both vehicle-treated control and Aβ-treated slices, there were no bands at the expected size (17 and 19 kDa) for cleaved caspase-3 (Figure 3.8D). This may be due to batch-dependent variability of the antibody, as the same antibody has previously been shown to label bands of the expected size in rat primary neurons (Garwood et al., 2011).

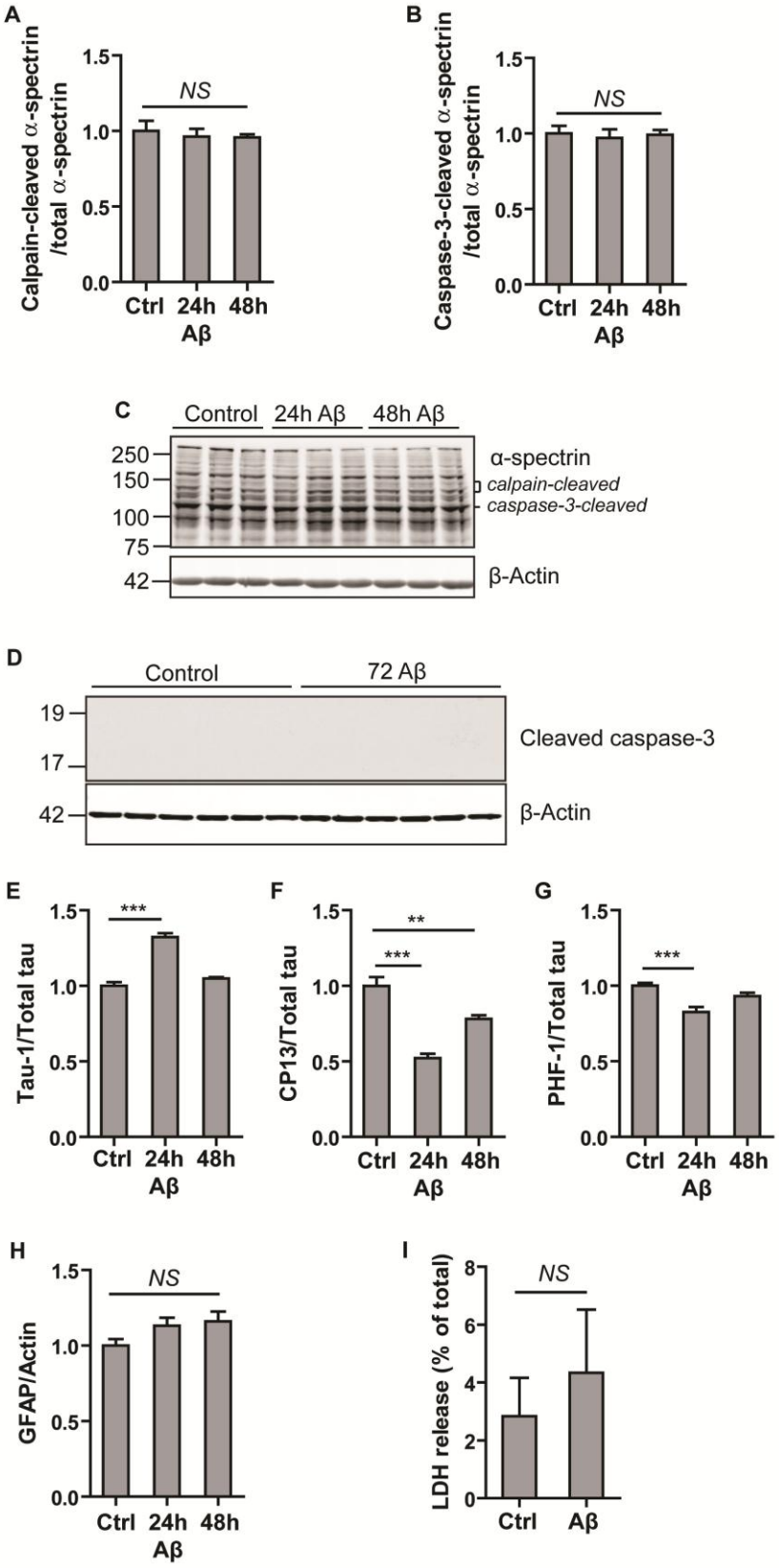

Figure 3.8 Aβ treatment of WT organotypic brain slice cultures

WT organotypic brain slices were treated with 10 μM soluble Aβ for 24, 48, or 72 hours and analysed on western blots, *n* = 6. WT slices were analysed for (A) calpain-cleaved α-spectrin and (B) caspase-3-cleaved α-spectrin. (C) Representative western blots of

brain slices treated with Aβ for 24h or 48h, probed with α-spectrin antibody. 145-150 kDa calpain-cleaved and 120 kDa caspase-3-cleaved bands are indicated. β-actin was used as a loading control. (D) Representative western blot of brain slices treated with Aβ for 72h, probed with cleaved caspase-3 antibody. β-actin was used as a loading control. WT slices were further analysed for (E) tau-1 (tau dephosphorylated at S199/202), (F) CP13 (tau pS202), (G) PHF-1 (tau pS396/404), and (H) GFAP expression. (I) LDH release was not significantly increased in 48 hour Aβ-treated slices compared to control, n = 3. Values represent mean ± SEM. One-way ANOVA, $^{**}p < 0.01$, $^{***}p < 0.001$, *NS* = not significant.

Brain slices (21 DIV) were then analysed for tau phosphorylation, as this has previously been shown to increase at specific epitopes in rat primary cortical neurons treated under the same conditions of Aβ (Garwood et al., 2011). All western blots quantified for tau phosphorylation were normalised to total tau. In contrast to previous results found in rat primary cortical neurons, the antibody against tau dephosphorylated at S199/S202 (Tau-1) revealed a statistically significant increase at 24 hours, but not at 48 hours of Aβ treatment, compared to control (Figure 3.8E). Accordingly, probing with CP13 (tau phosphorylated at S202) showed a parallel decrease in phosphorylation at this epitope after 24 and 48 hours of Aβ treatment, although the 48 hours treatment resulted in a lesser degree of S202 dephosphorylation (Figure 3.8F). Tau phosphorylated at the PHF-1 epitope (S396/S404) was also reduced at 24 hours, but not after 48 hours of Aβ treatment compared to control (Figure 3.8G). To investigate whether Aβ treatment affects the activity of astrocytes, immunoblots from treated and untreated slices were incubated with an antibody against glial fibrillary acidic protein (GFAP). These results show that there are no changes in the amount of GFAP in Aβ-treated slices compared to control, when normalised to β-actin (Figure 3.8H).

In conjunction with western blotting, the toxicity of soluble Aβ preparation was determined by LDH release as described above. Aβ treatment did not result in a statistically significant increase in LDH release (Figure 3.8I). These results show that WT organotypic brain slices are resistant to toxicity induced by this preparation of soluble Aβ oligomers at the concentration tested, which is sufficient to induce toxicity in primary neurons (Figure 3.7C). Taken together, these findings do not support the use of organotypic brain slice cultures for investigating the effects of Aβ on tau release, at least not while considering the experimental conditions used here.

3.2 Discussion

In this chapter, organotypic brain slices were used as a model system in which to investigate tau release from neurons. Organotypic brain slice cultures were chosen as a more physiologically relevant system than cultured primary cortical neurons because the slices maintain the normal cytoarchitecture of the cortex and hippocampus, which allows retention of synaptic connectivity. These slices also contain more physiologically proportionate ratios of neurons to glia, and they are synaptically functional (De Simoni et al., 2003; Cho et al., 2007). Taken together, these reasons support the use of organotypic brain slices to study physiological, synaptic activity-dependent processes such as tau release.

Initial studies were carried out to examine the presence of tau and the abundance of key synaptic proteins in WT and $fyn^{-/-}$ brain slices. The results described here show that tau is secreted from both WT and $fyn^{-/-}$ organotypic brain slices when neuronal activation is induced by KCl. Notably, the release of tau from brain slices is not accompanied by significant cell death, further suggesting that this is a physiological phenomenon that is observed in healthy neurons, as we previously reported (Pooler et al., 2013a). Interestingly, there was no significant difference in the amount of tau released in basal conditions, or following KCl stimulation, in the absence of fyn, suggesting that the fyn-dependent positioning of tau at plasma membranes is not an important criterion for tau release, at least not in this model.

A key question remains, however: what is the source of the activity-dependent extracellular tau? As the results above show, the release of neuronal tau is not due to the death of neurons, excluding the possibility of tau being released due to loss of membrane integrity. Although tau is mainly localised to the cytoplasm where it is found in abundance, both in the free state and bound to microtubules (Weingarten et al., 1975), tau is also associated with components of the plasma membrane (Brandt et al., 1995; Pooler et al., 2012). Additionally, tau is also found in detergent-resistant microdomains in neurons, to where it appears to be recruited by a fyn-dependent mechanism (Williamson et al., 2008). Furthermore, fyn is required for phosphorylation-dependent trafficking of tau to the plasma membrane (Pooler et al., 2012). Therefore, it is plausible that this pool of membrane-associated tau is a likely subcellular location from where tau can be released. Since fyn is necessary for tau translocation from the cytosol to the plasma membrane when tau is dephosphorylated, it was hypothesised that fyn may also play a regulatory role in tau secretion.

In support of this hypothesis, fyn has an established role as a membrane-associated protein that plays a role in trafficking of binding partners to the plasma membrane. Expression of fyn in COS7 cells results in increased cell surface expression of APP through tyrosine phosphorylation (Hoe et al., 2008). Moreover, fyn was shown to promote the recruitment of APP and Dab1 into lipid rafts (Minami et al., 2011). During signal transduction events in endothelial cells, activation of fyn is involved in the pathway regulating the transcytosis of albumin (Tiruppathi et al., 1997). In contrast to regulation of APP and Dab1, activation of fyn negatively regulates expression of ephrin-A at the cell surface (Baba et al., 2009). Thus, there is a wide body of evidence that fyn is involved in a variety of roles in trafficking intracellular proteins between the cytosol and the plasma membrane.

However, in opposition to the proposed hypothesis, the results in this chapter suggest that fyn does not play a major role in regulation of the spread of extracellular tau. There is currently no evidence indicating that fyn directly regulates the secretion of any intracellular protein from neurons; however, in mast cells, fyn does play a role in regulating secretion of inflammatory leukotrienes, cytokines, and chemokines, as well as vascular endothelial growth factor (Gomez et al., 2005; García-Román et al., 2010).

Changes in the amount of intracellular tau was not detected following stimulation of neuronal activity with KCl, though it has been reported previously that synaptic activity increases tau expression in the post-synaptic density fraction of primary cortical neurons (Frandemiche et al., 2014). However, the amount of total tau was not measured in that report. One possibility is that neuronal activity stimulates the translocation of tau from the cytosol to the plasma membrane immediately prior to tau secretion, without affecting the total amount of tau in the neuron. Another possibility is the limitation of the technique used because the amount of tau released may have been too low to be detected on western blots, as it is likely that the amount of secreted tau is a minor proportion of endogenous tau. Thus, a more sensitive method, such as ELISA, may have allowed detection of subtle changes in the amount of intracellular tau following stimulation of its release from neurons.

The spread of tau from cell to cell raises questions on the mechanism of uptake as well as its release. If tau does act as a signalling molecule in healthy neurons, it is logical to assume that it must be taken up by neighbouring neurons. The mechanism of tau uptake has been suggested to be by bulk endocytosis in neurons, but only tau aggregates and not endogenous extracellular tau were investigated in these studies (Frost et al., 2009; Kfoury et al., 2012; Wu et al., 2013).

In this chapter, uptake of extracellular tau was investigated in tau$^{-/-}$ organotypic brain slices exposed to conditioned medium from WT slices treated with KCl to stimulate tau release. Tau protein was absent from both membrane and cytosolic fractions of treated tau$^{-/-}$ slices. Despite the lack of tau seen in either fraction in slices treated with tau-containing medium, it cannot be concluded definitively that extracellular tau is not taken up by neurons since there are important limitations to this experiment. First of all, the amount of tau secreted is believed to be very low. For example, the amount of tau in the interstitial fluid of WT mice is in the range of 40-50 ng/ml (Yamada et al., 2011), and although KCl would have induced an increase in tau release of several-fold, the total amount of tau released from neurons may have been insufficient for detection in the recipient neurons. Column concentration of tau in the medium would have increased the amount of extracellular tau and should be considered for future studies. Furthermore, despite subcellular fractionation of the recipient neurons, the samples may not have been sufficiently concentrated to detect tau. Further subcellular fractionation into synaptosomes may be beneficial in concentrating the samples so that more protein can be loaded. Moreover, if the amount of extracellular tau taken up by recipient brain slices was too low to detect on western blots, immunocytochemistry could indicate whether individual neurons have taken up extracellular tau. Finally, it is possible that the duration of exposure to tau in the medium applied to the slices may not have been long enough for tau to become internalised in amounts large enough to be detectable on western blots. In contrast, exogenous tau aggregates have been shown to be taken up by neurons after 6 hours exposure, although this uptake is likely through a different mechanism from that required for uptake of soluble tau (Wu et al., 2013).

The final aim for this chapter was to investigate the effects of Aβ on tau release in organotypic brain slices, and it was necessary to first characterise the nature of the Aβ species present in the synthetic Aβ peptide preparation as well as its toxicity to neurons. Here, the results show that soluble Aβ is comprised primarily of monomeric Aβ, but that it also contains smaller amounts of Aβ dimers, trimers, and tetramers. To assess neuronal toxicity, primary cortical neurons were treated with 10 μM Aβ for 48 hours and medium was collected to quantify LDH release as a measure of cell death. Aβ treatment significantly increased LDH release into the culture medium compared to control cultures, indicating that under these conditions, Aβ is toxic to cultured primary neurons. Based on these results, the same conditions and preparation of Aβ was used to treat organotypic brain slices. However, extensive analysis on western blots to examine the effects of Aβ showed that Aβ treatment did not alter astrocytic activity, levels of phosphorylated tau, cleavage of α-spectrin, or activation of caspase-3 in

organotypic brain slices. This is in contrast to previous reports where, in primary neurons, soluble Aβ treatment was shown to increase tau phosphorylated at the PHF-1 epitope (S396/S404), and to decrease the amount of tau dephosphorylated at the Tau-1 epitope (S199/S202) (De Felice et al., 2008; Garwood et al., 2011). It was expected that phosphorylation at the CP13 epitope (S202) would increase correspondingly, but this was not observed here. Likewise, activation of caspase-3 in response to soluble Aβ has been shown in primary neurons and hippocampal slices, as well as calpain-mediated cleavage of α-spectrin (Garwood et al., 2011; Chen et al., 2013; Atherton et al., 2014). Again, these changes were not observed in organotypic brain slices. Indeed, Aβ did not appear to increase LDH release in organotypic brain slices, despite the same treatment eliciting an effect on primary neurons as shown earlier in this chapter (Figure 3.7).

It was also expected that Aβ treatment, under the same conditions, might have greater toxicity and an enhanced capacity to induce pathological changes in tau in brain slices compared to primary neurons, because it has been shown that astrocytes mediate Aβ-induced neurotoxicity and tau phosphorylation (Garwood et al., 2011). Immunocytochemistry has revealed a layer of astrocytes on both the upper and lower surfaces of the cultured brain slices, as previously reported by others (del Rio et al., 1991; Stoppini et al., 1991; del Rio and Soriano, 2010; Mewes et al., 2012). This “glial scar” that forms on brain slices in culture could also explain why Aβ treatment may not have induced toxicity. Thus, the abundant presence of astrocytes on top of and underneath the cultured brain slices, as shown earlier, could have hindered the access of Aβ to neurons in brain slices. In future, it may be necessary to directly inject the slice with Aβ preparations to enable it to penetrate through the layer of astrocytes. Another possibility would be to prepare brain slices from transgenic mouse models of AD, such as APP/Swe mice, and to compare these with WT brain slices, as APP/Swe mice secrete elevated levels of Aβ and develop progressive Aβ pathology with age (Savonenko et al., 2003).

Taken together, these results show that tau is released under basal and activity-stimulated conditions in WT and $fyn^{-/-}$ organotypic brain slices. The presence of fyn is not required for tau release, and the amount of tau released is a small proportion of total intracellular tau. Further work will be needed to determine the mechanisms of tau uptake, and the effects of Aβ on the physiological release and uptake of tau.

Chapter 4 Fyn binds to PXXP motifs in the proline-rich region of tau

The interaction between tau and fyn has drawn much attention due to the potential implications that tau-fyn interactions could have for the function of tau, both in normal and pathological conditions (Lee et al., 1998). In AD brain, fyn expression is increased in a subset of neurons that contain abnormally phosphorylated tau (Shirazi and Wood, 1993). Increased levels of activated fyn are also observed in AD brain (Larson et al., 2012). In parallel, tau phosphorylated at residue Y18, which is a fyn phosphorylation site, is found in neurofibrillary tangles in AD brain (Lee et al., 2004).

Mounting evidence supports the hypothesis that tau-fyn interactions play a role at the dendrite and thereby modulate synaptic function. An aberrant increase of interactions between tau and fyn caused by Aβ may result in synaptic dysfunction in AD. Tau has been reported to target fyn to the dendrite, where fyn stabilises the interaction of N-methyl-D-aspartate (NMDA) receptors with the postsynaptic density 95 protein (PSD-95). Fyn phosphorylates subunit 2 of the NMDA receptor (NR2b) at Y1472 (Nakazawa et al., 2001). The importance of these interactions for AD was revealed in an elegant series of experiments using several different transgenic mouse models (Ittner et al., 2010). In this paper it was shown that tau is required for the positioning of fyn in dendrites and that missorting of tau and fyn to the cell soma reduces the interaction of the fyn-dependent interaction of the NMDA receptor with PSD-95, suggesting that tau-fyn binding facilitates stabilisation of the NMDA receptor complex at the postsynaptic density (Ittner et al., 2010).

In addition, dephosphorylation of tau through inhibition of casein kinase Iδ (CK1δ) caused dynamic translocation of cytosolic tau to the plasma membrane, which was abolished in fyn-deficient neurons (Pooler et al., 2012). Inhibiting CK1δ also increased the association of tau with the SH3 domain of fyn, leading to the hypothesis that dephosphorylated tau moves to the membrane, possibly via a serine/threonine phosphorylation-dependent increased interaction of tau with the SH3 domain of fyn (Pooler et al., 2012).

Synaptic activity also triggers translocation of tau and synaptic markers such as fyn and PSD-95 from the dendritic shaft to the postsynaptic compartment (Frandemiche et al., 2014). Exposure to Aβ oligomers results in the same translocation but, in conjunction with synaptic activity, Aβ impairs the recruitment of tau to the postsynaptic compartment (Frandemiche et al., 2014). In addition, a signalling pathway that couples Aβ with fyn and tau via cellular prion protein (PrP^C) has also been proposed (Larson et

al., 2012). PrP^C co-immunoprecipitates with fyn and soluble Aβ dimers, which also co-localise at dendritic spines in AD brain (Larson et al., 2012). Aβ oligomer treatment induces activation of fyn, which is abolished in neurons lacking PrP^C (Um et al., 2012). PrP^C-deficient neurons also lacked the downstream phosphorylation of NR2b by fyn when treated with Aβ oligomers (Um et al., 2012). Likewise, deletion of PrP^C in APP mutant mice resulted in reduced amounts of active fyn, reduced levels of phosphorylated Y18 tau, and reduced tau missorting (Larson et al., 2012). NMDA receptor activation also increases the association of fyn with phosphorylated tau in synapses (Mondragon-Rodriguez et al., 2012). These data provide support for the hypothesis that interactions between tau and fyn may be impaired in AD and cause synaptic dysfunction.

Given that Aβ appears to exert synaptotoxicity that is mediated by tau and fyn, a rational option for therapy in AD might be to target fyn. Reduction of fyn has been shown to reduce Aβ-induced synaptotoxicity and early mortality in transgenic mice overexpressing mutant APP (Chin et al., 2004). However, mice lacking fyn exhibit impaired long-term potentiation and deficits in spatial learning (Grant et al., 1992). However, in apparent contrast to the study by Chin et al. (2004), reduction of striatal-enriched phosphatase 61 ($STEP_{61}$), which normally dephosphorylates and inhibits fyn activity, improved cognitive deficits in a mouse model of AD (Zhang et al., 2010). Moreover, in a subsequent study, genetic reduction of fyn in 3xTg mice, which express mutations in APP, presenilin-1, and tau, resulted in increased phosphorylation of tau compared to 3xTg controls. Reduction of fyn also resulted in impaired spatial learning in the Morris water maze task compared to control 3xTg mice (Minami et al., 2012).

Additionally, global tau reduction may not be an optimum therapeutic strategy, as genetic ablation of tau results in mice with complex and sometimes inconsistent phenotypes. For example, tau knockout mice are reported to display motor deficits (Ikegami et al., 2000; Lei et al., 2012; Ma et al., 2014) and cognitive deficits (Lei et al., 2014) although reports of the latter phenotype is inconsistent since it is not consistently reported (Morris et al., 2013; Li et al., 2014). Given the complexity that lies with the therapeutic approach of reducing levels of tau or fyn, it may be more prudent to investigate alternative options such as disrupting the interactions between tau and fyn.

Previous efforts to determine the molecular specifications of the tau-fyn interaction suggested that tau could bind to the SH3 domains of src family kinases, including fyn (Lee et al., 1998; Reynolds et al., 2008). However, src family kinases also contain other SH domains, such as SH2 domains which bind to tyrosine phosphorylated residues, suggesting that proteins harbouring tyrosine residues could also be potential binding

candidates for fyn-SH2 (Boggon and Eck, 2004). Indeed, tau was previously shown to interact with fyn-SH2, in a manner modulated by tyrosine phosphorylation of tau (Usardi et al., 2011).

Tau has a proline-rich region within its projection domain that contains several PXXP motifs (where P is a proline and X is any amino acid). SH3 domains recognise PXXP motifs on interacting proteins (Boggon and Eck, 2004). Earlier efforts to identify the binding site on tau for fyn *in vitro* demonstrated that truncated constructs with a deletion of 223-PXXP-236 and the C-terminal half of tau abolished the binding of tau to fyn-SH3 (Lee et al., 1998). More recently, using CHO cells expressing full length tau with PXXP-containing mutations, it was shown that mutation of proline 216 to alanine, but not proline 233 to alanine, reduced the amount of tau bound to fyn-SH3 (Usardi et al., 2011).

The discrepancy of the results obtained by Lee et al. (1998) and Usardi et al. (2011) may be due to differences in the methods employed. In the first study, truncated tau constructs (residues 1-221) were used for GST pull-down with fyn-SH3. As this construct excluded the seventh PXXP motif (233-236), Lee et al. (1998) suggested that the seventh PXXP motif was critical for tau-fyn binding. Additionally, a construct that contained the 233-PXXP-236 motif but lacked PXXP motifs N-terminal to P233 exhibited reduced binding to fyn-SH3 (Lee et al., 1998). Moreover, tau with an internal deletion at 228-236 was still able to bind fyn-SH3, suggesting that motifs N-terminal to P233 of tau are also important for tau-fyn binding (Lee et al., 1998). It is possible that the truncated tau fragments used by Lee et al. (1998) may result in a conformation of tau that is inaccessible to fyn-SH3, rendering it impossible for binding to occur *in vitro,* hence affecting the results of this study. Importantly, full-length intact tau was used in the studies carried out by Usardi et al. (2011). This approach is less likely to cause structural changes due to truncation of tau protein. Finally, the studies of Lee et al. (1998) were carried out with 0N3R tau, whereas Usardi et al. (2011) used 2N4R (full-length) tau. Interestingly, 3R tau was shown to bind with higher affinity to fyn-SH3 than 4R tau in surface plasmon resonance experiments, which may have also influenced the binding capacity of these tau fragments in these two different studies (Bhaskar et al., 2005). In a separate study, it was reported that fyn-SH3 preferentially interacts with two tandem PXXP motifs at residues 213-219, but not the seventh PXXP motif at 233-236 (Reynolds et al., 2008), contradicting those results from Lee et al. (1998) but in agreement with Usardi et al. (2011).

Additional studies have investigated the binding of tau and fyn-SH3 further. Using 293T cells co-expressing fyn and 2N4R tau, or truncated tau constructs (residues 1-221, and

1-196), full-length tau co-immunoprecipitates with fyn (Ittner et al., 2010). Tau 1-221, which excludes the seventh PXXP motif (233-236), was still shown to bind to fyn, whereas tau 1-196, which only includes the first two PXXP motifs, does not bind to fyn (Ittner et al., 2010). This work suggests that the PXXP motif at 233-236 is not the only critical motif for tau-fyn binding, further supporting the idea that PXXP motifs N-terminal to P233 are also important. More recently, a separate study demonstrated inhibition of binding to fyn-SH3 when proline 216, but not 233, of tau was mutated to alanine (Cochran et al., 2014), adding further support to the findings of Usardi et al. (2011).

However, the remaining four PXXP motifs in tau have yet to be formally tested for their ability to bind to fyn-SH3, in experiments designed to avoid potential modifications to tau structure. It is important to identify the binding site between tau and fyn so that the functional implications of disrupting this interaction can be elucidated. Downstream consequences of disrupting the tau-fyn interaction could include altered localisation of tau or fyn, changes in fyn kinase activity, or could impact on the spread of tau in normal and pathological conditions.

The aims of this chapter were therefore to characterise the interaction between tau and fyn and to investigate any downstream consequences of disrupting the interaction, by 1) confirming the binding of tau to fyn in primary neurons; 2) identifying the critical PXXP motif(s) for tau-fyn binding; and 3) exploring downstream consequences for tau function when tau-fyn interactions are modulated following disruption of key PXXP motif(s) in organotypic brain slices.

4.1 Results

4.1.1 Tau binds to both SH2 and SH3 domains of fyn *in vitro*

In order to confirm the interaction of tau with the SH2 and SH3 domains of fyn, primary neuronal lysates were subjected to glutathione S transferase (GST) pull-down assays. Recombinantly produced fyn-SH2 or fyn-SH3 were adsorbed onto glutathione agarose beads (GST-fyn-SH2 and GST-fyn-SH3, or GST alone) and were used in GST pull-down experiments (Section 2.2.7). To assess the GST proteins bound to the beads, samples collected from different stages of GST fusion bead preparation were run on 10% SDS-PAGE gels and stained with Coomassie blue to visualise the resolved proteins (Figure 4.1). Following induction of protein expression with IPTG, the presence of GST or GST-fyn-SH3 protein in the bacterial lysate was confirmed (Figure 4.1, lanes IPTG). Removal of the bacterial pellet also showed retention of GST proteins in the

supernatant (Figure 4.1, lanes Binding S/N). After coupling GST proteins to glutathione beads, the supernatant remaining following removal of GST beads showed a depletion of proteins corresponding to the sizes of GST and GST-fyn-SH3 (27 and 36 kDa, respectively) (Figure 4.1, lanes Beads S/N). As expected, GST and GST-fyn-SH3 bound to glutathione beads did not bind non-specifically to other proteins, as shown by single bands at the expected sizes (~27 kDa and 36 kDa, respectively). Similar results were obtained with GST-fyn-SH2 (data not shown).

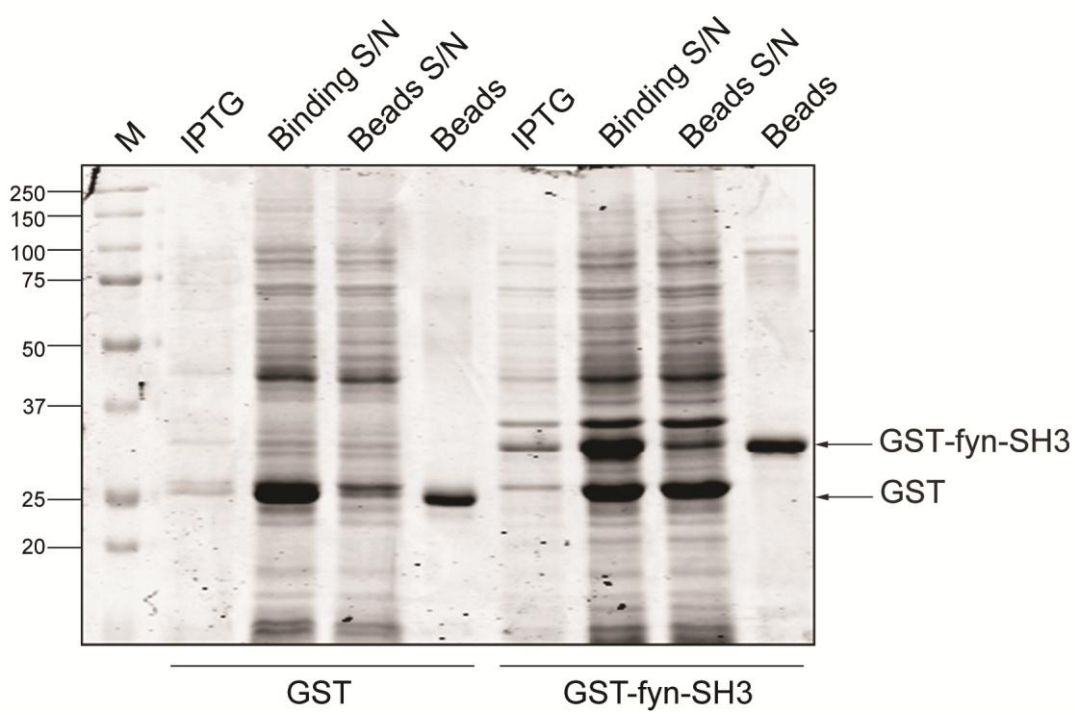

Figure 4.1 Preparation and purification of GST fusion proteins

Coomassie blue-stained 10% SDS-PAGE shows samples from different stages of preparation of GST fusion proteins. Bacterial lysates after induction of protein expression (IPTG) and cleared supernatants (Binding S/N) show GST or GST-fyn-SH3 at the expected sizes (27 and 36 kDa, respectively). Supernatant retained following protein-bead coupling (Beads S/N) and proteins bound to the glutathione beads (Beads) show specific coupling of GST or GST-fyn-SH3 to glutathione beads. Molecular weight markers are shown on the left (kDa).

Primary rat cortical neuronal lysates were subjected to pull-down with glutathione beads fused to GST-fyn-SH2, GST-fyn-SH3, or GST-only (Figure 4.2A). Bound proteins were resolved on SDS-PAGE and western blots were probed with an antibody against total tau (Figure 4.2B). Whole cell lysates were run alongside as a positive control, confirming that tau was expressed in the neurons at the time of harvest. As expected, GST-only beads did not pull-down tau protein. Tau was bound to GST-fyn-SH2 and GST-fyn-SH3 beads, as shown by bands at ~50 kDa. Tau was more abundant in the GST-fyn-SH3 beads, suggesting that tau binds with stronger affinity to fyn-SH3 than it does to fyn-SH2. These results agree with previously published reports using cultured neurons and CHO cells showing that tau binds to both SH2 and SH3 domains of fyn in rodent neurons (Usardi et al., 2011; Pooler et al., 2012).

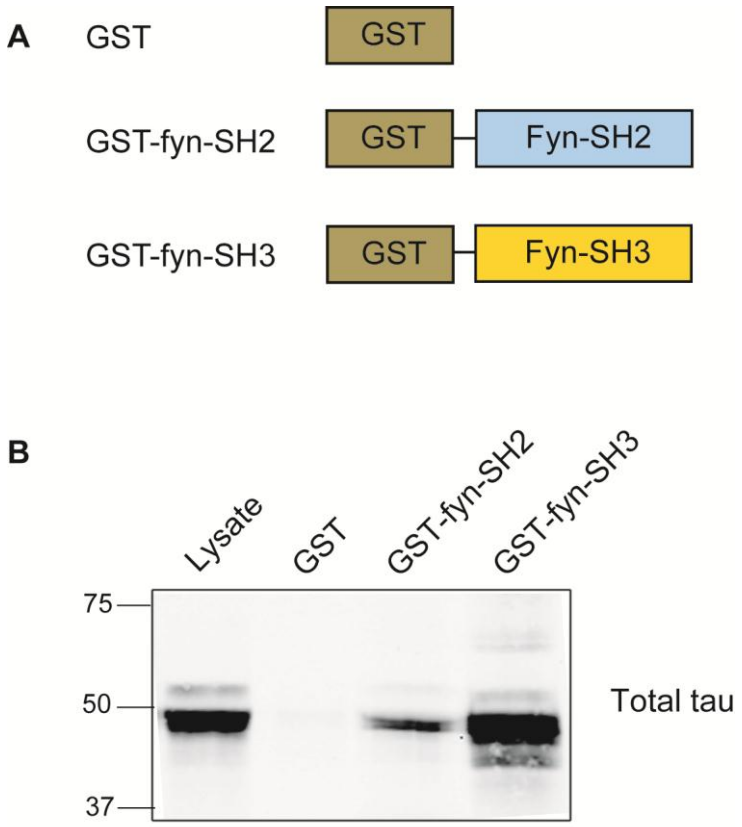

Figure 4.2 Tau from primary cortical neurons binds to fyn-SH2 and fyn-SH3

(A) Diagram illustrating constructs expressing SH2 and SH3 domains of fyn fused to GST. (B) Western blot shows binding of endogenous tau protein to fyn-SH2 and fyn-SH3. Primary cortical neurons were subjected to GST pull-down with GST, GST-fyn-SH2, or GST-fyn-SH3. Supernatants containing bound proteins, along with total lysate, were separated on 10% SDS-PAGE gels and western blots were probed with an antibody against tau. Molecular weight markers are shown on the left (kDa).

4.1.2 Site-directed mutagenesis of PXXP motifs in full-length tau

As the SH3 domain, rather than SH2 domain, of fyn is the predominant region for tau binding, further experiments were designed to investigate the precise binding site of tau to fyn-SH3. To identify which specific PXXP motif is important for binding of tau to the SH3 domain of fyn, tau constructs were made in which individual proline residues in each of the PXXP motifs were mutated to alanine (Figure 4.3). A total of eight constructs were generated by site-directed mutagenesis and these were used to identify the binding site between tau and fyn. Each proline (P) to alanine (A) substitution is marked by an asterisk in Figure 4.3.

V5-His-tagged 2N4R wild-type (WT) human tau cDNA was used as a template, and forward and reverse primers were designed to include the proline to alanine mutation for each individual construct. The P216A and P233A tau mutants had been generated previously (Usardi et al., 2011). All seven PXXP motifs were targeted individually, with the exception of the P216A tau construct (Usardi et al., 2011) which targets two PXXP motifs as the proline to alanine substitution overlaps two tandem motifs. The resulting tau cDNA products with individual P→A mutations were each amplified by PCR.

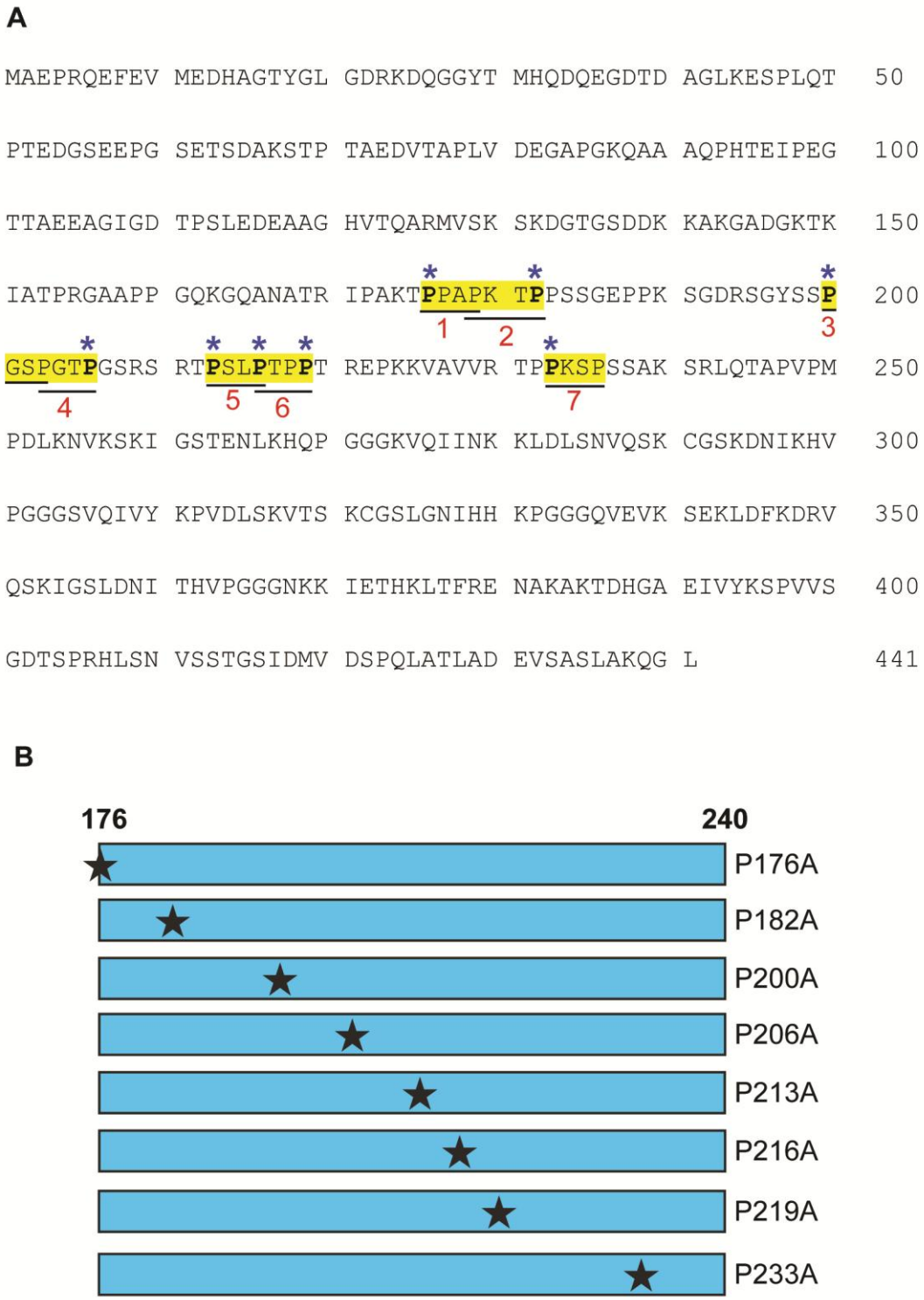

Figure 4.3 PXXP motifs in the proline-rich region of full-length tau

(A) Diagram illustrating the amino acid sequence of full-length tau, with the PXXP sequences highlighted in yellow. Individual PXXP motifs are numbered in red from 1 to 7. Individual proline to alanine mutations are indicated by an asterisk above each proline in blue, generating a total of eight constructs. (B) Asterisks indicate the sites of individual P→A mutations in the proline-rich region of tau for each construct.

Initial attempts using the standard PCR parameters as recommended by the manufacturer, using an annealing temperature of 60°C, resulted in successful generation only of the P182A tau construct with an expected size of 6.9 kbp (Figure 4.4A). A successful mutagenesis product should yield a single band; however, P176A, P200A, P206A, P213A, and P219A tau constructs resulted in multiple bands when separated on a 1% agarose gel (Figure 4.4A). This may have been due to mis-priming or to secondary structure formation. In order to increase the stringency of the reaction, the annealing temperature was increased to 68°C, which resulted in successful generation of P206A, P213A, and P219A tau mutants (Figure 4.4B).

The failure to generate products for the P176A and P200A tau constructs could be due to the high G-C content in the primers (58.6% and 73.9%, respectively), which could result in secondary structure formation. Therefore, new primers were designed for P176A and P200A tau. In particular, the P176A tau primers introduced a silent mutation (GCT instead of GCG) into the codon for alanine 176 to reduce the G-C content, and this resulted in successful generation of the P176A tau construct (Figure 4.4C). Primers for P200A tau were also re-designed to reduce G-C content and to lower the melting temperature, which also resulted in successful generation of PCR product (Figure 4.4D).

The tau mutant PCR products were each used to transform XL1-Blue competent *E.coli*, after which transformed cells were plated onto agar plates containing the appropriate antibiotic and incubated overnight. Transformed colonies were cultured in LB broth containing antibiotic and plasmids were purified and verified by sequencing (Eurofins MWG Operon, Wolverhampton, UK).

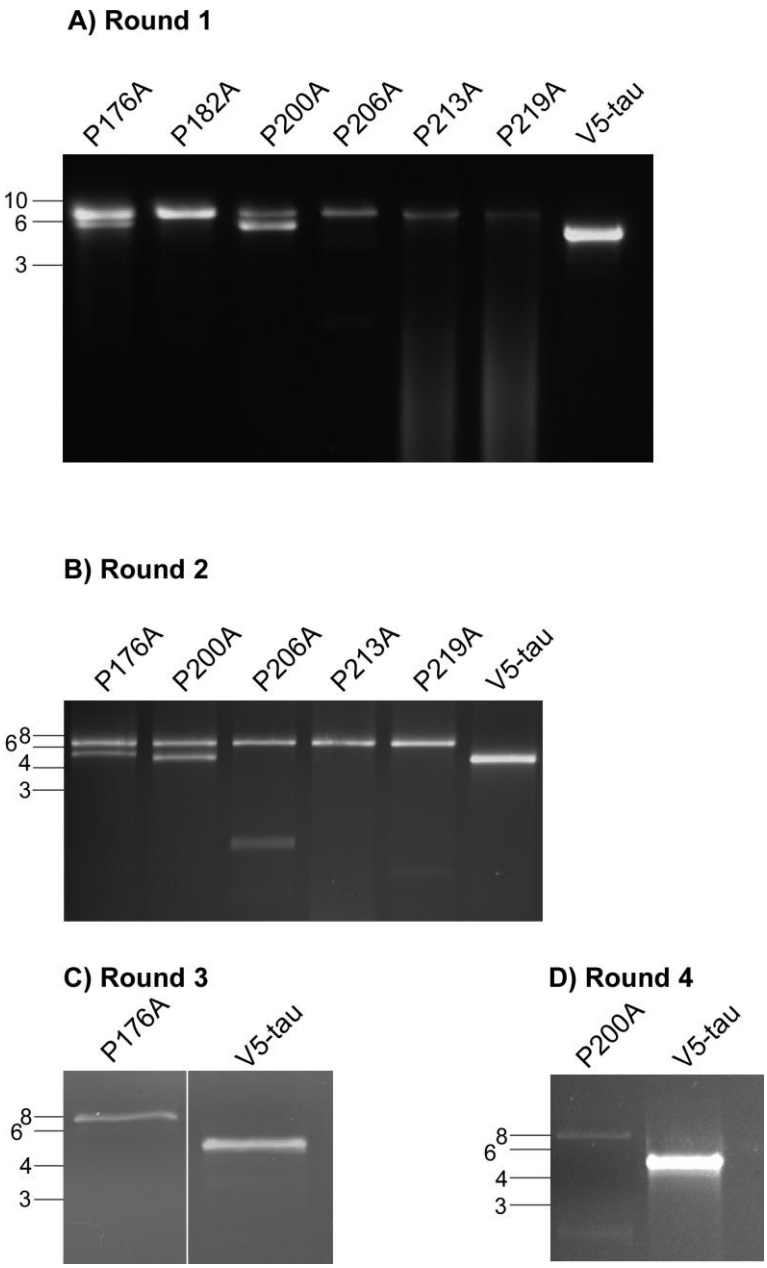

Figure 4.4 Preparation and verification of mutant PXXP tau constructs

Agarose gels of PCR products generated following site-directed mutagenesis of V5-His-tagged 2N4R wild-type human tau cDNA (V5-tau) and PCR to generate mutant P→A tau constructs. Following site-directed mutagenesis, samples were amplified by PCR and resolved on 1% agarose gels to confirm the correct proline to alanine substitution, as indicated by a single band at the expected size (6.9 kbp). (A) With a 60°C annealing temperature, P182A tau resulted in a single band of the correct size. (B) Increase of annealing temperature to 68°C resulted in successful generation of P206A, P213A, and P219A. Primers were re-designed for (C) P176A and (D) P200A which resulted in successful generation of constructs. Molecular weight markers are shown on the left (kbp).

4.1.3 P213-219 of tau is important for tau binding to the SH3 domain of fyn

To determine whether any of P→A mutant tau constructs altered binding between tau and fyn, constructs were expressed in CHO cells, the lysates of which were then subjected to a GST pull-down assay with GST-fyn-SH3 beads. GST-only beads served as a negative control, to account for any non-specific binding between tau and GST beads. CHO cell lysates were analysed on western blots probed with an antibody against tau and this confirmed that tau protein was correctly synthesised and expressed by all of the tau mutants (Figure 4.5A, lower panel). The amount of tau bound to the GST-fyn-SH3 beads was quantified and standardised against the amount of tau expressed in the equivalent CHO cell lysate for each tau construct (Figure 4.5A). Western blots were also probed with an antibody against GST to normalise for equal amounts of GST protein (Figure 4.5A).

Compared to WT tau, expression of P213A, P216A, and P219A tau each resulted in altered amount of tau bound to fyn-SH3 (Figure 4.5B). The expression of P216A tau impaired binding of tau to fyn-SH3, which agreed with previously reported results (Usardi et al., 2011; Cochran et al., 2014). Substitution of P219 by A219 also significantly reduced the amount of tau bound to fyn-SH3 to a similar extent as P216A tau. Conversely, tau in which P213 was mutated to alanine resulted in a significant increase in the amount of tau bound to fyn-SH3. Binding of fyn-SH3 to tau mutated at P176, P182, P200, P206, or P233 to alanine was unchanged compared to WT tau (Figure 4.5B).

These results indicate that the sequence of amino acids between 213-219 of tau is important for binding between fyn-SH3 and tau. Importantly, the sixth PXXP motif at 216-219 of tau plays a critical role for allowing tau binding to fyn-SH3, while the mutation at P213A of tau increased binding between tau and fyn-SH3 by 50% compared to WT tau. As expected, binding of P233A tau to fyn-SH3 was unchanged compared to WT tau, which agrees with previous reports (Usardi et al., 2011; Cochran et al., 2014). Although others have reported that deletion of the motif at 233-236 of tau disrupts binding to fyn-SH3 (Lee et al., 1998), mounting evidence, including data presented here, supports the idea that PXXP motifs N-terminal to P233 of tau are more important for tau-fyn binding. Furthermore, regions of tau other than the PXXP motifs may be important in tau binding to fyn-SH3, as neither P216A or P219A mutations completely abolished the interaction, but rather binding was reduced to only 0.65-fold of that seen for WT tau.

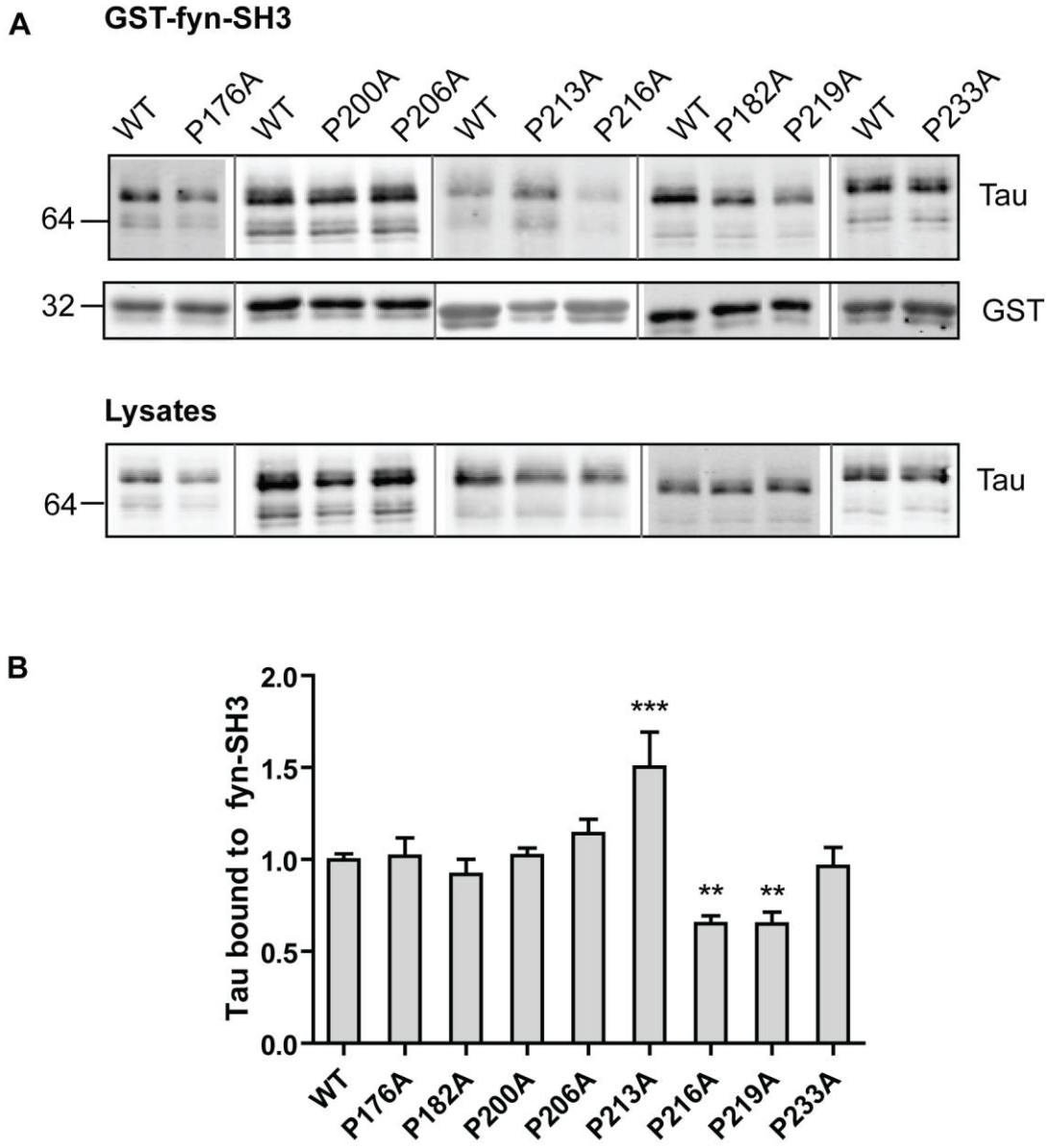

Figure 4.5 Identification of PXXP motifs critical for tau binding to fyn-SH3

Representative western blots of GST pull-downs of tau in lysates from CHO cells expressing WT or mutant P→A tau with GST-fyn-SH3 beads. CHO cells transiently transfected with WT tau or mutant P→A tau were subjected to GST pull-down with GST or GST-fyn-SH3. (A) Western blots of proteins bound to GST-fyn-SH3 were probed with antibodies against tau (upper panel) and GST (middle panel). Western blots of CHO cell lysates were probed with an antibody against tau for standardisation (lower panel). Molecular weight markers are shown on the left (kDa). (B) Bar chart showing the amount of tau immunoreactivity pulled down by GST-fyn-SH3, as a proportion of WT tau, following standardisation to total tau in the corresponding lysate. Values represent mean ± SEM, n=6-22. One-way ANOVA with post-hoc Dunnett's test, $^{**}p < 0.01$, $^{***}p < 0.001$.

4.1.4 Generation of lentiviral plasmids expressing wild-type and PXXP mutant tau

CHO cells are widely used for expression studies as they are a convenient system in which to express large amounts of target proteins. However, to examine the functional relevance of tau-fyn binding, such as downstream implications for tau release, a more physiologically relevant system was required.

Therefore, lentiviruses containing the expression constructs for wild-type and mutant PXXP tau were designed to transduce organotypic brain slices. This model enables expression of WT and mutant tau in a more physiological system. In addition to WT tau, the P213A, P216A, and P219A tau constructs were selected for further investigation because the results obtained previously indicated that these mutations were the most likely to induce significant alterations in tau-fyn interactions.

The lentivirus constructs required a neuron-specific promoter for tau expression only in neurons in the transduced organotypic slices. Furthermore, a fluorescent reporter was needed to verify the presence of the plasmid in transduced cells. Previous reports have shown that GFP fusion proteins can alter the localisation and/or metabolism of the proteins. Therefore, to circumvent this problem, an internal ribosome entry site (IRES) vector was used in these experiments. An alternative method of co-expressing two heterologous transcripts would be to use two independent promoters; however, promoter interference can occur and this could result in transcription from one promoter inhibiting transcription by the second promoter (Emerman and Temin, 1984). Using an IRES eliminates this problem, although it has been shown that IRES-dependent gene expression can vary from 6%-100% relative to the first gene expression (Mizuguchi et al., 2000). This potential lack of equivalent gene expression efficiency is not a problem for the planned experiments because it would be used solely for indicating successful lentivirus transduction.

The steps required to generate the PXXP tau lentiviruses are illustrated in Figure 4.6. This protocol utilised the existing plasmids (WT, P213A, P216A, P219A tau) generated by site-directed mutagenesis in Section 4.1.2, which were subsequently cloned into lentivirus expression vectors containing a neuron-specific promoter and IRES-dependent EGFP expression.

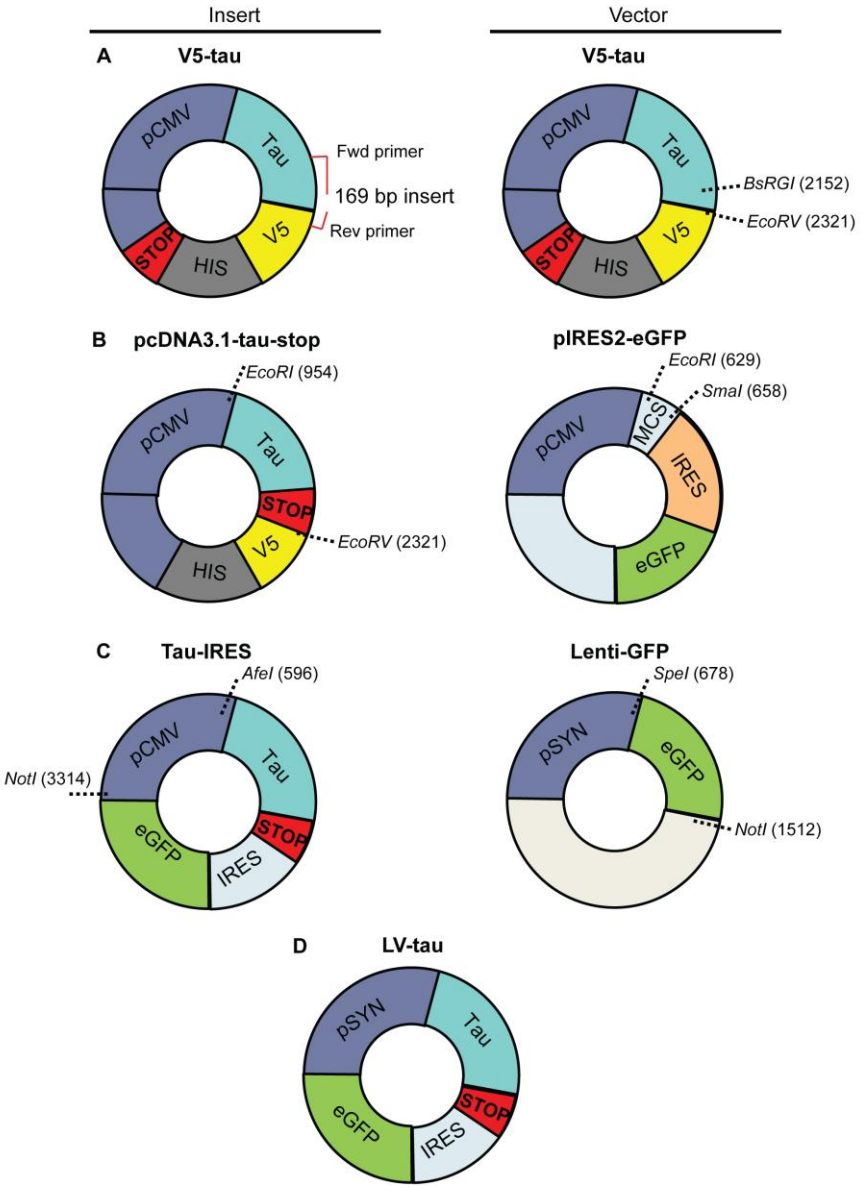

Figure 4.6 Schematic of protocol used to generate WT and mutant PXXP tau lentiviral constructs

The steps taken to generate WT and mutant PXXP tau lentiviral constructs are illustrated. Expression vectors are listed above each plasmid. Restriction enzyme sites are indicated by dashed lines and the position of cut is indicated in parentheses. (A) WT and mutant PXXP tau in pcDNA3.1-V5-His-TOPO vector were used as templates for PCR. Forward (fwd) and reverse (rev) primers to amplify a fragment to substitute one base pair to insert a stop codon are indicated (left). Insert and V5-tau were digested with *BsRGI* and *EcoRV* (right) and ligated to generate pcDNA3.1-tau-stop (B). (B) pcDNA3.1-tau-stop was digested with *EcoRI* and *EcoRV* (left) and was ligated to pIRES2-EGFP digested with *EcoRI* and *SmaI* (right) to generate tau-IRES (C). (C) Tau-IRES was digested with *AfeI* (left) and ligated to Lenti-GFP digested with *SpeI* and *NotI* (right). This generated LV-tau (D).

First, a stop codon was introduced after the tau coding sequence in WT, P213A, P216A, and P219A tau to prevent translation of V5 and His from the pcDNA3.1 vector. Primers were designed to substitute the A at nucleotide 2297 with T, introducing the stop codon (AGA→TGA):

Forward primer: 5'-TGACCTTCCGCGAGAACGCCAAAGCCAAG-3'
Reverse primer: 5'-GTGCTGGATATCTGCAGAATTGCCCTTTGATCACAAACC-3'
The A→T replacement is underlined.

These primers were used to PCR amplify a 230 bp sequence of pcDNA3.1-V5-His plasmid containing the tau sequence (V5-tau) flanking the stop codon (Figure 4.6A, left panel). The PCR product was separated on a 1.5% agarose gel and the 230 bp fragment (insert) was extracted and purified. The insert was digested with *BsrGI* and *EcoRV* and separated on a 1.5% agarose gel from which the 169 bp fragment containing the stop codon was extracted (Figure 4.6A, left panel). V5-tau was digested with *BsrGI* and *EcoRV*, and the 6650 bp tau-encoding fragment was extracted from a 0.7% agarose gel (6.7 kb) and ligated to the *BsrGI-EcoRV* insert containing the stop codon (Figure 4.6A, right panel). The ligated DNA was transformed into DH5α *E.coli* cells, and plasmid DNA was purified (Section 2.2.12). This resulted in generation of WT and mutant PXXP tau in the pcDNA3.1-V5-His vector, containing a stop codon (pcDNA3.1-tau-stop) (Figure 4.6B, left panel).

The pIRES2-EGFP plasmid was kindly provided by Dr Nina Balthasar (University of Bristol, UK). pcDNA3.1-tau-stop was digested with *EcoRI* and *EcoRV* (Figure 4.6B, left panel). pIRES-EGFP vector was digested with *EcoRI* and *SmaI* (Figure 4.6B, right panel). As *EcoRV* and *SmaI* leave blunt ends after digestion, the 3' cut ends are compatible for ligation. Double-digested pcDNA3.1-tau-stop and pIRES-EGFP plasmids were separated on a 0.7% agarose gel. The 1.37 kb fragment encoding tau containing a stop codon (insert) and 5.3 kb-digested pIRES-EGFP (vector) were extracted and ligated overnight to produce Tau-IRES (Figure 4.6C, left panel) (Section 2.2.12). Ligated DNA was transformed and plasmid DNA was isolated as above.

To confirm that tau protein was correctly expressed, Tau-IRES was transiently transfected into CHO cells. Lysed transfected CHO cells were analysed on western blots with antibodies against tau and GFP, which verified that tau and EGFP were translated (Figure 4.7A). CHO cells were also transfected with WT V5-tau and Lenti-GFP, the backbone for the lentiviral tau plasmids, as controls. Probing CHO cells expressing pcDNA3.1-tau-stop with an antibody against V5 showed that V5 was not translated from this plasmid and hence the stop codon was present (Figure 4.7A). β-actin antibody demonstrated equal loading of protein.

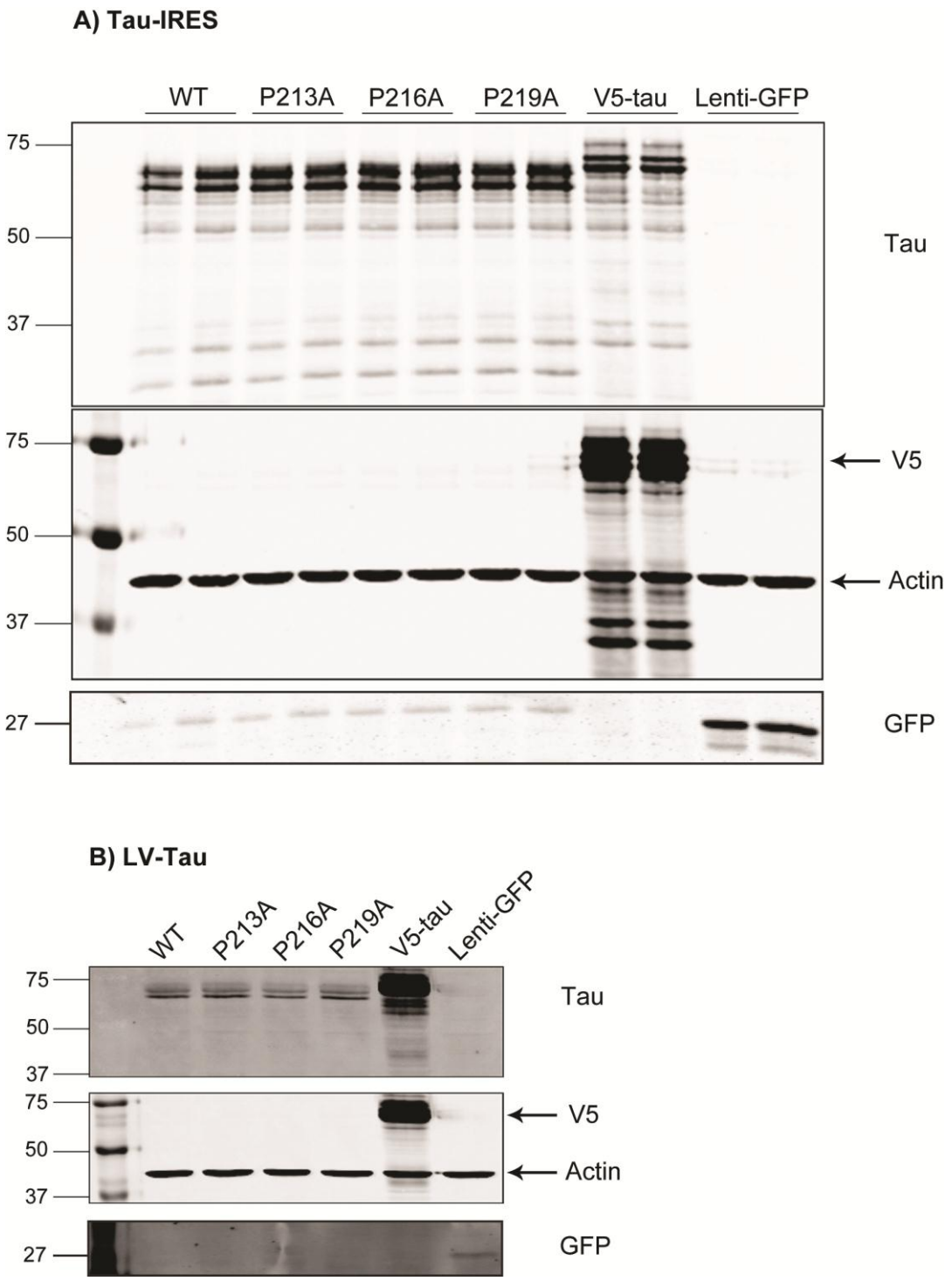

Figure 4.7 Transfection of tau-IRES and LV-tau in CHO cells

Western blots of CHO cells expressing Tau-IRES and LV-tau. WT and mutant PXXP Tau-IRES (A) and LV-tau (B) plasmids were transiently transfected in CHO cells to verify correct translation of tau. CHO cell lysates were separated on a 10% SDS-PAGE gel and western blots were probed with antibodies against tau and V5 to ensure the insertion of stop codon, GFP to ensure expression of EGFP under the IRES, and β-actin to visualise equal protein loading. CHO cells transfected with WT V5-tau and Lenti-GFP were included as controls. Molecular weight markers are shown on the left (kDa).

Finally, Tau-IRES was inserted into a lentiviral construct containing a human synapsin I promoter (Lenti-GFP), also provided by Dr Nina Balthasar (University of Bristol, UK). Tau-IRES was digested with *AfeI* and *NotI* (Figure 4.6C, left panel), separated on a 0.8% agarose gel, and the 2.7 kb tau-encoding insert was extracted. Lenti-GFP was digested with *SpeI* and *NotI* (Figure 4.6C, right panel). As *AfeI* (for Tau-IRES) is a blunt cutter, Lenti-GFP was blunted at the 5' *SpeI* site and the fragments were electrophoresed on a 0.8% agarose gel to separate the 8.2 kb cut vector (Section 2.2.12). *AfeI-NotI* Tau-IRES was ligated (Section 2.2.12) with *SpeI-NotI* Lenti-GFP overnight to generate LV-tau (Figure 4.6D), a lentiviral construct containing the synapsin promoter, WT or mutant tau, and IRES-EGFP.

Due to the instability and large size of the final construct (10.8 kb), SURE2 cells, which are deficient in the *E.coli* genes involved in DNA recombination, were used to transform LV-tau. Plasmid DNA was isolated as detailed in Section 2.2.12. The presence of each component of LV-tau was verified by sequencing. To confirm tau expression in the lentiviral plasmid, LV-tau was transiently transfected into CHO cells and cell lysates were analysed on western blots 24 hours later. Probing with an antibody against tau confirmed that the protein was translated in transfected CHO cells (Figure 4.7B). CHO cells were transfected with V5-tau and Lenti-GFP as controls. Probing with an antibody against V5 showed that V5 was not translated in LV-tau, due to the presence of the newly introduced stop codon (Figure 4.7B). GFP antibody recognised barely detectable expression of EGFP in the Lenti-GFP control but not in CHO cells expressing LV-tau or V5-tau, indicating a potential lack of sensitivity with this antibody (Figure 4.7B). β-actin antibody demonstrated equal loading of protein.

4.1.5 Expression of wild-type and PXXP mutant tau in organotypic brain slices and primary neurons

The aim of generating lentiviruses was to investigate the downstream consequences of expressing WT and mutant PXXP tau in neurons in organotypic brain slices, therefore optimisation of lentiviral transduction was carried out. Lentiviral plasmids expressing tau were used to produce lentiviral particles (Penn Vector Core, University of Pennsylvania, PA, USA).

To determine whether the lentiviruses were able to express tau, 8 DIV rat hippocampal neurons were transduced with lentiviruses equivalent to 10, 20, or 50 multiplicities of infection (MOI). An MOI of 10-20 is recommended for transduction of primary neurons, and 50 MOI has been found to result in neuronal death (Zhang et al., 2006; Castellani et al., 2010; Hutson et al., 2012). 10 days post-transduction, neurons were harvested and neuronal lysates were separated on a 10% SDS-PAGE gel and analysed on western blots. Probing blots with a rabbit polyclonal antibody that recognised mouse and human tau (total tau) together with a mouse monoclonal antibody specific for human tau (Tau-13) resulted in a positive signal at 70 kDa which was not detected in non-transduced neurons (NT) (Figure 4.8). The total tau antibody also recognised endogenous tau in the cultured neurons. However, probing transduced neurons with an antibody against GFP did not result in a positive signal (Figure 4.8), although EGFP should have been expressed by LV-tau.

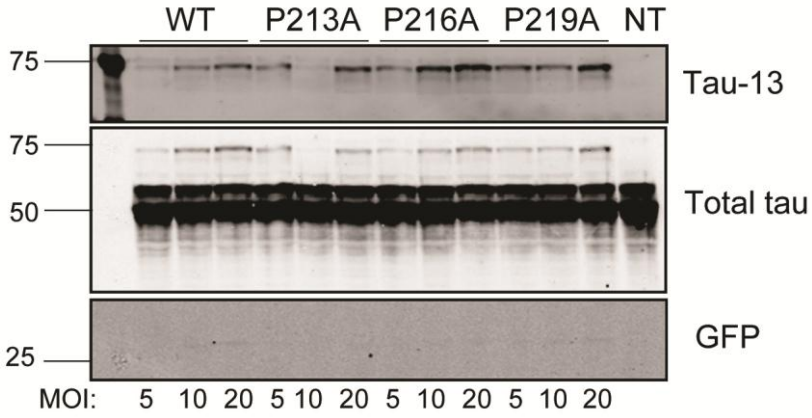

Figure 4.8 Optimisation of LV-tau transduction in rat primary cortical neurons

Western blots of primary rat hippocampal neurons transduced with LV-tau. Lentiviral particles were applied to the culture medium at 5, 10, or 20 multiplicities of infection (MOI) for 10 days prior to separating lysed neurons on a 10% SDS-PAGE gel. Neuronal lysates were probed with Tau-13, total tau, and GFP antibodies. Non-transduced (NT) neurons were included as a control. Molecular weight markers are shown on the left (kDa).

Delivery of lentivirus to primary neurons has been shown to be effective when lentiviral particles are added to the culture medium. However, because organotypic brain slices are cultured on an insert in wells containing 1 ml medium, this results in a substantial dilution of the lentiviruses, or the use of prohibitively large amounts of virus transducing units. Therefore, three different methods of lentiviral application were tested to determine the most efficient route of lentivirus administration. The first method applied lentivirus directly onto the top of the slice, the second method used injection of lentiviruses directly into the slice, and the third method involved addition of lentiviruses to the culture medium underneath the slice insert.

Organotypic brain slices were prepared from WT and tau$^{-/-}$ mice. Tau$^{-/-}$ brain slices were used so that endogenous tau would not compete with expression of lentiviral tau for binding to fyn-SH3 in functional experiments. Previous studies have demonstrated successful lentiviral transduction when viral particles are added on the day of plating the slices, prior to the growth of the glial layer surrounding the slice (Chapter 3) (Teschemacher et al., 2005a). Therefore, on the day of plating the slices, lentiviruses were diluted to 10^9 transducing units (TU)/ml in slice culture medium, and approximately 10^7 TU were applied directly to the upper surface of each slice. As previous reports indicate that lentiviral expression peaks eight days post-infection and remains stable for at least a further six days (Ehrengruber et al., 2001; Teschemacher

et al., 2005b; Hioki et al., 2007), brain slices were harvested two weeks post-transduction (14 DIV). Slice lysates, including non-transduced brain slices as a negative control, were resolved on western blots to detect expression of lentiviral-encoded tau (Figure 4.9A). Probing with the human tau-specific antibody (Tau-13) and the total tau antibody did not reveal any tau bands of the expected size for either endogenous tau (~50 kDa) or transduced tau (~70 kDa) (Figure 4.9A). The 42 kDa band visible in the Tau-13 blot does not appear to be tau, as it is also visible in the non-transduced $tau^{-/-}$ slice lysate. As the band is approximately the same molecular weight as β-actin, the Tau-13 bands could indicate non-specific binding to β-actin.

The second method was to inject the lentiviruses directly into the brain slices after they had attached to the insert. Two weeks after plating (14 DIV), approximately 10^7 TU were injected into WT and $tau^{-/-}$ brain slices at three equally spaced locations using a Hamilton syringe. Slices were harvested two weeks post-injection (28 DIV) and analysed on western blots as above. Probing with Tau-13 and total tau antibodies did not reveal tau bands of the expected size (Figure 4.9B). Injection of LV-tau into brain slices from WT mice did not reveal any expression of EGFP on western blots probed with antibodies against GFP (Figure 4.9C). β-actin antibody demonstrated equal protein loading.

A third approach was tested in 42 DIV WT brain slices. Slices were transduced at 20 MOI (approximately 10^7 TU) by addition to the medium underneath the slice culture insert for 48 hours before changing the medium at 44 DIV. Slices were cultured for a further four weeks before harvesting at 70 DIV to explore whether a longer duration post-transduction might improve lentiviral tau expression. Western blots of slice lysates probed with total tau antibody did not reveal any detectable tau at 70 kDa, nor any bands in the Tau-13 blot, despite the presence of endogenous mouse tau at ~50 kDa (Figure 4.9D).

Taken together, these results suggest that while the lentiviruses are able to translate tau protein that is detectable with an antibody recognising human tau, this has only been successfully transduced in primary neurons and not in organotypic brain slices. Despite attempting three different methods of transduction in slices, none of these approaches resulted in significant tau expression from the lentiviruses in neurons. As lentiviral expression of tau was successful in primary neurons, this indicates that the problem of lack of lentiviral tau expression may be a technical issue relating to the introduction of lentivirus into neurons in slice culture.

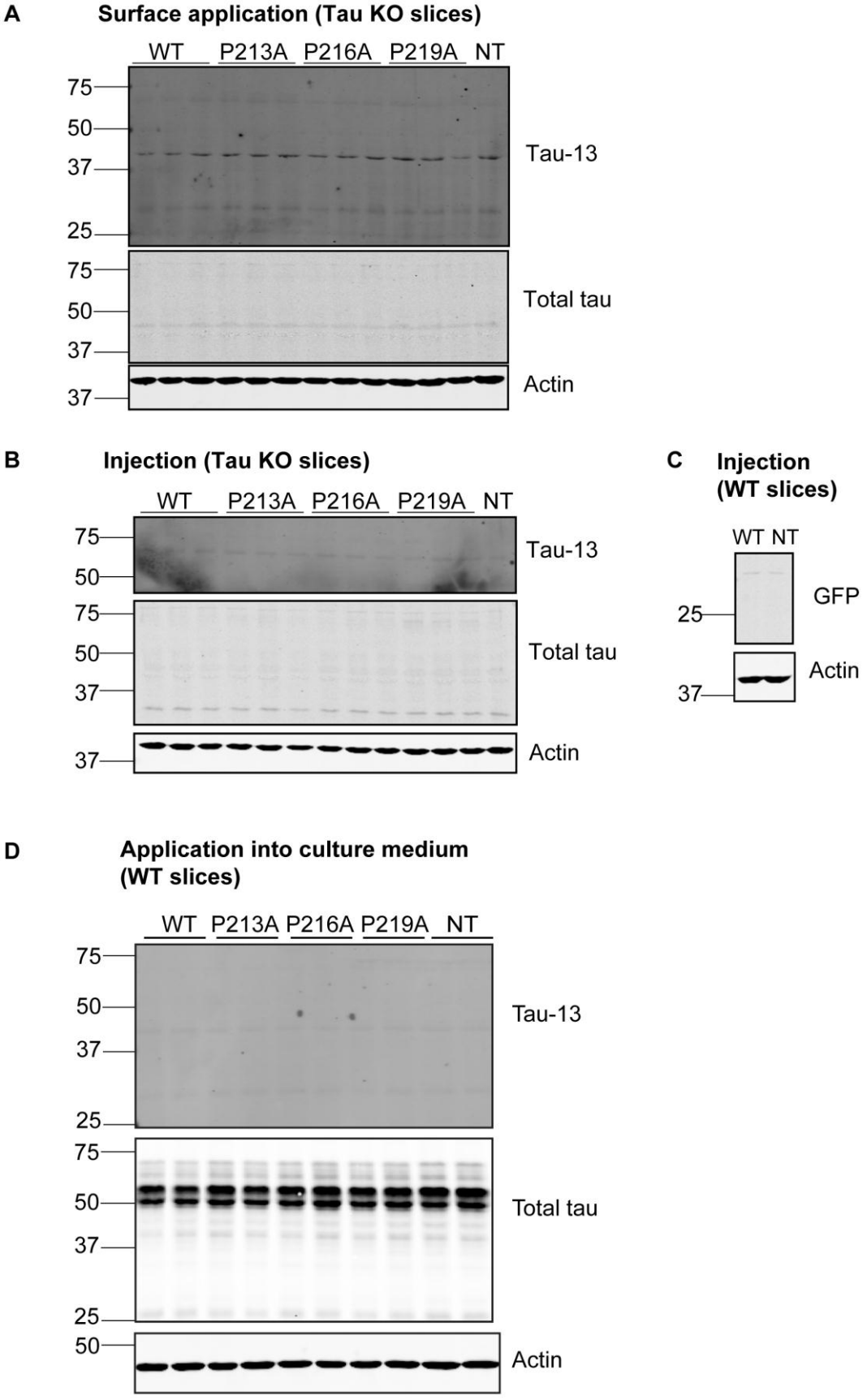

Figure 4.9 Optimisation of LV-tau transduction in organotypic brain slices

Western blots of total lysates from WT and tau$^{-/-}$ organotypic brain slices transduced with LV-tau. Different methods of transduction were used to test the expression of LV-

tau in WT and tau$^{-/-}$ organotypic brain slices. (A) Lentiviruses were applied directly to the surface of each slice on the day of plating and incubated for 2 weeks before harvesting. Total slice lysates were probed with antibodies against Tau-13 (recognises human tau), total tau, and β-actin to ensure equal protein loading. (B) Lentiviruses were injected into 14 DIV tau$^{-/-}$ brain slices and harvested 2 weeks post-transduction. Total slice lysates were probed with Tau-13, total tau, and β-actin. (C) Lentiviruses were injected into 14 DIV WT slices and total slice lysates were probed with antibodies against GFP and β-actin. (D) 42 DIV WT slices were transduced with 20 MOI and harvested at 70 DIV. Western blots of total slice lysates were probed with antibodies against Tau-13 and total tau. β-actin antibody was used to ensure equal protein loading. Non-transduced slices (NT) were included in all blots as a control. Molecular weight markers are shown on the left (kDa).

4.2 Discussion

4.2.1 Discussion and summary of results

These results show that tau can bind to both the SH2 and the SH3 domains of fyn in neurons. Tau preferentially binds to the SH3 domain of fyn relative to fyn-SH2, and further experiments were carried out to identify the critical binding site of tau with fyn-SH3. In this study, all seven PXXP motifs of tau were tested for their ability to bind to the SH3 domain of fyn. In transfected CHO cells, GST pull-downs showed that the P216A and P219A mutations of tau reduce its binding to fyn-SH3, while P213A increases the association between tau and fyn. This indicates that fyn-SH3 binds to the sixth PXXP motif of tau at residues 216-219, and that the fifth PXXP motif of tau at 213-216 also appears to play a role in regulating the association between tau and fyn-SH3.

PXXP ligands are classified as either class I or class II and the binding domains are usually flanked by positively charged amino acids. The localisation of the flanking amino acids at the N or C terminus of the motif determines its categorisation into class I or II. Class I ligands are characterised by a consensus sequence of RPLPPXP and class II ligands by XXXPXXPXR, where X denotes any amino acid (Alexandropoulos et al., 1995). The classification of the PXXP ligand defines the orientation by which it binds to the SH3 domain, and SH3 domains may exhibit a preference for either class of ligand. In the case of fyn, the SH3 domain can bind to both class I and II PXXP ligands (Alexandropoulos et al., 1995). In contrast to previous reports in which the seventh PXXP motif of tau at 233-236 appeared to be important for binding to fyn-SH3 (Lee et al., 1998; Ittner et al., 2010), the data shown here suggest instead that tau residues 213-219 (fifth and sixth PXXP motifs) are involved in this interaction, with the sixth motif enabling the binding between tau and fyn-SH3. The sequence surrounding the sixth

PXXP motif in tau is 211-RTPSL**PTPP**TREP-223, whilst that surrounding the seventh PXXP motif is 228-VVRTP**PKSP**SSAK-240. Comparing the amino acid sequences around these two PXXP motifs suggests that the sixth PXXP motif fits the consensus for a class II ligand, whereas the seventh PXXP motif conforms better to a class I ligand, and the fifth PXXP motif conforms to neither class of ligand. Even though fyn-SH3 can bind to both class I and II ligands, the conformation of tau could define the orientation with which it binds to fyn-SH3, which could mean that fyn-SH3 favours binding to the sixth PXXP motif as a class II ligand. However, this has not been examined and the functional implications of SH3 domain binding to class I or II PXXP ligands remains to be properly defined.

A previous study from this laboratory using truncated tau peptides to investigate tau-fyn-SH3 binding showed that inclusion of K224 and K225 in tau resulted in improved binding between fyn-SH3 and tau containing the fifth and sixth PXXP motifs, when compared to a peptide lacking residues K224 and K225 (Reynolds et al., 2008). The study by Lee et al. (1998), that identified tau residues 233-236 as important for tau-fyn-SH3 binding, used truncated tau constructs that excluded both the seventh PXXP motif and the lysine residues at 224 and 225, therefore the absence of K224 and K225 could also explain the lack of binding of this construct to fyn-SH3. It is also possible that fyn-SH3 can bind to different PXXP motifs depending on the experimental conditions used. This idea is supported by data shown in this chapter that the mutations at P216A and P219A did not completely abolish the interaction between tau and fyn-SH3. This suggests that tau can still bind to fyn-SH3 through another binding site, and it may be that other PXXP motifs, including the seventh motif, may also facilitate binding between tau and fyn-SH3. Further support for this conclusion comes from a study by Ittner et al. (2010) who reported that a truncated construct containing the N-terminus of tau and the first two PXXP motifs could not bind to fyn in co-transfected 293T cells, whereas another truncated N-terminal tau construct that included the sixth PXXP motif exhibited reduced binding to fyn compared to full-length tau. Therefore, the exclusion of the seventh PXXP motif in the Ittner et al. (2010) study was insufficient to completely abolish tau-fyn-SH3 binding. The contributions of other PXXP motifs on the binding between tau 216-219 and fyn-SH3 would have to undergo further investigation by double mutations, in particular at P219A/P233A.

Interestingly, we found that the P213A tau mutation resulted in an increased binding to fyn-SH3. The reasons for this are unclear. However, one possibility is that the alanine substitution at P213 results in an altered tau conformation that is favourable for binding to fyn-SH3, given the presence of the intact sixth PXXP motif. It has been shown that specific residues outside the core PXXP motif can contribute to the binding between

PXXP motifs and SH3 domains (Mayer, 2001), which could explain the increased affinity between tau P213A and fyn-SH3. For example, the serine residue downstream of the PXXP motif is important for binding to the SH3 domain of the protein Nck (Zhao et al., 2000). Residues C-terminal to PXXP ligands are also shown to modulate binding to fyn-SH3, although flanking residues N-terminal to PXXP have not been examined (Rickles et al., 1995). Thus, if fyn-SH3 binds to tau at residues 216-219, the proline to alanine substitution at residue 213 of tau upstream of the sixth PXXP motif could result in increased binding affinity with fyn-SH3. Another possibility is that the P213A mutation alters tau phosphorylation around this PXXP motif, which could enhance tau-fyn binding at the SH3 domain. The phosphorylation state of tau at S199/S202 has been shown to influence tau binding to fyn-SH3 (Pooler et al., 2012), but the precise residues and the effects of phosphorylation on tau-fyn binding have not been clearly identified. There is also no effect of tyrosine phosphorylation on tau binding to fyn-SH3, although phosphorylation at Y18 of tau was shown to regulate the interaction between tau and the SH2 domain of fyn (Usardi et al., 2011). The PXXP motifs of tau are located in a region that has a high density of phosphorylatable serine/threonine residues (Hanger et al., 2009). Therefore, it is likely that phosphorylation, or other post-translational modifications at residues surrounding the sixth PXXP motif of tau could influence its binding to fyn-SH3. In support of this idea, substitution of 18 serine and threonine residues to glutamate in the N-terminal half of tau, which mimics phosphorylation, inhibited binding between tau and fyn-SH3 (Reynolds et al., 2008). These mutations include residues S198, S199, S202, T205, S208, S210, T212, S214, T217, T220, and S235, which are located within the proline-rich region of tau. Fyn-SH3 was also unable to bind to Tau-Glu10, a construct that mimics phosphorylation at 10 serine/threonine sites throughout the sequence of tau, including 5 in the proline-rich region (S198, S199, S202, T231, S235) (Reynolds et al., 2008). Additionally, fyn-SH3 was unable to bind to highly phosphorylated tau isolated from AD brain (Reynolds et al., 2008). Thus it appears that phosphorylation of tau influences its binding to fyn-SH3, and much of this phosphorylation occurs around the PXXP motifs identified here as being important for tau-fyn-SH3 binding.

Lentiviruses were generated to express WT, P213A, P216A, and P219A tau constructs in order to investigate the effects of disrupting these PXXP motifs on downstream tau functions in organotypic brain slices. However, although these lentiviruses expressed tau in primary neurons, they did not express detectable amounts of tau in organotypic brain slices.

4.2.2 Limitations of lentiviruses expressing tau

In order to troubleshoot the problems with transduction of lentivirally-encoded tau in organotypic brain slices, the DNA and amino acid sequences of the lentiviral constructs were re-assessed. During this analysis, it became apparent that although the DNA and protein sequence of tau in LV-tau was correct, insertion of Tau-IRES into the lentiviral plasmid had resulted in the removal of a single base pair at the *SpeI*-blunt/*AfeI* insertion site. This change resulted in utilisation of a different ATG start codon at base pair 211, rather than at base pair 735. This use of an ATG at a more 5' position in the lentiviral vector resulted in translation of full-length tau with an additional 145 amino acids fused to the N-terminus of tau, giving a protein with a predicted molecular weight of 70 kDa. It is apparent therefore that the 70 kDa exogenous tau species detected in neurons corresponded to this tau fusion protein. The 5' sequence that formed the fusion protein was translated from part of the synapsin promoter. Despite the truncation of the synapsin promoter, and the additional encoded amino acids, full-length tau was translated, although the effect on the promoter may have resulted in reduced expression of lentiviral tau, compared to endogenous tau in primary neurons. However, the lack of lentiviral tau expression in organotypic brain slices does not appear to be caused by the additional amino acids fused to the N-terminus of tau. Rather, this suggests that the techniques used to deliver the lentivirus particles to organotypic brain slices were inefficient. In the future, it will be necessary to implement alternative lentiviral delivery techniques, such as direct injection into the brains of $tau^{-/-}$ mice prior to preparation of brain slices.

In summary, the results presented in this chapter has identified mechanisms by which tau interacts with fyn. Further investigation is required into whether phosphorylation at individual serine/threonine residues within the proline-rich region are critical regulators of tau-fyn interactions. This may provide additional insight as to whether inhibiting tau-fyn interactions would be a good target as a therapeutic strategy for AD. For example, if phosphorylation at a specific residue inhibits tau-fyn interactions, targeting kinase inhibition could be a viable option for treatment.

Chapter 5 Investigating interactions between tau and fyn in brain tissue

The first study which implicated fyn in the pathogenesis of AD was reported by Shirazi and Wood (1993). These authors observed increased fyn immunoreactivity in a subset of neurons containing abnormally phosphorylated tau in AD brain (Shirazi and Wood, 1993). *In vitro* studies demonstrating that oligomeric Aβ can upregulate fyn activity (Lambert et al., 1998; Williamson et al., 2002; Um et al., 2012) have further implicated fyn and its downstream signalling partners in the underlying mechanisms of AD.

During the progression of AD, the ratio of soluble to insoluble fyn in the brain decreases substantially, without any significant change to the total amount of fyn (Ho et al., 2005). Immunohistochemical analysis showed that fyn was mislocalised from its normal synaptic localisation to the neuronal cell body in AD, and this change became more prominent with disease severity (Ho et al., 2005). A proportion of neurons containing mislocalised fyn in the cell body also showed increased co-localisation with tau-containing tangles (Ho et al., 2005). Furthermore, the amount of soluble fyn correlated positively with a decrease in the mini mental state examination (MMSE) (Ho et al., 2005), which is a common clinical test used to determine cognitive ability (Folstein et al., 1975). In the same study, soluble fyn was inversely correlated with the cerebral load of tau-containing neurofibrillary tangles, but neither soluble nor insoluble fyn correlated with amyloid plaques (Ho et al., 2005). Nonetheless, these reported changes in fyn expression in AD brain need to be replicated independently in a larger cohort of individuals since the study by Ho et al. (2005) was limited by the small number of replicates of each group (n = 3-8 for each group).

In a larger cohort of subjects (n = 24-26 for each group), Larson et al. (2012) showed that the total amount of fyn was unchanged in AD patients compared to non-demented controls and individuals with mild cognitive impairment (MCI). However, although there was no relationship between levels of fyn and severity of dementia, a strong correlation was found between total fyn and cellular prion protein (PrP^C), regardless of the cognitive status of each individual (Larson et al., 2012). These authors also reported that the amount of active fyn, assessed by immunoprecipitation of fyn followed by western blotting with an antibody against the active form of fyn, was increased in AD brain compared to controls, and that in AD brain, but not in controls, the amount of active fyn was also significantly correlated with that of PrP^C (Larson et al., 2012). These data strengthen the hypothesis that Aβ signals through PrP^C and fyn to mediate synaptotoxicity and this could be an important mechanism underlying the development

of AD. However, to date, the relationship between tau and fyn has not been explored extensively in human brain tissue, which was the aim of this study.

Interactions between tau and fyn in rodents and in cell lines, however, have been observed in several studies. The first *in vitro* studies showed that tau could directly interact with the SH3 domain of fyn (Lee et al., 1998; Bhaskar et al., 2005; Pooler et al., 2012), which was confirmed by the results presented in Chapter 4 of this thesis. Subsequently it was demonstrated that tau also associates directly with the SH2 domain of fyn (Usardi et al., 2011). However, a greater challenge is to validate this binding *in vivo* in a physiologically relevant system.

Interaction assays pose a challenge because the nature of the interaction can interfere with the assay and there are many variables that can determine whether the assay is successful or not. For example, weak or transient interactions can be difficult to verify in an *in vivo* system using endogenous proteins. One of the most common methods of investigating interactions in a more physiologically relevant system is the co-immunoprecipitation assay (Berggård et al., 2007). It has recently been reported that tau and fyn can be co-immunoprecipitated in rodent brain tissue and synaptosomes using either tau or fyn antibodies for immunoprecipitation (Ittner et al., 2010; Mondragon-Rodriguez et al., 2012). However, in both of these previous studies, negative controls for co-immunoprecipitation experiments were not shown, and therefore the observed apparent interactions of tau and fyn could conceivably have been due to detection of non-specific bands. The necessary controls for this type of experiment usually include samples of lysates incubated with agarose beads in the absence of primary antibody, and/or the inclusion of an irrelevant antibody that does not bind either protein to determine whether the target protein is binding non-specifically to immunoglobulins present in the immunoprecipitate. In another study, using transgenic mice overexpressing both wild-type human tau and mutant APP, co-immunoprecipitation also revealed associations between tau and fyn (Chabrier et al., 2012). It should be noted, however, that this experiment was performed under conditions in which one of the target proteins was overexpressed. Therefore, although tau and fyn binding has been demonstrated in rodent brain tissue, it is important that this interaction is reproduced in an independent study examining the endogenous proteins, and with the inclusion of appropriate negative controls.

It is currently unclear whether tau and fyn are associated only at the dendrite, or whether these proteins can also interact in different subcellular locations. In addition, the relationship between tau phosphorylation and expression of fyn has not been well explored, particularly in the case of human brain. Therefore, the aims of this chapter

were 1) to determine whether an interaction of endogenously expressed tau and fyn in rodent brain could be detected, and if so, 2) to identify the subcellular localisation of this interaction, and 3) to investigate the relationship between tau phosphorylation and fyn in human AD post-mortem brain tissue.

5.1 Results

5.1.1 Optimisation of tau-fyn co-immunoprecipitation assays using lysates from primary neurons and brain tissue

A range of different conditions was tested to verify the tau-fyn interaction in lysates prepared from primary neurons and rodent brain tissue by co-immunoprecipitation. Several factors affect the success of co-immunoprecipitation experiments, including buffer composition, antibody-antigen accessibility, concentration of target proteins, and the nature of the interaction between the target proteins. A summary of all the conditions tested is shown in Table 5.1.

Different buffers containing a range of detergent types and concentrations were tested to find the optimal conditions for co-immunoprecipitation (see Section 2.1.4 for details of lysis buffers). Radioimmunoprecipitation assay (RIPA) buffer was used in the first instance, because fyn is a membrane-bound protein and we hypothesised that the additional ionic detergents SDS and sodium deoxycholate present in this buffer would aid in the disruption of membranes. Facilitating fyn solubilisation could hence provide more opportunity for its interaction with soluble tau. Due to concerns that RIPA buffer could also have the effect of disrupting tau-fyn interactions, lysis buffers containing non-ionic detergents were also tested. HEPES buffer containing the non-ionic detergent Triton X-100 was used to successfully demonstrate co-immunoprecipitation between tau and fyn in a previous study (Ittner et al., 2010), while NETF buffer contains a non-ionic detergent, Nonidet P-40, and has also been used in successful co-immunoprecipitation of V5-tagged tau (Derkinderen et al., 2005).

Primary antibodies directed against either tau or fyn were used to investigate the interaction in both directions. Since it is known that the SH3 domain of fyn binds to the proline-rich region of tau *in vitro*, efforts were made to find antibodies for immunoprecipitation with epitopes that did not bind to these identified binding regions.

The sources used were rat primary cortical neurons, mouse brain tissue, and CHO cells co-expressing tau (V5-His-tagged) and fyn. In some cases, primary neurons were

treated with IC261, an inhibitor of casein kinases 1δ and ε (CK1δ and CK1ε, respectively), as this has been shown to increase the association between tau and fyn-SH3 *in vitro* (Pooler et al., 2012). Another approach was to crosslink proteins using Dithiobis[succinimidyl propionate] (DSP), since this can aid in detecting weak or transient protein-protein interactions. Mouse brain tissue was separated into membrane and cytosolic fractions because fyn is predominantly found in association with membranes. Finally, CHO cells expressing tau and fyn were treated with sodium pervanadate, a tyrosine phosphatase inhibitor, because a previous study showed that pervanadate increases the association between tau and fyn-SH2 *in vitro* (Usardi et al., 2011).

Regardless of the type of sample (primary neurons, brain tissue, or cultured non-neuronal cells), treatment, lysis buffer, or primary antibody used, the co-immunoprecipitation protocol remained the same (Section 2.2.8). Prepared samples were pre-incubated with washed protein A agarose beads to clear endogenous immunoglobulins, and the pre-cleared samples were incubated with primary antibody overnight to allow binding to antigen. Lysates containing antibody-antigen complexes were bound to protein A agarose beads, and bound proteins were eluted and analysed on western blots with antibodies against tau or fyn to verify the presence of co-immunoprecipitated proteins. Lysates without primary antibody, or incubated with an irrelevant antibody raised in the same species as the tau or fyn antibody, were bound to beads and eluates were included on western blots as controls. Total lysates were also run on western blots as a positive control for the target proteins and to ensure that the amount of antigen input was detectable.

Western blots were probed with antibodies raised in a different species than the primary antibody used for immunoprecipitation, to avoid detection of the heavy-chain IgG proteins immunoprecipitated with the antibody-antigen-bead complex. Because tau is ~50 kDa, and fyn is 59 kDa, the heavy chain IgG (50 kDa) interferes with the detection of tau and fyn. Since preliminary studies had shown that commercial mouse monoclonal antibodies did not specifically detect fyn with much sensitivity, and therefore the best option was to use a rabbit polyclonal antibody, the combinations of binding and detection antibodies were necessarily limited for these studies.

To identify an association between tau and fyn in cultured neurons, rat primary cortical neurons were subjected to immunoprecipitation of fyn in RIPA, HEPES, or NETF buffer with the following antibodies: polyclonal fyn (Sigma), monoclonal fyn (BD Biosciences), polyclonal fyn (Cell Signalling Technologies; CST), polyclonal fyn sc-16 (Santa Cruz Biotechnology), monoclonal fyn sc-434 (Santa Cruz Biotechnology), and monoclonal

fyn 1S (Abcam). A representative western blot of co-immunoprecipitation of fyn using the polyclonal fyn (Sigma) antibody from rat cortical neurons is shown in Figure 5.1. Rat cortical neurons were also subjected to tau immunoprecipitation in RIPA buffer with a monoclonal tau antibody (Tau-5) and the following polyclonal antibodies: tau (DAKO), C-terminal epitope of tau (TP70), and N-terminal epitope of tau (TP007). In addition, rat cortical neurons were treated with IC261 to inhibit CK1δ/ε, or DSP to cross-link proteins. IC261 treatment was followed by immunoprecipitation with fyn (Sigma), fyn (BD Biosciences), fyn (CST), or total tau (DAKO) antibodies. DSP treatment was followed by immunoprecipitation with the following antibodies: fyn (CST), fyn sc-16, fyn 1S (Abcam), tau (DAKO), and tau-5. Western blots of immunoprecipitates from monoclonal antibodies were probed with polyclonal antibodies against tau and fyn, and polyclonal immunoprecipitates were probed with monoclonal tau and fyn antibodies.

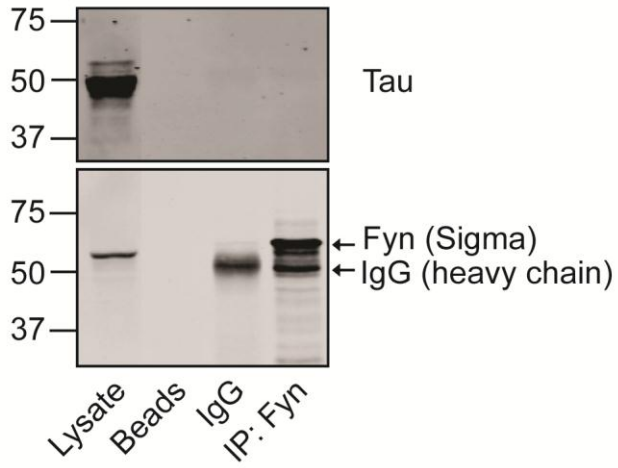

Figure 5.1 Co-immunoprecipitation of fyn from rat cortical neurons

Western blot of co-immunoprecipitation from rat cortical neurons. Fyn was immunoprecipitated from rat cortical neurons with the polyclonal fyn (Sigma) antibody. As negative controls, neuronal lysates were incubated without primary antibody (beads), or an with an irrelevant polyclonal antibody (IgG). Western blots of neuronal lysate, immunoprecipitates, and negative controls were probed with a monoclonal antibody against tau (upper panel) and the same polyclonal fyn (Sigma) antibody used for immunoprecipitation (lower panel). The 50 kDa heavy chain band is indicated (arrow) and is distinct from the 59 kDa fyn band (lower panel). Molecular weight markers are shown on the left (kDa).

Whole brain mouse homogenates were subjected to fyn immunoprecipitation in RIPA, HEPES, or NETF buffer as above, and analysed on western blots. In addition, membrane and cytosolic fractions of mouse brain tissue were immunoprecipitated with fyn (CST), tau (TP70), or tau (TP007) antibodies. Western blots were probed with tau and fyn antibodies as above.

Finally, CHO cells co-expressing tau (V5-His-tagged) and fyn were treated with pervanadate and subjected to immunoprecipitation with fyn (CST) and V5 antibodies. Western blots were probed with tau and fyn antibodies as above.

In all the conditions tested (Table 5.1), western blots showed that tau and fyn were both present in the total lysate. Samples immunoprecipitated with tau or fyn antibody were all strongly positive for tau or fyn, respectively, showing that the immunoprecipitation of the target antigen was successful. However, tau was not detected in any of the fyn

	Buffer			Treatment				IP antibody									
								Fyn antibodies					Tau antibodies				
Sample	RIPA	HEPES	NETF	IC261	Fractionation	Pervanadate	DSP	Sigma	Fyn BD	Fyn CST	sc-16	sc-434	Fyn 1S	DAKO	TP70	TP007	Tau-5	V5
Rat cortical neurons	x													x				
	x							x										
	x			x				x										
	x											x						
	x										x							
	x								x									
	x			x					x									
	x			x						x				x				
	x			x						x								
	x									x								
		x								x								
			x							x								
	x						x			x								
	x						x				x							
	x						x							x				
	x						x						x					
	x						x										x	
Mouse brain tissue	x											x						
	x								x									
	x							x										
	x										x							
	x									x								
	x									x								
		x								x								
			x							x								
	x									x								
	x													x				
		x													x			
		x														x		
		x																
CHO V5-tau + Fyn	x					x				x								
	x					x												x

Table 5.1 Conditions used for co-immunoprecipitation of tau and fyn

immunoprecipitates and neither was fyn detected in any of the tau immunoprecipitates under any of the conditions tested in these studies. These results are in contrast to the study by Ittner and colleagues (2010), in which the authors used fyn antibodies sc-434 and sc-16 (both from Santa Cruz Biotechnology) to successfully demonstrate co-immunoprecipitation in both directions. It is unclear which antibody was used for immunoprecipitation and which for determining the co-immunoprecipitation, but both antibodies were tested here (Table 5.1). Through personal communication with the authors of the study (Ittner et al., 2010), it appeared that fyn antibodies obtained from Santa Cruz Biotechnology demonstrated considerable batch to batch variability. It was subsequently determined that the batch number used in the studies reported herein differed from that used by Ittner et al. (2010), which could provide a possible explanation for the discrepancy between the results obtained from each laboratory.

It remains possible that the tau-fyn interaction is weak or transient and that successful co-immunoprecipitation requires a precisely optimised combination of factors to detect tau or fyn in the co-immunoprecipitates. The stoichiometry of the tau-fyn interaction is also unclear. It is not known how much tau is normally bound to fyn, and vice versa. The absence of follow-up studies that reproduce an endogenous tau-fyn interaction *in vivo*, in contrast to the abundance of *in vitro* studies using recombinant or overexpressed tau or fyn proteins, suggests that the tau-fyn interaction may not be a robust, stable association, at least under normal conditions. Further methods to concentrate the target proteins, such as additional fractionation into synaptosomes where the tau-fyn interaction is thought to occur, may be necessary to facilitate detection of their binding by co-immunoprecipitation. Alternatively, assays such as Duolink may be capable of detecting transient interactions within cells. Duolink is a proximity ligation assay which detects protein-protein interactions by utilising probes that bind to primary antibodies in fixed cells or tissues. If the target proteins are in close enough proximity (<40 nm), the probes ligate to elicit a reaction that can be visualised under a fluorescent microscope. This approach would also allow visualisation of the subcellular localisation of the tau-fyn interaction.

5.1.2 Fyn expression in the human brain

To investigate fyn expression in human brain, antibodies against fyn were first optimised for use in human post-mortem brain tissue. Brain homogenates from WT and $fyn^{-/-}$ mouse brain tissue were used as controls. Human brain tissue from a control individual without AD that had previously been shown to contain undegraded protein was used as the optimisation sample. Human and mouse brain tissue were separated on 10% SDS-PAGE gels and western blots were probed with antibodies targeting fyn, with β-actin antibody as a loading control.

The polyclonal fyn (Sigma) antibody detected a single, prominent band at 59 kDa in all samples except for $fyn^{-/-}$ mouse brain (Figure 5.2A). Fyn antibodies from Abcam, Invitrogen, and Santa Cruz Biotechnology (sc-434) did not reveal any positive signal in human brain tissue (Figure 5.2A). A second antibody from Santa Cruz Biotechnology (sc-16) did recognise a 59 kDa band in both human and WT mouse brain tissue, but not in $fyn^{-/-}$ brain tissue (Figure 5.2A). However, sc-16 also recognised a non-specific band at 50 kDa in all brain samples. The antibody from Cell Signalling Technologies (CST) also recognised fyn at 59 kDa in human brain tissue. However, the best signal was obtained using the polyclonal fyn (Sigma) antibody which provided a clear fyn band at 59 kDa in both mouse and human brain tissue in the absence of non-specific bands (Figure 5.2A).

An antibody directed against the active form of fyn was also tested for immunoreactivity in mouse and human brain tissue. The src pY420 antibody (CST) recognises fyn and cross-reacts with other src family members only when they are phosphorylated at Y420, which indicates an active conformation. As controls, CHO cells expressing tau and fyn with and without pervanadate treatment were used. Pervanadate inhibits tyrosine phosphatases, resulting in increased tyrosine phosphorylation and increased association of recombinant tau with fyn-SH3 (Usardi et al., 2011). As expected, probing western blots with the fyn (Sigma) antibody revealed a 59 kDa band in all samples except for $fyn^{-/-}$ mouse brain tissue (Figure 5.2B). Conversely, the pY420 antibody only recognised active fyn in CHO cells expressing fyn (Figure 5.2B). This could have been due to the relatively small amount of endogenous fyn in human and mouse brain tissue compared to CHO cells that were overexpressing fyn, or that little of the fyn protein present in human and mouse brain tissue was active under basal conditions.

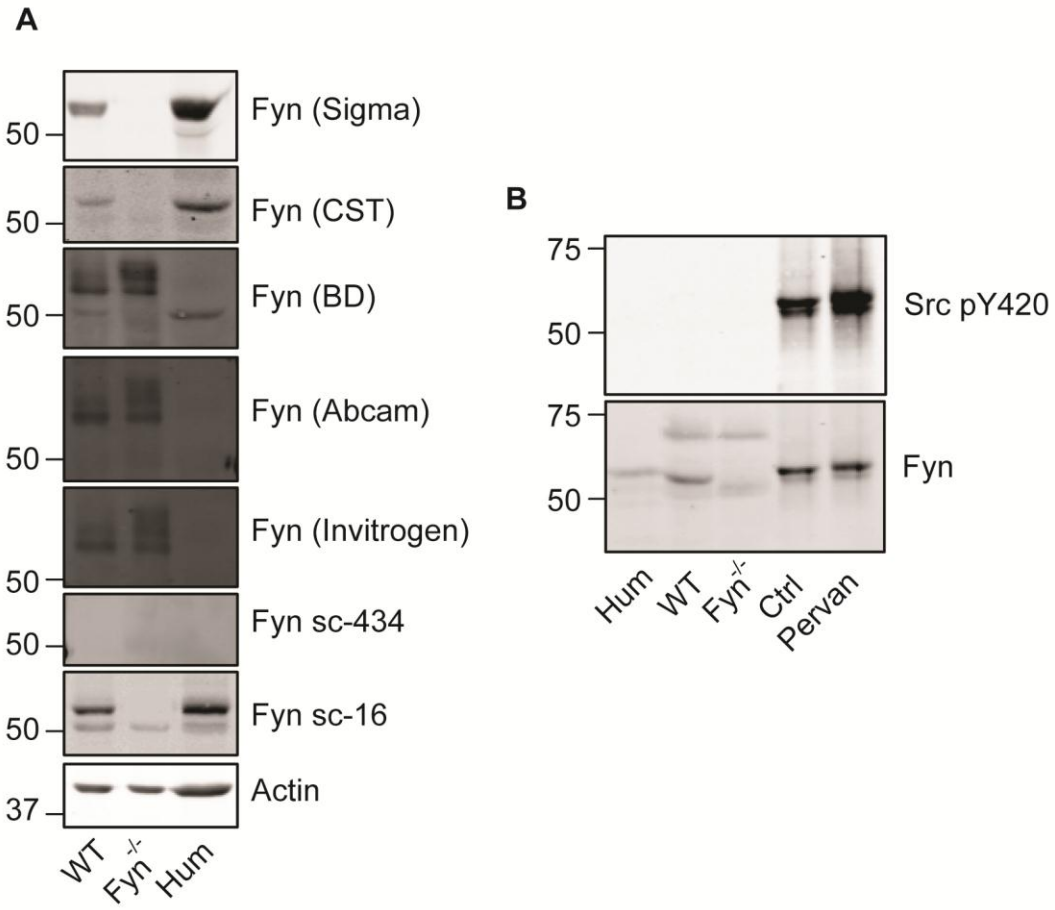

Figure 5.2 Optimisation of antibodies against fyn

Western blots of wild-type (WT) and fyn$^{-/-}$ mouse brain tissue, CHO cells expressing V5-His-tagged tau and fyn, and post-mortem human brain tissue. (A) A panel of polyclonal and monoclonal antibodies directed against fyn were tested in lysates prepared from WT and fyn$^{-/-}$ mouse brain tissue, and human brain tissue (Hum). β-actin antibody was used as a loading control. CST, Cell Signalling Technologies. BD, BD Biosciences. (B) An antibody directed against src phosphorylated at Y420, which cross-reacts with active fyn, was tested in human brain tissue, WT and fyn$^{-/-}$ mouse brain tissue, and CHO cells expressing tau and fyn treated with (Pervan) to increase tyrosine phosphorylation, and vehicle-treated (Ctrl) cells. Pervanadate treatment of CHO cells decreases the mobility of fyn on SDS-PAGE. Molecular weight markers are shown on the left (kDa).

To concentrate the amount of fyn in samples, immunoprecipitation of fyn would facilitate a greater chance of detecting phosphorylation at Y420. This approach would also specifically indicate the amount of active fyn, rather than Y420 detected in other src family members. Therefore, fyn was immunoprecipitated with a monoclonal antibody against fyn (BD Biosciences), using control and AD human brain tissue. Samples were also immunoprecipitated without the addition of a primary antibody as a negative control. Western blots of immunoprecipitated fyn and total brain homogenates (input) were probed with the polyclonal antibodies fyn (Sigma) and src pY420, to avoid cross-reaction with immunoglobulin bands. Probing with the total fyn antibody (Sigma) showed that fyn was present in human brain tissue, but there was considerably less fyn protein immunoprecipitated with the monoclonal fyn (BD Biosciences) antibody (Figure 5.3). The pY420 blot showed the absence of a band at the expected size (59 kDa) in the immunoprecipitates and total lysates, but there appeared to be some cross-reaction with the fyn immunoprecipitation antibody as a band corresponding to the size of the immunoglobulin heavy chain (50 kDa) was recognised (Figure 5.3A). This was likely due to the relatively low amount of fyn that was immunoprecipitated from the brain. A potential cause of the weak immunoprecipitation is the monoclonal antibody used. Its ability to recognise fyn in total lysates is apparent, but its epitope may not be easily accessible in the native form of fyn. To determine whether this is the case, an alternative fyn antibody could be used for immunoprecipitation. However, time constraints meant that optimisation of fyn immunoprecipitation in these samples was not feasible at this time.

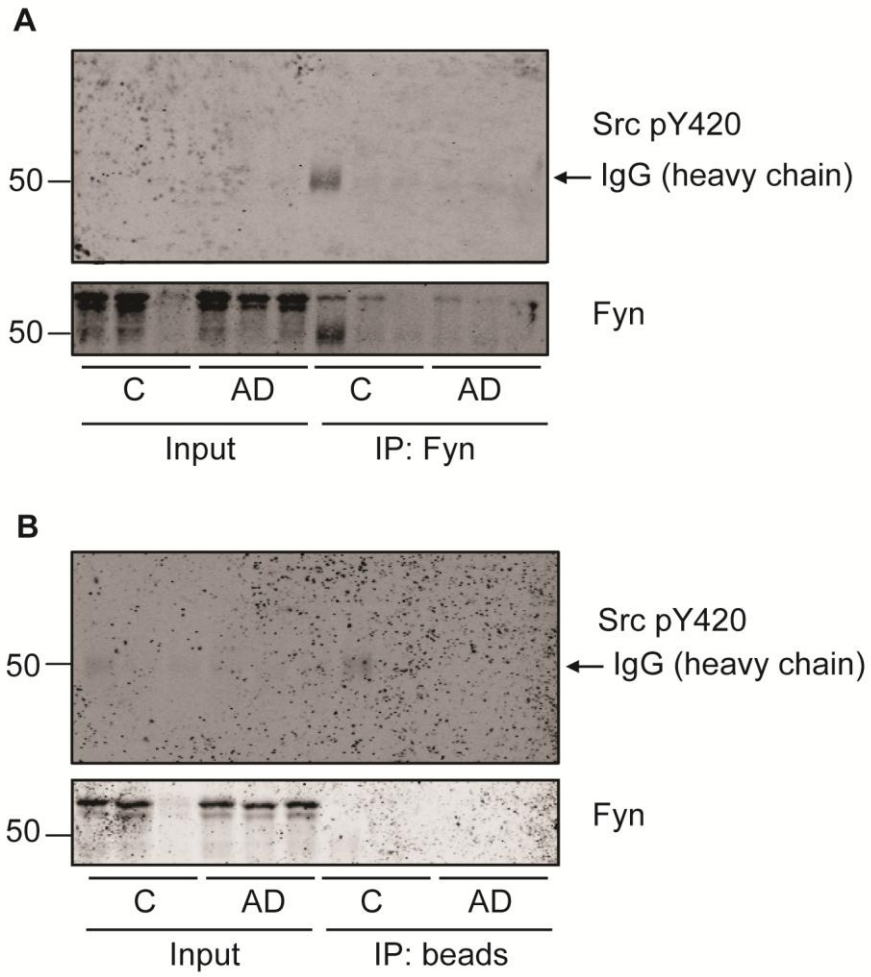

Figure 5.3 Immunoprecipitation of fyn in human post-mortem brain tissue

Western blots of total lysates (input) and immunoprecipitates from human post-mortem brain tissue. (A) Fyn was immunoprecipitated from control (C) and Alzheimer's disease (AD) human brain tissue using a monoclonal fyn antibody. (B) Beads-only immunoprecipitates were included as negative controls. Western blots were probed with polyclonal antibodies against fyn and src phosphorylated at Y420. The 50 kDa heavy chain band is indicated (arrow). Molecular weight markers are shown on the left (kDa).

5.1.3 Alterations in tau and fyn expression during the progression of AD

To investigate any disease-related changes in tau and fyn expression in AD, age-matched human cortical post-mortem brain tissue from control and individuals with sporadic AD (Braak stages I-VI) was homogenised in extra strong lysis buffer (Section 2.1.4) and separated on 10% SDS-PAGE gels. Phosphorylation of tau at several epitopes was investigated by probing western blots with the following tau antibodies: PHF-1 (recognises tau phosphorylated at S396/S404), Tau-1 (tau dephosphorylated at S199/S202), CP13 (tau phosphorylated at S202), pS214, and pS262. All phosphorylated tau species are expressed relative to the total amount of tau. The cohort of brain samples investigated here included brains classified as normal aging controls and Braak stages I-VI (AD). Due to the low numbers of available samples at each Braak stage, the brains were grouped into controls, Braak stages I-II, III-IV, and V-VI.

The amount of total tau was initially measured, relative to neuron-specific enolase (NSE) expression, to determine whether there were any differences in the amount of total tau present in neurons in control and AD brain. NSE was used for normalisation since this neuron-specific protein allows standardisation of samples whilst taking into account neuron loss and gliosis that occurs during the progression of AD. There was wide variation in the total amount of tau relative to NSE in AD brain (Figure 5.4A), although the amount of tau present in control brain appeared to be considerably less than that of AD brains at all Braak stages. Quantification of the western blots showed that tau was significantly increased at Braak stages I-II and Braak stages V-VI, compared to controls (Figure 5.4A).

Tau phosphorylated at the PHF-1 and CP13 epitopes (S396/S404 and S202, respectively) was detectable at Braak stages V-VI, but not in controls or during Braak stages I-IV brain tissues (Figure 5.4B, C). However, the wide variation in phosphorylated tau at Braak stages V-VI meant that no statistically significant difference from controls was determined. Interestingly, the amount of tau phosphorylated at S396/S404 appeared to be significantly increased at Braak stages V-VI compared to earlier Braak stages I-II. However, the significant difference between Braak stages I-II, but not control or Braak stages III-IV, and Braak stages V-VI is not reflected on the western blots as the presence of PHF-1 immunoreactivity is only observed in Braak stages V-VI. Therefore the statistical difference is likely caused by the wide variation in total tau (Figure 5.4B).

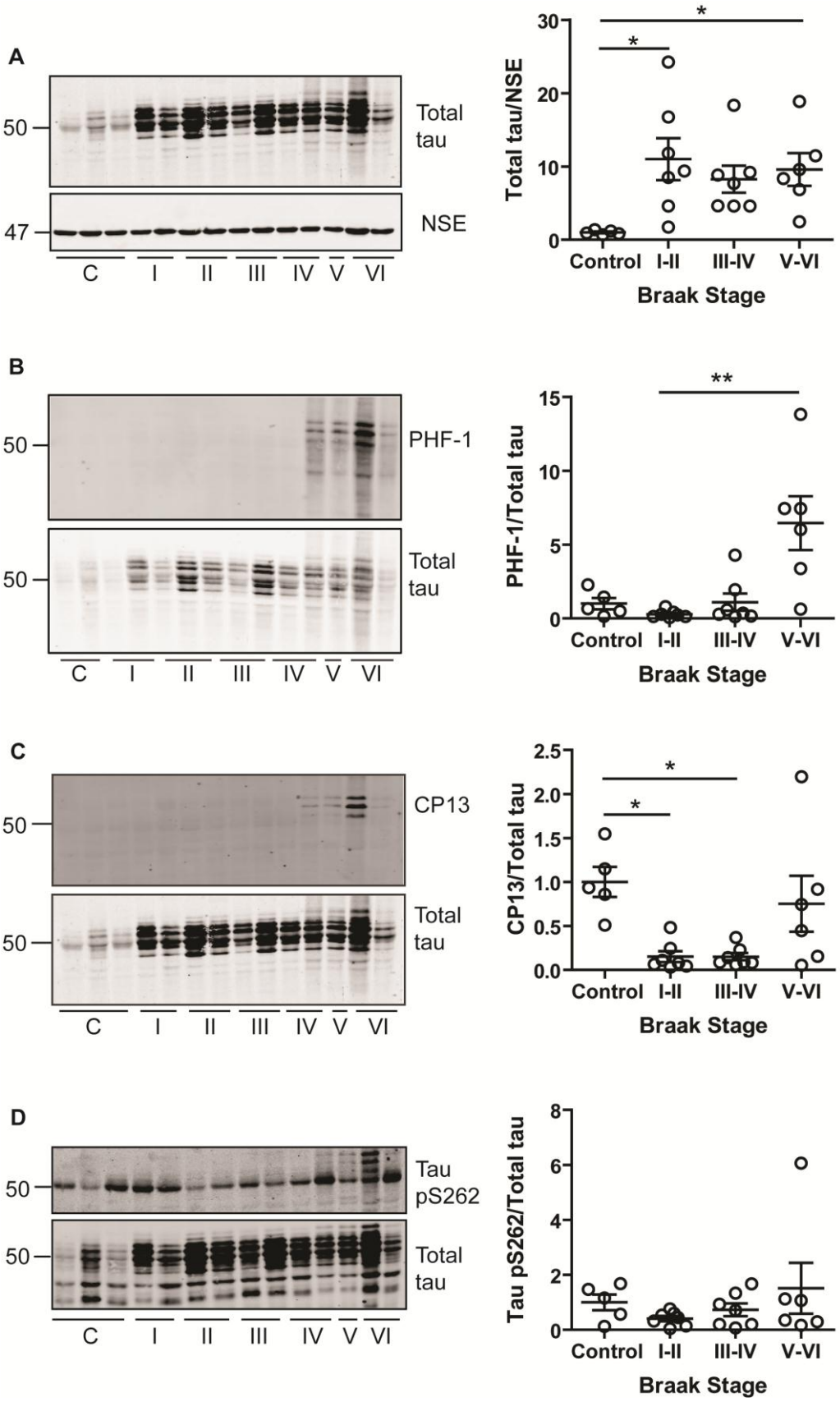
A
50
47
Total tau
NSE
C I II III IV V VI
Total tau/NSE
30
20
10
0
*
*
Control I-II III-IV V-VI
Braak Stage
B
50
50
PHF-1
Total tau
C I II III IV V VI
PHF-1/Total tau
15
10
5
0
**
Control I-II III-IV V-VI
Braak Stage
C
50
50
CP13
Total tau
C I II III IV V VI
CP13/Total tau
2.5
2.0
1.5
1.0
0.5
0.0
*
*
Control I-II III-IV V-VI
Braak Stage
D
50
50
Tau pS262
Total tau
C I II III IV V VI
Tau pS262/Total tau
8
6
4
2
0
Control I-II III-IV V-VI
Braak Stage

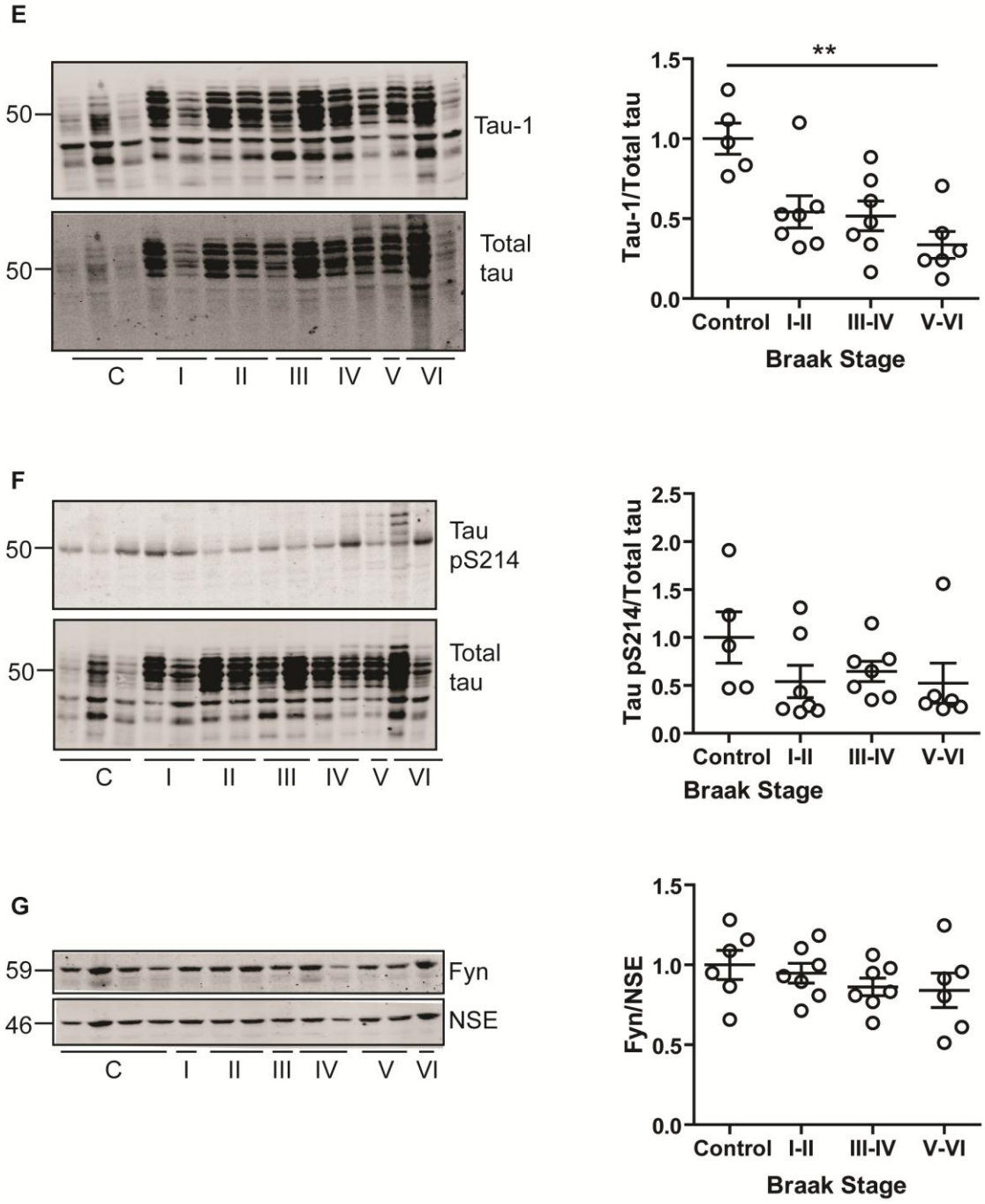

Figure 5.4 Changes in tau phosphorylation over time in AD

Representative western blots of control and AD (Braak stages I-VI) human post-mortem brain tissue. Western blots were probed for (A) total tau, or phosphorylated tau with (B) PHF-1, (C) CP13, (D) tau pS262, (E) Tau-1, and (F) tau pS214. Quantification of total tau is shown in graphs following normalisation to neuron-specific enolase (NSE) amounts in each sample. Quantification of phosphorylated tau is shown in graphs to the right of each western blot following normalisation to total tau amounts in each sample. (G) Western blots were also probed with an antibody against fyn and quantification of fyn was normalised to NSE. Molecular weight markers are shown on the left (kDa). Values represent mean ± SEM, n=6-7 per group. Kruskal-Wallis with post-hoc Dunn's test, *$p < 0.05$, **$p < 0.01$.

In addition, phosphorylation of tau at the CP13 epitope (S202) appeared to be reduced at Braak stages I-IV compared to control brain (Figure 5.4C), but this is likely due to the variation in total tau (Figure 5.4C) rather than any reduction in tau phosphorylation at S202 at Braak stages I-IV.

Phosphorylation of tau at S262 and S214 was detected in control and AD brain of all Braak stages, but the amount of tau phosphorylation at these epitopes, relative to total tau, was not significantly different between controls and AD samples of all stages (Figure 5.4D, F). However, tau species phosphorylated at S262 and S214 appeared to have a higher molecular weight in a subset of Braak stage V-VI AD brain, indicating increased phosphorylation, but this did not reach statistical significance when compared to control brain (Figure 5.4D, F). Nevertheless, this suggests the presence of highly phosphorylated species that are recognised by the pS214 and pS262 tau antibodies in late stage AD brain. The Tau-1 antibody, which recognises tau dephosphorylated at S199/S202, detected tau in both control and AD brain in all samples tested. Notably, tau dephosphorylated at S199/S202 was significantly decreased at Braak stages V-VI compared to control brain (Figure 5.4E), indicating an increase of tau phosphorylated at the S199/S202 in late stage AD brain.

Probing with an antibody against fyn showed that it was present as a 59 kDa band in both control and AD brain (Figure 5.4G). There appeared to be a slight trend towards decreased fyn in subjects in AD brain homogenates of increasing Braak stage (Figure 5.4G). However, this did not reach statistical significance. Levels of fyn protein were normalised to NSE to account for any potential variations in neuronal loss between the different brain samples (Figure 5.4G).

Taken together, these results suggest that increased tau phosphorylation, at least at the epitopes examined here, can be observed in late stage AD brain (Braak V-VI). There appears to be a wide range in the total amount of tau in different AD brains, but these data suggest an accumulation of tau with increasing Braak stage. Phosphorylation of tau at several epitopes (S214, S202, S262, S396/S404) increases with progression of AD as defined by the Braak stage, but some of these results were only shown qualitatively by western blot. The lack of statistical significance apparent following quantification of some of these data is likely caused by the large variations in the total amount of tau present, compounded by the relatively small number of AD brain samples available at each Braak stage.

5.1.4 Tau and fyn expression in the soluble fraction of human brain

It was previously reported that fyn is decreased in the soluble fraction of AD brain and that the increased fyn in the insoluble fraction is correlated with progression of disease (Ho et al., 2005). There is also substantial evidence that tau pathology correlates with the severity of disease (Augustinack et al., 2002). To investigate the relationship between soluble tau and fyn in AD, human post-mortem brain tissue from controls and sporadic AD patients (Braak stages II-VI) were homogenised in detergent-free lysis buffer (Section 2.1.4). Since there are no denaturing or reducing agents in the lysis buffer, insoluble components in the sample are retained in the pellet after centrifugation. The supernatant of homogenised brain tissue was separated on 10% SDS-PAGE gels, analysed on western blots and probed with antibodies targeting tau and fyn.

Samples were grouped into controls, Braak stages II, III-IV, and V-VI, due to a low number of replicates available for each Braak stage. AD brain tissue at Braak stage I was unavailable at this time. Quantification of western blots showed that total tau in AD brain was significantly increased in AD brain at Braak stages V-VI compared to control brain tissue after normalisation to NSE to account for variations in neuronal loss between control and AD brain (Figure 5.5A). However, soluble fyn was unchanged between controls and AD brain across all Braak stages (Figure 5.5B). Interestingly, the bands recognised by the fyn antibody in human brain tissue did not appear as a single prominent band of 59 kDa, but up to four bands ranging from ~48-62 kDa were visible (Figure 5.5B). It is unclear whether these bands are modified species of fyn, or whether they represent different isoforms of fyn. It is possible that the preparation of these samples resulted in protein degradation, reflecting the presence of the lower molecular weight bands of fyn. In addition, the buffer used to prepare these samples does not contain detergent, which may not have been effective at lysis of fyn, a membrane-associated protein. Therefore, this may represent a different pool of fyn which could comprise of different fyn species as compared to membrane-associated fyn. Thus, although the increase in total tau in the soluble fraction of AD brain reflects the previous results using total brain homogenate, the amount of soluble fyn was unchanged in AD brain, in contrast to the results reported by Ho et al. (2005).

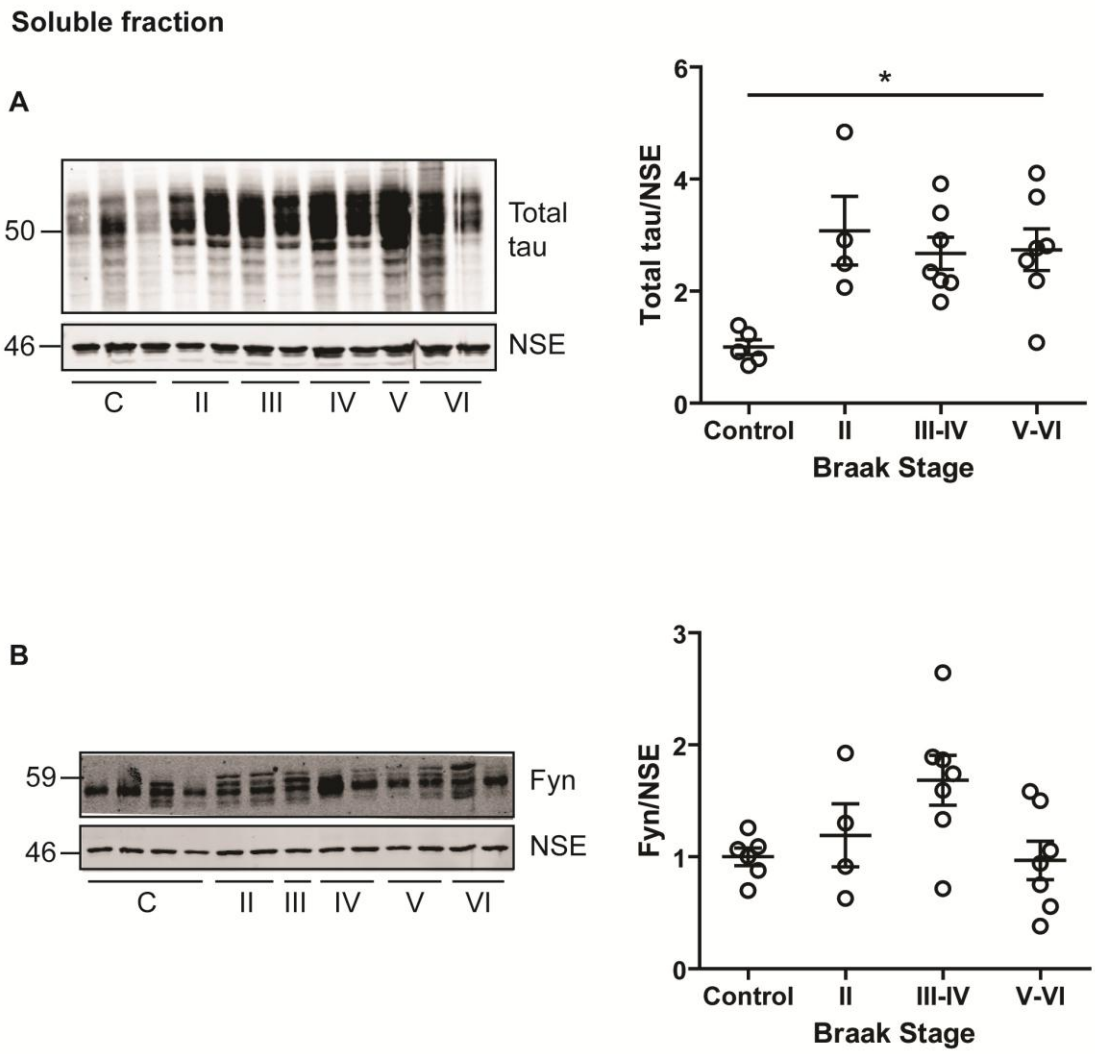

Figure 5.5 Tau and fyn expression in soluble fractions of AD brain

Representative western blots of soluble fractions of control and AD (Braak stages II-VI) post-mortem human brain tissue were probed with antibodies against (A) total tau and (B) fyn. Molecular weight markers are shown on the left (kDa). Quantification of western blots normalised to neuron-specific enolase (NSE) is shown on the right. Values represent mean ± SEM, n=4-7 per group, Kruskal-Wallis with post-hoc Dunn's test, *$p < 0.05$.

5.1.5 Disease-related changes in tau and fyn in the human brain

The number of independent replicates used in the previous experiments shown above is low because samples from early and mid-Braak stages were not readily available. The low replicate number combined with high variability within groups is likely to have influenced the statistical analyses performed. We hypothesised that alterations of fyn levels and tau phosphorylation would be most prominent in the late stages of AD where severe tau pathology is observed. Hence, tau and fyn expression were investigated further in a larger cohort of control and Braak stages V-VI AD brain to increase the statistical power of the experiments.

All samples showed prominent tau staining with the distinctive banding pattern of human tau (Figure 5.6A). After normalisation to NSE to account for variability in neuronal loss, the total amount of tau was shown to be significantly increased in AD brain (Braak stages V-VI) compared to control brain (Figure 5.6A). The total amount of tau also appears to have wide variation in AD brain, which is not seen in control brain, in agreement with previous results shown earlier in this chapter (Figure 5.6A). Western blots showed barely any immunoreactivity to PHF-1 antibody in control brain, as shown previously (Figure 5.6B). Quantification of PHF-1 bands showed a significant increase of PHF-1 immunoreactive tau in AD brains at Braak stages V-VI compared to control (Figure 5.6B), suggesting that phosphorylation of tau at this site is a feature of AD brain. Likewise, tau immunoreactivity to CP13 antibody was barely detectable in control samples but higher molecular weight bands at ~65-70 kDa were recognised by this antibody in AD brain (Figure 5.6C). Quantification of these tau species relative to total tau revealed that CP13 immunoreactivity was significantly increased in AD brains compared to control (Figure 5.6C). The pS262 tau antibody revealed higher molecular weight bands (65-70 kDa) in AD, but not control, samples, and these species were also found to be significantly increased in AD (Figure 5.6D). Phosphorylation of tau at S214, which is located close to the PXXP motifs important for tau-fyn binding (Chapter 4), was also investigated in human brain tissue. pS214 tau antibody revealed a 50 kDa band present in all brain samples, which co-localised with tau (Figure 5.6E). However, quantification showed that tau phosphorylated at S214 relative to total tau was not significantly different between AD and control brains (Figure 5.6E). Tau-1, an antibody which recognises dephosphorylated tau at S199/S202, revealed prominent bands in all samples tested (Figure 5.6F). Quantification of Tau-1 bands relative to total tau showed a significant decrease of Tau-1 immunoreactivity in AD samples compared to control, indicating phosphorylation at S199/S202 is increased in AD (Figure 5.6F). This reflects the increase of CP13-immunoreactive bands in AD samples, as CP13 recognises phosphorylated tau at S202.

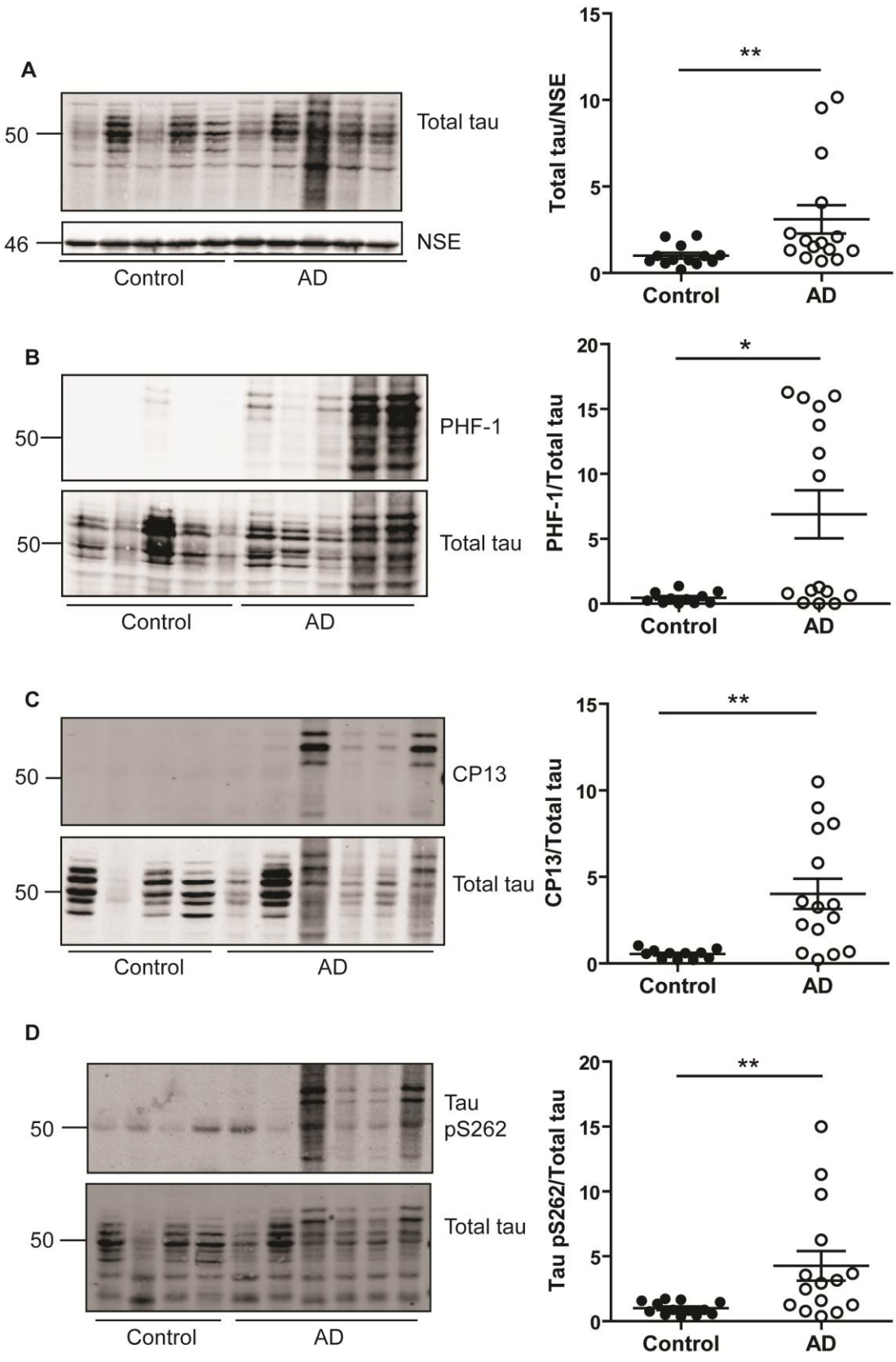
A
50
Total tau
46
NSE
Control
AD
Total tau/NSE
15
10
5
0
**
Control
AD
B
50
PHF-1
50
Total tau
Control
AD
PHF-1/Total tau
20
15
10
5
0
*
Control
AD
C
50
CP13
50
Total tau
Control
AD
CP13/Total tau
15
10
5
0
**
Control
AD
D
50
Tau
pS262
50
Total tau
Control
AD
Tau pS262/Total tau
20
15
10
5
0
**
Control
AD

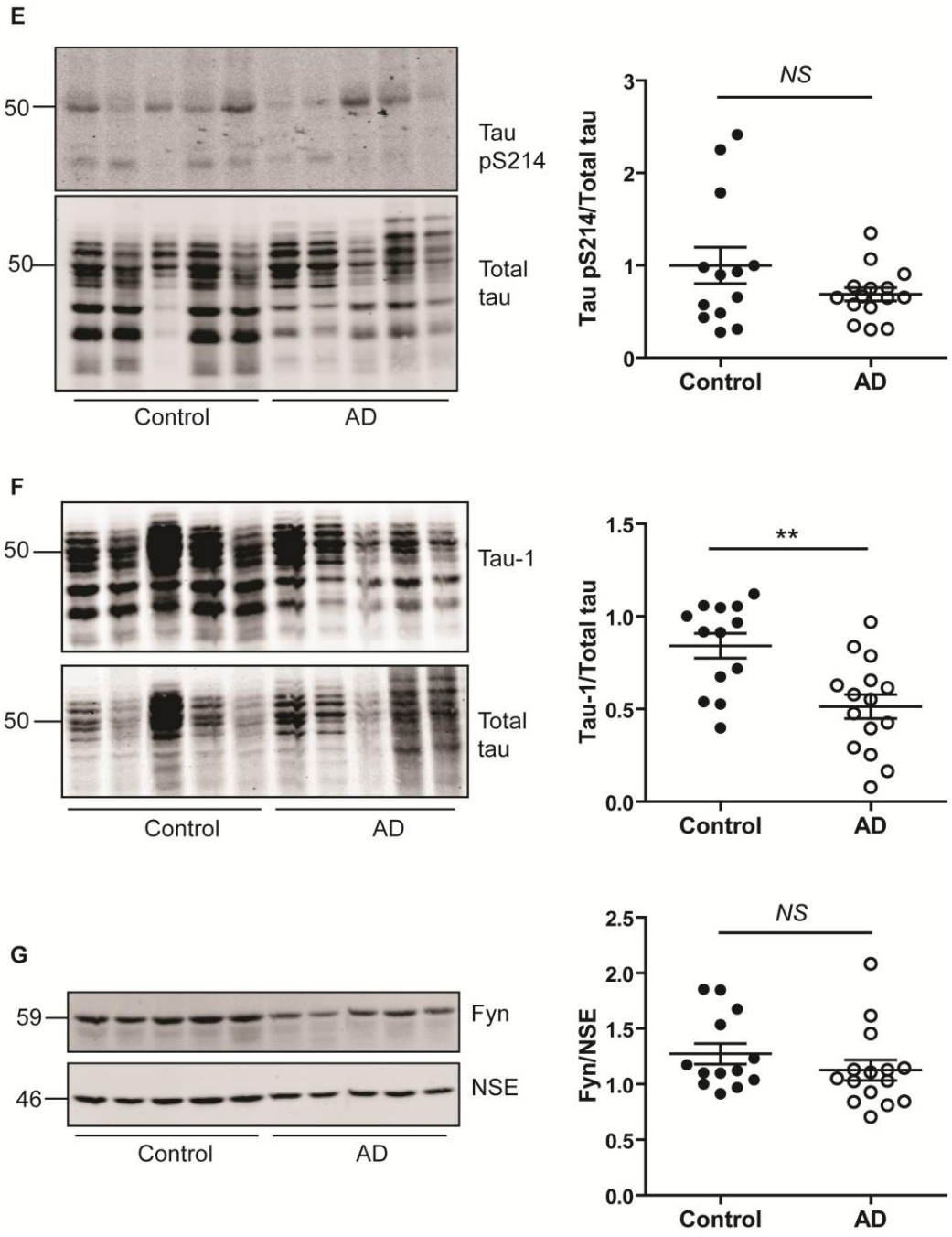

Figure 5.6 Altered tau and fyn expression at late stages of AD (Braak stages V-VI)

Representative western blots of control and AD (Braak stages V-VI) post-mortem human brain tissue were probed with antibodies against (A) total tau and phosphorylated tau. Tau phosphorylation was detected with antibodies (B) PHF-1, (C) CP13, (D) tau pS262, (E) Tau-1, and (F) tau pS214. Quantification of total tau was normalised to neuron-specific enolase (NSE). Quantification of phosphorylated tau is shown to the right of each western blot and normalised to total tau. (G) Western blots were also probed with an antibody against fyn and quantification of fyn was normalised to NSE. Molecular weight markers are shown on the left (kDa). Values represent mean ± SEM, *n*=13-16 per group. Mann-Whitney non-parametric test, *$p < 0.05$, **$p < 0.01$, *NS* = not significant.

To determine whether any changes in the amount of fyn protein could be observed in AD, western blots of human brain tissue were probed with an antibody against fyn. The amount of fyn protein was normalised to NSE to ensure any alterations in fyn protein were not due to neuronal loss. Quantification of fyn bands showed that levels of fyn protein, relative to NSE, appeared to be slightly decreased in AD compared to control brains, but this decrease did not reach significance (Figure 5.6G). A summary of the statistical significance between control and AD brains for phosphorylated tau and total fyn is shown in Table 5.2.

Table 5.2 Summary of significance values from western blots of tau and fyn in control and AD brain tissue

	Antibody						
	Total tau	**PHF-1**	**CP13**	**Tau pS262**	**Tau-1**	**Tau pS214**	**Fyn**
Control vs late stage	0.0075	0.0292	0.0022	0.0099	0.0017	0.1281	0.0668
Control vs I-II	*	*NS*	*	*NS*	*NS*	*NS*	*NS*
Control vs III-IV	*NS*	*NS*	*	*NS*	*NS*	*NS*	*NS*
Control vs V-VI	*	*NS*	*NS*	*NS*	**	*NS*	*NS*
I-II vs III-IV	*NS*	*NS*	*NS*	*NS*	*NS*	*NS*	*NS*
I-II vs V-VI	*NS*	**	*NS*	*NS*	*NS*	*NS*	*NS*
III-IV vs V-VI	*NS*	*NS*	*NS*	*NS*	*NS*	*NS*	*NS*

Table 5.2 shows the significance values obtained following statistical analysis of total tau relative to NSE, tau phosphorylation at the epitopes PHF-1, CP13, pS262, Tau-1, and pS214 normalised to total tau, and fyn levels normalised to NSE, in controls and AD post-mortem human brain tissue. Mann-Whitney test was carried out to determine the difference between means of controls and late-stage AD (Braak stages V-VI, Figure 5.6), while the Kruskal-Wallis with post-hoc Dunn's test was carried out to determine the difference between means of controls and AD groups (Braak stages I-II, III-IV, V-VI, Figure 5.4). * $p < 0.05$, ** $p < 0.01$, *NS* = not significant.

To determine if there was any correlation between levels of fyn protein in AD and tau phosphorylation at the epitopes above, non-parametric Spearman correlation analysis was carried out. Correlation between tau and fyn was first investigated in the cohort of control and late-stage (Braak V-VI) AD patients as a combined group, to investigate whether there was any association irrespective of the neuropathological status (Figure 5.7). Notably, fyn was significantly correlated with pS214 tau in both control and AD brain (Figure 5.7F). When the control and AD groups were combined, the amount of fyn was not associated with that of total tau (Figure 5.7A), phosphorylated tau at S396/S404 (Figure 5.7B), S202 (Figure 5.7C), S262 (Figure 5.7D), or S199/S202 (Figure 5.7E).

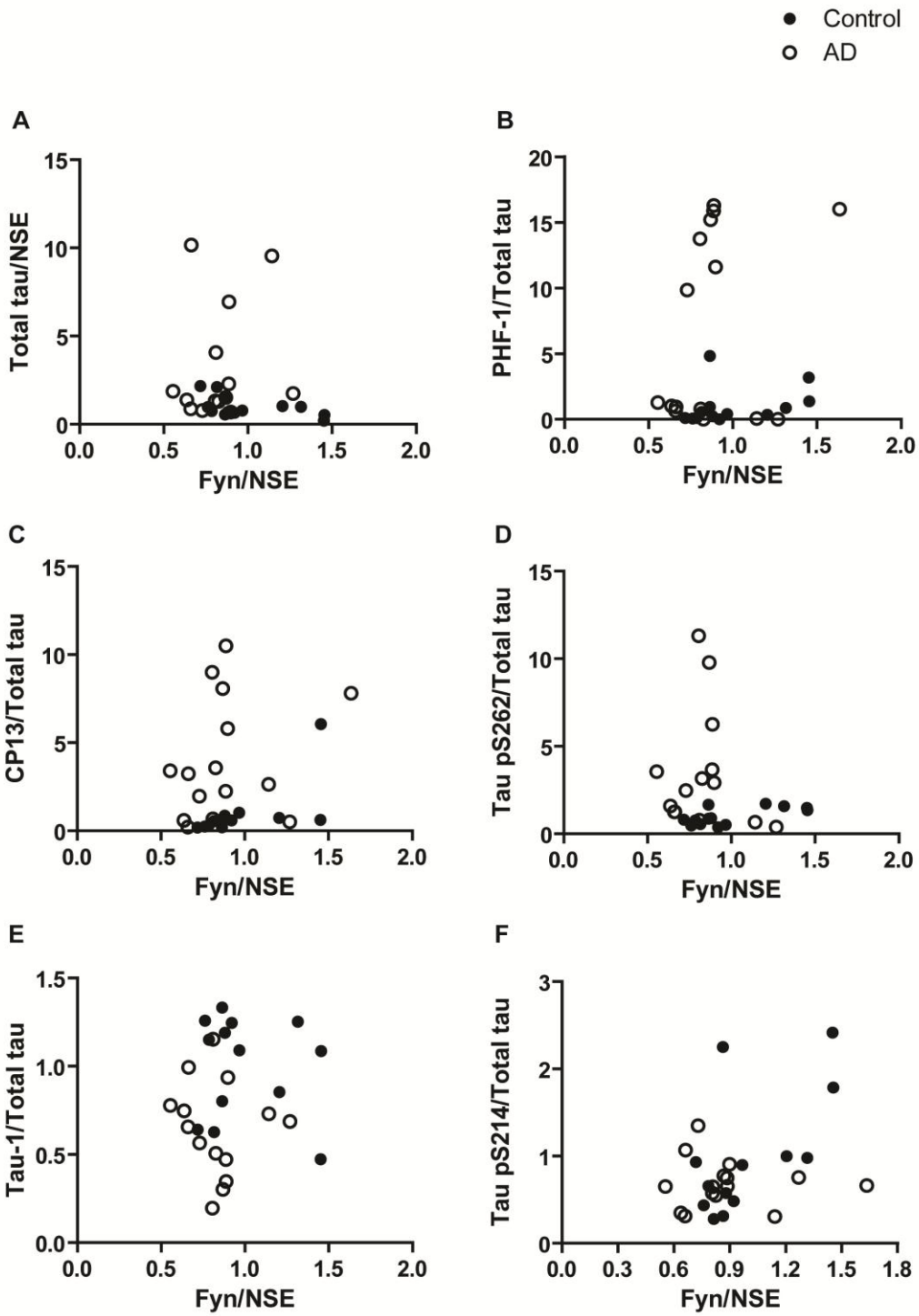

Figure 5.7 Correlation between disease-related changes in tau and fyn in AD brain

Spearman's rank correlation analysis of the (A) total amount of tau, phosphorylated tau at (B) PHF-1, (C) CP13, (D) pS262, (E) tau-1 (F) pS214 epitopes relative to fyn in post-mortem control and AD human brain. See Table 5.3 for details of significant correlations. Filled circles, control. Open circles, AD.

To investigate whether the correlation between fyn and tau was altered due to neuropathological AD status, the cohort was separated into controls and AD samples and re-analysed for correlation. A summary of Spearman's rank correlation coefficients and significance levels for correlation between fyn and tau in control and AD brain is shown in Table 5.3. Statistically significant results are highlighted in purple. Interestingly, this analysis showed that the amount of fyn was positively correlated with tau phosphorylated at S202 (CP13) and S214 in control brain, but not in AD brain (Table 5.3). There appeared to be a negative correlation between the amount of total tau and fyn in control brain, but this was not statistically significant (Table 5.3). Tau phosphorylated at S396/S404 (PHF-1) appeared to be positively correlated with the amount of fyn in control brain, but this did not reach statistical significance (Table 5.3).

Table 5.3 Analysis of correlation between the amounts of tau and fyn in control and AD brain

	Control		AD	
Fyn vs	***r***	***p***	***r***	***p***
Total tau	-0.5257	0.065	0.156	0.5942
PHF-1	0.5055	0.0812	0.1752	0.5293
CP13	0.8741	0.0004	0.2857	0.3012
Tau pS262	0.4670	0.1103	-0.1209	0.6806
Tau-1	-0.1504	0.6238	-0.1198	0.6833
Tau pS214	0.6099	0.0269	-0.0699	0.8045

Spearman's rank correlation coefficients (*r*) and significance values (*p*) corresponding to associations between fyn, and total and phosphorylated tau. Correlation analyses were carried out on brains from controls only or AD only.

This suggests that tau phosphorylation at S202 and S214 correlates with the amount of fyn in normal brain, but that this correlation is lost in AD. These data support the hypothesis that tau and fyn are associated under normal conditions, but that pathological activation of fyn by Aβ or other alterations in fyn in AD may directly or indirectly alter downstream regulation of tau phosphorylation.

5.2 Discussion

In this chapter, co-immunoprecipitation was used to identify an interaction between tau and fyn *in vivo*. In addition, to investigate whether the expression levels of fyn is associated with the pathogenesis of AD, human post-mortem tissue of control and AD brain was analysed on western blots. Moreover, the accumulation of phosphorylated tau was investigated in controls and AD brain. Statistical analyses showed that the amount of fyn does not correlate with increased tau phosphorylation in AD.

Both tau and fyn were successfully immunoprecipitated from mouse brain tissue, primary rat cortical neurons, and CHO cells expressing tau and fyn. However, the presence of fyn in tau immunoprecipitates and tau in fyn immunoprecipitates was not observed, suggesting that either these two proteins do not co-immunoprecipitate, that any binding is transient, or that the amounts of associated proteins were below the level of detection using these antibodies. A large number of different conditions were applied in order to optimise the co-immunoprecipitation. A decisive factor is likely the combination of binding and detection antibodies, although antibodies that did not overlap with the SH3 domain of fyn or the proline-rich region in tau were used for immunoprecipitation. Given that several studies have now confirmed that tau and fyn can directly interact *in vitro* (Lee et al., 1998; Bhaskar et al., 2005; Usardi et al., 2011; Pooler et al., 2012; Cochran et al., 2014), and two independent studies have verified the tau-fyn interaction using endogenous proteins *in vivo* by co-immunoprecipitation (Ittner et al., 2010; Mondragon-Rodriguez et al., 2012), it is likely that the tau-fyn interaction may well exist *in vivo*. It is probable that this interaction is transient, as the major function of tau is to bind to microtubules. In addition, only a small proportion of tau is bound to the plasma membrane (Maas et al., 2000; Pooler et al., 2012; Liu and Götz, 2013), and a similarly small pool of tau is found at the dendrite (Ittner et al., 2010; Mondragon-Rodriguez et al., 2012; Liu and Götz, 2013; Frandemiche et al., 2014). It is not clear what proportion of fyn is normally bound to tau. Therefore, the amount of tau bound to fyn may be only a very minor proportion of the total amount of tau in neurons. It is possible that for the studies with successful co-immunoprecipitation between tau and fyn, much larger amounts of protein were used as the starting material in order to concentrate the target proteins. However, in the experiments presented herein, a considerable amount of fyn and tau protein was immunoprecipitated from the starting material, suggesting that this is not the sole reason for the lack of co-immunoprecipitation.

An interesting question would be to identify the precise cellular localisation of the tau-fyn interaction. Fyn is required for phosphorylation-dependent trafficking of tau to the

membrane, although the amount of tau at the membrane under basal conditions does not appear to be affected by the presence of fyn (Pooler et al., 2012). Fyn is also required for recruitment of tau to lipid rafts (Williamson et al., 2008; Usardi et al., 2011). In parallel, tau is required for the localisation of fyn at the dendrite. Does the interaction occur at the dendrite, as suggested by Ittner et al. (2010), or in the cytosol from where the complex is transported to dendrites? Further investigation is required to answer this question. One approach would be to utilise imaging methods such as Duolink, in which interaction of endogenous proteins can be detected and quantified in fixed cells. Identification of the tau-fyn localisation would aid in developing specific therapeutics for AD, if unique components of a pathological tau-fyn interaction can be targeted dependent on its subcellular localisation.

Although there is now compelling evidence for a signalling cascade via fyn triggered by Aβ (Larson et al., 2012; Um et al., 2012; Rushworth et al., 2013), data from this chapter show that the amount of fyn is not altered in AD brain relative to control tissue. Thus, the role of fyn in the pathogenesis of AD does not appear to be related to the fyn expression. Fyn activity, as determined by immunoprecipitation of fyn followed by western blots with an antibody against the active form of fyn, has been shown to increase in AD patients compared to controls (Larson et al., 2012). The amount of fyn is also correlated with that of PrP^{C} in both control and AD brains (Larson et al., 2012). However, the relationship of fyn with total tau or tau phosphorylation has not been investigated previously. Here, data from this chapter show that the amount of fyn does not correlate with tau phosphorylation in AD, suggesting that regulation of tau phosphorylation, at least at the serine/threonine residues examined here, is not the major pathogenic mechanism of fyn in AD. It will be interesting to determine whether the amount of fyn correlates with tau phosphorylation at tyrosine residues in human brain. However, in this study, fyn kinase activity was not examined and this would likely provide more accurate data as to the role of fyn in regulating downstream effects of tau phosphorylation. Further investigations to determine the relationship between fyn kinase activity and tau phosphorylation, including the tyrosine phosphorylation of tau, in human brains will be important in developing novel therapeutics for AD.

Intriguingly, although no correlation was found between levels of fyn and tau phosphorylation at S199, S262, or S396/S404, there was a significant correlation between fyn and tau phosphorylated at S202 and S214 in control brain tissue. This correlation was not apparent in AD brain, suggesting that at least during the late stages of AD, underlying pathogenic mechanisms may result in disruption of the association between fyn and tau phosphorylated at these epitopes. Notably, inhibition of CK1δ, which results in increased tau dephosphorylated at S199/S202, increases the

association of tau with fyn-SH3, while okadaic acid, which induces tau phosphorylation at multiple sites, including S199/S202, decreases the tau-fyn association (Pooler et al., 2012). Phosphomimics of tau at S202 have altered affinity for fyn *in vitro* dependent on the insertion of microtubule-binding repeats of tau (Bhaskar et al., 2005). Phosphorylation at S214 of tau has been shown to inhibit binding between tau and microtubules, as well as preventing aggregation of tau fibrils (Illenberger et al., 1998; Schneider et al., 1999). Detachment of tau from microtubules might increase the likelihood of tau associating with fyn. Interestingly, although tau phosphorylation at S262 is also important for microtubule binding with tau (Schneider et al., 1999), the amount of tau phosphorylated at S262 did not correlate with fyn in control or AD brain. It is possible that tau phosphorylated at S202 and S214 can bind to fyn normally, but at late stages of AD, tau becomes increasingly phosphorylated at other epitopes which might alter the subcellular localisation of tau and cause the loss of tau-fyn binding. The progressive accumulation of tau into aggregates in AD could also result in the loss of the association with fyn. However, it is important to note that correlation analyses do not imply causation. Hence, further investigation is required to fully understand the relationship between fyn and tau phosphorylation, in particular at the epitopes S214 and S202, and to determine what relevance this has for AD.

These data suggest that therapies targeting the expression level of fyn may not be beneficial to AD patients, but a fyn kinase inhibitor is currently being tested in phase IIa clinical trials as a therapy for AD (Nygaard et al., 2014). If successful, this will provide proof-of-concept evidence that reducing fyn kinase activity can be therapeutically beneficial for AD patients. It will be interesting to investigate whether fyn inhibition affects downstream targets such as tau phosphorylation at specific epitopes, tau localisation, tau function, and slow disease progression in AD.

Chapter 6 Discussion

The primary aims of this thesis were to investigate and characterise the functional implications of interactions between tau and fyn in AD and how this association might contribute to mechanisms underlying the development of neurodegenerative disease.

For several years, research into tau and Aβ-mediated neurodegeneration has dominated the field of AD research. The amyloid cascade hypothesis has been a leading guide for much of this research (Hardy and Higgins, 1992), although the original hypothesis has required significant modification over the years (Hardy, 2009; Karran et al., 2011). The amyloid cascade hypothesis posits that the accumulation of toxic Aβ peptide in the brain triggers downstream changes in tau, leading to synaptotoxicity and neurotoxicity. However, the mechanisms that link Aβ and tau have so far been unclear. Mounting evidence points to the tyrosine kinase fyn as an important mediator in the signalling cascade between Aβ and tau. Upregulation of fyn activity is induced by Aβ (Williamson et al., 2002; Um et al., 2012), and increased fyn activity is found in AD brain (Larson et al., 2012). Fyn is a known tau kinase (Lee et al., 2004), and both tau and fyn co-localise in a subset of degenerating neurons in AD (Shirazi and Wood, 1993). The presence of fyn is also required for phosphorylation-dependent trafficking of tau (Usardi et al., 2011; Pooler et al., 2012). Thus, identifying the mechanisms by which tau and fyn may contribute to neurodegeneration will aid in understanding the missing mechanisms that link the pathogenesis of Aβ and tau and lead to the development of AD.

The primary findings of the work presented in this thesis are that:

- Tau is released through activity-dependent mechanisms in organotypic brain slices, but this process does not appear to be regulated by fyn.
- The PXXP motifs located between residues 213-219 of tau are critical for the interaction between tau and fyn.
- The amount of fyn is not altered during the progression of AD, nor is it correlated with tau phosphorylation in AD, suggesting that fyn-dependent pathways are regulated by the activity, rather than the total amount of fyn in AD brain.

6.1 Regulation of extracellular tau release

The presence of extracellular tau supports the hypothesis that tau pathology can spread in a stereotypic, trans-synaptic manner in the brain of some neurodegenerative diseases. Spreading of tau pathology via anatomically-connected pathways was first shown in 2009. Injection of brain extracts obtained from P301S tau transgenic mice into WT human tau-overexpressing mice resulted in the formation of tau filaments and over time, tau pathology spread beyond the injection site, which could not be explained by diffusion alone (Clavaguera et al., 2009). Two further studies have since been published that confirm these findings *in vivo* in mice in which P301L tau expression is restricted to the entorhinal cortex. In these mice, tau pathology spreads progressively in an age-dependent manner along anatomical pathways to hippocampal neurons that do not express the transgene (de Calignon et al., 2012; Liu et al., 2012). Induction of tau fibrils was also observed when young P301S tau transgenic mice were injected with brain extract from aged P301S tau mice at a time when the recipients were pre-symptomatic (Ahmed et al., 2014). Tau pathology spread to the contralateral side of the brain, as well as to other regions that are anatomically connected to the injection site, further supporting the conclusion that tau propagation is trans-synaptic. Taken together, these results suggest that rather than tau pathology being spread by diffusion of cell contents as a result of cell death, tau propagation is an active process. Notably, neurodegeneration or severe neuronal loss was not detected in any of these models, suggesting that mechanisms other than the toxic effects of abnormally folded and aggregated tau may lead to a loss of neurons in AD. This also indicates that the species of transmitted tau may not be solely responsible for neurodegeneration and that other toxic tau species are involved, or that propagation of tau pathology occurs at an earlier stage of disease prior to widespread neurodegeneration or neuronal loss. At a recent meeting, it was reported that mice expressing P301L tau restricted to the entorhinal cortex exhibit hypometabolism in the entorhinal cortex and hippocampus by two years of age, as determined by functional magnetic resonance imaging (Duff et al., 2013). Even at two years of age, there is no change in cognitive function as assessed by the Morris water maze test (Duff et al., 2013). This is similar to AD patients with neuropathology classified as Braak stage I or II, as these individuals exhibit hypometabolism but without any overt cognitive symptoms (Duff et al., 2013).

The mechanisms underlying the spread of tau pathology are not yet understood. If tau propagation is indeed trans-synaptic, it must exit the neuron in order to cross the synapse into the connected neuron. Hence, it is plausible that tau is normally released as a physiological process, and in pathological conditions, toxic species of tau are

transmitted, leading to the spread of tau pathology. Tau can be detected in the interstitial fluid and cerebrospinal fluid of WT and P301S tau-expressing mice at an age when no overt neurodegeneration is detected, suggesting that tau can be secreted into the extracellular space under physiological conditions *in vivo* (Yamada et al., 2011).

In this thesis, organotypic brain slices were validated for use as a physiologically relevant *ex vivo* alternative to primary neurons, since brain slices express synaptic markers within two weeks of preparation and are cultured in the presence of astrocytes and glia. The data presented in Chapter 3 show that, similar to primary neurons, tau in organotypic brain slices is released into the extracellular medium in an activity-dependent manner. Importantly, this release of tau is not associated with a significant increase in cell death, as measured by lactate dehydrogenase assay. These results confirm previous findings in primary rat cortical neurons that tau release can be stimulated by neuronal activity (Pooler et al., 2013a). In agreement with these findings, it was recently reported that an increase of endogenous tau in the interstitial fluid of WT mice could be observed following neuronal depolarisation by potassium chloride. This activity-dependent secretion of tau increased from 1-3 hours following stimulation, and tau in the interstitial fluid gradually returned to baseline within 5 hours after neuronal depolarisation (Yamada et al., 2014). In the studies presented in this thesis, extracellular tau in the medium was increased 10-fold following potassium chloride stimulation of neuronal activity in organotypic brain slices. Time points longer than 30 minutes were not examined, although it could be anticipated that the rise in extracellular tau and subsequent return to baseline would mirror that observed *in vivo* by Yamada et al. (2014). Herein, the amount of intracellular tau was unchanged following activity-dependent secretion of tau, suggesting that the amount of both basal and stimulated tau release was very low when considered as a proportion of total endogenous tau. The total amount of tau released into the medium was not measured in this study, but extracellular tau has been reported to be approximately 40-50 ng/ml in the interstitial fluid of WT mice (Yamada et al., 2011). In primary mouse cortical neurons, the amount of extracellular tau present under resting conditions has been determined to be approximately 2-3% of intracellular tau (Karch et al., 2012). This estimate is likely to be similar to the organotypic brain slices used in this thesis, as the primary neurons used by Karch et al. (2012) were grown on an astrocyte monolayer, reflecting the mixed cell population in organotypic brain slice culture. Given that the concentration of neuronal tau is estimated to be 1-2 μM (Iqbal et al., 2010; Zempel and Mandelkow, 2014), if the proportion of extracellular tau is 2-3% of total tau, the concentration of tau would be approximately 20-60 nM in the culture medium.

6.1.1 The role of fyn in tau release

To investigate the intracellular source from which extracellular tau might originate, we hypothesised that a pool of membrane-associated tau, which is a small proportion of the total amount of endogenous tau, is released upon stimulation of neuronal activity. Fyn is required for the phosphorylation-dependent trafficking of tau to the membrane (Pooler et al., 2012), leading to the hypothesis that fyn is required for tau release. Interestingly, the results in Chapter 3 show that organotypic brain slices prepared from fyn knockout mice did not exhibit a change in the amount of tau released compared to that released from WT brain slices. There was also no change in the amount of basal tau release in $fyn^{-/-}$ organotypic brain slices compared to WT. These results suggest that while fyn plays a role in trafficking proteins, such as tau, ephrin-A, Dab1, and APP, to the membrane (Hoe et al., 2008; Baba et al., 2009; Minami et al., 2011; Pooler et al., 2012), fyn is not involved in the regulation of tau secretion. These results could also indicate that the extracellular tau does not originate from the membrane-associated pool of tau. It should be noted that the presence of fyn does not affect basal levels of membrane tau, so it is also possible that stimulation of neuronal activity would result in fyn-independent release of membrane tau. Because phosphorylation of tau changes its dynamic association with the membrane through a fyn-dependent mechanism (Pooler et al., 2012), another possibility is that phosphorylation of tau could alter tau release by a fyn-dependent mechanism. Although this idea was not examined here, the results obtained in this thesis suggest that there may be more than one mechanism underlying tau release, and that this could be triggered either by neuronal activity or tau phosphorylation. Further investigation is required to examine how phosphorylation of tau affects its release and whether or not this is a separate mechanism to activity-stimulated tau release. If so, it will be important to determine whether fyn is involved in either mechanism of tau release.

6.1.2 Implications of activity-dependent tau release for AD

A worthy avenue of investigation is to examine how tau secretion is altered under pathological conditions because dysregulation of this process could have implications for the propagation of tau pathology in AD. Aggregates of truncated tau injected into the brains of mutant P301S tau transgenic mice resulted in decreased tau presence in the interstitial fluid *in vivo* compared to controls (Yamada et al., 2011). Moreover, P301S tau transgenic mice secrete reduced amounts of tau into the interstitial fluid over time from 6-12 months, whereas the amount of tau in the interstitial fluid remains stable in

WT mice over the same period of time (Yamada et al., 2011). As P301S tau mice accumulate tau tangles from 6 months of age, the reduction of tau in the interstitial fluid accompanies the accumulation of aggregated tau and the corresponding decrease in intracellular soluble tau, neither of which events occurs in WT mice (Yamada et al., 2011). These results suggest that sequestration of soluble tau into aggregates results in decreased tau secretion and reduced levels of extracellular tau. In addition, destabilisation of microtubules with pseudolaric acid, a microtubule-destabilising agent, led to significantly increased extracellular tau amounts, indicating that loss of binding to microtubules, one of the major functions of tau, also has significant consequences for tau release (Karch et al., 2012). In addition, HEK293T cells expressing mutant P301S, P301L, or R406W tau produce less extracellular tau than WT tau-expressing cells under basal conditions, in the absence of any detectable changes in the amount of intracellular tau (Karch et al., 2012), indicating that some disease-relevant species of tau have altered capacity to be released. Activity-dependent tau secretion was also unchanged in the presence of soluble Aβ oligomers, nor did the level of basal tau decrease with Aβ treatment (Pooler et al., 2013a). Conversely, HeLa cells expressing a phospho-mutant of tau in which 12 residues were mutated to glutamate, to mimic a state of phosphorylation, secreted considerably more tau than cells expressing WT tau (Plouffe et al., 2012). In another study, tau secretion was investigated in primary cortical neurons under stress conditions (Mohamed et al., 2014). Nutrient deprivation and inhibition of lysosomal function resulted in increased stress and elevated basal tau secretion that was not associated with loss of cell viability (Mohamed et al., 2014). Hence, a wealth of published literature shows that conditions mimicking disease can not only alter intracellular tau function and phosphorylation, but also dysregulate tau release, all in the absence of neuronal death.

Previous work showed that activity-dependent tau secretion, and intracellular tau amounts, were unchanged in the presence of soluble Aβ oligomers (Pooler et al., 2013a). It was an intention of this study to investigate the effects of Aβ on tau release in a more physiologically relevant slice culture model. However, results presented in this thesis show that it was difficult to demonstrate any biological activity of soluble Aβ, including induction of synaptotoxicity, in organotypic brain slices as described in Chapter 3. Aβ is known to alter tau phosphorylation and localisation in cultured neurons, and therefore it would be of interest to determine whether the effects of Aβ also extend to extracellular tau. Further investigation into the effects of abnormal tau phosphorylation, excitotoxicity, and Aβ-induced synaptotoxicity will be important in determining the mechanisms that distinguish physiological and pathogenic tau release.

6.1.3 Uptake of extracellular tau

Since tau appears to be propagated between neurons via synapses, it follows that the released tau must be taken up by connecting neurons. Therefore, organotypic brain slices were examined for uptake of released tau. Medium from WT organotypic brain slices stimulated with potassium chloride were collected and used as the source of extracellular tau, since we previously found that depolarisation of neurons by potassium chloride induces a 10-fold increase of extracellular tau. The medium from stimulated neurons was used to treat $tau^{-/-}$ organotypic brain slices, so that the uptake of exogenous tau could be identified. Unfortunately, it was not possible to detect uptake of tau into neurons on western blots. It is likely that this apparent absence of tau internalisation may be due to methodological issues, and more sensitive methods such as ELISA should be used in future studies. In one study, exogenous low molecular weight tau aggregates, mainly comprised of dimers and trimers of tau, added to the culture medium of $tau^{-/-}$ primary neurons were internalised after six hours of incubation (Wu et al., 2013). It was also demonstrated that approximately 100 ng of tau aggregates per mg of total protein was taken up (Wu et al., 2013). Thus, if the ratio of internalised tau to total tau was similar in the experiments carried out in Chapter 3, given that the concentration of extracellular tau is likely to be very low, the minute amount of internalised tau may not be detectable by on western blots. In addition, the rate of extracellular tau uptake may be slow and, in the experiments carried out in Chapter 3, there may have been insufficient contact time (4 hours) with extracellular tau for internalisation. The characterisation of endogenous tau uptake in neurons should be further investigated, with increased incubation of tau-containing medium with the slices, in combination with a more sensitive detection method such as ELISA or immunofluorescence. The former method would allow for quantification of the ratio of internalised tau to total extracellular tau, and the latter method would enable identification of the subcellular localisation of internalised tau.

Preliminary data by Karen Duff's laboratory has shown that cyan fluorescent protein-tagged tau is released by neurons prepared from rTg4510 mice expressing mutant P301L tau, and is subsequently taken up by tau knockout neurons. Once internalised, which can take up to six days, extracellular tau accumulates at dendritic spine-like structures. Uptake of endogenous tau was also investigated using conditioned media from neurons derived from induced pluripotent stem cells (iPSC). When conditioned media from WT iPSC-neurons was incubated with neurons prepared from tau knockout mice, human tau was also taken up by the mouse neurons, where it accumulated in lysosomes as determined by co-localisation with lysosomal-associated membrane protein 1 (Lamp1) (Karen Duff, personal communication). These preliminary results

indicate that endogenous, non-pathogenic tau can be transmitted between neurons. Nevertheless, it will be important to characterise endogenous tau uptake in organotypic brain slices, as the presence of glial cells may influence the uptake of extracellular tau.

Several different mechanisms for neuronal uptake of tau have been proposed (Figure 6.1). The precise mechanisms of tau uptake may be dependent on the form of secreted tau. Some groups have reported that extracellular tau could be associated with vesicular membranes, such as exosomes or ectosomes, which could lead to fusion of vesicle-associated tau with the plasma membrane of recipient neurons (Lee et al., 2012; Saman et al., 2012; Simón et al., 2012b; Dujardin et al., 2014). However, we and others have reported that the majority of soluble full-length extracellular tau is not associated with exosomes, suggesting that tau is not secreted within a membranous structure (Karch et al., 2012; Pooler et al., 2013a). Non-exosomal tau could be taken up by endocytosis, or by direct penetration of the plasma membrane and this may depend on the conformation of extracellular tau. One study by Wu et al. (2013) suggests that pathological forms of tau are taken up by bulk endocytosis in neurons. Using a microfluidic chamber culture system that separates primary neurons into somatodendritic and axonal compartments, aggregated tau was added to the somatodendritic compartment (Wu et al., 2013). Tau aggregates bound to the neurons and were anterogradely transported to the axon, and tau was also internalised and transported retrogradely upon addition of tau aggregates to the axonal compartment (Wu et al., 2013). Internalised tau co-localised with dextran and was trafficked to lysosomes, indicating that tau aggregates were taken up by bulk endocytosis (Wu et al., 2013). Macropinocytosis, a form of bulk endocytosis, has also been proposed to underlie the uptake of aggregated tau (Holmes et al., 2013; Falcon et al., 2014). Alternatively, nanotubes, which are extracellular tunnel-like structures that connect two cells, have been proposed as a method for transmission of pathological forms of proteins, such as the pathogenic prion protein and mutant huntingtin, between neurons (Gousset et al., 2009; Costanzo et al., 2013). Thus transmission of pathological forms of neuronal tau could also involve nanotubes.

The uptake of monomeric, physiological tau is less well-studied and recombinant monomeric tau has been reported to be rapidly internalised by human neuroblastoma cells within 1 hour (Michel et al., 2014). Receptor-mediated endocytosis has also been suggested to be responsible for uptake of monomeric tau. Addition of tau protein to COS-7 cells results in direct interaction of tau with M1 muscarinic receptors, leading to receptor activation and induction of intracellular calcium currents (Gómez-Ramos et al., 2009). This suggests that soluble, monomeric tau could play a role in signalling pathways under physiological conditions, in addition to its pathological propagation.

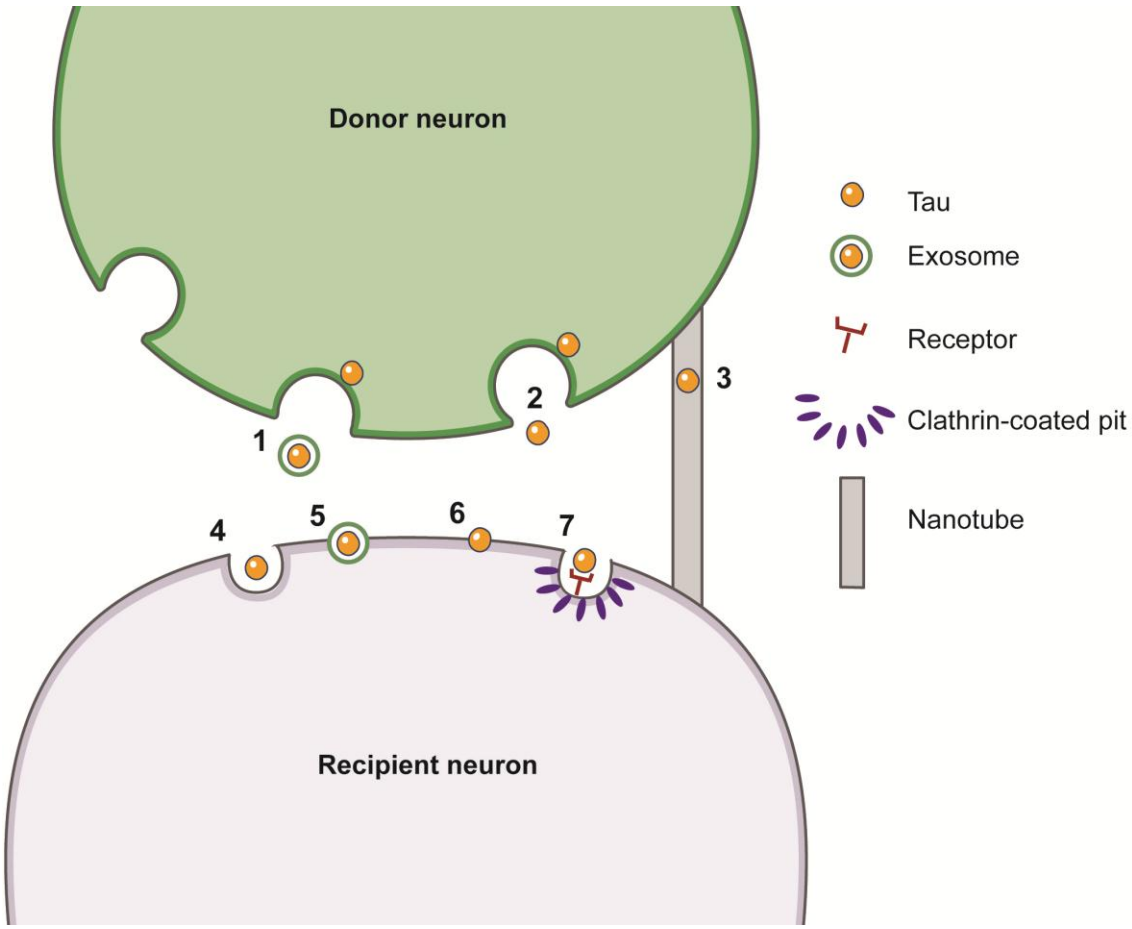

Figure 6.1 Potential mechanisms of tau secretion and uptake in neurons

Possible mechanisms underlying cell-to-cell transmission of neuronal tau. Tau can be released into the extracellular space as (1) vesicle-bound tau, such as in exosomes, or (2) free tau. (3) Tau could also be transferred between neurons through nanotubes. Uptake of tau could result from (4) bulk endocytosis, (5) exosomal fusion to the plasma membrane of the recipient cell, (6) direct penetration of tau into the plasma membrane, or (7) receptor-mediated endocytosis.

Acetylcholine, a muscarinic agonist, has been shown to potentiate NMDA receptor currents in response to NMDA and glutamate (Markram and Segal, 1990). The potentiating effect on NMDA receptor currents of carbachol, a muscarinic receptor agonist, was blocked by M1-toxin (Marino et al., 1998). As M1-toxin is a highly specific M1 muscarinic receptor antagonist, these data suggest that NMDA receptor currents can be mediated by M1 muscarinic receptor agonists. If extracellular tau can indeed bind to M1, and in fact tau has been shown to elicit greater calcium responses than acetylcholine alone (Gómez-Ramos et al., 2009), this would suggest that tau-mediated M1 receptor activation can modulate NMDA receptor currents. A proposed model that might explain this could involve the activation of M1 receptors by extracellular tau, eliciting an intracellular calcium response (Figure 6.2). In this model, extracellular tau could be internalised by M1 receptor-mediated endocytosis. While it remains at the post-synaptic density, endocytosed tau could bind to fyn, promoting its association with PSD-95 and the NR2b subunit of the NMDA receptor. This postsynaptic complex would stabilise the NMDA receptor, potentiating NMDA receptor-mediated activity, leading to increased intracellular calcium currents. If this model is correct, under pathological conditions, aberrant tau release could lead to increased intracellular calcium mediated by M1 and subsequently NMDA receptors. This would provide an explanation for the NMDA-receptor mediated excitotoxicity observed in AD.

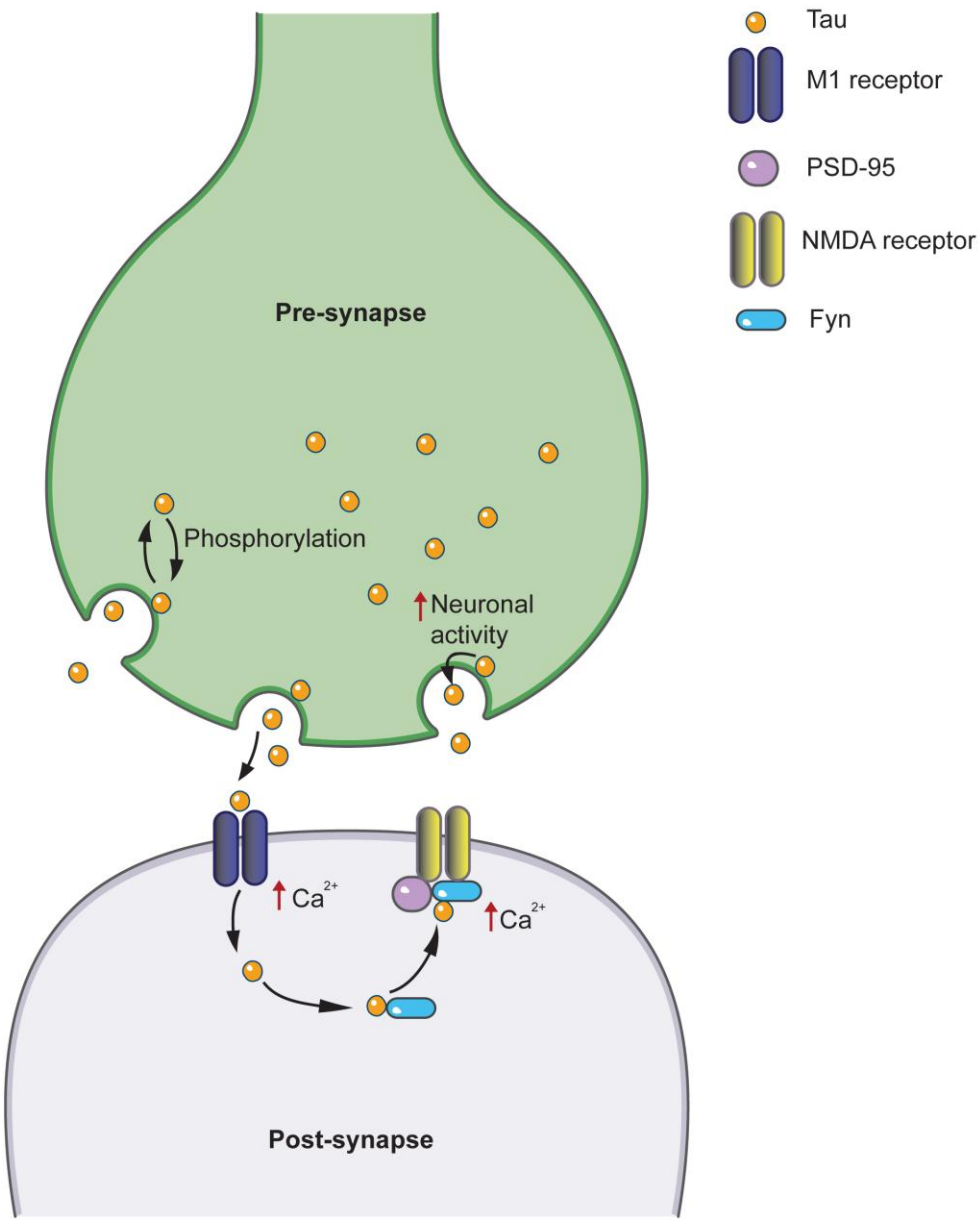

Figure 6.2 Model of extracellular tau binding on M1 and modulation of NMDA receptors

This schematic illustrates a candidate role of extracellular tau in neuronal signalling. Dynamic phosphorylation of tau regulates its trafficking from the cytosol to the plasma membrane. Upon induction of neuronal activity, tau is released at the pre-synaptic terminal. This pool of tau could originate from the cytosol, or from the membrane. Extracellular tau binds to and activates post-synaptic M1 muscarinic receptors. Internalised tau can then bind to dendritic fyn, and both proteins co-translocate to the NMDA receptors where fyn phosphorylates the NR2b subunit and forms a complex with PSD-95. This facilitates NMDA receptor signalling. In pathological conditions, aberrant tau release could enhance rises in intracellular calcium, leading to excitotoxicity.

6.1.4 Extracellular tau as a therapeutic target

Extracellular tau makes an attractive target for therapy because it is more accessible to tau-targeted therapies than intracellular tau. The discovery that tau pathology can be transmitted from cell to cell suggests that targeting the extracellular tau may be able to stop or slow the progression of tau-mediated neurodegeneration. However, data presented in this thesis and elsewhere (Pooler et al., 2013b; Yamada et al., 2014) indicate that tau can be secreted from neurons under physiological conditions, in a process regulated by synaptic activity. For this reason, therapeutics that target extracellular tau should be designed to distinguish between physiological and pathological forms of extracellular tau, to avoid side effects originating from loss-of-function of normal tau. It is therefore important to determine if the species of secreted tau differs in physiological and pathological conditions. In addition, AD-related excitotoxicity could also contribute to aberrant tau release. In AD, tau becomes missorted to the somatodendritic area, where it normally interacts with fyn to stabilise the NMDA receptor complex with PSD-95, a postsynaptic scaffolding protein (Ittner et al., 2010). Under pathological conditions, increased association of tau and fyn caused by mislocalisation of tau could lead to NMDA receptor-mediated excitotoxicity. Since tau release is regulated by neuronal activity via AMPA and NMDA receptors (Pooler et al., 2013a; Yamada et al., 2014), this could lead to increased release of tau at the synapse due to positive feedback mechanisms. Such a mechanism would induce local spreading of tau pathology, as it has been shown that tau pathology can spread in both anterograde and retrograde directions (Wu et al., 2013).

Passive antibody immunisation is one strategy that can be used to target extracellular tau and the efficacy of such treatments has been demonstrated both *in vitro* and *in vivo*. A mouse monoclonal antibody raised against tau, HJ9.3, prevented tau aggregation in acceptor cells when co-cultured with donor cells expressing fluorescently-tagged tau (Kfoury et al., 2012). In this study, HEK293 cells were transfected with a tau fragment containing only microtubule repeat domains of tau, which leads to formation of fibrils when expressed in cultured cells. The donor cells expressed this truncated tau construct containing two aggregant-prone mutations within the repeat domain, while a form of tau containing only one mutation in the repeat domain was expressed in the acceptor cells. The tau constructs were tagged with yellow or cyan fluorescent protein, which enabled quantification of aggregate formation by fluorescence resonance energy transfer. This treatment was deemed to be specific for extracellular tau, because addition of antibody HJ9.3 did not prevent intracellular tau aggregation in a single cell population expressing the repeat domain of tau with aggregant-promoting mutations (Kfoury et al., 2012). Labelling with an anti-mouse

secondary antibody to detect HJ9.3 showed that tau fibrils bound to antibody complexes were mainly found at the cell surface, suggesting that HJ9.3 blocks uptake of extracellular tau by sequestration outside the cell (Kfoury et al., 2012). Passive and active immunisation targeting tau phosphorylated at S396/S404 has also been shown to effectively reduce insoluble tau aggregates and ameliorate some behavioural tests in P301L tau transgenic mice, although these studies did not determine whether the antibodies entered the cells and bound to intracellular tau (Boutajangout et al., 2011; Chai et al., 2011).

Immunotherapy studies have also been carried out using antibodies that target different epitopes in 3xTg mice which express mutations in APP, tau, and presenilin (Walls et al., 2014), htau mice overexpressing all six isoforms of human WT tau in the absence of mouse tau (Castillo-Carranza et al., 2014a), P301S tau mice (Yanamandra et al., 2013), and P301L tau mice (Castillo-Carranza et al., 2014b). Immunisation of 3xTg mice with the AT8 antibody, which recognises phosphorylated tau at S202/T205, transiently decreased the amount of tau at the somatodendritic area and overall AT8 immunoreactivity without affecting Aβ pathology from 7-14 days post-immunisation (Walls et al., 2014). In contrast, immunisation of 3xTg mice with the 4G8 antibody, which recognises Aβ, reduces both Aβ pathology and neurofibrillary tangles within a week (Walls et al., 2014). Chronic injection of a monoclonal antibody recognising oligomeric tau (TOMA) in htau mice resulted in improved cognitive function as assessed by the novel object recognition task, and reduced levels of oligomeric tau (Castillo-Carranza et al., 2014a). In addition, immunisation of P301S mice with anti-tau antibodies reduced AT8 tau-positive immunoreactivity as well as insoluble tau levels, and rescued deficits in contextual fear conditioning (Yanamandra et al., 2013). Furthermore, injection of the antibody TOMA into P301L mice improved deficits in the rotarod test, reduced the level of oligomeric tau, and reduced phosphorylation of tau at several epitopes (Castillo-Carranza et al., 2014b). Moreover, immunotherapy has been shown to be effective for clearance of other pathological proteins relevant to neurodegenerative disease, such as Aβ (Bard et al., 2000; Morgan et al., 2000; Sigurdsson et al., 2001), α-synuclein (Masliah et al., 2011; Bae et al., 2012; Tran et al., 2014), and superoxide dismutase 1 (SOD1) (Gros-Louis et al., 2010). It remains to be seen whether the results from tau immunotherapy studies in animal models can translate to efficacy in humans. These studies are therefore proof-of-principle experiments that demonstrate the effectiveness of extracellular tau as a therapeutic target. Alternative approaches to further refine drug treatments that inhibit tau propagation without affecting physiological tau signalling should be encouraged.

6.2 Association between tau and fyn in AD

Altered gene or protein expression, or altered localisation or structure of a protein in pathological conditions, points towards a mechanistic role for that protein in disease. Fyn expression, as well as the ratio of soluble to insoluble fyn, is altered in AD (Shirazi and Wood, 1993; Ho et al., 2005). The accumulation of insoluble fyn protein is associated with the progression of AD, when correlated with cognitive measures including the MMSE score, and with the progressive accumulation of neurofibrillary tangles (Ho et al., 2005). Moreover, fyn activity is increased in brains of AD patients compared to controls and individuals with MCI (mild cognitive impairment), whereas total levels of fyn remain unchanged over the course of disease (Larson et al., 2012). Fyn phosphorylates tau at Y18, and increased phosphorylation at this epitope can be observed in some neurofibrillary tangles in AD (Lee et al., 2004). Together, these data indicate that the relationship between fyn and tau is important in AD.

To determine whether changes in the association of these proteins were apparent in AD brain, samples of brain tissue from AD and control individuals were analysed by western blot for tau and fyn expression. Statistical analyses were carried out in order to establish whether there is a relationship between tau and fyn expression. Total levels of fyn were unchanged between control and late-stage AD (Braak stages V-VI) samples, confirming previously reported findings (Ho et al., 2005; Larson et al., 2012). Fyn expression over the course of disease was also investigated in controls and AD samples ranging from Braak stages I-VI. There was no change in total fyn expression over time in AD compared with control whole brain homogenates. In contrast to findings from Ho et al. (2005), levels of soluble fyn were also unchanged during the progression of disease, although this discrepancy may have been due to the low numbers of samples used here. Although total levels of fyn were unchanged throughout all stages of AD, we hypothesised that expression of fyn could correlate with tau phosphorylation, as it has been shown that fyn levels correlate with PrP^C irrespective of AD status (Larson et al., 2012).

This is the first study to investigate relationships between fyn expression and tau phosphorylation in AD. Although phosphorylation at several epitopes of tau (S199, S262, S396/S404) was increased at late stages of AD, there was no relationship between increases in the amount of tau phosphorylated at these epitopes and the amount of fyn present in the same brain samples. Interestingly, although tau phosphorylated at S214 was unchanged between control and AD samples, the amount of fyn was significantly correlated with tau phosphorylation at S214 in control samples, but not AD brain. Likewise, fyn was significantly correlated with phosphorylation at

S202 of tau in control, but not in AD brain. These results indicate that there is a relationship between fyn and tau phosphorylated at S202 and S214 under normal conditions, but this link is lost in AD, at least in Braak stages V-VI.

It is apparent that one of the disease mechanisms underlying AD triggers the dissociation between tau pS202/pS214 and fyn. Phosphorylation at S202 of tau can increase its propensity to polymerise (Rankin et al., 2005), and as this epitope is increasingly phosphorylated in AD, the structural changes of tau that is caused by phosphorylation at this site may result in the inability of tau to bind to fyn during the late stages of AD. Phosphorylation at S214 regulates tau binding to microtubules. If tau S214 is increasingly phosphorylated in AD, and fyn levels are no longer correlated in pathogenic conditions, this could suggest that fyn is unable to associate with tau during late stage AD. Interestingly, mice expressing a constitutively active form of fyn have increased tau phosphorylation at S202/T205 (Xia and Gotz, 2014). This suggests that fyn has an indirect effect on phosphorylation at this epitope, which the results presented here suggest could be out-competed in AD as other kinases and phosphatases become dysregulated.

Unexpectedly, given the wealth of data supporting a direct interaction between tau and fyn, we were unable to identify this interaction by co-immunoprecipitation of the endogenous rodent proteins, in contrast to other groups (Ittner et al., 2010; Mondragon-Rodriguez et al., 2012). Data presented in this thesis and previously published literature have demonstrated that tau and fyn can interact directly in neurons *in vitro* (Lee et al., 1998; Usardi et al., 2011; Pooler et al., 2012), although many of these studies involved the use of recombinant SH2 or SH3 domains of fyn. Taken together, these findings could suggest that the tau-fyn interaction is transient *in vivo* and requires very specific conditions in order to be detected biochemically. Furthermore, the stoichiometry of the tau-fyn interaction is not known. Of the total amount of tau present in neurons, it is likely that the majority of tau is bound to microtubules, and only a minor fraction of unbound tau is present at the dendrite. This small amount of tau may be sufficient to carry out its functions in neuronal signalling, in conjunction with fyn, but it may be insufficient for detection biochemically unless a large amount of starting material is available. To fully understand the interaction between tau and fyn, it will be important to determine the nature of the tau that is bound to fyn, and the temporal nature of fyn activation in relation to tau binding. This can be determined by immunofluorescence using specific antibodies recognising phosphorylated forms of tau to examine which species of tau co-localises with fyn. In addition, imaging methods, such as Duolink, enable detection of protein-protein interactions in neurons, using

proximity measures. These experiments could be used in conjunction with phospho-specific antibodies to tau and fyn without resorting to over-expression of either protein.

6.3 Identification of the binding site between tau and fyn

The interaction of tau and fyn at dendritic spines in neurons has implications for AD, as mislocalisation of tau to the dendrite, in association with fyn, may facilitate increased NMDA receptor-mediated excitotoxicity (Ittner et al., 2010). This hypothesis is supported by data showing that exposure to Aβ induces translocation of tau and fyn from the dendritic shaft to the postsynaptic density, ensuring that these proteins are in the correct place to perform their function of stabilising NMDA receptors (Frandemiche et al., 2014). Increased NMDA receptor activity promotes association of fyn with phosphorylated tau at the synapse, which could result in a positive feedback cycle of NMDA receptor-mediated excitotoxicity (Mondragon-Rodriguez et al., 2012). Thus targeting tau or fyn, or inhibiting their interaction, is a rational target for AD therapy.

To do that, it is critical to find the binding site between tau and fyn, which was one of the principal aims of Chapter 4. Fyn, like other members of the src kinase family, is comprised of four src homology (SH) domains. The binding between tau and fyn was first confirmed in primary neurons, where tau binds to both fyn-SH2 and fyn-SH3 (Figure 6.3), confirming previous studies (Reynolds et al., 2008; Usardi et al., 2011; Pooler et al., 2012). As the dominant domain of interaction between tau and fyn appears to be fyn-SH3, the binding site between tau and fyn-SH3 was selected for further investigation. SH3 domains are known to recognise and bind to PXXP sequences (proline-X-X-proline, where X is any amino acid) (Ren et al., 1993; Cheadle et al., 1994; Sparks et al., 1994). In its proline-rich region, tau contains seven PXXP motifs that are possible candidates for interacting with fyn-SH3. The studies carried out in Chapter 4 are the first to examine each PXXP motif in tau for their ability to bind to fyn-SH3 while conserving the structure of full-length intact tau in the experimental design. First, single proline residues within PXXP motifs of tau were substituted with alanine, generating tau constructs harbouring individual mutations in each PXXP motif. Using GST pull-down assays with fyn-SH3 beads and CHO cells expressing WT or tau containing mutant PXXP motifs, the sixth PXXP motif at 216-219 of tau was identified as a critical binding site for fyn-SH3. The residues surrounding 216-PXXP-219 of tau can also modulate the interaction of tau with fyn-SH3, as it was shown that substitution of proline 213 of tau with alanine enhanced the binding affinity between tau and fyn-SH3. Taken together, the work here shows that the sixth PXXP motif of tau is a major site for interaction with fyn-SH3, whereas modification of residues, particularly in close proximity to the sixth motif, could alter tau-fyn-SH3 binding.

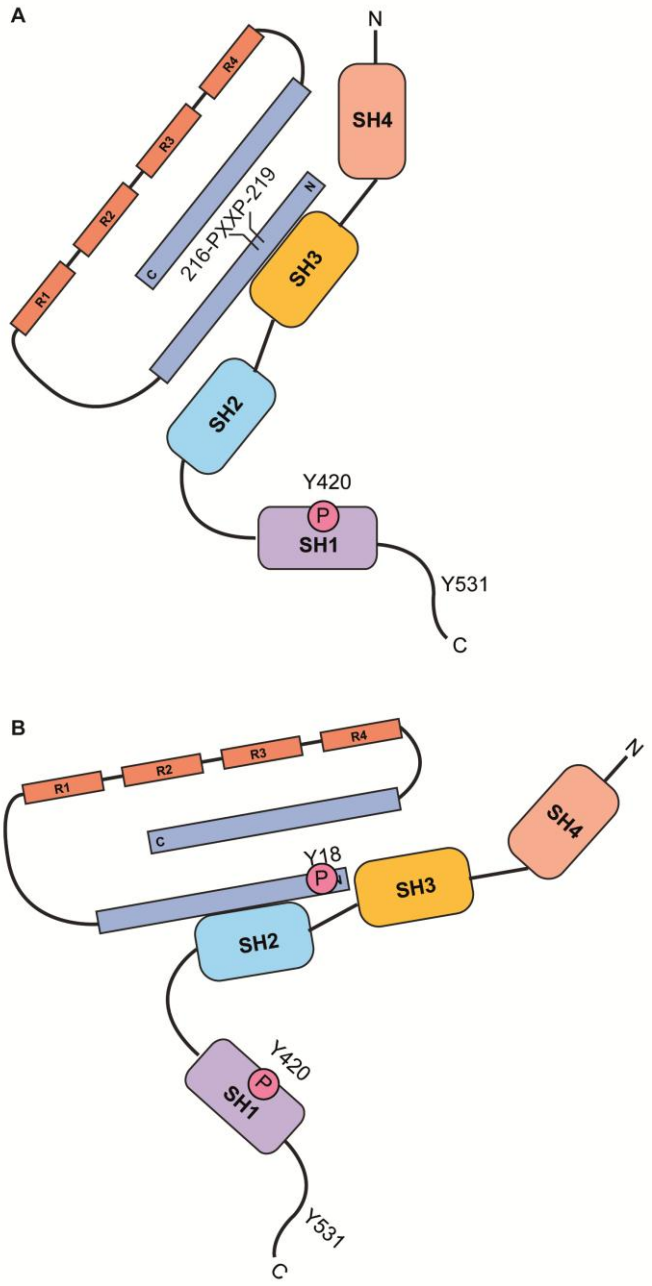

Figure 6.3 Interactions between tau and fyn-SH2 and SH3 domains

Fyn contains 4 SH (src homology) domains (SH1-4), of which the SH2 domain recognises tyrosine residues, and the SH3 domain recognises PXXP motifs. Tau can bind to fyn at either the SH2 or SH3 domain. (A) The major binding site for tau-fyn interaction is located between PXXP motifs at residues 216-219 of tau and fyn-SH3. (B) Tau also binds to fyn-SH2 but with weaker affinity. The binding site on tau is not known, but phosphorylation at Y18 of tau regulates binding between tau and fyn-SH2. The microtubule binding repeats of tau are labelled as R1-4 and the N- and C-termini are indicated. Further information about the functions of the SH domains is discussed in Chapter 1.

Previous *in vitro* studies undertaken to identify the binding site between tau and fyn-SH3 utilised truncated tau constructs or tau peptides. The first of these studies proposed that the seventh PXXP motif at tau residues 233-236 was the major binding site for fyn-SH3 (Lee et al., 1998). In this report, tau peptides containing C-terminal deletions, generating truncated tau constructs with or without PXXP motifs, were incubated with fyn-SH3 in a GST pull-down assay. Deletion of tau 222-441 abolished binding with fyn-SH3, leading to the conclusion that the PXXP motif at 233-236 was required for tau-fyn binding (Lee et al., 1998). A subsequent *in vitro* binding assay showed that a recombinant tau peptide spanning the two tandem motifs at 213-219, but not 233-236, of tau could bind to fyn-SH3 (Reynolds et al., 2008). Further investigation by Ittner et al. (2010) revealed that deletion of the PXXP motif at 233-236 and the C-terminal half of tau significantly decreased interaction of tau with fyn. However, binding was not completely abolished until PXXP constructs C-terminal to tau residue 196 were removed (Ittner et al., 2010). The nature of truncated tau peptides could lead to conformational changes in tau that could influence protein-protein interactions, which underscores the importance of using intact tau constructs for such experiments. More recently, two additional studies have attempted to identify the PXXP motif recognised by fyn-SH3 using intact full-length tau. In agreement with our findings, both studies conclude that of the PXXP motifs investigated, PXXP motifs in the region of 213-219 of tau are the most likely sites for binding with fyn-SH3 (Usardi et al., 2011; Cochran et al., 2014).

The experiments presented in this thesis address many of the pitfalls of using truncated tau mentioned above by instead using intact full-length tau expressed in CHO cells for GST pull-down with fyn-SH3 beads. This allows examination of the tau-fyn interaction in a cellular system which is more physiologically relevant than testing the binding efficacy of recombinant peptides *in vitro*. Nevertheless, CHO cells are a non-neuronal cell line and hence these experiments in CHO cells were intended as preliminary experiments to identify the binding site for tau and fyn. In particular, the aims were to determine what the effects of PXXP mutations would have on tau release and on tau and fyn trafficking, and whether the PXXP mutations influenced the susceptibility of neurons to Aβ toxicity. Since both tau and fyn are reported to play roles in trafficking to the dendrite and the plasma membrane (Ittner et al., 2010; Pooler et al., 2012), inhibition of tau-fyn binding would be expected to sequester both proteins in the cytosol. Moreover, given that reduction of tau or fyn confers neuroprotection from Aβ toxicity (Lambert et al., 1998; Rapoport et al., 2002; Chin et al., 2004; Roberson et al., 2007; Shipton et al., 2011), inhibiting the interaction between tau and fyn may also be sufficient for resistance to Aβ toxicity. Thus, the constructs containing mutations in

P213, P216, and P219 of tau were used to generate lentiviruses, as mutations at these sites had the most significant effects on tau-fyn binding. Lentiviruses were engineered to contain a synapsin promoter to enable neuron-specific expression of tau, along with an independently expressed fluorescent EGFP reporter protein. Subsequent generation of lentiviruses expressing tau with individual mutations in PXXP motifs were to be used to investigate functional downstream consequences on tau and fyn in organotypic brain slices. Expression of lentiviral tau was successful in primary neurons, but unfortunately this was not detectable following lentiviral transduction of organotypic brain slices. This lack of expression was likely due to methodological difficulties caused by inaccessibility of lentivirus particles to the neurons in slice cultures. It is possible that, with further optimisation, lentiviral expression of mutant PXXP tau in organotypic brain slices would have been sufficient to allow further functional experiments, but this remains to be determined experimentally. One alternative approach would be to inject lentivirus into the brains of $tau^{-/-}$ mice prior to the preparation of organotypic brain slices, to circumvent possible obstruction of virus internalisation by the glial scar that forms over cultured brain slices. Another approach could be to treat organotypic brain slices from WT mice with a peptide spanning the sixth PXXP motif to attempt to block the interaction of fyn with endogenous tau.

6.3.1 Inhibition of tau-fyn interaction: a viable therapy?

It is important to note that the substitution of proline with alanine at residues P216 and P219 in tau did not completely abolish its binding to fyn. Likewise, although neuronal tau preferentially binds to fyn-SH3 relative to fyn-SH2, data presented in Chapter 4 demonstrate that tau can also bind to fyn-SH2 in neurons, in agreement with a previous report from this laboratory (Usardi et al., 2011). Therefore, although the majority of the tau-fyn interaction is likely mediated by the SH3 domain of fyn, it is possible that inhibition of binding between tau and fyn-SH3 may not entirely prevent the association of tau with fyn. It is possible, however, that the downstream functional effects on tau may differ according to which domain of fyn is bound to tau. Blocking the interaction between tau and fyn-SH2, as opposed to fyn-SH3, could confer different consequences for tau function and/or phosphorylation, and for mediating Aβ neurotoxicity. For example, Y18 was previously shown to mediate binding between tau and fyn-SH2, and altering the tyrosine phosphorylation of tau disrupts its trafficking to lipid rafts (Usardi et al., 2011). It is important to determine which binding site mediates the pathological downstream effects on tau if inhibiting the tau-fyn interaction is to become a therapeutic target.

More investigation is also needed to determine how modifications of tau affect its affinity with fyn. For example, 3R tau binds to fyn-SH3 with higher affinity than 4R tau (Bhaskar et al., 2005; Cochran et al., 2014). In addition, phosphorylation of tau at epitopes abnormally phosphorylated in AD has been shown to increase the association of tau with fyn-SH3 (Bhaskar et al., 2005; Cochran et al., 2014). Furthermore, pseudophosphorylation of tau by amino acid substitution of serine/threonine to glutamate at tau residues S199, S202, T205, S262, S293, S324, S356, or S404 increases the association of 4R tau with fyn (Bhaskar et al., 2005; Cochran et al., 2014). These data are in contrast to results from the study by Reynolds et al. (2008). In this study, the authors investigated binding of phosphorylated 2N4R tau to fyn-SH3 by using tau constructs that contained substitutions of 10 or 18 serine/threonine tau residues to glutamate to mimic phosphorylation (residues S198, S199, S202, T231, S235, S396, S404, S409, S413, S422; or residues S46, T50, T69, T111, T153, T175, T181, S198, S199, S202, T205, S208, S210, T212, S214, T217, T231, S235, respectively). It was reported that the pseudophosphorylated tau constructs exhibited reduced binding to fyn-SH3 compared to WT tau (Reynolds et al., 2008). Discrepancies of the results obtained from the tau-fyn binding assays could stem from the combination of phospho-epitopes that were mutated in the tau constructs in the Reynolds et al. (2008) study, as opposed to the individual glutamate substitutions in the two former studies. Nonetheless, further experiments are required to clarify the effect of tau phosphorylation on its association with fyn-SH3. Collectively, these studies suggest that modifications of tau that lead to structural or phosphorylation changes could regulate tau-fyn interactions. In AD, the oligomerisation and abnormal phosphorylation of tau could result in altered tau-fyn binding, leading to dysfunction in the stabilisation of NMDA receptors and possibly other downstream effects.

One recently published study has suggested the use of small peptides to inhibit tau-fyn binding as a potential therapy for AD. A fluorescent cell-based assay (bioluminescence resonance energy transfer; BRET) has been developed to screen molecules for their ability to modify the interaction between tau and fyn-SH3 (Cochran et al., 2014). In this study, fyn-SH3 was tagged with click beetle green luciferase, while 2N4R tau was tagged with a far red fluorescent reporter. Upon association of tau with fyn-SH3, the donor luciferase fused to fyn-SH3 is in close proximity to the fluorescent acceptor-tagged tau, leading to energy transfer that can be measured by fluorescence. Dozens of compounds were screened with the BRET assay and several hits were identified that could inhibit the tau-fyn interaction (Cochran et al., 2014). Using this assay, it will be possible to identify hits that can modify interactions between pseudophosphorylated tau and fyn-SH3, which may be of relevance for AD. Importantly, the results presented in

this thesis indicate that the effects of post-translational modification of residues surrounding the sixth PXXP motif at residues 216-219 of tau should be taken into account when screening for tau-fyn-SH3 small molecule inhibitors. Since the pathological conditions in AD induce aberrant tau phosphorylation and structural changes, kinases that phosphorylate residues surrounding the sixth PXXP motif may be putative candidates. In addition, it would be interesting to modify the BRET assay so that compounds that block tau and fyn-SH2 interactions can be screened, which would provide additional insight into the functional effects of tau-fyn-SH2 binding.

6.4 Concluding remarks

Research in AD has grown from focusing on the pathogenic roles of tau and Aβ in neurons to studying the involvement of many other proteins and cell types. Multiple proteins are dysregulated in AD, and several pathways have been identified that might contribute to AD pathogenesis. This thesis focuses on the roles of tau and fyn in AD and contributes novel findings to elucidate the relationship between tau and fyn in normal and pathogenic conditions. Thus, release of tau can be induced by neuronal activity in organotypic brain slices, but this process does not seem to be regulated by the presence of fyn. Moreover, tau binds to both fyn-SH2 and fyn-SH3 in neurons, but shows more preference for binding with fyn-SH3 compared to fyn-SH2. Interactions between tau and fyn-SH3 are mediated primarily by the sixth PXXP motif at residues 216-219 of tau, and residues surrounding these motifs can also modulate the degree of binding between tau and fyn-SH3. In particular, phosphorylation of serine/threonine residues in close proximity to this PXXP motif such as S210, T212, S214, and T217 of tau, which are detected in AD brain, could regulate the interaction between tau and fyn-SH3. Finally, a correlation was observed between tau phosphorylation at specific residues and fyn protein amounts in control, but not AD human brain tissue, suggesting that the functional associations between these two proteins could be dysregulated in AD. The work presented in this thesis paves the way for further research to address questions that remain unanswered concerning the physiological and pathological consequences of tau interactions with fyn.

In particular, the role of extracellular tau remains to be elucidated. If tau is involved in normal neuronal signalling, then this is a novel role for tau that is not properly understood. Activation of muscarinic receptors by tau has been demonstrated (Gómez-Ramos et al., 2009), but in a relatively artificial system and therefore this needs to be replicated with endogenous proteins in neurons. Additionally, the effects of

phosphorylation on tau release are unclear; in particular, evidence is needed to demonstrate whether tau phosphorylation regulates the amount and to identify the species of tau that is released from neurons.

It is important to determine the effect of Aβ on tau-fyn interactions, and in particular whether Aβ potentiates or disrupts the tau-fyn interaction. Previous studies have shown that Aβ treatment causes translocation of tau to dendrites, activation of fyn, and phosphorylation of tau at Y18, but any functional effects of fyn-mediated Y18 phosphorylation under pathological conditions have yet to be described. Y18 tau phosphorylation can regulate association of tau with fyn-SH2, but not fyn-SH3 (Usardi et al., 2011). Tyrosine phosphorylation of tau can also regulate its association with lipid rafts (Usardi et al., 2011). Because fyn is required for this process (Usardi et al., 2011; Pooler et al., 2012), it could mean that fyn-mediated phosphorylation of tau at Y18 influences its association with membranes. It will be important to determine whether binding of tau with fyn-SH2 results in different downstream effects than interaction with fyn-SH3, since these effects appear to be differentially regulated by phosphorylation at serine, threonine, and tyrosine residues. Although the binding site between tau and fyn-SH3 has been identified, SH2 domains do not recognise PXXP motifs. Thus the structural characteristics of interaction with tau and fyn-SH2 may differ, and experiments to block tau-fyn-SH2 binding will also be important to elucidate the functional consequences of tau-fyn interactions in pathological conditions.

Collectively, results from this thesis show that further investigation into interaction between tau and fyn in AD will be important for further understanding the role of these proteins in AD pathogenesis and for developing future therapeutics that may be able to halt or slow disease progression. Furthermore, the work presented here also highlights activity-dependent extracellular tau as a potential target for AD therapy.

References

Abraha A, Ghoshal N, Gamblin TC, Cryns V, Berry RW, Kuret J, Binder LI (2000) C-terminal inhibition of tau assembly in vitro and in Alzheimer's disease. J Cell Sci 113:3737-3745.

Agarwal-Mawal A, Qureshi HY, Cafferty PW, Yuan Z, Han D, Lin R, Paudel HK (2003) 14-3-3 connects glycogen synthase kinase-3β to tau within a brain microtubule-associated tau phosphorylation complex. J Biol Chem 278:12722-12728.

Aguzzi A, O'Connor T (2010) Protein aggregation diseases: pathogenicity and therapeutic perspectives. Nature reviews Drug discovery 9:237-248.

Ahmed Z, Cooper J, Murray T, Garn K, McNaughton E, Clarke H, Parhizkar S, Ward M, Cavallini A, Jackson S, Bose S, Clavaguera F, Tolnay M, Lavenir I, Goedert M, Hutton M, O'Neill M (2014) A novel in vivo model of tau propagation with rapid and progressive neurofibrillary tangle pathology: the pattern of spread is determined by connectivity, not proximity. Acta Neuropathol 127:667-683.

Alexandropoulos K, Cheng G, Baltimore D (1995) Proline-rich sequences that bind to Src homology 3 domains with individual specificities. Proc Natl Acad Sci U S A 92:3110-3114.

Alonso AdC, Zaidi T, Novak M, Grundke-Iqbal I, Iqbal K (2001) Hyperphosphorylation induces self-assembly of τ into tangles of paired helical filaments/straight filaments. Proc Natl Acad Sci U S A 98:6923-6928.

Alzheimer A (1907) About a peculiar disease of the cerebral cortex. [in German]. Centralblatt für Nervenheilkunde Psychiatrie 30:177–179.

Andorfer C, Kress Y, Espinoza M, De Silva R, Tucker KL, Barde Y-A, Duff K, Davies P (2003) Hyperphosphorylation and aggregation of tau in mice expressing normal human tau isoforms. J Neurochem 86:582-590.

Andreadis A, Brown WM, Kosik KS (1992) Structure and novel exons of the human tau gene. Biochemistry (Mosc) 31:10626-10633.

Anfossi M, Bernardi L, Gallo M, Geracitano S, Colao R, Puccio G, Curcio SA, Frangipane F, Mirabelli M, Tomaino C, Smirne N, Maletta R, Bruni AC (2011) MAPT V363I variation in a sporadic case of frontotemporal dementia: variable penetrant mutation or rare polymorphism? Alzheimer Dis Assoc Disord 25:96-99.

Arrasate M, Pérez M, Avila J (2000) Tau dephosphorylation at tau-1 site correlates with its association to cell membrane. Neurochem Res 25:43-50.

Arriagada PV, Growdon JH, Hedley-Whyte ET, Hyman BT (1992) Neurofibrillary tangles but not senile plaques parallel duration and severity of Alzheimer's disease. Neurology 42:631.

Atherton J, Kurbatskaya K, Bondulich M, Croft CL, Garwood CJ, Chhabra R, Wray S, Jeromin A, Hanger DP, Noble W (2014) Calpain cleavage and inactivation of the sodium calcium exchanger-3 occur downstream of Aβ in Alzheimer's disease. Aging Cell 13:49-59.

Augustinack JC, Schneider A, Mandelkow EM, Hyman BT (2002) Specific tau phosphorylation sites correlate with severity of neuronal cytopathology in Alzheimer's disease. Acta Neuropathol 103:26-35.

Baba A, Akagi K, Takayanagi M, Flanagan JG, Kobayashi T, Hattori M (2009) Fyn tyrosine kinase regulates the surface expression of glycosylphosphatidylinositol-linked ephrin via the modulation of sphingomyelin metabolism. J Biol Chem 284:9206-9214.

Babus LW, Little EM, Keenoy KE, Minami SS, Chen E, Song JM, Caviness J, Koo S-Y, Pak DTS, Rebeck GW, Turner RS, Hoe H-S (2011) Decreased dendritic spine density and abnormal spine morphology in Fyn knockout mice. Brain Res 1415:96-102.

Bae EJ, Lee HJ, Rockenstein E, Ho DH, Park EB, Yang NY, Desplats P, Masliah E, Lee SJ (2012) Antibody-aided clearance of extracellular alpha-synuclein prevents cell-to-cell aggregate transmission. J Neurosci 32:13454-13469.

Bahr BA, Tiriveedhi S, Park GY, Lynch G (1995) Induction of calpain-mediated spectrin fragments by pathogenic treatments in long-term hippocampal slices. J Pharmacol Exp Ther 273:902-908.

Baker M, Litvan I, Houlden H, Adamson J, Dickson D, Perez-Tur J, Hardy J, Lynch T, Bigio E, Hutton M (1999) Association of an extended haplotype in the tau gene with progressive supranuclear palsy. Hum Mol Genet 8:711-715.

Bard F et al. (2000) Peripherally administered antibodies against amyloid beta-peptide enter the central nervous system and reduce pathology in a mouse model of Alzheimer disease. Nat Med 6:916-919.

Barghorn S, Zheng-Fischhöfer Q, Ackmann M, Biernat J, von Bergen M, Mandelkow EM, Mandelkow E (2000) Structure, microtubule interactions, and paired helical filament aggregation by tau mutants of frontotemporal dementias. Biochemistry (Mosc) 39:11714-11721.

Baumann K, Mandelkow EM, Biernat J, Piwnica-Worms H, Mandelkow E (1993) Abnormal Alzheimer-like phosphorylation of tau-protein by cyclin-dependent kinases cdk2 and cdk5. FEBS Lett 336:417-424.

Benilova I, Karran E, De Strooper B (2012) The toxic Abeta oligomer and Alzheimer's disease: an emperor in need of clothes. Nat Neurosci 15:349-357.

Benzing WC, Mufson EJ (1995) Apolipoprotein E immunoreactivity within neurofibrillary tangles: relationship to tau and PHF in Alzheimer's disease. Exp Neurol 132:162-171.

Berggård T, Linse S, James P (2007) Methods for the detection and analysis of protein–protein interactions. Proteomics 7:2833-2842.

Bhandari V, Lim KL, Pallen CJ (1998) Physical and functional interactions between receptor-like protein-tyrosine phosphatase α and p59 fyn. J Biol Chem 273:8691-8698.

Bhaskar K, Yen S-H, Lee G (2005) Disease-related modifications in tau affect the interaction between fyn and tau. J Biol Chem 280:35119-35125.

Bian F, Nath R, Sobocinski G, Booher RN, Lipinski WJ, Callahan MJ, Pack A, Wang KK, Walker LC (2002) Axonopathy, tau abnormalities, and dyskinesia, but no neurofibrillary tangles in p25-transgenic mice. J Comp Neurol 446:257-266.

Binder LI, Frankfurter A, Rebhun LI (1985) The distribution of tau in the mammalian central nervous system. J Cell Biol 101:1371-1378.

Blacker D, Haines JL, Rodes L, Terwedow H, Go RC, Harrell LE, Perry RT, Bassett SS, Chase G, Meyers D, Albert MS, Tanzi R (1997) ApoE-4 and age at onset of Alzheimer's disease: the NIMH genetics initiative. Neurology 48:139-147.

Boggon TJ, Eck MJ (2004) Structure and regulation of Src family kinases. Oncogene 23:7918-7927.

Borchelt DR, Thinakaran G, Eckman CB, Lee MK, Davenport F, Ratovitsky T, Prada C-M, Kim G, Seekins S, Yager D, Slunt HH, Wang R, Seeger M, Levey AI, Gandy SE, Copeland NG, Jenkins NA, Price DL, Younkin SG, Sisodia SS (1996) Familial Alzheimer's disease–linked presenilin 1 variants elevate Aβ1–42/1–40 ratio in vitro and in vivo. Neuron 17:1005-1013.

Boutajangout A, Ingadottir J, Davies P, Singurdsson EM (2011) Passive immunization targeting pathological phospho-tau protein in a mouse model reduces functional decline and clears tau aggregates from the brain. J Neurochem 118:658-667.

Braak H, Braak E (1991) Neuropathological stageing of Alzheimer-related changes. Acta Neuropathol 82:239-259.

Braak H, Del Tredici K (2011) Alzheimer’s pathogenesis: is there neuron-to-neuron propagation? Acta Neuropathol 121:589-595.

Braak H, Thal DR, Ghebremedhin E, Del Tredici K (2011) Stages of the pathologic process in Alzheimer disease: age categories from 1 to 100 years. J Neuropathol Exp Neurol 70:960-969.

Braak H, Zetterberg H, Tredici K, Blennow K (2013) Intraneuronal tau aggregation precedes diffuse plaque deposition, but amyloid-β changes occur before increases of tau in cerebrospinal fluid. Acta Neuropathol 126:631-641.

Brady RM, Zinkowski RP, Binder LI (1995) Presence of tau in isolated nuclei from human brain. Neurobiol Aging 16:479-486.

Brandt R, Léger J, Lee G (1995) Interaction of tau with the neural plasma membrane mediated by tau's amino-terminal projection domain. J Cell Biol 131:1327-1340.

Bugiani O, Murrell JR, Giaccone G, Hasegawa M, Ghigo G, Tabaton M, Morbin M, Primavera A, Carella F, Solaro C, Grisoli M, Savoiardo M, Spillantini MG, Tagliavini F, Goedert M, Ghetti B (1999) Frontotemporal dementia and corticobasal degeneration in a family with a P301S mutation in tau. J Neuropathol Exp Neurol 58:667-677.

Burton EA, Hunter S, Wu SC, Anderson SM (1997) Binding of src-like kinases to the β-subunit of the interleukin-3 receptor. J Biol Chem 272:16189-16195.

Caffrey TM, Joachim C, Wade-Martins R (2008) Haplotype-specific expression of the N-terminal exons 2 and 3 at the human MAPT locus. Neurobiol Aging 29:1923-1929.

Castellani S, Di Gioia S, Trotta T, Maffione AB, Conese M (2010) Impact of Lentiviral Vector-Mediated Transduction on the Tightness of a Polarized Model of Airway Epithelium and Effect of Cationic Polymer Polyethylenimine. J Biomed Biotechnol 2010:11.

Castillo-Carranza DL, Gerson JE, Sengupta U, Guerrero-Munoz MJ, Lasagna-Reeves CA, Kayed R (2014a) Specific targeting of tau oligomers in Htau mice prevents cognitive impairment and tau toxicity following injection with brain-derived tau oligomeric seeds. J Alzheimers Dis 40 Suppl 1:S97-S111.

Castillo-Carranza DL, Sengupta U, Guerrero-Munoz MJ, Lasagna-Reeves CA, Gerson JE, Singh G, Estes DM, Barrett AD, Dineley KT, Jackson GR, Kayed R (2014b) Passive immunization with Tau oligomer monoclonal antibody reverses tauopathy phenotypes without affecting hyperphosphorylated neurofibrillary tangles. J Neurosci 34:4260-4272.

Chabrier MA, Blurton-Jones M, Agazaryan AA, Nerhus JL, Martinez-Coria H, LaFerla FM (2012) Soluble abeta promotes wild-type tau pathology in vivo. J Neurosci 32:17345-17350.

Chai X, Dage JL, Citron M (2012) Constitutive secretion of tau protein by an unconventional mechanism. Neurobiol Dis.

Chai X, Wu S, Murray TK, Kinley R, Cella CV, Sims H, Buckner N, Hanmer J, Davies P, O'Neill MJ, Hutton ML, Citron M (2011) Passive immunization with anti-Tau antibodies in two transgenic models: reduction of Tau pathology and delay of disease progression. J Biol Chem 286:34457-34467.

Chartier-Hariln M-C, Parfitt M, Legrain S, Pérez-Tur J, Brousseau T, Evans A, Berr C, Vldal O, Roques P, Gourlet V, Fruchart J-C, Delacourte A, Rossor M, Amouyel P (1994) Apolipoprotein E, ε4 allele as a major risk factor for sporadic early and late-onset forms of Alzheimer's disease: analysis of the 19q13.2 chromosomal region. Hum Mol Genet 3:569-574.

Chartier-Harlin M-C, Crawford F, Houlden H, Warren A, Hughes D, Fidani L, Goate A, Rossor M, Roques P, Hardy J, Mullan M (1991) Early-onset Alzheimer's disease caused by mutations at codon 717 of the β-amyloid precursor protein gene. Nature 353:844-846.

Cheadle C, Ivashchenko Y, South V, Searfoss GH, French S, Howk R, Ricca GA, Jaye M (1994) Identification of a Src SH3 domain binding motif by screening a random phage display library. J Biol Chem 269:24034-24039.

Chen J, Kanai Y, Cowan NJ, Hirokawa N (1992) Projection domains of MAP2 and tau determine spacings between microtubules in dendrites and axons. Nature 360:674-677.

Chen X, Lin R, Chang L, Xu S, Wei X, Zhang J, Wang C, Anwyl R, Wang Q (2013) Enhancement of long-term depression by soluble amyloid β protein in rat hippocampus is mediated by metabotropic glutamate receptor and involves activation of p38MAPK, STEP and caspase-3. Neuroscience 253:435-443.

Chin J, Palop JJ, Yu G-Q, Kojima N, Masliah E, Mucke L (2004) Fyn kinase modulates synaptotoxicity, but not aberrant sprouting, in human amyloid precursor protein transgenic mice. J Neurosci 24:4692-4697.

Chin J, Palop JJ, PuolivÃ¤li J, Massaro C, Bien-Ly N, Gerstein H, Scearce-Levie K, Masliah E, Mucke L (2005) Fyn kinase induces synaptic and cognitive impairments in a transgenic mouse model of Alzheimer's disease. J Neurosci 25:9694-9703.

Cho J-H, Johnson GVW (2003) Glycogen synthase kinase 3β phosphorylates tau at both primed and unprimed sites: differential impact on microtubule binding. J Biol Chem 278:187-193.

Cho S, Wood A, Bowby MR (2007) Brain slices as models for neurodegenerative disease and screening platforms to identify novel therapeutics. Current Neuropharmacology 5:19-33.

Citron M, Oltersdorf T, Haass C, McConlogue L, Hung AY, Seubert P, Vigo-Pelfrey C, Lieberburg I, Selkoe DJ (1992) Mutation of the β-amyloid precursor protein in familial Alzheimer's disease increases β-protein production. Nature 360:672-674.

Citron M et al. (1997) Mutant presenilins of Alzheimer's disease increase production of 42-residue amyloid β-protein in both transfected cells and transgenic mice. Nat Med 3:67-72.

Clark RF et al. (1995) The structure of the presenilin 1 (S182) gene and identification of six novel mutations in early onset AD families. Nat Genet 11:219-222.

Clavaguera F, Bolmont T, Crowther RA, Abramowski D, Frank S, Probst A, Fraser G, Stalder AK, Beibel M, Staufenbiel M, Jucker M, Goedert M, Tolnay M (2009) Transmission and spreading of tauopathy in transgenic mouse brain. Nat Cell Biol 11:909-913.

Clavaguera F, Akatsu H, Fraser G, Crowther RA, Frank S, Hench J, Probst A, Winkler DT, Reichwald J, Staufenbiel M, Ghetti B, Goedert M, Tolnay M (2013) Brain homogenates from human tauopathies induce tau inclusions in mouse brain. Proc Natl Acad Sci U S A 110:9535-9540.

Cleveland DW, Hwo S-Y, Kirschner MW (1977) Purification of tau, a microtubule-associated protein that induces assembly of microtubules from purified tubulin. J Mol Biol 116:207-225.

Cochran JN, Diggs PV, Nebane NM, Rasmussen L, White EL, Bostwick R, Maddry JA, Suto MJ, Roberson ED (2014) AlphaScreen HTS and live-cell bioluminescence resonance energy transfer (BRET) assays for identification of tau–fyn SH3 interaction inhibitors for Alzheimer disease. J Biomol Screen 19:1338-1349.

Congdon EE, Wu JW, Myeku N, Figueroa YH, Herman M, Marinec PS, Gestwicki JE, Dickey CA, Yu WH, Duff KE (2012) Methylthioninium chloride (methylene blue) induces autophagy and attenuates tauopathy in vitro and in vivo. Autophagy 8:609-622.

Cooke MP, Perlmutter RM (1989) Expression of a novel form of the fyn proto-oncogene in hematopoietic cells. New Biol 1:66-74.

Corder EH, Saunders AM, Strittmatter WJ, Schmechel DE, Gaskell PC, Small GW, Roses AD, Haines JL, Pericak-Vance MA (1993) Gene dose of apolipoprotein E type 4 allele and the risk of Alzheimer's disease in late onset families. Science 261:921-923.

Corneveaux JJ et al. (2010) Association of CR1, CLU and PICALM with Alzheimer's disease in a cohort of clinically characterized and neuropathologically verified individuals. Hum Mol Genet 19:3295-3301.

Costanzo M, Abounit S, Marzo L, Danckaert A, Chamoun Z, Roux P, Zurzolo C (2013) Transfer of polyglutamine aggregates in neuronal cells occurs in tunneling nanotubes. J Cell Sci 126:3678-3685.

Couchie D, Nunez J (1985) Immunological characterization of microtubule-associated proteins specific for the immature brain. FEBS Lett 188:331-335.

Cuchillo-Ibanez I, Seereeram A, Byers HL, Leung K-Y, Ward MA, Anderton BH, Hanger DP (2008) Phosphorylation of tau regulates its axonal transport by controlling its binding to kinesin. FASEB J 22:3186-3195.

D'Souza I, Poorkaj P, Hong M, Nochlin D, Lee VM, Bird TD, Schellenberg GD (1999) Missense and silent tau gene mutations cause frontotemporal dementia with parkinsonism-chromosome 17 type, by affecting multiple alternative RNA splicing regulatory elements. Proc Natl Acad Sci U S A 96:5598-5603.

Dawson HN, Ferreira A, Eyster MV, Ghoshal N, Binder LI, Vitek MP (2001) Inhibition of neuronal maturation in primary hippocampal neurons from τ deficient mice. J Cell Sci 114:1179-1187.

De Felice FG, Wu D, Lambert MP, Fernandez SJ, Velasco PT, Lacor PN, Bigio EH, Jerecic J, Acton PJ, Shughrue PJ, Chen-Dodson E, Kinney GG, Klein WL (2008) Alzheimer's disease-type neuronal tau hyperphosphorylation induced by Aβ oligomers. Neurobiol Aging 29:1334-1347.

De Simoni A, Griesinger CB, Edwards FA (2003) Development of rat CA1 neurones in acute Versus organotypic slices: role of experience in synaptic morphology and activity. J Physiol 550:135-147.

de Calignon A, Polydoro M, Suárez-Calvet M, William C, Adamowicz David H, Kopeikina Kathy J, Pitstick R, Sahara N, Ashe Karen H, Carlson George A, Spires-Jones Tara L, Hyman Bradley T (2012) Propagation of tau pathology in a model of early Alzheimer's disease. Neuron 73:685-697.

Dean J, Riddle A, Maire J, Hansen K, Preston M, Barnes A, Sherman L, Back S (2011) An organotypic slice culture model of chronic white matter injury with maturation arrest of oligodendrocyte progenitors. Mol Neurodegener 6:46.

DeKosky ST, Scheff SW (1990) Synapse loss in frontal cortex biopsies in Alzheimer's disease: correlation with cognitive severity. Ann Neurol 27:457-464.

del Rio JA, Soriano E (2010) Regenerating cortical connections in a dish: the entorhino-hippocampal organotypic slice co-culture as tool for pharmacological screening of molecules promoting axon regeneration. Nat Protocols 5:217-226.

del Rio JA, Heimrich B, Soriano E, Schwegler H, Frotscher M (1991) Proliferation and differentiation of glial fibrillary acidic protein-immunoreactive glial cells in organotypic slice cultures of rat hippocampus. Neuroscience 43:335-347.

Delobel P, Lavenir I, Fraser G, Ingram E, Holzer M, Ghetti B, Spillantini MG, Crowther RA, Goedert M (2008) Analysis of tau phosphorylation and truncation in a mouse model of human tauopathy. Am J Pathol 172:123-131.

Deramecourt V, Lebert F, Maurage CA, Fernandez-Gomez FJ, Dujardin S, Colin M, Sergeant N, Buee-Scherrer V, Clot F, Ber IL, Brice A, Pasquier F, Buee L (2012) Clinical, neuropathological, and biochemical characterization of the novel tau mutation P332S. J Alzheimers Dis 31:741-749.

Derkinderen P, Scales TME, Hanger DP, Leung K-Y, Byers HL, Ward MA, Lenz C, Price C, Bird IN, Perera T, Kellie S, Williamson R, Noble W, Van Etten RA, Leroy K, Brion J-P, Reynolds CH, Anderton BH (2005) Tyrosine 394 is phosphorylated in Alzheimer's paired helical filament tau and in fetal tau with c-Abl as the candidate tyrosine kinase. J Neurosci 25:6584-6593.

Desplats P, Lee H-J, Bae E-J, Patrick C, Rockenstein E, Crews L, Spencer B, Masliah E, Lee S-J (2009) Inclusion formation and neuronal cell death through neuron-to-neuron transmission of α-synuclein. Proc Natl Acad Sci U S A 106:13010-13015.

Di Fede G et al. (2009) A recessive mutation in the APP gene with dominant-negative effect on amyloidogenesis. Science 323:1473-1477.

Dixit R, Ross JL, Goldman YE, Holzbaur ELF (2008) Differential regulation of dynein and kinesin motor proteins by tau. Science 319:1086-1089.

Drewes G, Ebneth A, Preuss U, Mandelkow EM, Mandelkow E (1997) MARK, a novel family of protein kinases that phosphorylate microtubule-associated proteins and trigger microtubule disruption. Cell 89:297-308.

Drubin DG, Kirschner MW (1986) Tau protein function in living cells. J Cell Biol 103:2739-2746.

Dubois B et al. (2010) Revising the definition of Alzheimer's disease: a new lexicon. Lancet Neurol 9:1118-1127.

Dubois B et al. (2014) Advancing research diagnostic criteria for Alzheimer's disease: the IWG-2 criteria. Lancet Neurol 13:614-629.

Duff K, Noble W, Gaynor K, Matsuoka Y (2002) Organotypic slice cultures from transgenic mice as disease model systems. J Mol Neurosci 19:317-320.

Duff K, Liu L, Wu JW, Small SA (2013) Propagation of AD-related pathology and functional decline in transgenic models. In: The 11th International Conference on Alzheimer's and Parkinson's Diseases. Florence, Italy.

Duff K, Eckman C, Zehr C, Yu X, Prada C-M, Perez-tur J, Hutton M, Buee L, Harigaya Y, Yager D, Morgan D, Gordon MN, Holcomb L, Refolo L, Zenk B, Hardy J, Younkin S (1996) Increased amyloid-β42(43) in brains of mice expressing mutant presenilin 1. Nature 383:710-713.

Dujardin S, Bégard S, Caillierez R, Lachaud C, Delattre L, Carrier S, Loyens A, Galas M-C, Bousset L, Melki R, Aurégan G, Hantraye P, Brouillet E, Buée L, Colin M (2014) Ectosomes: a new mechanism for non-exosomal secretion of tau protein. PLoS ONE 9:e100760.

Dumanchin C, Camuzat A, Campion D, Verpillat P, Hannequin D, Dubois B, Saugier-Veber P, Martin C, Penet C, Charbonnier F, Agid Y, Frebourg T, Brice A (1998) Segregation of a missense mutation in the microtubule-associated protein tau gene with familial frontotemporal dementia and parkinsonism. Hum Mol Genet 7:1825-1829.

Dunah AW, Sirianni AC, Fienberg AA, Bastia E, Schwarzschild MA, Standaert DG (2004) Dopamine D1-Dependent trafficking of striatal N-methyl-d-aspartate glutamate receptors requires fyn protein tyrosine kinase but not DARPP-32. Mol Pharmacol 65:121-129.

Ehrengruber MU, Hennou S, Büeler H, Naim HY, Déglon N, Lundstrom K (2001) Gene transfer into neurons from hippocampal slices: comparison of recombinant Semliki Forest virus, adenovirus, adeno-associated virus, lentivirus, and measles virus. Mol Cell Neurosci 17:855-871.

Emerman M, Temin HM (1984) Genes with promoters in retrovirus vectors can be independently suppressed by an epigenetic mechanism. Cell 39:459-467.

Engen JR, Wales TE, Hochrein JM, Meyn MA, 3rd, Banu Ozkan S, Bahar I, Smithgall TE (2008) Structure and dynamic regulation of Src-family kinases. Cell Mol Life Sci 65:3058-3073.

Falcon B, Cavallini A, Angers R, Glover S, Murray TK, Barnham L, Jackson S, O'Neill MJ, Isaacs AM, Hutton ML, Szekeres PG, Goedert M, Bose S (2014) Conformation determines the seeding potencies of native and recombinant tau aggregates. J Biol Chem Advance online publication.

Fernandez-Nogales M, Cabrera JR, Santos-Galindo M, Hoozemans JJM, Ferrer I, Rozemuller AJM, Hernandez F, Avila J, Lucas JJ (2014) Huntington's disease is a four-repeat tauopathy with tau nuclear rods. Nat Med advance online publication.

Folstein MF, Folstein SE, McHugh PR (1975) “Mini-mental state”: A practical method for grading the cognitive state of patients for the clinician. J Psychiatr Res 12:189-198.

Frandemiche ML, De Seranno S, Rush T, Borel E, Elie A, Arnal I, Lanté F, Buisson A (2014) Activity-dependent tau protein translocation to excitatory synapse is disrupted by exposure to amyloid-beta oligomers. J Neurosci 34:6084-6097.

Frost B, Jacks RL, Diamond MI (2009) Propagation of tau misfolding from the outside to the inside of a cell. J Biol Chem 284:12845-12852.

Fujio K, Sato M, Uemura T, Sato T, Sato-Harada R, Harada A (2007) 14-3-3 proteins and protein phosphatases are not reduced in tau-deficient mice. Neuroreport 18:1049-1052.

Fulga TA, Elson-Schwab I, Khurana V, Steinhilb ML, Spires TL, Hyman BT, Feany MB (2007) Abnormal bundling and accumulation of F-actin mediates tau-induced neuronal degeneration in vivo. Nat Cell Biol 9:139-148.

Gähwiler BH (1981) Organotypic monolayer cultures of nervous tissue. J Neurosci Methods 4:329-342.

Gähwiler BH, Capogna M, Debanne D, McKinney RA, Thompson SM (1997) Organotypic slice cultures: a technique has come of age. Trends Neurosci 20:471-477.

Games D et al. (1995) Alzheimer-type neuropathology in transgenic mice overexpressing V717F β-amyloid precursor protein. Nature 373:523-527.

García-Román J, Ibarra-Sánchez A, Lamas M, González Espinosa C (2010) VEGF secretion during hypoxia depends on free radicals-induced Fyn kinase activity in mast cells. Biochem Biophys Res Commun 401:262-267.

Garwood CJ, Pooler AM, Atherton J, Hanger DP, Noble W (2011) Astrocytes are important mediators of Aβ-induced neurotoxicity and tau phosphorylation in primary culture. Cell Death Dis 2:e167.

Gerrish A et al. (2012) The role of variation at AβPP, PSEN1, PSEN2, and MAPT in late onset Alzheimer's disease. J Alzheimers Dis 28:377-387.

Giaccone G, Rossi G, Farina L, Marcon G, Di Fede G, Catania M, Morbin M, Sacco L, Bugiani O, Tagliavini F (2005) Familial frontotemporal dementia associated with the novel MAPT mutation T427M. J Neurol 252:1543-1545.

Giannakopoulos P, Herrmann FR, Bussiere T, Bouras C, Kovari E, Perl DP, Morrison JH, Gold G, Hof PR (2003) Tangle and neuron numbers, but not amyloid load, predict cognitive status in Alzheimer's disease. Neurology 60:1495-1500.

Glenner GG, Wong CW (1984) Alzheimer's disease: Initial report of the purification and characterization of a novel cerebrovascular amyloid protein. Biochem Biophys Res Commun 120:885-890.

Goate A, Chartier-Harlin MC, Mullan M, Brown J, Crawford F, Fidani L, Giuffra L, Haynes A, Irving N, James L, et al. (1991) Segregation of a missense mutation in the amyloid precursor protein gene with familial Alzheimer's disease. Nature 349:704-706.

Goedert M, Jakes R (1990) Expression of separate isoforms of human tau protein: correlation with the tau pattern in brain and effects on tubulin polymerization. EMBO J 9:4225-4230.

Goedert M, Crowther RA, Garner CC (1991) Molecular characterization of microtubule-associated proteins tau and map2. Trends Neurosci 14:193-199.

Goedert M, Spillantini MG, Crowther RA (1992) Cloning of a big tau microtubule-associated protein characteristic of the peripheral nervous system. Proc Natl Acad Sci U S A 89:1983-1987.

Goedert M, Jakes R, Crowther RA (1999) Effects of frontotemporal dementia FTDP-17 mutations on heparin-induced assembly of tau filaments. FEBS Lett 450:306-311.

Goedert M, Spillantini MG, Potier MC, Ulrich J, Crowther RA (1989a) Cloning and sequencing of the cDNA encoding an isoform of microtubule-associated protein tau containing four tandem repeats: differential expression of tau protein mRNAs in human brain. EMBO J 8:393-399.

Goedert M, Spillantini MG, Jakes R, Rutherford D, Crowther RA (1989b) Multiple isoforms of human microtubule-associated protein tau: sequences and localization in neurofibrillary tangles of Alzheimer's disease. Neuron 3:519-526.

Goldsmith JF, Hall CG, Atkinson TP (2002) Identification of an alternatively spliced isoform of the fyn tyrosine kinase. Biochem Biophys Res Commun 298:501-504.

Gómez-Isla T, Hollister R, West H, Mui S, Growdon JH, Petersen RC, Parisi JE, Hyman BT (1997) Neuronal loss correlates with but exceeds neurofibrillary tangles in Alzheimer's disease. Annals of Neurology 41:17-24.

Gómez-Ramos A, Díaz-Hernández M, Cuadros R, Hernández F, Avila J (2006) Extracellular tau is toxic to neuronal cells. FEBS Lett 580:4842-4850.

Gómez-Ramos A, Díaz-Hernández M, Rubio A, Díaz-Hernández JI, Miras-Portugal MT, Avila J (2009) Characteristics and consequences of muscarinic receptor activation by tau protein. Eur Neuropsychopharmacol 19:708-717.

Gomez G, Gonzalez-Espinosa C, Odom S, Baez G, Cid ME, Ryan JJ, Rivera J (2005) Impaired FcεRI-dependent gene expression and defective eicosanoid and cytokine production as a consequence of fyn deficiency in mast cells. J Immunol 175:7602-7610.

Gousset K, Schiff E, Langevin C, Marijanovic Z, Caputo A, Browman DT, Chenouard N, de Chaumont F, Martino A, Enninga J, Olivo-Marin J-C, Mannel D, Zurzolo C (2009) Prions hijack tunnelling nanotubes for intercellular spread. Nat Cell Biol 11:328-336.

Grant S, O'Dell T, Karl K, Stein P, Soriano P, Kandel E (1992) Impaired long-term potentiation, spatial learning, and hippocampal development in fyn mutant mice. Science 258:1903-1910.

Grant SG, Karl KA, Kiebler MA, Kandel ER (1995) Focal adhesion kinase in the brain: novel subcellular localization and specific regulation by Fyn tyrosine kinase in mutant mice. Genes Dev 9:1909-1921.

Gros-Louis F, Soucy G, Lariviere R, Julien JP (2010) Intracerebroventricular infusion of monoclonal antibody or its derived Fab fragment against misfolded forms of SOD1 mutant delays mortality in a mouse model of ALS. J Neurochem 113:1188-1199.

Grover A, England E, Baker M, Sahara N, Adamson J, Granger B, Houlden H, Passant U, Yen SH, DeTure M, Hutton M (2003) A novel tau mutation in exon 9 (1260V) causes a four-repeat tauopathy. Exp Neurol 184:131-140.

Guerreiro R et al. (2013) TREM2 variants in Alzheimer's disease. N Engl J Med 368:117-127.

Guo JL, Lee VM-Y (2011) Seeding of normal tau by pathological tau conformers drives pathogenesis of Alzheimer-like tangles. J Biol Chem 286:15317-15331.

Haase C, Stieler JT, Arendt T, Holzer M (2004) Pseudophosphorylation of tau protein alters its ability for self-aggregation. J Neurochem 88:1509-1520.

Haass C, Selkoe DJ (1993) Cellular processing of β-amyloid precursor protein and the genesis of amyloid β-peptide. Cell 75:1039-1042.

Hanger DP, Noble W (2011) Functional implications of glycogen synthase kinase-3-mediated tau phosphorylation. Int J Alzheimers Dis 2011.

Hanger DP, Anderton BH, Noble W (2009) Tau phosphorylation: the therapeutic challenge for neurodegenerative disease. Trends Mol Med 15:112-119.

Hanger DP, Hughes K, Woodgett JR, Brion JP, Anderton BH (1992) Glycogen synthase kinase-3 induces Alzheimer's disease-like phosphorylation of tau: generation of

paired helical filament epitopes and neuronal localisation of the kinase. Neurosci Lett 147:58-62.

Harada A, Oguchi K, Okabe S, Kuno J, Terada S, Ohshima T, Sato-Yoshitake R, Takei Y, Noda T, Hirokawa N (1994) Altered microtubule organization in small-calibre axons of mice lacking tau protein. Nature 369:488-491.

Hardy J (2009) The amyloid hypothesis for Alzheimer's disease: a critical reappraisal. J Neurochem 110:1129-1134.

Hardy J, Allsop D (1991) Amyloid deposition as the central event in the aetiology of Alzheimer's disease. Trends Pharmacol Sci 12:383-388.

Hardy J, Higgins G (1992) Alzheimer's disease: the amyloid cascade hypothesis. Science 256:184-185.

Hardy J, Selkoe DJ (2002) The amyloid hypothesis of Alzheimer's disease: progress and problems on the road to therapeutics. Science 297:353-356.

Harold D et al. (2009) Genome-wide association study identifies variants at CLU and PICALM associated with Alzheimer's disease. Nat Genet 41:1088-1093.

Harris JA, Koyama A, Maeda S, Ho K, Devidze N, Dubal DB, Yu G-Q, Masliah E, Mucke L (2012) Human P301L-Mutant Tau Expression in Mouse Entorhinal-Hippocampal Network Causes Tau Aggregation and Presynaptic Pathology but No Cognitive Deficits. PLoS ONE 7:e45881.

Hayashi S, Toyoshima Y, Hasegawa M, Umeda Y, Wakabayashi K, Tokiguchi S, Iwatsubo T, Takahashi H (2002) Late-onset frontotemporal dementia with a novel exon 1 (Arg5His) tau gene mutation. Ann Neurol 51:525-530.

He HJ, Xing SW, Rong P, Wang DL, Liu MN, He RQ (2009) The proline-rich domain of tau plays a role in interactions with actin. BMC Cell Biol 10:1-12.

Hendriks L, van Duijn CM, Cras P, Cruts M, Van Hul W, van Harskamp F, Warren A, McInnis MG, Antonarakis SE, Martin J-J, Hofman A, Van Broeckhoven C (1992) Presenile dementia and cerebral haemorrhage linked to a mutation at codon 692 of the β-amyloid precursor protein gene. Nat Genet 1:218-221.

Himmler A, Drechsel D, Kirschner MW, Martin DW (1989) Tau consists of a set of proteins with repeated C-terminal microtubule-binding domains and variable N-terminal domains. Mol Cell Biol 9:1381-1388.

Hioki H, Kameda H, Nakamura H, Okunomiya T, Ohira K, Nakamura K, Kuroda M, Furuta T, Kaneko T (2007) Efficient gene transduction of neurons by lentivirus with enhanced neuron-specific promoters. Gene Ther 14:872-882.

Hirokawa N, Shiomura Y, Okabe S (1988) Tau proteins: the molecular structure and mode of binding on microtubules. J Cell Biol 107:1449-1459.

Ho GJ, Hashimoto M, Adame A, Izu M, Alford MF, Thal LJ, Hansen LA, Masliah E (2005) Altered p59Fyn kinase expression accompanies disease progression in Alzheimer's disease: implications for its functional role. Neurobiol Aging 26:625-635.

Hoe HS, Minami SS, Makarova A, Lee J, Hyman BT, Matsuoka Y, Rebeck GW (2008) Fyn modulation of Dab1 effects on amyloid precursor protein and ApoE receptor 2 processing. J Biol Chem 283:6288-6299.

Hof Wvt, Resh MD (1997) Rapid plasma membrane anchoring of newly synthesized p59 fyn: selective requirement for NH2-terminal myristoylation and palmitoylation at cysteine-3. J Cell Biol 136:1023-1035.

Hogg M et al. (2003) The L266V tau mutation is associated with frontotemporal dementia and Pick-like 3R and 4R tauopathy. Acta Neuropathol 106:323-336.

Hollingworth P et al. (2012) Genome-wide association study of Alzheimer's disease with psychotic symptoms. Mol Psychiatry 17:1316-1327.

Holmes BB, DeVos SL, Kfoury N, Li M, Jacks R, Yanamandra K, Ouidja MO, Brodsky FM, Marasa J, Bagchi DP, Kotzbauer PT, Miller TM, Papy-Garcia D, Diamond MI (2013) Heparan sulfate proteoglycans mediate internalization and propagation of specific proteopathic seeds. Proc Natl Acad Sci U S A 110:E3138-3147.

Holtzman DM, Morris JC, Goate AM (2011) Alzheimer's disease: the challenge of the second century. Science translational medicine 3:77sr71.

Hoover BR, Reed MN, Su J, Penrod RD, Kotilinek LA, Grant MK, Pitstick R, Carlson GA, Lanier LM, Yuan LL, Ashe KH, Liao D (2010) Tau mislocalization to dendritic spines mediates synaptic dysfunction independently of neurodegeneration. Neuron 68:1067-1081.

Houlden H et al. (2001) Corticobasal degeneration and progressive supranuclear palsy share a common tau haplotype. Neurology 56:1702-1706.

Hsieh H, Boehm J, Sato C, Iwatsubo T, Tomita T, Sisodia S, Malinow R (2006) AMPAR removal underlies Abeta-induced synaptic depression and dendritic spine loss. Neuron 52:831-843.

Hutson TH, Foster E, Dawes JM, Hindges R, Yáñez-Muñoz RJ, Moon LDF (2012) Lentiviral vectors encoding short hairpin RNAs efficiently transduce and knockdown LINGO-1 but induce an interferon response and cytotoxicity in central nervous system neurones. J Gene Med 14:299-315.

Hutton M et al. (1998) Association of missense and 5[prime]-splice-site mutations in tau with the inherited dementia FTDP-17. Nature 393:702-705.

Iijima M, Tabira T, Poorkaj P, Schellenberg GD, Trojanowski JQ, Lee VM, Schmidt ML, Takahashi K, Nabika T, Matsumoto T, Yamashita Y, Yoshioka S, Ishino H (1999) A distinct familial presenile dementia with a novel missense mutation in the tau gene. Neuroreport 10:497-501.

Ikegami S, Harada A, Hirokawa N (2000) Muscle weakness, hyperactivity, and impairment in fear conditioning in tau-deficient mice. Neurosci Lett 279:129-132.

Illenberger S, Zheng-Fischhöfer Q, Preuss U, Stamer K, Baumann K, Trinczek B, Biernat J, Godemann R, Mandelkow E-M, Mandelkow E (1998) The endogenous and cell cycle-dependent phosphorylation of tau protein in living cells: implications for Alzheimer's disease. Mol Biol Cell 9:1495-1512.

Iqbal K, Liu F, Gong CX, Grundke-Iqbal I (2010) Tau in Alzheimer disease and related tauopathies. Curr Alzheimer Res 7:656-664.

Iseki E, Matsumura T, Marui W, Hino H, Odawara T, Sugiyama N, Suzuki K, Sawada H, Arai T, Kosaka K (2001) Familial frontotemporal dementia and parkinsonism with a novel N296H mutation in exon 10 of the tau gene and a widespread tau accumulation in the glial cells. Acta Neuropathol 102:285-292.

Ishiguro K, Takamatsu M, Tomizawa K, Omori A, Takahashi M, Arioka M, Uchida T, Imahori K (1992) Tau protein kinase I converts normal tau protein into A68-like component of paired helical filaments. J Biol Chem 267:10897-10901.

Ishiguro K, Shiratsuchi A, Sato S, Omori A, Arioka M, Kobayashi S, Uchida T, Imahori K (1993) Glycogen synthase kinase 3β is identical to tau protein kinase I generating several epitopes of paired helical filaments. FEBS Lett 325:167-172.

Ittner LM, Ke YD, Götz J (2009) Phosphorylated tau interacts with c-Jun N-terminal kinase-interacting protein 1 (JIP1) in Alzheimer disease. J Biol Chem 284:20909-20916.

Ittner LM, Ke YD, Delerue F, Bi M, Gladbach A, van Eersel J, Wölfing H, Chieng BC, Christie MJ, Napier IA, Eckert A, Staufenbiel M, Hardeman E, Götz J (2010) Dendritic function of tau mediates amyloid-β toxicity in Alzheimer's disease mouse models. Cell 142:387-397.

Jarrett JT, Berger EP, Lansbury PT (1993) The carboxy terminus of the .beta. amyloid protein is critical for the seeding of amyloid formation: Implications for the pathogenesis of Alzheimer's disease. Biochemistry (Mosc) 32:4693-4697.

Jeganathan S, von Bergen M, Brutlach H, Steinhoff H-J, Mandelkow E (2006) Global hairpin folding of tau in solution. Biochemistry (Mosc) 45:2283-2293.

Jenkins SM, Johnson GV (1998) Tau complexes with phospholipase C-gamma in situ. Neuroreport 9:67-71.

Jin M, Shepardson N, Yang T, Chen G, Walsh D, Selkoe DJ (2011) Soluble amyloid β-protein dimers isolated from Alzheimer cortex directly induce Tau hyperphosphorylation and neuritic degeneration. Proc Natl Acad Sci U S A 108:5819-5824.

Jonsson T et al. (2013) Variant of TREM2 associated with the risk of Alzheimer's disease. N Engl J Med 368:107-116.

Jonsson T et al. (2012) A mutation in APP protects against Alzheimer's disease and age-related cognitive decline. Nature 488:96-99.

Jurd R, Tretter V, Walker J, Brandon NJ, Moss SJ (2010) Fyn kinase contributes to tyrosine phosphorylation of the GABAA receptor γ2 subunit. Mol Cell Neurosci 44:129-134.

Kamboh MI et al. (2012) Genome-wide association study of Alzheimer's disease. Transl Psychiatry 2:e117.

Kanaan NM, Pigino GF, Brady ST, Lazarov O, Binder LI, Morfini GA (2013) Axonal degeneration in Alzheimer's disease: when signaling abnormalities meet the axonal transport system. Exp Neurol 246:44-53.

Kanai Y, Chen J, Hirokawa N (1992) Microtubule bundling by tau proteins in vivo: analysis of functional domains. EMBO J 11:3953-3961.

Kang J, Müller-Hill B (1990) Differential splicing of Alzheimer's disease amyloid A4 precursor RNA in rat tissues: PreA4695 mRNA is predominantly produced in rat and human brain. Biochem Biophys Res Commun 166:1192-1200.

Kang J, Lemaire H-G, Unterbeck A, Salbaum JM, Masters CL, Grzeschik K-H, Multhaup G, Beyreuther K, Muller-Hill B (1987) The precursor of Alzheimer's disease amyloid A4 protein resembles a cell-surface receptor. Nature 325:733-736.

Karch CM, Jeng AT, Goate AM (2012) Extracellular tau levels are influenced by variability in tau that is associated with tauopathies. J Biol Chem 287:42751-42762.

Karran E, Mercken M, Strooper BD (2011) The amyloid cascade hypothesis for Alzheimer's disease: an appraisal for the development of therapeutics. Nature reviews Drug discovery 10:698-712.

Kempf M, Clement A, Faissner A, Lee G, Brandt R (1996) Tau binds to the distal axon early in development of polarity in a microtubule- and microfilament-dependent manner. J Neurosci 16:5583-5592.

Kfoury N, Holmes BB, Jiang H, Holtzman DM, Diamond MI (2012) Trans-cellular propagation of tau aggregation by fibrillar species. J Biol Chem 287:19440-19451.

Kimberly WT, LaVoie MJ, Ostaszewski BL, Ye W, Wolfe MS, Selkoe DJ (2003) γ-Secretase is a membrane protein complex comprised of presenilin, nicastrin, aph-1, and pen-2. Proc Natl Acad Sci U S A 100:6382-6387.

Kimura T, Whitcomb DJ, Jo J, Regan P, Piers T, Heo S, Brown C, Hashikawa T, Murayama M, Seok H, Sotiropoulos I, Kim E, Collingridge GL, Takashima A, Cho K (2014) Microtubule-associated protein tau is essential for long-term depression in the hippocampus. Philos Trans R Soc Lond B Biol Sci 369.

Klein C, KrÃ¤mer E-M, Cardine A-M, Schraven B, Brandt R, Trotter J (2002) Process outgrowth of oligodendrocytes is promoted by interaction of fyn kinase with the cytoskeletal protein tau. J Neurosci 22:698-707.

Kobayashi K, Hayashi M, Kidani T, Nakano H, Miyazu K, Ujike H, Kuroda S, Koshino Y (2002) Pick's disease in 2 brothers with S305N mutation: note in supplement to an earlier communication. Clin Neuropathol 21:191-193.

Kobayashi T, Ota S, Tanaka K, Ito Y, Hasegawa M, Umeda Y, Motoi Y, Takanashi M, Yasuhara M, Anno M, Mizuno Y, Mori H (2003) A novel L266V mutation of the tau gene causes frontotemporal dementia with a unique tau pathology. Ann Neurol 53:133-137.

Koffie RM, Hashimoto T, Tai H-C, Kay KR, Serrano-Pozo A, Joyner D, Hou S, Kopeikina KJ, Frosch MP, Lee VM, Holtzman DM, Hyman BT, Spires-Jones TL (2012) Apolipoprotein E4 effects in Alzheimer’s disease are mediated by synaptotoxic oligomeric amyloid-β. Brain 135:2155-2168.

Kojima N, Ishibashi H, Obata K, Kandel ER (1998) Higher seizure susceptibility and enhanced tyrosine phosphorylation of N-methyl-d-aspartate receptor subunit 2B in fyn transgenic mice. Learn Mem 5:429-445.

Kojima N, Wang J, Mansuy IM, Grant SGN, Mayford M, Kandel ER (1997) Rescuing impairment of long-term potentiation in fyn-deficient mice by introducing Fyn transgene. Proc Natl Acad Sci U S A 94:4761-4765.

Kolarova M, Garcia-Sierra F, Bartos A, Ricny J, Ripova D (2012) Structure and pathology of tau protein in Alzheimer disease. Int J Alzheimers Dis 2012:731526.

Kopeikina KJ, Polydoro M, Tai H-C, Yaeger E, Carlson GA, Pitstick R, Hyman BT, Spires-Jones TL (2013) Synaptic alterations in the rTg4510 mouse model of tauopathy. J Comp Neurol 521:1334-1353.

Kouri N, Carlomagno Y, Baker M, Liesinger AM, Caselli RJ, Wszolek ZK, Petrucelli L, Boeve BF, Parisi JE, Josephs KA, Uitti RJ, Ross OA, Graff-Radford NR, DeTure MA, Dickson DW, Rademakers R (2014) Novel mutation in MAPT exon 13 (p.N410H) causes corticobasal degeneration. Acta Neuropathol 127:271-282.

Kovacs GG, Pittman A, Revesz T, Luk C, Lees A, Kiss E, Tariska P, Laszlo L, Molnar K, Molnar MJ, Tolnay M, de Silva R (2008) MAPT S305I mutation: implications for argyrophilic grain disease. Acta Neuropathol 116:103-118.

Kowalska A, Hasegawa M, Miyamoto K, Akiguchi I, Ikemoto A, Takahashi K, Araki W, Tabira T (2002) A novel mutation at position +11 in the intron following exon 10 of the tau gene in FTDP-17. Journal of applied genetics 43:535-543.

Krämer-Albers E-M, White R (2011) From axon–glial signalling to myelination: the integrating role of oligodendroglial Fyn kinase. Cell Mol Life Sci 68:2003-2012.

Kuchibhotla KV, Wegmann S, Kopeikina KJ, Hawkes J, Rudinskiy N, Andermann ML, Spires-Jones TL, Bacskai BJ, Hyman BT (2014) Neurofibrillary tangle-bearing neurons are functionally integrated in cortical circuits in vivo. Proc Natl Acad Sci U S A 111:510-514.

LaFerla FM, Green KN, Oddo S (2007) Intracellular amyloid-β in Alzheimer's disease. Nat Rev Neurosci 8:499-509.

Lambert J-C et al. (2009) Genome-wide association study identifies variants at CLU and CR1 associated with Alzheimer's disease. Nat Genet 41:1094-1099.

Lambert MP, Barlow AK, Chromy BA, Edwards C, Freed R, Liosatos M, Morgan TE, Rozovsky I, Trommer B, Viola KL, Wals P, Zhang C, Finch CE, Krafft GA, Klein WL (1998) Diffusible, nonfibrillar ligands derived from Aβ1-42 are potent central nervous system neurotoxins. Proc Natl Acad Sci U S A 95:6448-6453.

Larson M, Sherman MA, Amar F, Nuvolone M, Schneider JA, Bennett DA, Aguzzi A, Lesné SE (2012) The complex PrPc-fyn couples human oligomeric Aβ with pathological tau changes in Alzheimer's disease. J Neurosci 32:16857-16871.

Lasagna-Reeves CA, Castillo-Carranza DL, Sengupta U, Clos AL, Jackson GR, Kayed R (2011) Tau oligomers impair memory and induce synaptic and mitochondrial dysfunction in wild-type mice. Mol Neurodegener 6:39.

Lauren J, Gimbel D, Nygaard H, Gilbert J, Strittmatter S (2009) Cellular prion protein mediates impairment of synaptic plasticity by amyloid-beta oligomers. Nature 457:1128 - 1132.

Lee G, Newman ST, Gard DL, Band H, Panchamoorthy G (1998) Tau interacts with src-family non-receptor tyrosine kinases. J Cell Sci 111 (Pt 21):3167-3177.

Lee G, Thangavel R, Sharma VM, Litersky JM, Bhaskar K, Fang SM, Do LH, Andreadis A, Van Hoesen G, Ksiezak-Reding H (2004) Phosphorylation of tau by fyn: implications for Alzheimer's disease. J Neurosci 24:2304-2312.

Lee M-s, Kwon YT, Li M, Peng J, Friedlander RM, Tsai L-H (2000) Neurotoxicity induces cleavage of p35 to p25 by calpain. Nature 405:360-364.

Lee S, Kim W, Li Z, Hall GF (2012) Accumulation of vesicle-associated human tau in distal dendrites drives degeneration and tau secretion in an in situ cellular tauopathy model. Int J Alzheimers Dis 2012:172837.

Lei P, Ayton S, Moon S, Zhang Q, Volitakis I, Finkelstein D, Bush A (2014) Motor and cognitive deficits in aged tau knockout mice in two background strains. Mol Neurodegener 9:29.

Lei P, Ayton S, Finkelstein DI, Spoerri L, Ciccotosto GD, Wright DK, Wong BXW, Adlard PA, Cherny RA, Lam LQ, Roberts BR, Volitakis I, Egan GF, McLean CA, Cappai R, Duce JA, Bush AI (2012) Tau deficiency induces parkinsonism with dementia by impairing APP-mediated iron export. Nat Med 18:291-295.

Lemere CA, Lopera F, Kosik KS, Lendon CL, Ossa J, Saido TC, Yamaguchi H, Ruiz A, Martinez A, Madrigal L, Hincapie L, Arango JC, Anthony DC, Koo EH, Goate AM, Selkoe DJ, Arango JC (1996) The E280A presenilin 1 Alzheimer mutation produces increased A beta 42 deposition and severe cerebellar pathology. Nat Med 2:1146-1150.

Lesort M, Jope RS, Johnson GVW (1999) Insulin transiently increases tau phosphorylation: Involvement of glycogen synthase kinase-β and Fyn tyrosine kinase. J Neurochem 72:576-584.

Levy-Lahad E, Wasco W, Poorkaj P, Romano DM, Oshima J, Pettingell WH, Yu CE, Jondro PD, Schmidt SD, Wang K, et al. (1995) Candidate gene for the chromosome 1 familial Alzheimer's disease locus. Science 269:973-977.

Li S, Hong S, Shepardson NE, Walsh DM, Shankar GM, Selkoe D (2009) Soluble oligomers of amyloid Beta protein facilitate hippocampal long-term depression by disrupting neuronal glutamate uptake. Neuron 62:788-801.

Li Z, Hall AM, Kelinske M, Roberson ED (2014) Seizure resistance without parkinsonism in aged mice after tau reduction. Neurobiol Aging 35:2617-2624.

Liang X, Lu Y, Wilkes M, Neubert TA, Resh MD (2004) The N-terminal SH4 region of the src family kinase fyn is modified by methylation and heterogeneous fatty acylation. J Biol Chem 279:8133-8139.

Lindwall G, Cole RD (1984) Phosphorylation affects the ability of tau protein to promote microtubule assembly. J Biol Chem 259:5301-5305.

Lippa CF, Zhukareva V, Kawarai T, Uryu K, Shafiq M, Nee LE, Grafman J, Liang Y, St George-Hyslop PH, Trojanowski JQ, Lee VM (2000) Frontotemporal dementia with novel tau pathology and a Glu342Val tau mutation. Ann Neurol 48:850-858.

Liu BH, Yang Y, Paton JFR, Li F, Boulaire J, Kasparov S, Wang S (2006) GAL4-NF-[kappa]B fusion protein augments transgene expression from neuronal

promoters in the rat brain. Molecular therapy : the journal of the American Society of Gene Therapy 14:872-882.

Liu C, Götz J (2013) Profiling murine tau with 0N, 1N and 2N isoform-specific antibodies in brain and peripheral organs reveals distinct subcellular localization, with the 1N isoform being enriched in the nucleus. PLoS ONE 8:e84849.

Liu F, Iqbal K, Grundke-Iqbal I, Gong CX (2002) Involvement of aberrant glycosylation in phosphorylation of tau by cdk5 and GSK-3beta. FEBS Lett 530:209-214.

Liu F, Grundke-Iqbal I, Iqbal K, Gong C-X (2005) Contributions of protein phosphatases PP1, PP2A, PP2B and PP5 to the regulation of tau phosphorylation. Eur J Neurosci 22:1942-1950.

Liu L, Drouet V, Wu JW, Witter MP, Small SA, Clelland C, Duff K (2012) Trans-synaptic spread of tau pathology *in vivo*. PLoS ONE 7:e31302.

Llado A, Ezquerra M, Sanchez-Valle R, Rami L, Tolosa E, Molinuevo JL (2007) A novel MAPT mutation (P301T) associated with familial frontotemporal dementia. Eur J Neurol 14:e9-10.

Loomis PA, Howard TH, Castleberry RP, Binder LI (1990) Identification of nuclear tau isoforms in human neuroblastoma cells. Proc Natl Acad Sci U S A 87:8422-8426.

Lossos A, Reches A, Gal A, Newman JP, Soffer D, Gomori JM, Boher M, Ekstein D, Biran I, Meiner Z, Abramsky O, Rosenmann H (2003) Frontotemporal dementia and parkinsonism with the P301S tau gene mutation in a Jewish family. J Neurol 250:733-740.

Lovestone S, Reynolds CH, Latimer D, Davis DR, Anderton BH, Gallo JM, Hanger D, Mulot S, Marquardt B, Stabel S, et al. (1994) Alzheimer's disease-like phosphorylation of the microtubule-associated protein tau by glycogen synthase kinase-3 in transfected mammalian cells. Curr Biol 4:1077-1086.

Lu P-J, Wulf G, Zhou XZ, Davies P, Lu KP (1999) The prolyl isomerase Pin1 restores the function of Alzheimer-associated phosphorylated tau protein. Nature 399:784-788.

Lucas JJ, Hernández F, Gómez-Ramos P, Morán MA, Hen R, Avila J (2001) Decreased nuclear β-catenin, tau hyperphosphorylation and neurodegeneration in GSK-3β conditional transgenic mice. EMBO J 20:27-39.

Ma QL, Zuo X, Yang F, Ubeda OJ, Gant DJ, Alaverdyan M, Kiosea NC, Nazari S, Chen PP, Nothias F, Chan P, Teng E, Frautschy SA, Cole GM (2014) Loss of MAP function leads to hippocampal synapse loss and deficits in the Morris Water Maze with aging. J Neurosci 34:7124-7136.

Maas T, Eidenmüller J, Brandt R (2000) Interaction of tau with the neural membrane cortex is regulated by phosphorylation at sites that are modified in paired helical filaments. J Biol Chem 275:15733-15740.

Malkani R, D'Souza I, Gwinn-Hardy K, Schellenberg GD, Hardy J, Momeni P (2006) A MAPT mutation in a regulatory element upstream of exon 10 causes frontotemporal dementia. Neurobiol Dis 22:401-403.

Mandelkow E-M, Mandelkow E (2012) Biochemistry and cell biology of tau protein in neurofibrillary degeneration. Cold Spring Harb Perspect Med 2.

Marino MJ, Rouse ST, Levey AI, Potter LT, Conn PJ (1998) Activation of the genetically defined m1 muscarinic receptor potentiates N-methyl-d-aspartate (NMDA) receptor currents in hippocampal pyramidal cells. Proc Natl Acad Sci U S A 95:11465-11470.

Markram H, Segal M (1990) Acetylcholine potentiates responses to N-methyl-d-aspartate in the rat hippocampus. Neurosci Lett 113:62-65.

Martin SJ, O'Brien GA, Nishioka WK, McGahon AJ, Mahboubi A, Saido TC, Green DR (1995) Proteolysis of fodrin (non-erythroid spectrin) during apoptosis. J Biol Chem 270:6425-6428.

Masliah E, Rockenstein E, Mante M, Crews L, Spencer B, Adame A, Patrick C, Trejo M, Ubhi K, Rohn TT, Mueller-Steiner S, Seubert P, Barbour R, McConlogue L, Buttini M, Games D, Schenk D (2011) Passive immunization reduces behavioral and neuropathological deficits in an alpha-synuclein transgenic model of Lewy body disease. PLoS ONE 6:e19338.

Masters CL, Simms G, Weinman NA, Multhaup G, McDonald BL, Beyreuther K (1985) Amyloid plaque core protein in Alzheimer disease and Down syndrome. Proc Natl Acad Sci U S A 82:4245-4249.

Mastrangelo M, Bowers W (2008) Detailed immunohistochemical characterization of temporal and spatial progression of Alzheimer's disease-related pathologies in male triple-transgenic mice. BMC Neurosci 9:81.

Mayer BJ (2001) SH3 domains: complexity in moderation. J Cell Sci 114:1253-1263.

Mc Donald JM, Savva GM, Brayne C, Welzel AT, Forster G, Shankar GM, Selkoe DJ, Ince PG, Walsh DM (2010) The presence of sodium dodecyl sulphate-stable Aβ dimers is strongly associated with Alzheimer-type dementia. Brain 133:1328-1341.

McLean CA, Cherny RA, Fraser FW, Fuller SJ, Smith MJ, Konrad V, Bush AI, Masters CL (1999) Soluble pool of Aβ amyloid as a determinant of severity of neurodegeneration in Alzheimer's disease. Ann Neurol 46:860-866.

Messing L, Decker JM, Joseph M, Mandelkow E, Mandelkow E-M (2013) Cascade of tau toxicity in inducible hippocampal brain slices and prevention by aggregation inhibitors. Neurobiol Aging 34:1343-1354.

Mewes A, Franke H, Singer D (2012) Organotypic brain slice cultures of adult transgenic P301S mice--a model for tauopathy studies. PLoS One 7:e45017.

Meyer MR, Tschanz JT, Norton MC, Welsh-Bohmer KA, Steffens DC, Wyse BW, Breitner JCS (1998) APOE genotype predicts when--not whether--one is predisposed to develop Alzheimer disease. Nat Genet 19:321-322.

Michel CH, Kumar S, Pinotsi D, Tunnacliffe A, St. George-Hyslop P, Mandelkow E, Mandelkow E-M, Kaminski CF, Kaminski Schierle GS (2014) Extracellular monomeric tau protein is sufficient to initiate the spread of tau protein pathology. J Biol Chem 289:956-967.

Michel G, Mercken M, Murayama M, Noguchi K, Ishiguro K, Imahori K, Takashima A (1998) Characterization of tau phosphorylation in glycogen synthase kinase-3beta and cyclin dependent kinase-5 activator (p23) transfected cells. Biochim Biophys Acta 1380:177-182.

Minami SS, Hoe H-S, Rebeck GW (2011) Fyn kinase regulates the association between amyloid precursor protein and Dab1 by promoting their localization to detergent-resistant membranes. J Neurochem 118:879-890.

Minami SS, Clifford TG, Hoe H-S, Matsuoka Y, Rebeck GW (2012) Fyn knock-down increases Aβ, decreases phospho-tau, and worsens spatial learning in 3×Tg-AD mice. Neurobiol Aging 33:825.e815-825.e824.

Mitchison T, Kirschner M (1984) Dynamic instability of microtubule growth. Nature 312:237-242.

Miyamoto K, Kowalska A, Hasegawa M, Tabira T, Takahashi K, Araki W, Akiguchi I, Ikemoto A (2001) Familial frontotemporal dementia and parkinsonism with a novel mutation at an intron 10+11-splice site in the tau gene. Ann Neurol 50:117-120.

Mizuguchi H, Xu Z, Ishii-Watabe A, Uchida E, Hayakawa T (2000) IRES-dependent second gene expression is significantly lower than cap-dependent first gene expression in a bicistronic vector. Molecular therapy : the journal of the American Society of Gene Therapy 1:376-382.

Mohamed NV, Plouffe V, Remillard-Labrosse G, Planel E, Leclerc N (2014) Starvation and inhibition of lysosomal function increased tau secretion by primary cortical neurons. Scientific reports 4:5715.

Momeni P, Wickremaratchi MM, Bell J, Arnold R, Beer R, Hardy J, Revesz T, Neal JW, Morris HR (2010) Familial early onset frontotemporal dementia caused by a novel S356T MAPT mutation, initially diagnosed as schizophrenia. Clin Neurol Neurosurg 112:917-920.

Momeni P, Pittman A, Lashley T, Vandrovcova J, Malzer E, Luk C, Hulette C, Lees A, Revesz T, Hardy J, de Silva R (2009) Clinical and pathological features of an Alzheimer's disease patient with the MAPT Delta K280 mutation. Neurobiol Aging 30:388-393.

Mondragon-Rodriguez S, Trillaud-Doppia E, Dudilot A, Bourgeois C, Lauzon M, Leclerc N, Boehm J (2012) Interaction of endogenous tau with synaptic proteins is regulated by NMDA-receptor dependent tau phosphorylation. J Biol Chem 287:32040-32053.

Morgan D, Diamond DM, Gottschall PE, Ugen KE, Dickey C, Hardy J, Duff K, Jantzen P, DiCarlo G, Wilcock D, Connor K, Hatcher J, Hope C, Gordon M, Arendash GW (2000) A beta peptide vaccination prevents memory loss in an animal model of Alzheimer's disease. Nature 408:982-985.

Morin-Brureau M, De Bock F, Lerner-Natoli M (2013) Organotypic brain slices: a model to study the neurovascular unit micro-environment in epilepsies. Fluids Barriers CNS 10:11.

Morris M, Hamto P, Adame A, Devidze N, Masliah E, Mucke L (2013) Age-appropriate cognition and subtle dopamine-independent motor deficits in aged Tau knockout mice. Neurobiol Aging 34:1523-1529.

Morsch R, Simon W, Coleman PD (1999) Neurons may live for decades with neurofibrillary tangles. J Neuropathol Exp Neurol 58:188-197.

Mouillet-Richard S, Ermonval M, Chebassier C, Laplanche JL, Lehmann S, Launay JM, Kellermann O (2000) Signal transduction through prion protein. Science 289:1925-1928.

Mullan M, Crawford F, Axelman K, Houlden H, Lilius L, Winblad B, Lannfelt L (1992) A pathogenic mutation for probable Alzheimer's disease in the APP gene at the N-terminus of β-amyloid. Nat Genet 1:345-347.

Münch C, O'Brien J, Bertolotti A (2011) Prion-like propagation of mutant superoxide dismutase-1 misfolding in neuronal cells. Proc Natl Acad Sci U S A 108:3548-3553.

Munoz DG, Ros R, Fatas M, Bermejo F, de Yebenes JG (2007) Progressive nonfluent aphasia associated with a new mutation V363I in tau gene. American journal of Alzheimer's disease and other dementias 22:294-299.

Murrell J, Farlow M, Ghetti B, Benson MD (1991) A mutation in the amyloid precursor protein associated with hereditary Alzheimer's disease. Science 254:97-99.

Murrell JR, Spillantini MG, Zolo P, Guazzelli M, Smith MJ, Hasegawa M, Redi F, Crowther RA, Pietrini P, Ghetti B, Goedert M (1999) Tau gene mutation G389R causes a tauopathy with abundant pick body-like inclusions and axonal deposits. J Neuropathol Exp Neurol 58:1207-1226.

Myers AJ, Kaleem M, Marlowe L, Pittman AM, Lees AJ, Fung HC, Duckworth J, Leung D, Gibson A, Morris CM, de Silva R, Hardy J (2005) The H1c haplotype at the MAPT locus is associated with Alzheimer's disease. Hum Mol Genet 14:2399-2404.

Myers AJ, Pittman AM, Zhao AS, Rohrer K, Kaleem M, Marlowe L, Lees A, Leung D, McKeith IG, Perry RH, Morris CM, Trojanowski JQ, Clark C, Karlawish J, Arnold S, Forman MS, Van Deerlin V, de Silva R, Hardy J (2007) The MAPT H1c risk haplotype is associated with increased expression of tau and especially of 4 repeat containing transcripts. Neurobiol Dis 25:561-570.

Nacharaju P, Lewis J, Easson C, Yen S, Hackett J, Hutton M, Yen S-H (1999) Accelerated filament formation from tau protein with specific FTDP-17 missense mutations. FEBS Lett 447:195-199.

Nada S, Okada M, MacAuley A, Cooper JA, Nakagawa H (1991) Cloning of a complementary DNA for a protein-tyrosine kinase that specifically phosphorylates a negative regulatory site of p60c-src. Nature 351:69-72.

Nada S, Yagi T, Takeda H, Tokunaga T, Nakagawa H, Ikawa Y, Okada M, Aizawa S (1993) Constitutive activation of Src family kinases in mouse embryos that lack Csk. Cell 73:1125-1135.

Nakazawa T, Komai S, Tezuka T, Hisatsune C, Umemori H, Semba K, Mishina M, Manabe T, Yamamoto T (2001) Characterization of fyn-mediated tyrosine phosphorylation sites on GluRε2 (NR2B) subunit of the N-methyl-d-aspartate receptor. J Biol Chem 276:693-699.

Naruse S, Igarashi S, Kobayashi H, Aoki K, Inuzuka T, Kaneko K, Shimizu T, Iihara K, Kojima T, Miyatake T, et al. (1991) Mis-sense mutation Val-Ile in exon 17 of

amyloid precursor protein gene in Japanese familial Alzheimer's disease. Lancet 337:978-979.

Necula M, Kayed R, Milton S, Glabe CG (2007) Small molecule inhibitors of aggregation indicate that amyloid-β oligomerization and fibrillization pathways are independent and distinct. J Biol Chem 282:10311-10324.

Nelson PT, Braak H, Markesbery WR (2009) Neuropathology and cognitive impairment in Alzheimer disease: a complex but coherent relationship. J Neuropathol Exp Neurol 68:1-14.

Neumann M, Diekmann S, Bertsch U, Vanmassenhove B, Bogerts B, Kretzschmar HA (2005) Novel G335V mutation in the tau gene associated with early onset familial frontotemporal dementia. Neurogenetics 6:91-95.

Neumann M, Schulz-Schaeffer W, Crowther RA, Smith MJ, Spillantini MG, Goedert M, Kretzschmar HA (2001) Pick's disease associated with the novel Tau gene mutation K369I. Ann Neurol 50:503-513.

Neve RL, Harris P, Kosik KS, Kurnit DM, Donlon TA (1986) Identification of cDNA clones for the human microtubule-associated protein tau and chromosomal localization of the genes for tau and microtubule-associated protein 2. Brain Res 387:271-280.

Nguyen T-H, Liu J, Lombroso PJ (2002) Striatal enriched phosphatase 61 dephosphorylates fyn at phosphotyrosine 420. J Biol Chem 277:24274-24279.

Nicholl DJ, Greenstone MA, Clarke CE, Rizzu P, Crooks D, Crowe A, Trojanowski JQ, Lee VM, Heutink P (2003) An English kindred with a novel recessive tauopathy and respiratory failure. Ann Neurol 54:682-686.

Nicholson AM, Ferreira A (2009) Increased membrane cholesterol might render mature hippocampal neurons more susceptible to beta-amyloid-induced calpain activation and tau toxicity. J Neurosci 29:4640-4651.

Nilsberth C, Westlind-Danielsson A, Eckman CB, Condron MM, Axelman K, Forsell C, Stenh C, Luthman J, Teplow DB, Younkin SG, Naslund J, Lannfelt L (2001) The 'Arctic' APP mutation (E693G) causes Alzheimer's disease by enhanced Aβ protofibril formation. Nat Neurosci 4:887-893.

Noble W, Hanger DP, Miller CC, Lovestone S (2013) The importance of tau phosphorylation for neurodegenerative diseases. Frontiers in neurology 4.

Noble W, Planel E, Zehr C, Olm V, Meyerson J, Suleman F, Gaynor K, Wang L, LaFrancois J, Feinstein B, Burns M, Krishnamurthy P, Wen Y, Bhat R, Lewis J, Dickson D, Duff K (2005) Inhibition of glycogen synthase kinase-3 by lithium correlates with reduced tauopathy and degeneration in vivo. Proc Natl Acad Sci U S A 102:6990-6995.

Noble W, Olm V, Takata K, Casey E, Mary O, Meyerson J, Gaynor K, LaFrancois J, Wang L, Kondo T, Davies P, Burns M, Veeranna, Nixon R, Dickson D, Matsuoka Y, Ahlijanian M, Lau LF, Duff K (2003) Cdk5 is a key factor in tau aggregation and tangle formation in vivo. Neuron 38:555-565.

Nygaard H, van Dyck C, Strittmatter S (2014) Fyn kinase inhibition as a novel therapy for Alzheimer's disease. Alzheimer's research & therapy 6:8.

O'Brien RJ, Wong PC (2011) Amyloid precursor protein processing and Alzheimer's disease. Annu Rev Neurosci 34:185-204.

Oddo S, Caccamo A, Cheng D, Jouleh B, Torp R, LaFerla FM (2007) Genetically augmenting tau levels does not modulate the onset or progression of Aβ pathology in transgenic mice. J Neurochem 102:1053-1063.

Ono K, Yoshiike Y, Takashima A, Hasegawa K, Naiki H, Yamada M (2003) Potent anti-amyloidogenic and fibril-destabilizing effects of polyphenols in vitro: implications for the prevention and therapeutics of Alzheimer's disease. J Neurochem 87:172-181.

Paholikova K, Salingova B, Opattova A, Skrabana R, Majerova P, Zilka N, Kovacech B, Zilkova M, Barath P, Novak M (2015) N-terminal truncation of microtubule associated protein tau dysregulates its cellular localization. J Alzheimers Dis 43:915-926.

Pastor P, Pastor E, Carnero C, Vela R, Garcia T, Amer G, Tolosa E, Oliva R (2001) Familial atypical progressive supranuclear palsy associated with homozigosity for the delN296 mutation in the tau gene. Ann Neurol 49:263-267.

Patrick GN, Zukerberg L, Nikolic M, de la Monte S, Dikkes P, Tsai L-H (1999) Conversion of p35 to p25 deregulates Cdk5 activity and promotes neurodegeneration. Nature 402:615-622.

Peeraer E, Bottelbergs A, Van Kolen K, Stancu I-C, Vasconcelos B, Mahieu M, Duytschaever H, Ver Donck L, Torremans A, Sluydts E, Van Acker N, Kemp JA, Mercken M, Brunden KR, Trojanowski JQ, Dewachter I, Lee VMY, Moechars D (2014) Intracerebral injection of preformed synthetic tau fibrils initiates widespread tauopathy and neuronal loss in the brains of tau transgenic mice. Neurobiol Dis 73:83-95.

Pereira DB, Chao MV (2007) The tyrosine kinase Fyn determines the localization of TrkB receptors in lipid rafts. J Neurosci 27:4859-4869.

Perez M, Santa-Maria I, De Barreda EG, Zhu X, Cuadros R, Cabrero JR, Sanchez-Madrid F, Dawson HN, Vitek MP, Perry G, Smith MA, Avila J (2009) Tau – an inhibitor of deacetylase HDAC6 function. J Neurochem 109:1756-1766.

Pickering-Brown S, Baker M, Yen S-H, Liu W-K, Hasegawa M, Cairns N, Lantos PL, Rossor M, Iwatsubo T, Davies Y, Allsop D, Furlong R, Owen F, Hardy J, Mann D, Hutton M (2000) Pick's disease is associated with mutations in the tau gene. Ann Neurol 48:859-867.

Pickering-Brown SM, Baker M, Nonaka T, Ikeda K, Sharma S, Mackenzie J, Simpson SA, Moore JW, Snowden JS, de Silva R, Revesz T, Hasegawa M, Hutton M, Mann DM (2004) Frontotemporal dementia with Pick-type histology associated with Q336R mutation in the tau gene. Brain 127:1415-1426.

Pittman AM, Fung H-C, de Silva R (2006) Untangling the tau gene association with neurodegenerative disorders. Hum Mol Genet 15:R188-R195.

Plattner F, Angelo M, Giese KP (2006) The roles of cyclin-dependent kinase 5 and glycogen synthase kinase 3 in tau hyperphosphorylation. J Biol Chem 281:25457-25465.

Plouffe V, Mohamed N-V, Rivest-McGraw J, Bertrand J, Lauzon M, Leclerc N (2012) Hyperphosphorylation and cleavage at D421 enhance tau secretion. PLoS ONE 7:e36873.

Pooler AM, Phillips EC, Lau DHW, Noble W, Hanger DP (2013a) Physiological release of endogenous tau is stimulated by neuronal activity. EMBO Rep 14:389-394.

Pooler AM, Usardi A, Evans CJ, Philpott KL, Noble W, Hanger DP (2012) Dynamic association of tau with neuronal membranes is regulated by phosphorylation. Neurobiol Aging 33:431.e427-431.e438.

Pooler AM, Polydoro M, Wegmann S, Nicholls SB, Spires-Jones TL, Hyman BT (2013b) Propagation of tau pathology in Alzheimer's disease: identification of novel therapeutic targets. Alzheimer's research & therapy 5:49.

Poorkaj P, Bird TD, Wijsman E, Nemens E, Garruto RM, Anderson L, Andreadis A, Wiederholt WC, Raskind M, Schellenberg GD (1998) Tau is a candidate gene for chromosome 17 frontotemporal dementia. Ann Neurol 43:815-825.

Poorkaj P, Muma NA, Zhukareva V, Cochran EJ, Shannon KM, Hurtig H, Koller WC, Bird TD, Trojanowski JQ, Lee VM, Schellenberg GD (2002) An R5L tau mutation in a subject with a progressive supranuclear palsy phenotype. Ann Neurol 52:511-516.

Porat Y, Mazor Y, Efrat S, Gazit E (2004) Inhibition of islet amyloid polypeptide fibril formation: a potential role for heteroaromatic interactions. Biochemistry (Mosc) 43:14454-14462.

Qian W, Shi J, Yin X, Iqbal K, Grundke-Iqbal I, Gong C-X, Liu F (2010) PP2A regulates tau phosphorylation directly and also indirectly via activating GSK-3β. Journal of Alzheimer's Disease 19:1221-1229.

Rankin CA, Sun Q, Gamblin TC (2005) Pseudo-phosphorylation of tau at Ser202 and Thr205 affects tau filament formation. Brain Res Mol Brain Res 138:84-93.

Rapoport M, Dawson HN, Binder LI, Vitek MP, Ferreira A (2002) Tau is essential to β-amyloid-induced neurotoxicity. Proc Natl Acad Sci U S A 99:6364-6369.

Reed LA, Grabowski TJ, Schmidt ML, Morris JC, Goate A, Solodkin A, Van Hoesen GW, Schelper RL, Talbot CJ, Wragg MA, Trojanowski JQ (1997) Autosomal dominant dementia with widespread neurofibrillary tangles. Ann Neurol 42:564-572.

Ren R, Mayer BJ, Cicchetti P, Baltimore D (1993) Identification of a ten-amino acid proline-rich SH3 binding site. Science 259:1157-1161.

Resh MD (1998) Fyn, a Src family tyrosine kinase. Int J Biochem Cell Biol 30:1159-1162.

Reynolds CH, Garwood CJ, Wray S, Price C, Kellie S, Perera T, Zvelebil M, Yang A, Sheppard PW, Varndell IM, Hanger DP, Anderton BH (2008) Phosphorylation regulates tau interactions with src homology 3 domains of phosphatidylinositol 3-kinase, phospholipase Cγ1, Grb2, and src family kinases. J Biol Chem 283:18177-18186.

Rhinn H, Fujita R, Qiang L, Cheng R, Lee JH, Abeliovich A (2013) Integrative genomics identifies APOE epsilon4 effectors in Alzheimer's disease. Nature 500:45-50.

Rickles RJ, Botfield MC, Zhou XM, Henry PA, Brugge JS, Zoller MJ (1995) Phage display selection of ligand residues important for Src homology 3 domain binding specificity. Proc Natl Acad Sci U S A 92:10909-10913.

Ripoli C, Cocco S, Li Puma DD, Piacentini R, Mastrodonato A, Scala F, Puzzo D, D'Ascenzo M, Grassi C (2014) Intracellular accumulation of amyloid-beta protein plays a major role in Abeta-induced alterations of glutamatergic synaptic transmission and plasticity. J Neurosci 34:12893-12903.

Rizzini C, Goedert M, Hodges JR, Smith MJ, Jakes R, Hills R, Xuereb JH, Crowther RA, Spillantini MG (2000) Tau gene mutation K257T causes a tauopathy similar to Pick's disease. J Neuropathol Exp Neurol 59:990-1001.

Rizzu P, Van Swieten JC, Joosse M, Hasegawa M, Stevens M, Tibben A, Niermeijer MF, Hillebrand M, Ravid R, Oostra BA, Goedert M, van Duijn CM, Heutink P (1999) High prevalence of mutations in the microtubule-associated protein tau in a population study of frontotemporal dementia in the Netherlands. Am J Hum Genet 64:414-421.

Roberson ED, Scearce-Levie K, Palop JJ, Yan F, Cheng IH, Wu T, Gerstein H, Yu G-Q, Mucke L (2007) Reducing endogenous tau ameliorates amyloid β-induced deficits in an Alzheimer's disease mouse model. Science 316:750-754.

Roberson ED, Halabisky B, Yoo JW, Yao J, Chin J, Yan F, Wu T, Hamto P, Devidze N, Yu G-Q, Palop JJ, Noebels JL, Mucke L (2011) Amyloid-β/fyn–induced synaptic, network, and cognitive impairments depend on tau levels in multiple mouse models of Alzheimer's disease. J Neurosci 31:700-711.

Rogaev EI et al. (1995) Familial Alzheimer's disease in kindreds with missense mutations in a gene on chromosome 1 related to the Alzheimer's disease type 3 gene. Nature 376:775-778.

Rohrer JD, Paviour D, Vandrovcova J, Hodges J, de Silva R, Rossor MN (2011) Novel L284R MAPT mutation in a family with an autosomal dominant progressive supranuclear palsy syndrome. Neurodegener Dis 8:149-152.

Ros R, Thobois S, Streichenberger N, Kopp N, Sanchez MP, Perez M, Hoenicka J, Avila J, Honnorat J, de Yebenes JG (2005) A new mutation of the tau gene, G303V, in early-onset familial progressive supranuclear palsy. Arch Neurol 62:1444-1450.

Rossi G, Bastone A, Piccoli E, Mazzoleni G, Morbin M, Uggetti A, Giaccone G, Sperber S, Beeg M, Salmona M, Tagliavini F (2012) New mutations in MAPT gene causing frontotemporal lobar degeneration: biochemical and structural characterization. Neurobiol Aging 33:834 e831-836.

Rosso SM, van Herpen E, Deelen W, Kamphorst W, Severijnen LA, Willemsen R, Ravid R, Niermeijer MF, Dooijes D, Smith MJ, Goedert M, Heutink P, van Swieten JC (2002) A novel tau mutation, S320F, causes a tauopathy with inclusions similar to those in Pick's disease. Ann Neurol 51:373-376.

Rushworth JV, Griffiths HH, Watt NT, Hooper NM (2013) Prion protein-mediated toxicity of amyloid-β oligomers requires lipid rafts and the transmembrane LRP1. J Biol Chem 288:8935-8951.

Sahara N, Lewis J, DeTure M, McGowan E, Dickson DW, Hutton M, Yen S-H (2002) Assembly of tau in transgenic animals expressing P301L tau: alteration of phosphorylation and solubility. J Neurochem 83:1498-1508.

Saito YD, Jensen AR, Salgia R, Posadas EM (2010) Fyn: a novel molecular target in cancer. Cancer 116:1629-1637.

Sala C, Sheng M (1999) The fyn art of N-methyl-D-aspartate receptor phosphorylation. Proc Natl Acad Sci U S A 96:335-337.

Saman S, Kim W, Raya M, Visnick Y, Miro S, Saman S, Jackson B, McKee AC, Alvarez VE, Lee NCY, Hall GF (2012) Exosome-associated tau is secreted in tauopathy models and is selectively phosphorylated in cerebrospinal fluid in early Alzheimer disease. J Biol Chem 287:3842-3849.

SantaCruz K, Lewis J, Spires T, Paulson J, Kotilinek L, Ingelsson M, Guimaraes A, DeTure M, Ramsden M, McGowan E, Forster C, Yue M, Orne J, Janus C, Mariash A, Kuskowski M, Hyman B, Hutton M, Ashe KH (2005) Tau suppression in a neurodegenerative mouse model improves memory function. Science 309:476-481.

Santuccione A, Sytnyk V, Leshchyns'ka I, Schachner M (2005) Prion protein recruits its neuronal receptor NCAM to lipid rafts to activate p59fyn and to enhance neurite outgrowth. J Cell Biol 169:341 - 354.

Sasaki Y, Cheng C, Uchida Y, Nakajima O, Ohshima T, Yagi T, Taniguchi M, Nakayama T, Kishida R, Kudo Y, Ohno S, Nakamura F, Goshima Y (2002) Fyn and cdk5 mediate semaphorin-3A signaling, which is involved in regulation of dendrite orientation in cerebral cortex. Neuron 35:907-920.

Sato Y, Tao YX, Su Q, Johns RA (2008) Post-synaptic density-93 mediates tyrosine-phosphorylation of the N-methyl-d-aspartate receptors. Neuroscience 153:700-708.

Savonenko AV, Xu GM, Price DL, Borchelt DR, Markowska AL (2003) Normal cognitive behavior in two distinct congenic lines of transgenic mice hyperexpressing mutant APPSWE. Neurobiol Dis 12:194-211.

Scheuner D et al. (1996) Secreted amyloid beta-protein similar to that in the senile plaques of Alzheimer's disease is increased in vivo by the presenilin 1 and 2 and APP mutations linked to familial Alzheimer's disease. Nat Med 2:864-870.

Schmitz M, Greis C, Ottis P, Silva C, Schulz-Schaeffer W, Wrede A, Koppe K, Onisko B, Requena J, Govindarajan N, Korth C, Fischer A, Zerr I (2014) Loss of prion protein leads to age-dependent behavioral abnormalities and changes in cytoskeletal protein expression. Mol Neurobiol:1-14.

Schneider A, Biernat J, von Bergen M, Mandelkow E, Mandelkow EM (1999) Phosphorylation that detaches tau protein from microtubules (ser262, ser214) also protects it against aggregation into Alzheimer paired helical filaments. Biochemistry (Mosc) 38:3549-3558.

Selkoe DJ (2011) Alzheimer’s disease. Cold Spring Harb Perspect Biol 3.

Serrano-Pozo A, Frosch MP, Masliah E, Hyman BT (2011) Neuropathological alterations in Alzheimer disease. Cold Spring Harb Perspect Med 1.

Seshadri S, Fitzpatrick AL, Ikram M, et al. (2010) Genome-wide analysis of genetic loci associated with Alzheimer disease. JAMA 303:1832-1840.

Shahpasand K, Uemura I, Saito T, Asano T, Hata K, Shibata K, Toyoshima Y, Hasegawa M, Hisanaga S (2012) Regulation of mitochondrial transport and inter-microtubule spacing by tau phosphorylation at the sites hyperphosphorylated in Alzheimer's disease. J Neurosci 32:2430-2441.

Shankar GM, Bloodgood BL, Townsend M, Walsh DM, Selkoe DJ, Sabatini BL (2007) Natural oligomers of the Alzheimer amyloid-beta protein induce reversible synapse loss by modulating an NMDA-type glutamate receptor-dependent signaling pathway. J Neurosci 27:2866-2875.

Shankar GM, Li S, Mehta TH, Garcia-Munoz A, Shepardson NE, Smith I, Brett FM, Farrell MA, Rowan MJ, Lemere CA, Regan CM, Walsh DM, Sabatini BL, Selkoe DJ (2008) Amyloid-β protein dimers isolated directly from Alzheimer's brains impair synaptic plasticity and memory. Nat Med 14:837-842.

Sharma VM, Litersky JM, Bhaskar K, Lee G (2007) Tau impacts on growth-factor-stimulated actin remodeling. J Cell Sci 120:748-757.

Sherrington R et al. (1996) Alzheimer's disease associated with mutations in presenilin 2 is rare and variably penetrant. Hum Mol Genet 5:985-988.

Sherrington R et al. (1995) Cloning of a gene bearing missense mutations in early-onset familial Alzheimer's disease. Nature 375:754-760.

Shipton OA, Leitz JR, Dworzak J, Acton CE, Tunbridge EM, Denk F, Dawson HN, Vitek MP, Wade-Martins R, Paulsen O, Vargas-Caballero M (2011) Tau protein is required for amyloid β-induced impairment of hippocampal long-term potentiation. J Neurosci 31:1688-1692.

Shirao T, Kojima N, Nabeta Y, Obata K (1989) Two forms of drebrins, developmentally regulated brain proteins, in rat. Proc Jpn Acad Ser B Phys Biol Sci 65:169-172.

Shirazi SK, Wood JG (1993) The protein tyrosine kinase, fyn, in Alzheimer's disease pathology. Neuroreport 4:435-437.

Sigurdsson EM, Scholtzova H, Mehta PD, Frangione B, Wisniewski T (2001) Immunization with a nontoxic/nonfibrillar amyloid-β homologous peptide reduces Alzheimer's disease-associated pathology in transgenic mice. Am J Pathol 159:439-447.

Simón D, García-García E, Royo F, Falcón-Pérez JM, Avila J (2012a) Proteostasis of tau. Tau overexpression results in its secretion via membrane vesicles. FEBS Lett 586:47-54.

Simón D, García-García E, Gómez-Ramos A, Falcón-Pérez JM, Díaz-Hernández M, Hernández F, Avila J (2012b) Tau overexpression results in its secretion via membrane vesicles. Neurodegener Dis 10:73-75.

Sjöberg MK, Shestakova E, Mansuroglu Z, Maccioni RB, Bonnefoy E (2006) Tau protein binds to pericentromeric DNA: a putative role for nuclear tau in nucleolar organization. J Cell Sci 119:2025-2034.

Skoglund L, Viitanen M, Kalimo H, Lannfelt L, Jonhagen ME, Ingelsson M, Glaser A, Herva R (2008) The tau S305S mutation causes frontotemporal dementia with parkinsonism. Eur J Neurol 15:156-161.

Snyder EM, Nong Y, Almeida CG, Paul S, Moran T, Choi EY, Nairn AC, Salter MW, Lombroso PJ, Gouras GK, Greengard P (2005) Regulation of NMDA receptor trafficking by amyloid-β. Nat Neurosci 8:1051-1058.

Sparks AB, Quilliam LA, Thorn JM, Der CJ, Kay BK (1994) Identification and characterization of Src SH3 ligands from phage-displayed random peptide libraries. J Biol Chem 269:23853-23856.

Sperber BR, Boyle-Walsh ÃiA, Engleka MJ, Gadue P, Peterson AC, Stein PL, Scherer SS, McMorris FA (2001) A unique role for fyn in CNS myelination. J Neurosci 21:2039-2047.

Sperfeld AD, Collatz MB, Baier H, Palmbach M, Storch A, Schwarz J, Tatsch K, Reske S, Joosse M, Heutink P, Ludolph AC (1999) FTDP-17: an early-onset phenotype with parkinsonism and epileptic seizures caused by a novel mutation. Ann Neurol 46:708-715.

Spillantini MG, Goedert M (2013) Tau pathology and neurodegeneration. Lancet Neurol 12:609-622.

Spillantini MG, Crowther RA, Kamphorst W, Heutink P, van Swieten JC (1998a) Tau pathology in two Dutch families with mutations in the microtubule-binding region of tau. Am J Pathol 153:1359-1363.

Spillantini MG, Murrell JR, Goedert M, Farlow MR, Klug A, Ghetti B (1998b) Mutation in the tau gene in familial multiple system tauopathy with presenile dementia. Proc Natl Acad Sci U S A 95:7737-7741.

Spillantini MG, Yoshida H, Rizzini C, Lantos PL, Khan N, Rossor MN, Goedert M, Brown J (2000) A novel tau mutation (N296N) in familial dementia with swollen achromatic neurons and corticobasal inclusion bodies. Ann Neurol 48:939-943.

Spina S, Murrell JR, Yoshida H, Ghetti B, Bermingham N, Sweeney B, Dlouhy SR, Crowther RA, Goedert M, Keohane C (2007) The novel Tau mutation G335S: clinical, neuropathological and molecular characterization. Acta Neuropathol 113:461-470.

Stanford PM, Halliday GM, Brooks WS, Kwok JB, Storey CE, Creasey H, Morris JG, Fulham MJ, Schofield PR (2000) Progressive supranuclear palsy pathology caused by a novel silent mutation in exon 10 of the tau gene: expansion of the disease phenotype caused by tau gene mutations. Brain 123 (Pt 5):880-893.

Stanford PM, Shepherd CE, Halliday GM, Brooks WS, Schofield PW, Brodaty H, Martins RN, Kwok JB, Schofield PR (2003) Mutations in the tau gene that cause an increase in three repeat tau and frontotemporal dementia. Brain 126:814-826.

Stefansson H et al. (2005) A common inversion under selection in Europeans. Nat Genet 37:129-137.

Stoppini L, Buchs PA, Muller D (1991) A simple method for organotypic cultures of nervous tissue. J Neurosci Methods 37:173-182.

Stoppini L, Parisi L, Oropesa C, Muller D (1997) Sprouting and functional recovery in co-cultures between old and young hippocampal organotypic slices. Neuroscience 80:1127-1136.

Strassnig M, Ganguli M (2005) About a peculiar disease of the cerebral cortex: Alzheimer's original case revisited. Psychiatry (Edgmont) 2:30-33.

Strittmatter WJ, Saunders AM, Schmechel D, Pericak-Vance M, Enghild J, Salvesen GS, Roses AD (1993) Apolipoprotein E: high-avidity binding to beta-amyloid and increased frequency of type 4 allele in late-onset familial Alzheimer disease. Proc Natl Acad Sci U S A 90:1977-1981.

Sultan A, Nesslany F, Violet M, Bégard S, Loyens A, Talahari S, Mansuroglu Z, Marzin D, Sergeant N, Humez S, Colin M, Bonnefoy E, Buée L, Galas M-C (2011) Nuclear tau, a key player in neuronal DNA protection. J Biol Chem 286:4566-4575.

Sumi SM, Bird TD, Nochlin D, Raskind MA (1992) Familial presenile dementia with psychosis associated with cortical neurofibrillary tangles and degeneration of the amygdala. Neurology 42:120-127.

Sun G, Sharma AK, Budde RJ (1998) Autophosphorylation of Src and Yes blocks their inactivation by Csk phosphorylation. Oncogene 17:1587-1595.

Superti-Furga G, Fumagalli S, Koegl M, Courtneidge SA, Draetta G (1993) Csk inhibition of c-Src activity requires both the SH2 and SH3 domains of Src. EMBO J 12:2625-2634.

Suzuki T, Okamuranoji K (1995) NMDA receptor subunits ε1 (NR2A) and ε2 (NR2B) are substrates for fyn in the postsynaptic density fraction isolated from the rat brain. Biochem Biophys Res Commun 216:582-588.

Tai H-C, Serrano-Pozo A, Hashimoto T, Frosch MP, Spires-Jones TL, Hyman BT (2012) The synaptic accumulation of hyperphosphorylated tau oligomers in Alzheimer disease is associated with dysfunction of the ubiquitin-proteasome system. Am J Pathol 181:1426-1435.

Tai H-C, Wang B, Serrano-Pozo A, Frosch M, Spires-Jones T, Hyman B (2014) Frequent and symmetric deposition of misfolded tau oligomers within presynaptic and postsynaptic terminals in Alzheimer's disease. Acta neuropathologica communications 2:146.

Tanzi RE, Vaula G, Romano DM, Mortilla M, Huang TL, Tupler RG, Wasco W, Hyman BT, Haines JL, Jenkins BJ, et al. (1992) Assessment of amyloid beta-protein precursor gene mutations in a large set of familial and sporadic Alzheimer disease cases. Am J Hum Genet 51:273-282.

Tavares IA, Touma D, Lynham S, Troakes C, Schober M, Causevic M, Garg R, Noble W, Killick R, Bodi I, Hanger DP, Morris JDH (2013) Prostate-derived sterile 20-like kinases (PSKs/TAOKs) phosphorylate tau protein and are activated in tangle-bearing neurons in Alzheimer disease. J Biol Chem 288:15418-15429.

Terry RD, Masliah E, Salmon DP, Butters N, DeTeresa R, Hill R, Hansen LA, Katzman R (1991) Physical basis of cognitive alterations in Alzheimer's disease: synapse loss is the major correlate of cognitive impairment. Ann Neurol 30:572-580.

Teschemacher AG, Paton JFR, Kasparov S (2005a) Imaging living central neurones using viral gene transfer. Adv Drug Deliv Rev 57:79-93.

Teschemacher AG, Wang S, Lonergan T, Duale H, Waki H, Paton JFR, Kasparov S (2005b) Targeting specific neuronal populations using adeno- and lentiviral vectors: applications for imaging and studies of cell function. Exp Physiol 90:61-69.

Tezuka T, Umemori H, Akiyama T, Nakanishi S, Yamamoto T (1999) PSD-95 promotes Fyn-mediated tyrosine phosphorylation of the N-methyl-D-aspartate receptor subunit NR2A. Proc Natl Acad Sci U S A 96:435-440.

Thies W, Bleiler L (2011) 2011 Alzheimer's disease facts and figures. Alzheimers Dement 7:208-244.

Tiruppathi C, Song W, Bergenfeldt M, Sass P, Malik AB (1997) Gp60 activation mediates albumin transcytosis in endothelial cells by tyrosine kinase-dependent pathway. J Biol Chem 272:25968-25975.

Toescu EC (1999) Activity of voltage-operated calcium channels in rat cerebellar granule neurons and neuronal survival. Neuroscience 94:561-570.

Town T, Zolton J, Shaffner R, Schnell B, Crescentini R, Wu Y, Zeng J, DelleDonne A, Obregon D, Tan J, Mullan M (2002) p35/Cdk5 pathway mediates soluble amyloid-β peptide-induced tau phosphorylation in vitro. J Neurosci Res 69:362-372.

Townsend M, Shankar GM, Mehta T, Walsh DM, Selkoe DJ (2006) Effects of secreted oligomers of amyloid β-protein on hippocampal synaptic plasticity: a potent role for trimers. J Physiol 572:477-492.

Trabzuni D, Wray S, Vandrovcova J, Ramasamy A, Walker R, Smith C, Luk C, Gibbs JR, Dillman A, Hernandez DG, Arepalli S, Singleton AB, Cookson MR, Pittman AM, de Silva R, Weale ME, Hardy J, Ryten M (2012) MAPT expression and splicing is differentially regulated by brain region: relation to genotype and implication for tauopathies. Hum Mol Genet 21:4094-4103.

Tran Hien T, Chung Charlotte H-Y, Iba M, Zhang B, Trojanowski John Q, Luk Kelvin C, Lee Virginia MY (2014) α-Synuclein Immunotherapy Blocks Uptake and Templated Propagation of Misfolded α-Synuclein and Neurodegeneration. Cell Rep 7:2054-2065.

Tucker KL, Meyer M, Barde Y-A (2001) Neurotrophins are required for nerve growth during development. Nat Neurosci 4:29-37.

Uchihara T, Nakamura A, Yamazaki M, Mori O (2001) Evolution from pretangle neurons to neurofibrillary tangles monitored by thiazin red combined with Gallyas method and double immunofluorescence. Acta Neuropathol 101:535-539.

Um JW, Nygaard HB, Heiss JK, Kostylev MA, Stagi M, Vortmeyer A, Wisniewski T, Gunther EC, Strittmatter SM (2012) Alzheimer amyloid-β oligomer bound to postsynaptic prion protein activates Fyn to impair neurons. Nat Neurosci 15:1227–1235.

Um Ji W, Kaufman Adam C, Kostylev M, Heiss Jacqueline K, Stagi M, Takahashi H, Kerrisk Meghan E, Vortmeyer A, Wisniewski T, Koleske Anthony J, Gunther Erik C, Nygaard Haakon B, Strittmatter Stephen M (2013) Metabotropic

glutamate receptor 5 is a coreceptor for Alzheimer Aβ oligomer bound to cellular prion protein. Neuron 79:887-902.

Umemori H, Sato S, Yagi T, Aizawa S, Yamamoto T (1994) Initial events of myelination involve Fyn tyrosine kinase signalling. Nature 367:572-576.

Usardi A, Pooler AM, Seereeram A, Reynolds CH, Derkinderen P, Anderton B, Hanger DP, Noble W, Williamson R (2011) Tyrosine phosphorylation of tau regulates its interactions with Fyn SH2 domains, but not SH3 domains, altering the cellular localization of tau. FEBS J 278:2927-2937.

van der Flier WM, Pijnenburg YAL, Fox NC, Scheltens P (2011) Early-onset versus late-onset Alzheimer's disease: the case of the missing APOE ε4 allele. Lancet Neurol 10:280-288.

van der Zee J, Rademakers R, Engelborghs S, Gijselinck I, Bogaerts V, Vandenberghe R, Santens P, Caekebeke J, De Pooter T, Peeters K, Lubke U, Van den Broeck M, Martin JJ, Cruts M, De Deyn PP, Van Broeckhoven C, Dermaut B (2006) A Belgian ancestral haplotype harbours a highly prevalent mutation for 17q21-linked tau-negative FTLD. Brain 129:841-852.

van Duijn CM, Hendriks L, Cruts M, Hardy JA, Hofman A, Van Broeckhoven C (1991) Amyloid precursor protein gene mutation in early-onset Alzheimer's disease. Lancet 337:978.

van Herpen E, Rosso SM, Serverijnen LA, Yoshida H, Breedveld G, van de Graaf R, Kamphorst W, Ravid R, Willemsen R, Dooijes D, Majoor-Krakauer D, Kros JM, Crowther RA, Goedert M, Heutink P, van Swieten JC (2003) Variable phenotypic expression and extensive tau pathology in two families with the novel tau mutation L315R. Ann Neurol 54:573-581.

Vassar R et al. (1999) β-Secretase cleavage of Alzheimer's amyloid precursor protein by the transmembrane aspartic protease BACE. Science 286:735-741.

von Bergen M, Friedhoff P, Biernat J, Heberle J, Mandelkow E-M, Mandelkow E (2000) Assembly of τ protein into Alzheimer paired helical filaments depends on a local sequence motif (306VQIVYK311) forming β structure. Proc Natl Acad Sci U S A 97:5129-5134.

von Bergen M, Barghorn S, Li L, Marx A, Biernat J, Mandelkow EM, Mandelkow E (2001) Mutations of tau protein in frontotemporal dementia promote aggregation of paired helical filaments by enhancing local beta-structure. J Biol Chem 276:48165-48174.

Wagner U, Utton M, Gallo JM, Miller CC (1996) Cellular phosphorylation of tau by GSK-3 beta influences tau binding to microtubules and microtubule organisation. J Cell Sci 109:1537-1543.

Walls KC, Ager RR, Vasilevko V, Cheng D, Medeiros R, LaFerla FM (2014) p-Tau immunotherapy reduces soluble and insoluble tau in aged 3xTg-AD mice. Neurosci Lett 575:96-100.

Wang Y, Loomis PA, Zinkowski RP, Binder LI (1993) A novel tau transcript in cultured human neuroblastoma cells expressing nuclear tau. J Cell Biol 121:257-267.

Wasco W, Pettingell WP, Jondro PD, Schmidt SD, Gurubhagavatula S, Rodes L, DiBlasi T, Romano DM, Guenette SY, Kovacs DM, et al. (1995) Familial Alzheimer's chromosome 14 mutations. Nat Med 1:848.

Wei Y, Qu M-H, Wang X-S, Chen L, Wang D-L, Liu Y, Hua Q, He R-Q (2008) Binding to the minor groove of the double-strand, tau protein prevents DNA from damage by peroxidation. PLoS ONE 3:e2600.

Weingarten MD, Lockwood AH, Hwo SY, Kirschner MW (1975) A protein factor essential for microtubule assembly. Proc Natl Acad Sci U S A 72:1858-1862.

Wille H, Drewes G, Biernat J, Mandelkow EM, Mandelkow E (1992) Alzheimer-like paired helical filaments and antiparallel dimers formed from microtubule-associated protein tau in vitro. J Cell Biol 118:573-584.

William Rebeck G, Reiter JS, Strickland DK, Hyman BT (1993) Apolipoprotein E in sporadic Alzheimer's disease: Allelic variation and receptor interactions. Neuron 11:575-580.

Williamson R, Usardi A, Hanger DP, Anderton BH (2008) Membrane-bound β-amyloid oligomers are recruited into lipid rafts by a fyn-dependent mechanism. FASEB J 22:1552-1559.

Williamson R, Scales T, Clark BR, Gibb G, Reynolds CH, Kellie S, Bird IN, Varndell IM, Sheppard PW, Everall I, Anderton BH (2002) Rapid tyrosine phosphorylation of neuronal proteins including tau and focal adhesion kinase in response to amyloid-β peptide exposure: involvement of src family protein kinases. J Neurosci 22:10-20.

Wolfe MS (2009) Tau mutations in neurodegenerative diseases. J Biol Chem 284:6021-6025.

Wszolek ZK, Pfeiffer RF, Bhatt MH, Schelper RL, Cordes M, Snow BJ, Rodnitzky RL, Wolters EC, Arwert F, Calne DB (1992) Rapidly progressive autosomal dominant parkinsonism and dementia with pallido-ponto-nigral degeneration. Ann Neurol 32:312-320.

Wu JW, Herman M, Liu L, Simoes S, Acker CM, Figueroa H, Steinberg JI, Margittai M, Kayed R, Zurzolo C, Di Paolo G, Duff KE (2013) Small misfolded tau species are internalized via bulk endocytosis and anterogradely and retrogradely transported in neurons. J Biol Chem 288:1856-1870.

Xia D, Gotz J (2014) Premature lethality, hyperactivity, and aberrant phosphorylation in transgenic mice expressing a constitutively active form of Fyn. Frontiers in molecular neuroscience 7:40.

Yagi T (1999) Molecular mechanisms of Fyn-tyrosine kinase for regulating mammalian behaviors and ethanol sensitivity. Biochem Pharmacol 57:845-850.

Yamada K, Cirrito JR, Stewart FR, Jiang H, Finn MB, Holmes BB, Binder LI, Mandelkow EM, Diamond MI, Lee VM, Holtzman DM (2011) In vivo microdialysis reveals age-dependent decrease of brain interstitial fluid tau levels in P301S human tau transgenic mice. J Neurosci 31:13110-13117.

Yamada K, Holth JK, Liao F, Stewart FR, Mahan TE, Jiang H, Cirrito JR, Patel TK, Hochgrafe K, Mandelkow EM, Holtzman DM (2014) Neuronal activity regulates extracellular tau in vivo. J Exp Med 211:387-393.

Yanamandra K, Kfoury N, Jiang H, Mahan Thomas E, Ma S, Maloney Susan E, Wozniak David F, Diamond Marc I, Holtzman David M (2013) Anti-tau antibodies that block tau aggregate seeding in vitro markedly decrease pathology and improve cognition in vivo. Neuron 80:402-414.

Yasuda M, Takamatsu J, D'Souza I, Crowther RA, Kawamata T, Hasegawa M, Hasegawa H, Spillantini MG, Tanimukai S, Poorkaj P, Varani L, Varani G, Iwatsubo T, Goedert M, Schellenberg DG, Tanaka C (2000) A novel mutation at position +12 in the intron following exon 10 of the tau gene in familial frontotemporal dementia (FTD-Kumamoto). Ann Neurol 47:422-429.

Yoshiyama Y, Higuchi M, Zhang B, Huang SM, Iwata N, Saido TC, Maeda J, Suhara T, Trojanowski JQ, Lee VM (2007) Synapse loss and microglial activation precede tangles in a P301S tauopathy mouse model. Neuron 53:337-351.

Yu J-Z, Rasenick MM (2006) Tau associates with actin in differentiating PC12 cells. FASEB J 20:1452-1461.

Yuan A, Kumar A, Peterhoff C, Duff K, Nixon RA (2008) Axonal transport rates in vivo are unaffected by tau deletion or overexpression in mice. J Neurosci 28:1682-1687.

Yue T-L, Wang C, Romanic AM, Kikly K, Keller P, DeWolf Jr WE, Hart TK, Thomas HC, Storer B, Gu J-L, Wang X, Feuerstein GZ (1998) Staurosporine-induced Apoptosis in Cardiomyocytes: A Potential Role of Caspase-3. J Mol Cell Cardiol 30:495-507.

Zarranz JJ, Ferrer I, Lezcano E, Forcadas MI, Eizaguirre B, Atares B, Puig B, Gomez-Esteban JC, Fernandez-Maiztegui C, Rouco I, Perez-Concha T, Fernandez M, Rodriguez O, Rodriguez-Martinez AB, de Pancorbo MM, Pastor P, Perez-Tur J (2005) A novel mutation (K317M) in the MAPT gene causes FTDP and motor neuron disease. Neurology 64:1578-1585.

Zempel H, Mandelkow E (2014) Lost after translation: missorting of Tau protein and consequences for Alzheimer disease. Trends Neurosci.

Zempel H, Thies E, Mandelkow E, Mandelkow EM (2010) Abeta oligomers cause localized Ca(2+) elevation, missorting of endogenous Tau into dendrites, Tau phosphorylation, and destruction of microtubules and spines. J Neurosci 30:11938-11950.

Zhang XD, Gillespie SK, Hersey P (2004) Staurosporine induces apoptosis of melanoma by both caspase-dependent and -independent apoptotic pathways. Mol Cancer Ther 3:187-197.

Zhang Y, Wang H, Pan H, Bao X, Li M, Jin J, Wu X (2006) Gene delivery into primary cerebral cortical neurons by lentiviral vector. Cell Biol Int 30:777-783.

Zhang Y, Kurup P, Xu J, Carty N, Fernandez SM, Nygaard HB, Pittenger C, Greengard P, Strittmatter SM, Nairn AC, Lombroso PJ (2010) Genetic reduction of striatal-enriched tyrosine phosphatase (STEP) reverses cognitive and cellular deficits in an Alzheimer's disease mouse model. Proc Natl Acad Sci U S A 107:19014-19019.

Zhao Z-s, Manser E, Lim L (2000) Interaction between PAK and Nck: a template for Nck targets and role of PAK autophosphorylation. Mol Cell Biol 20:3906-3917.

Zheng-Fischhöfer Q, Biernat J, Mandelkow E-M, Illenberger S, Godemann R, Mandelkow E (1998) Sequential phosphorylation of Tau by glycogen synthase kinase-3β and protein kinase A at Thr212 and Ser214 generates the Alzheimer-specific epitope of antibody AT100 and requires a paired-helical-filament-like conformation. Eur J Biochem 252:542-552.

Zhou X, Moon C, Zheng F, Luo Y, Soellner D, Nunez JL, Wang H (2009) N-methyl-D-aspartate-stimulated ERK1/2 signaling and the transcriptional up-regulation of plasticity-related genes are developmentally regulated following in vitro neuronal maturation. J Neurosci Res 87:2632-2644.